Freie Universität Berlin

f-Vector Spaces of Polytopes, Spheres, and Eulerian Lattices

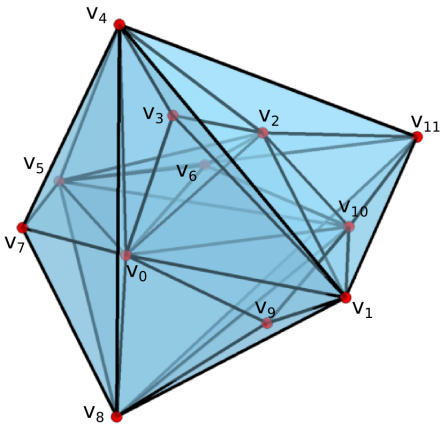

Dissertation zur Erlangung des Grades
eines Doktors der Naturwissenschaften (Dr. rer. nat.)
am Fachbereich Mathematik und Informatik
der Freien Universität Berlin

von

Philip Brinkmann

Berlin
06. Oktober 2016

Betreuer: Prof. Günter M. Ziegler, PhD
Zweitgutachter: Prof. Dr. Dr. h.c. Bernd Sturmfels, PhD

Tag der Disputation: 27. September 2016

THE ROAD TO WISDOM

The road to wisdom? - Well, it's
plain and simple to express:

Err
and err
and err again,
but less
and less
and less.

(A *Grook* by Piet Hein)

Acknowledgements

First of all I want to thank my supervisor Günter M. Ziegler who gave me enough freedom to study what I found interesting, but who also gave at the right moments valuable hints and directions to go further. I also thank Bernd Sturmfels who agreed to be the second referee for this thesis.
I am grateful for many math and non-math conversations, help and encouragement which helped me during my time as a PhD-student. For this I want to thank my mentor Tibor Szabó, as well as Katy Beeler, Marge Bayer, Hao Chen, Moritz Firsching, Tobias Friedl, Francesco Grande, Lauri Loiskekoski, Arnau Padrol, Nevena Palic, Raman Sanyal, Moritz Schmitt, Hannah Schäfer Sjöberg, Christian Stump, and all other people in and around the Villa. I was supported by the Deutsche Forschungsgemeinschaft within the research training group "Methods for Discrete Structures" (GRK1408). I would like to thank Elke Pose and Dorothea Kiefer for administrative support and everybody from the IT-support who kept the *allegro*-cluster running.
As life is not work alone I am really happy that I have my friends and family, especially DJ Dahlem, who give me support, comfort and joy.
Most of all I want to mention Geeske. Thank you for everything.

Contents

Introduction

Among the main objects in convex geometry are the *convex polytopes*, which are simply called *polytopes* throughout this thesis. Polytopes have already been studied by the ancient Greeks (like the *Platonic solids*), but it was not until Euler discovered the relation between the face numbers of polytopes (see Equation 1) that there was much progress on the combinatorics of polytopes, and still until the middle of the 19th century the focus was on the three dimensional case. However, since then a lot of new theory has been developed, which is partially due to the different fields where polytopes naturally occur. Among these applications for polytopes the probably best known is *linear programming*, which is, in short, maximising (or minimising) a linear functional over a set bounded by hyperplanes (so, the feasible region of the linear program is a polyhedron). The foundation of the modern theory of convex polytopes was laid by Grünbaum in his book [35], which also contains a wider overview over the history of the field. Also to mention is the book by Ziegler [76]. Both books are the reference for the basic concepts presented here.

A d-dimensional *polytope* (for short *d-polytope*) is the convex hull of finitely many points in Euclidean space such that the dimension of a smallest affine subspace containing it is d. Equivalently, one can define a d-polytope to be the intersection of finitely many halfspaces in $\mathbb{R}^d$ with the extra conditions that this intersection is full-dimensional and bounded. If this intersection is allowed to be unbounded, we call it a *polyhedron*.

For a d-polytope P we can define its *faces* as P itself, the empty set, as well as the intersections $P \cap H$, where H is a *supporting hyperplane* of P (i.e. a hyperplane such that $P \subset H^+$). Clearly, all faces are polytopes as well. They have dimensions ranging from -1 (empty face) to d (P itself). The 0-faces are called *vertices*, the 1-faces are *edges*, the $(d-2)$-faces are *ridges*, and the $(d-1)$-faces are called *facets*. The set of faces ordered by inclusion forms the *face lattice* of the polytope P. We say two polytopes P and Q are *combinatorially equivalent* if there is an inclusion-preserving bijection between their face lattices.

Basic examples of polytopes are the *d-simplices*, which are the convex hulls of $d+1$ affinely independent points. This means that a 1-simplex is a line segment, the 2-simplex is a triangle, and the 3-simplex is a tetrahedron. In a certain sense the d-simplex is the smallest d-polytope, since no other d-polytope can have less than or equally many vertices. The simplices also have a special face structure: Every combination of vertices yields a face of the simplex, and all faces are again simplices. If all facets of a polytope P are simplices we call it *simplicial*. They define an important subclass of polytopes, as they are in many cases easier to study than

general polytopes (see g-Theorem in Section 1.1). The dual polytopes to simplicial polytopes are called *simple polytopes*, and can be characterised as having all vertex degrees d. The simplices and the polygons are the only polytopes that are both simplicial and simple.

One important combinatorial invariant of a d-polytope P is its *f-vector*

$$f(P) := (f_{-1}(P), f_0(P), \ldots, f_{d-1}(P), f_d(P)),$$

where $f_i(P)$ is the number of i-dimensional faces of P. Since every d-polytope has exactly one face of dimension -1 and d, we have $f_{-1}(P) = f_d(P) = 1$, and these values are often omitted. We also often write f_i instead of $f_i(P)$ when the polytope is clear. One relation between the f-numbers is Euler's equation, which reads

$$f_0 - f_1 + \ldots + (-1)^{d-1} f_{d-1} = 1 - (-1)^d. \tag{1}$$

To encode more information about the combinatorics of a polytope we can extend the f-vector to the *flag-vector*, which we denote by $fl(P)$. The entries of the flag-vector are indexed by the sets $S \subset \{0, \ldots, d-1\}$ and are defined as

$$f_S(P) := |\{F_{i_1} \subset \cdots \subset F_{i_s} \subset P \,:\, S = \{i_1, \ldots, i_s\},\ \dim F_{i_j} = i_j\}|, \tag{2}$$

which is the number of ascending chains (flags) of faces of P with dimensions prescribed through the elements of S. Here, $f_\emptyset = f_{-1}$ and $f_{\{i\}} = f_i$. For convenience, we will often just write $f_{i_1 \cdots i_s}$ instead of $f_{\{i_1,\ldots,i_s\}}$.

For simplicial polytopes we can define another useful combinatorial invariant: the g-vector, which was introduced by McMullen & Walkup [50]. (It is useful, since it makes formulas nicer.) In order to define it, the notion of the h-vector of a simplicial d-polytope comes in handy. The h-vector $(h_0, h_1, \ldots, h_d)$, which was introduced by McMullen [48] and related to toric varieties by Stanley [63], is defined as

$$h_k := \sum_{i=0}^{k} (-1)^{k-i} \binom{d-i}{d-k} f_{i-1}. \tag{3}$$

With this, the g-vector $(g_0, g_1, \ldots, g_{\lfloor d/2 \rfloor})$ is defined as

$$g_0 := h_0,\ g_i := h_i - h_{i-1},\ 1 \leq i \leq \left\lfloor \frac{d}{2} \right\rfloor. \tag{4}$$

The Dehn–Sommerville relations (Dehn [29], Sommerville [60], see also [35, Ch. 9])

$$h_i = h_{d-i} \tag{5}$$

assert that for a simplicial polytope only half of the f-, resp. h-vector is needed to describe the entire one – and this explains why the g-vector is only defined for $i \leq \lfloor d/2 \rfloor$. For $d = 4$ the g-vector reads:

$$g_0 = 1, \tag{6}$$
$$g_1 = f_0 - 5, \tag{7}$$
$$g_2 = f_1 - 4f_0 + 10. \tag{8}$$

In general we get

$$g_j = f_{j-1} + \sum_{i=0}^{j-1} (-1)^{j-i} \binom{d+1-i}{d+1-j} f_{i-1}. \tag{9}$$

Due to Stanley [65] we can also define h- and g-vectors for general polytopes, but this is a bit more involved than in the simplicial case. These vectors are also called *toric* h-, resp. g-vector and denoted by h^{tor}, resp. g^{tor}. We will follow Bayer [12] to give Stanley's combinatorial formula [65]. Let P be a d-polytope. Define $h^{tor}(P,t) := \sum_{i=0}^{d} h_i^{tor} t^{d-i}$ and $g^{tor}(P,t) := \sum_{i=0}^{\lfloor d/2 \rfloor} g_i^{tor} t^i$, where $h^{tor}(P) := (h_0^{tor}, \ldots, h_d^{tor})$, $g^{tor}(P) := (g_0^{tor}, \ldots, g_{\lfloor d/2 \rfloor}^{tor})$ are the h^{tor}-, resp. g^{tor}-vector of P. Furthermore, we have the recursion

$$g^{tor}(\emptyset, t) = h^{tor}(\emptyset, t) = 1, \tag{10}$$

$$h^{tor}(P,t) = \sum_{G \subsetneq P \text{ face}} g^{tor}(G,t)(t-1)^{d-1-\dim G}, \tag{11}$$

and the definition $g_0^{tor} := h_0^{tor}$, $g_i^{tor} := h_i^{tor} - h_{i-1}^{tor}$ for $1 \leq i \leq \lfloor d/2 \rfloor$. Bayer [12] gives also a nice algorithm to compute the h^{tor}-vector, but we will just state those values (of the g^{tor}-vector) that are most important for this thesis (here, the dimension is $d = 4$):

$$g_0^{tor} = 1, \tag{12}$$

$$g_1^{tor} = f_0 - 5, \tag{13}$$

$$g_2^{tor} = f_1 + f_{02} - 3f_2 - 4f_0 + 10. \tag{14}$$

Note that if P is simplicial, the definitions of the h- and g-vectors coincide with those of the h^{tor}- and g^{tor}-vectors.

Now that we have defined these combinatorial invariants for polytopes, the next question is which values these can obtain. Let us denote by $\mathcal{P}^d$ ($\mathcal{P}_s^d$) the set of all combinatorial types of (simplicial) d-polytopes. The set of all f-vectors of d-polytopes is denoted by $f(\mathcal{P}^d)$, and that of flag-vectors by $f\ell(\mathcal{P}^d)$. Their analogues for the simplicial case are then $f(\mathcal{P}_s^d)$, resp. $f\ell(\mathcal{P}_s^d)$. The first interesting case $d = 3$ was solved by Steinitz [66] in 1906 (cf. Theorem 1.1.1), but already for $d = 4$ we are somehow stuck. In 1987 Bayer [11] collected the known inequalities for $f\ell(\mathcal{P}^4)$ (see Theorems 1.1.14 and 1.1.15). However, there are flag-vectors that satisfy all known inequalities, but that do not occur for any 4-polytope (cf. Höppner & Ziegler [39]).

In the case of simplicial (and dually simple) d-polytopes things look different: In 1971 McMullen [49] stated the g-Conjecture, which was later proven by Billera & Lee [15, 16] and Stanley [61]. This conjecture, now known as the g-Theorem (cf. Theorem 1.1.10), describes the set $f(\mathcal{P}_s^d) \cong f\ell(\mathcal{P}_s^d)$ entirely.

Viewed from a combinatorial perspective, another interesting question concerns the relation of the sets of f- and flag-vectors of (simplicial) d-polytopes compared to those of more general objects such as strongly regular $(d-1)$-spheres, Eulerian $(d-1)$-manifolds, and strongly connected Eulerian lattices of rank $(d+1)$.

A *strongly regular complex* is a pure finite regular CW complex with the intersection property (for an introduction to complexes see e.g. [18, Sec. 4.7], or [28]). If the underlying

space of the complex is a $(d-1)$-sphere, then we will call it *strongly regular* $(d-1)$*-sphere*. A cell complex is *regular* if all closed cells are homeomorphic to unit balls. A complex K has the *intersection property* if the intersection of any two cells of K is again a cell of K (i.e. any two cells intersect in a common face). A *cellular manifold* is a strongly regular complex, where the underlying space is a connected manifold and where all vertex links are PL-spheres. For convenience, we simply call it *manifold* as well. If the manifold satisfies Euler's equation (1), then we call it *Eulerian* (with the natural definition of f-vector; see also below). Clearly, every odd-dimensional $(d-1)$-manifold and every strongly regular $(d-1)$-sphere is an Eulerian (cellular) $(d-1)$-manifold.

Now, let M be an Eulerian $(d-1)$-manifold, and L be the set of faces of M given as sets of vertices (including the empty face) together with the set containing all vertices of M. There is a natural partial order $<_L$ on L given by set-inclusion. Therefore, $(L, <_L)$ forms a *poset*, which is even a *lattice*. This lattice is called *face lattice* of M, analogous to the face lattice of a polytope. Since M is Eulerian, L is *Eulerian* as well (i.e. L is ranked and every interval has the same number of elements of even and odd rank). Moreover, by the connectedness of M it follows that every interval I of L of length $l(I) \geq 3$ has a connected *atom-coatom-graph*. In general, we will call a lattice with this property *strongly connected*. See Stanley [64] for more about posets and lattices. The following example motivates the notion of *strongly connected Eulerian lattices*.

Example. Let P be the face lattice of the d-simplex, d even, and construct a new Eulerian lattice Q of rank $(d+1)$ by taking n copies of P and identifying the least, resp. largest elements ($\hat{0}$ and $\hat{1}$) with each other. Since the atom-coatom-graph of Q is not connected, Q is not the face lattice of an Eulerian manifold. Moreover, this example works in all even dimensions, resp. odd rank. The case of two triangles is shown in Figure 1. Since the product of two Eulerian lattices is again an Eulerian lattice, we can easily construct Eulerian lattices from this example where the atom-coatom-graph of the entire lattice is connected, but not that of every interval. Still these lattices cannot appear as face lattices of Eulerian manifolds.

Analogous to the polytope case, define $\mathcal{S}^{d-1}$, $\mathcal{M}_e^{d-1}$, resp. $\mathcal{EL}^{d+1}$ to be the sets of all combinatorial types of strongly regular $(d-1)$-spheres, Eulerian $(d-1)$-manifolds, resp. strongly connected Eulerian lattices of rank $d+1$. If we add an "s" as in $\mathcal{S}_s^{d-1}$ the respective set is restricted to the simplicial case. By the face structures of spheres and manifolds, and via the ranks of the elements of an Eulerian lattice, we can naturally extend the notions of f-, and flag-vectors to strongly regular spheres, Eulerian manifolds and strongly connected Eulerian lattices. Again, the terms $f(\cdot)$ and $f\ell(\cdot)$ refer to the sets of f-, resp. flag-vectors of the respective set of objects. Since every polytope boundary is a sphere, which is in turn an Eulerian manifold, and the face lattice of every Eulerian manifold is an Eulerian lattice, it is clear that

$$f(\mathcal{P}^d) \subset f(\mathcal{S}^{d-1}) \subset f(\mathcal{M}_e^{d-1}) \subset f(\mathcal{EL}^{d+1}), \tag{15}$$

$$f\ell(\mathcal{P}^d) \subset f\ell(\mathcal{S}^{d-1}) \subset f\ell(\mathcal{M}_e^{d-1}) \subset f\ell(\mathcal{EL}^{d+1}). \tag{16}$$

The question is now whether these inclusions are strict or not (resp. in which cases). Clearly, for $d \leq 2$ there is no difference. A first non-trivial result is Steinitz' Theorem (Theorem 0.1) from which it follows that all strongly connected Eulerian lattices of rank 4 are face lattices of 3-polytopes, so equality in (15) for $d = 3$ follows.

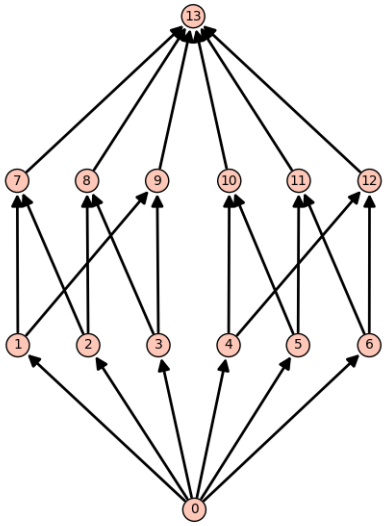

Figure 1: The Hasse diagram of the Eulerian lattice obtained by taking twice the face lattice of a triangle and identifying the $\hat{0}$, $\hat{1}$ resp. This lattice is not strongly connected.

Theorem 0.1 (Steinitz' Theorem [67], see also [76])**.** *A graph G is the graph of a 3-polytope if and only if it is simple, planar and 3-connected.*

Proposition 0.2. *Every strongly connected Eulerian lattice of length $d+1=4$ is the face lattice of a d-polytope.*

Proof. Let E be such an Eulerian lattice. Then E is the face lattice of a connected 2-manifold of Euler characteristic 2, so we have a sphere. The lattice property corresponds to what Steinitz calls "Bedingung des Nichtübergreifens" [68, S. 179], which is exactly the intersection property for a 2-sphere. Steinitz's Theorem 0.1 yields that every such 2-sphere can be realized as a convex polytope. □

In the simplicial case (15) refers to the g-Conjecture for spheres (cf. Section 1.1), which is still open. For general polytopes and spheres and higher dimensions there are a lot of results showing that $\mathcal{P}^d \subsetneqq \mathcal{S}^{d-1}$ for all $d \geq 4$. For example there are the upper bounds on the numbers of combinatorial types of polytopes by Goodman & Pollack [33] as well as lower bounds for spheres by Kalai [41], Pfeifle & Ziegler [57], and Nevo, Santos & Wilson [52]. However, all the non-polytopal 3-spheres studied so far turned out to have an f-vector (and even flag-vector) that is also the f- (resp. flag-) vector of some 4-polytope: This was observed repeatedly, from the first examples (such as the Brückner and Barnette spheres, see e.g. Grünbaum [35, Sect. 11.5] and Ewald [31, Sect. III.4]) to the systematic enumerations of spheres with few vertices by Altshuler et al. (see e.g. [6] as well as [35, p. 96b]).

The aim of this thesis is to study the relations in (15) in more detail. For this Section 1.1 collects known results on the shape of the sets of f- and flag-vectors of polytopes, spheres and lattices. Furthermore, we will show there that simplicial strongly connected Eulerian lattices

are Eulerian pseudomanifolds (Theorem 1.1.7), with which we can extend the Lower Bound Theorem (Theorem 1.1.3). Moreover, we will show that every strongly connected Eulerian lattices of rank 5 is the face lattice of some Eulerian 3-manifold (Theorem 1.1.8). Finally, we will show there that strongly connected Eulerian lattices and Eulerian manifolds have strictly larger sets of f-vectors than polytopes (Theorem 1.1.11). In Section 1.2 we will show new bounds for the sets of f- and flag-vectors of certain classes of strongly regular 3-spheres (Propositions 1.2.3 and 1.2.7, Lemma 1.2.8, and Corollary 1.2.9). Chapter 2 reports on some new enumeration results of 3-manifolds, which we will use in Chapter 3 to prove the main results of this thesis:

Theorem 3.1. *There is a unique strongly regular 3-sphere, but no convex 4-polytope, with flag-vector given by*

$$(f_0, f_1, f_2, f_3; f_{02}) = (12, 40, 40, 12; 120).$$

Thus, the set of flag-vectors of 4-polytopes is a proper subset of the set of flag-vectors of strongly regular 3-spheres:

$$f\ell(\mathcal{P}^4) \subsetneqq f\ell(\mathcal{S}^3).$$

Moreover, this is the smallest 2s2s flag-vector for which there is a 3-sphere but no 4-polytope.

Theorem 3.2. *The set of f-vectors of 4-polytopes is a strict subset of that of f-vectors of strongly regular 3-spheres:*

$$f(\mathcal{P}^4) \subsetneqq f(\mathcal{S}^3).$$

In particular, there are strongly regular 3-spheres, but no 4-polytopes, with the f-vectors

$$\begin{aligned}
(f_0, f_1, f_2, f_3) &= (10, 32, 33, 11),\\
(f_0, f_1, f_2, f_3) &= (11, 33, 32, 10),\\
(f_0, f_1, f_2, f_3) &= (10, 33, 35, 12),\\
(f_0, f_1, f_2, f_3) &= (12, 35, 33, 10),\\
(f_0, f_1, f_2, f_3) &= (11, 35, 35, 11),\\
(f_0, f_1, f_2, f_3) &= (12, 40, 40, 12).
\end{aligned}$$

Moreover, the f-vectors $(10, 32, 33, 11)$ and $(11, 33, 32, 10)$ are the smallest ones with that property and there are no other f-vectors of size $\mathrm{size}(f) := f_0 + f_3 - 10 \leq 12$ for which there are 3-spheres but no 4-polytopes other than the listed ones.

Finally, Section 3.3 reports on connections between the different notions of realisability of a sphere (cf. Conjecture 2) and proves some non-implications (Proposition 3.3.3).

Chapter 1

Bounds on f- and flag-vectors

1.1 Sets of f- and flag-vectors

In this section we will collect known results on the shape of the sets of f- and flag-vectors of polytopes, spheres and lattices. Furthermore, we will show that simplicial strongly connected Eulerian lattices are Eulerian pseudomanifolds (Theorem 1.1.7), with which we can extend the lower Bound Theorem (Theorem 1.1.3). Moreover, we will show that every strongly connected Eulerian lattice of rank 5 is the face lattice of some Eulerian 3-manifold (Theorem 1.1.8). Finally, we will show that strongly connected Eulerian lattices and Eulerian manifolds have strictly larger sets of f-vectors than polytopes (Theorem 1.1.11).

Theorem 1.1.1 (Steinitz [66], see also [35], [68])**.** *The set of f-vectors of 3-polytopes is the set of all integer points in a 2-dimensional cone with apex at $(4, 6, 4)$, the f-vector of the tetrahedron:*

$$f(\mathcal{P}^3) = \{(f_0, f_1, f_2) \in \mathbb{Z}^3 \,:\, f_0 - f_1 + f_2 = 2,\ f_0 \leq 2f_2 - 4,\ f_2 \leq 2f_0 - 4\}.$$

Moreover, the set of f-vectors of simplicial 3-polytopes is given by

$$f(\mathcal{P}_s^3) = \{((f_0, f_1, f_2) \in \mathbb{Z}^3 \,:\, f_1 = 3f_0 - 6,\ f_2 = 2f_0 - 4,\ f_0 \geq 4\}.$$

Since the flag-vector of a 3-polytope is completely determined by the f-vector, this result extends to $f\ell(\mathcal{P}^3)$. Moreover, Steinitz' Theorem (Theorem 0.1) implies that $\mathcal{S}^2 = \mathcal{P}^3$, and so Theorem 1.1.1 also describes $f(\mathcal{S}^2)$ and $f\ell(\mathcal{S}^2)$.

For higher dimensions the question of how to completely describe $f(\mathcal{P}^d)$, $f\ell(\mathcal{P}^d)$, $f(\mathcal{S}^{d-1})$, and $f\ell(\mathcal{S}^{d-1})$ remains open. However, there are some partial results. Grünbaum [35, p. 131] showed that the Euler equation (1) is the only linear equation that holds for all f-vectors of d-polytopes, so the affine hull of $f(\mathcal{P}^d)$ is a hyperplane in $\mathbb{R}^d$ ($\dim \operatorname{aff}(f(\mathcal{P}^d)) = d - 1$). For simplicial polytopes the Dehn–Sommerville relations (see Equation 5) imply that only half of the f-vector is needed to know the entire f-vector ($\dim \operatorname{aff}(f(\mathcal{P}_s^d)) = \lfloor d/2 \rfloor$). These relations were generalised by Bayer & Billera to the flag-vectors of Eulerian posets:

Theorem 1.1.2 (Generalised Dehn–Sommerville relations, Bayer & Billera [13]). *For all rank $d+1$ Eulerian posets, the flag-vector satisfies*

$$\sum_{j=i+1}^{k-1} (-1)^{j-i-1} f_{S\cup\{j\}} = (1-(-1)^{k-i-1}) f_S$$

whenever $i,k \in S \cup \{-1,d\}$ with $i \leq k-2$ and $S \cap \{i+1,\ldots,k-1\} = \emptyset$.

In particular, for $d=4$ we get:

(i) $S=\{3\}$, $i=-1$, $k=3$, $f_{03}-f_{13}+f_{23}=2f_3$;

(ii) $S=\{2\}$, $i=-1$, $k=2$, $f_{02}-f_{12}=0$;

(iii) $S=\{2\}$, $i=2$, $k=4$, $f_{23}=2f_2$;

(iv) $S=\{1\}$, $i=1$, $k=4$, $f_{12}-f_{13}=0$;

(v) $S=\{0\}$, $i=0$, $k=4$, $f_{01}-f_{02}+f_{03}=2f_0$.

From the theorem follows $\dim \mathrm{aff}(f\ell(\mathcal{P}^d)) = F_d - 1$ [13], where F_d is the d-th *Fibonacci number* ($F_1=F_2=1, F_n=F_{n-1}+F_{n-2}$). In particular, $\dim \mathrm{aff}(f\ell(\mathcal{P}^4)) = 4$.

Another important result on the f-vectors of simplicial polytopes is Barnette's Lower Bound Theorem (LBT) [7, 9], which gives lower bounds on the numbers f_i of i-faces in terms of the number of vertices f_0. Billera & Lee [15] extended this theorem in proving that equality holds for $d>3$ if and only if the polytope is stacked, and Kalai [40] and Tay [70] extended it to pseudomanifolds. A *pseudomanifold* is a pure simplicial complex, where every ridge is in exactly two facets and which dual graph (with the facets as vertices and ridges as edges) is connected (see [14] for more).

Theorem 1.1.3 (Lower Bound Theorem (LBT)). *For a $(d-1)$-dimensional pseudomanifold Δ with $f_0=n$ vertices,*

$$f_i(\Delta) \geq \begin{cases} \binom{d}{i} n - \binom{d+1}{i+1} i & \text{for } 1 \leq i \leq d-2 \\ (d-1)n - (d-2)(d+1) & \text{for } i = d-1. \end{cases}$$

Moreover, for $d \geq 4$ equality holds if and only if Δ is isomorphic to the boundary complex of a stacked d-polytope.

A textbook version of the proof for polytopes can be found in [27] and a different approach via shellings was used by Blind & Blind [19]. The LBT was later generalised to all d-polytopes as well as to triangulated manifolds with boundary.

Theorem 1.1.4 (Generalised LBT (gLBT), Kalai [40], Whiteley [73]). *For a d-polytope P with $f_0=n$ vertices*

$$f_1(P) + \sum_{k\geq 3} (k-3) f_2^k(P) \geq dn - \binom{d+1}{2},$$

where $f_2^k(P)$ denotes the number of k-gonal 2-faces of P.

Remark. In terms of the toric g-vector, Theorem 1.1.4 states that $g_2^{tor} \geq 0$ for all polytopes.

Theorem 1.1.5 (LBT for triangulated manifolds with boundary, Björner [17] and Kalai [40])**.** *For a triangulated $(d-1)$-dimensional manifold Δ, $d \geq 3$, with n_b boundary vertices and n_i interior vertices,*

$$f_i(\Delta) \geq \begin{cases} \binom{d-1}{i} n_b + \binom{d}{i} n_i - \binom{d}{i+1} k & \text{for } 1 \leq i \leq d-2 \\ n_b + (d-1) n_i - (d-1) & \text{for } i = d-1. \end{cases}$$

Moreover, if equality holds for some i, then Δ is a stacked $(d-1)$-ball.

We will now extend the LBT to simplicial strongly connected Eulerian lattices by showing that they are actually pseudomanifolds. For this define the *dual graph* of an Eulerian lattice L to be the graph with vertices corresponding to the elements of corank 1 and corank 2, and edges between two vertices if one of the two is larger than the other in L.

Proposition 1.1.6. *Let L be a finite, graded, strongly connected lattice. Then the dual graph of L is connected.*

Proof. Let $x, y \in L$ be of corank 1 or of corank 2, and let $x = x_0, \ldots, x_n = y$ be a path P in the Hasse diagram of L, where for all $i = 0, \ldots, n$ either x_i covers x_{i-1} or the other way around and no x_i is $\hat{0}$, or $\hat{1}$. Such a path exists by L being strongly connected. Now, let x_k be of least rank in the path. If x_k has corank 2, we are done. Otherwise, consider the interval $[x_k, \hat{1}]$ in L. Its atom-coatom-graph is connected, hence there is a path P' in $[x_k, \hat{1}]$ from x_{k-1} to x_{k+1} avoiding x_k and $\hat{1}$. Substitution of x_k in P by P' will give a new path from x to y with one element less of rank $\mathrm{rk}(x_k)$. Iteration yields the desired result, namely a path from x to y using only coatoms and elements of corank 2, which will translate to a path between x and y in the dual graph. □

Theorem 1.1.7. *Let L be a strongly connected Eulerian lattice of rank $d+1$ and let $L - \{\hat{1}\}$ be simplicial. Then L is the face lattice of an Eulerian pseudomanifold of dimension $d-1$.*

Proof. Construct the simplicial complex Δ as follows:

(i) the atoms of L are the vertices of Δ;

(ii) an element $x \in L - \{\hat{1}\}$ corresponds to the face of Δ with the vertices corresponding to the atoms smaller than x.

Since $L - \{\hat{1}\}$ is simplicial, this gives a simplicial complex. Since L is graded, Δ is pure, and, since L is Eulerian, every ridge of Δ is in exactly 2 facets. By Proposition 1.1.6 the dual graph of Δ is connected.

Now, consider the link of some element $x \in L - \{\hat{1}\}$. This is $\mathrm{lk}(x) = \{y \in L : y \geq x\} = [x, \hat{1}]$. Since L is Eulerian, this has the right Euler characteristic. Therefore, L is also Eulerian as a pseudomanifold. □

This theorem would extend to the non-simplicial case, if we would not have defined pseudomanifolds to be simplicial. Since strongly connected Eulerian lattices of rank $d \leq 4$ are face lattices of polytopes (cf. Steinitz' Theorem 0.1), we directly get:

Theorem 1.1.8. *If L is a strongly connected Eulerian lattice of rank 5, then L is the face lattice of an Eulerian 3-manifold.*

A somehow "dual" result to the Lower Bound Theorem is the Upper Bound Theorem (UBT) for polytopes due to McMullen [48]. A textbook version of this can be found in Ziegler [76]. Stanley [62] extended the UBT to spheres, and Novik [53] showed that it holds for Eulerian manifolds.

Theorem 1.1.9 (Upper Bound Theorem (UBT) for Eulerian manifolds)**.** *The f-vector of an Eulerian $(d-1)$-manifold M with $f_0(M) = n$ vertices is componentwise bounded from above by the f-vector of a d-dimensional cyclic polytope on n vertices:*

$$f_k(M) \leq f_k(Cyc_d(n)),\ 1 \leq k \leq d.$$

A remarkable combination of the Lower and Upper Bound Theorem is McMullen's g-Conjecture [49], which characterises the sets of f-vectors of simplicial d-polytopes $f(\mathcal{P}_s^d)$ for all d. This conjecture was later proven by Billera & Lee [15, 16] and Stanley [61]. For more details and explanation of M-sequences, see Ziegler [76, Lecture 8].

Theorem 1.1.10 (g-Theorem)**.** *A sequence $g = (g_0, g_1, \ldots, g_{\lfloor \frac{d}{2} \rfloor})$ is the g-vector of a simplicial d-polytope if and only if it is an M-sequence. In particular, this means*

$$g_i \geq 0.$$

Remark. Combining LBT and UBT one can see directly that the g-Theorem also holds for d-spheres with $d \leq 5$. For simplicial spheres of dimension $d-1 \geq 5$ the g-Conjecture is still open. For an overview over the different g-Conjectures see [69].

Theorem 1.1.11. *The f-vector spaces of d-polytopes and $(d-1)$-manifolds do not coincide for $d \geq 6$. In particular, there are simplicial (Eulerian) $(d-1)$-manifolds that violate the g-Theorem for all $d \geq 6$:*

$$f(\mathcal{P}_s^d) \subsetneqq f(\mathcal{M}_s^{d-1}).$$

For $d \geq 6$ even:

$$f(\mathcal{P}_s^d) \subsetneqq f(\mathcal{M}_{e,s}^{d-1}).$$

For $d \geq 7$ odd:

$$f(\mathcal{P}^d) \subsetneqq f(\mathcal{EL}^{d+1}).$$

Proof. Frank Lutz' thesis [45, pp. 56-58] lists a triangulation of the 5-manifold $S^4 \times S^1$ with the f-vector $(13, 78, 195, 260, 195, 65)$. The corresponding g-vector is $(1, 6, 21, -35)$. Hence, it violates the g-Theorem, and so this f-vector cannot occur for a 6-polytope. In general we can construct such manifolds as follows ($d \geq 6$):

(i) Take a stacked d-polytope P that has two facets F_0, F_1 s.t. no facet of P intersects both of them; the g-vector is then $g(P) = (1, f_0(P) - d - 1, 0, \ldots, 0)$;

(ii) Identify F_0 with F_1 to obtain a $(d-1)$-manifold M with f-vector given by $f_i(M) = f_i(P) - f_i(\Delta^{d-1})$, $0 \leq i \leq d-2$, and $f_{d-1}(M) = f_{d-1}(P) - 2$, where Δ^{d-1} is the $(d-1)$-simplex; with (9) we then get for $k \neq 1$:

$$\begin{aligned} g_k(M) &= g_k(P) - f_{k-1}(\Delta^{d-1}) - \sum_{i=0}^{k-1}(-1)^{k-i}\binom{d+1-i}{d+1-k} f_{i-1}(\Delta^{d-1}) \\ &= g_k(P) - \binom{d}{k} - \sum_{i=1}^{k}(-1)^{k-i}\binom{d+1-i}{k-i}\binom{d}{i}. \end{aligned}$$

Since

$$g_k(\Delta^{d-1}) = \binom{d}{k} + \sum_{i=0}^{k}(-1)^{k-i}\binom{d+1-i}{k-i}\binom{d}{i} = \delta_{0,k}$$

we get for $k \geq 1$

$$g_k(M) = g_k(P) + (-1)^k\binom{d+1}{k},$$

which is negative for odd $k \geq 3$.

Since in even dimensions the resulting manifold M is Eulerian, we get the first two claims. For the third one take the product of the face lattice of M with the 2-element Eulerian lattice (suspension with a point) to get a manifold M' with $f_i(M') = f_i(M) + f_{i-1}(M)$, $i \geq 1$:

$$\begin{aligned} g_k(M') &= f_{k-1}(M) + f_{k-2}(M) + \sum_{i=0}^{k-1}(-1)^{k-i}\binom{d+2-i}{d+2-k} f_{i-1} \\ &\quad + \sum_{i=1}^{k-1}(-1)^{k-i}\binom{d+2-i}{d+2-k} f_{i-2} \\ &= f_{k-1}(M) + \sum_{i=0}^{k-1}(-1)^{k-i}\binom{d+2-i}{d+2-k} f_{i-1} + \sum_{i=0}^{k-1}(-1)^{k-i+1}\binom{d+2-(i+1)}{d+2-k} f_{i-1} \\ &= f_{k-1}(M) + \sum_{i=0}^{k-1}(-1)^{k-i}\left(\binom{d+2-i}{d+2-k} - \binom{d+1-i}{d+2-k}\right) f_{i-1} \\ &= f_{k-1}(M) + \sum_{i=0}^{k-1}(-1)^{k-i}\binom{d+1-i}{d+1-k} f_{i-1} \\ &= g_k(M). \end{aligned}$$

Again, for odd $k \geq 3$ this is negative if M is as constructed above. □

Besides extending the g-Theorem to simplicial spheres or other manifolds, one can also ask for a similar result on the toric g-vectors for general polytopes. Theorem 1.1.4 ensures the non-negativity of g_2^{tor}. For the general case, this is due to Karu [42]:

Theorem 1.1.12. *The toric g-vector of a d-polytope P is non-negative, i.e.*

$$g_k^{tor}(P) \geq 0 \quad \forall\, 0 \leq k \leq \left\lfloor \frac{d}{2} \right\rfloor .$$

Again one can ask for generalisations to spheres. See Section 1.2 for some results in the case $d = 4$.

Another direction in which there has been some progress, is to restrict the dimension d. The following theorems give restrictions to the sets of f-, and flag-vectors of 4-polytopes, strongly regular 3-spheres, and Eulerian 3-manifolds. With the generalised Dehn–Sommerville relations we can write:

$$f_2 = f_3 + f_1 - f_0,\ f_{01} = 2f_1,\ f_{02} = f_{12} = f_{13} = f_{03} - 2f_0 + 2f_1. \tag{1.1}$$

Therefore, instead of taking the entire flag-vector it suffices to consider the values f_0, f_1, f_2, and f_{02}, or f_0, f_1, f_3, and f_{03}. Note that the precise choice of necessary parameters is rather arbitrary. Since depending on the context, each of the two has its advantages, we will give some of the inequalities for flag-vectors in both versions.

Theorem 1.1.13 (Barnette [8])**.** *Let M be an Eulerian 3-manifold with f-vector $f(M) = (f_0, f_1, f_2, f_3)$. Then,*

(i) $f_2 \leq \frac{3}{2}f_3 + \frac{1}{4}(f_0^2 - 3f_0)$,

(ii) $f_2 \leq \frac{1}{2}f_0 + \frac{1}{4}(f_3^2 + f_3)$,

(iii) $f_2 \geq \frac{1}{8}(3f_0 - 10 + 15f_3)$,

(iv) $f_2 \geq \frac{1}{8}(7f_0 - 10 + 11f_3)$.

Remark. Barnette proved this theorem for 4-polytopes, but he uses only the fact that all facets are 3-polytopes, and a lower bound inequality for simplicial polytopes that Walkup [71] actually proved for all simplicial 3-manifolds. Therefore, this theorem is valid for all 3-manifolds.

Theorem 1.1.14 (Bayer [11])**.** *Flag-vectors $(f_0, f_1, f_2, f_3; f_{02}, f_{03})$ of 4-polytopes satisfy*

(i) $f_{02} - 3f_2 \geq 0$, *resp.* $-f_0 + f_1 + 3f_3 - f_{03} \leq 0$,

(ii) $f_{02} - 3f_1 \geq 0$, *resp.* $2f_0 + f_1 - f_{03} \leq 0$,

(iii) $f_{02} - 3f_2 + f_1 - 4f_0 \geq 10$, *resp.* $3f_0 + 3f_3 - f_{03} \leq 10$,

(iv) $6f_1 - 6f_0 - f_{02} \geq 0$, *resp.* $4f_0 - 4f_1 + f_{03} \leq 0$,

(v) $f_0 \geq 5$,

(vi) $f_3 \geq 5$.

Except for (iii)*, all of these are knwon to hold for strongly connected Eulerian lattices of rank* 5 *in general.*

In addition to the linear inequalities, Bayer also proved some quadratic constraints. She proved them for 4-polytopes, but again the reasoning is valid for strongly connected Eulerian lattices of rank 5 in general.

Theorem 1.1.15 (Bayer [11])**.** *Flag-vectors* $(f_0, f_1, f_2, f_3; f_{02}, f_{03})$ *of strongly connected Eulerian lattices of rank* 5 *satisfy*

(i) $2(f_{02} - 3f_2) + f_1 \leq \binom{f_0}{2}$, *resp.* $2f_0 - f_1 - 6f_3 + 2f_{03} \leq \binom{f_0}{2}$,

(ii) $2(f_{02} - 3f_1) + f_1 \leq \binom{f_2 - f_1 + f_0}{2}$, *resp.* $-5f_0 - f_1 + f_3 + 2f_{03} \leq \binom{f_3}{2}$,

(iii) $f_{02} - 4f_2 + 3f_1 - 2f_0 \leq \binom{f_0}{2}$, *resp.* $f_1 - 4f_3 + f_{03} \leq \binom{f_0}{2}$,

(iv) $f_{02} + f_2 - 2f_1 - 2f_0 \leq \binom{f_2 - f_1 + f_0}{2}$, *resp.* $-5f_0 + f_1 + f_3 + f_{03} \leq \binom{f_3}{2}$.

Additionally, there are some (families of) inequalities that are proven only for the sets of flag-vectors of 4-polytopes (the proof relies at some point on the geometry).

Theorem 1.1.16 (Ling [43])**.** *Flag-vectors* $(f_0, f_1, f_2; f_{02})$ *of* 4*-polytopes satisfy*

(i) $(k-1)f_{02} - \binom{k+1}{2}f_2 + f_1 + 1 \leq \binom{f_0}{2}$, *for any integer* $k \geq 4$,

(ii) $f_{02}(f_{02} - 3f_2) \leq 2f_2\left[\binom{f_0}{2} - f_1\right]$,

(iii) $2(k-1)f_{02} - k(k+1)f_2 + (k^2 - 3k + 4)f_1 - k(k-3)f_0 \leq 4\binom{f_0}{2}$, *for any integer* k,

(iv) $(2f_{02} - f_2 - 3f_1 + 3f_0)^2 - 8(f_2 - f_1 + f_0)\left[2\binom{f_0}{2} + f_{02} - 2f_1\right] \leq (f_2 - f_1 + f_0)^2$,

as well as the dual versions of these.

All of these theorems restrict the set of f-, resp. flag-vectors further: While there are 171 potential f-vectors with $f_0 = 9$ satisfying the trivial bounds ($\binom{f_0}{2} \geq f_1 \geq 2f_0$, $f_2 \geq 2f_3$, $\binom{f_0}{4} \geq f_3 \geq 5$), Theorem 1.1.13 reduces their number to 81. Out of these, one can construct 4692 potential flag-vectors satisfying the trivial bounds ($4f_3 \leq f_{03} \leq (f_0 - 1)f_3$). With Theorems 1.1.14 and 1.1.15 there are only 392 potential flag-vectors with $f_0 = 9$ left. Theorem 1.1.16 reduces their number to 365. However, not all vectors that satisfy all these inequalities are f-, resp. flag-vectors of 4-polytopes (see Höppner & Ziegler [39] and Chapters 2, 3).

1.2 Fatness and Complexity

Two parameters that might help to distinguish between the f-vector spaces of 4-polytopes and 3-spheres are the *fatness*, which has been introduced by Eppstein et. al. [30] and Ziegler [74], and the *complexity*. We will use the definitions from Ziegler [74].

Definition 1.2.1. The *fatness* of a strongly regular 3-sphere is

$$F(S) := \frac{f_1(S) + f_2(S) - 20}{f_0(S) + f_3(S) - 10}. \tag{1.2}$$

The *complexity* of a strongly regular 3-sphere is

$$C(S) := \frac{f_{03}(S) - 20}{f_0(S) + f_3(S) - 10}. \tag{1.3}$$

Note that the constants in both parameters are designed in a way that for the simplex, both the numerator and denominator vanish. Therefore, they are not defined for the 4-simplex or its boundary.

Remark. Since the f-vector of the dual of a polytope or a strongly regular sphere is the reversed vector of the primal, the fatness and the complexity are invariant under taking duals.

The two parameters are linked via

$$C \leq 2F - 2, \; F \leq 2C - 2, \tag{1.4}$$

which follows from the generalised Dehn−Sommerville relations and the inequalities Theorem 1.1.14 (i) and (ii). Moreover, Theorem 1.1.14 (iii) is equivalent to

$$C \geq 3, \tag{1.5}$$

which holds for 4-polytopes and simple resp. simplicial strongly regular 3-spheres. With (1.4) it easily follows that

$$F \geq \frac{5}{2}. \tag{1.6}$$

Therefore, finding a 3-sphere with complexity $C < 3$ or fatness $F < \frac{5}{2}$ would result in an example of a flag-, resp. f-vector that occurs for spheres but not for polytopes. In the remainder of this section we will see some negative results in this direction, meaning that for some classes of 3-spheres a lower bound on the fatness of $F \geq \frac{5}{2}$ will be established. But let us start with some easier bounds.

Proposition 1.2.2 (Trivial Bound)**.** *For any strongly regular 3-sphere S the complexity and fatness satisfy*

$$C(S) \geq 2, \quad F(S) \geq 2.$$

Proof. This follows directly from $f_1 \geq 2f_0$, $f_2 \geq 2f_3$, and the first inequality in (1.4). These are obtained since any 2-face is contained in exactly two facets, and both facets contain at least four 2-faces. On the other hand, any edge contains two vertices and any vertex is contained in at least four edges. □

Remark. Equality holds if and only if the sphere S is both simple and simplicial, which is the case only if S is the boundary of the 4-simplex, for which the complexity and fatness are not defined, so $C, F > 2$.

Remark. We obtain another quite simple lower bound for large values of f_{03}. If S is a 3-sphere with $f_{03} \geq 6 \cdot \max\{f_0, f_3\}$, then Theorem 1.1.14 (iii) holds trivially. Therefore, we have $C \geq 3$ and $F \geq \frac{5}{2}$ for S. With the same argument, we can also show that $C \geq 3$ and $F \geq \frac{5}{2}$ hold if $\min\{f_0, f_3\} \leq 10$ and $f_{03} \geq 5 \cdot \max\{f_0, f_3\}$. However, there are potential flag-vectors with few vertices that do not satisfy these conditions.

For spheres with $f_0 \leq 8$ (or, dually, $f_3 \leq 8$) there are classifications by Barnette [10] and Altshuler & Steinberg [5, 6]. With these, we can easily verify that Theorem 1.1.14 (iii) holds for strongly regular 3-spheres with $f_0 \leq 8$[1].

With Theorem 1.1.13 we can prove a lower bound on the fatness of some 3-spheres.

Proposition 1.2.3. *Let S be a strongly regular 3-sphere with f-vector $f(S) = (f_0, f_1, f_2, f_3)$. If $3f_0 - f_3 \leq 20$ (or, dually, $3f_3 - f_0 \leq 20$) then the fatness of S is*

$$F(S) \geq \frac{5}{2}.$$

Remark. Since we use in the proof only inequalities that hold for the f-vectors of all Eulerian 3-manifolds, this proposition would extend to 3-manifolds as well. However, we have not defined fatness in that context.

Proof. We will use $f_2 \geq \frac{1}{8}(3f_0 - 10 + 15f_3)$ from Theorem 1.1.13 (iii). So we can deduce

$$\begin{aligned}
3f_0 - f_3 &\leq 20 \\
\Rightarrow 20f_0 + 20f_3 - 200 &\leq 14f_0 + 22f_3 - 180 \\
\Rightarrow 5(f_0 + f_3 - 10) &\leq 2(\frac{7}{4}f_0 + \frac{11}{4}f_3 - \frac{90}{4}) = 2(f_0 - f_3 - 20 + 2\frac{3f_0 - 10 + 15f_3}{8}) \\
\Rightarrow 5(f_0 + f_3 - 10) &\leq 2(f_0 + 2f_2 - f_3 - 20) \\
\Rightarrow \frac{5}{2} &\leq \frac{f_0 + 2f_2 - f_3 - 20}{f_0 + f_3 - 10} = \frac{f_1 + f_2 - 20}{f_0 + f_3 - 10} = F(S).
\end{aligned}$$

The proof for the case $3f_3 - f_0 \leq 20$ follows from duality. □

In the following we will mainly consider *2-simple 2-simplicial* 3-spheres, which were first studied by Grünbaum [35].

Definition 1.2.4. A 3-sphere $S \subset \mathbb{R}^4$ is *2-simplicial* (*2-simple*) if all 2-faces are triangles (all edges are in precisely three facets). The sphere S is *2-simple 2-simplicial* (abbreviated with 2s2s) if it is both 2-simple and 2-simplicial.

Lemma 1.2.5 (see [75])**.** *Every 2s2s 3-sphere has a symmetric f-vector, that is $f_0 = f_3$ and $f_1 = f_2$.*

[1] The papers refer to enumerations of all strongly regular 3-spheres with 8 vertices. The potential flag-vectors with fewer vertices that violate the gLBT can be reduced to the case of 8 vertices by stacking.

Remark. Since every 2-face of a 2s2s 3-sphere S is a triangle, we have that $f_{02}(S) = 3f_2$, and since every edge is in exactly three facets, we get $f_{13}(S) = 3f_1$.

Proposition 1.2.6 (see [75])**.** *The flag-vector of a 3-sphere S satisfies the inequality*

$$2f_{03} \geq (f_1 + f_2) + 2(f_0 + f_3).$$

Moreover, equality holds if and only if S is 2s2s.

Proof. This inequality is equivalent to $F \leq 2C - 2$ from (1.4). The equality case follows from combining $f_0 = f_3$ and $f_1 = f_2$ for 2s2s 3-spheres and Theorem 1.1.14 (ii). □

With the lower bounds for simplicial spheres we can now show a lower bound on the fatness for 2-simplicial resp. 2-simple spheres.

Proposition 1.2.7. *Let S be a strongly regular 3-sphere with $f_{03} \leq 2f_2$, or dually with $f_{03} \leq 2f_1$. Then the fatness of S is*

$$F(S) \geq \frac{5}{2}.$$

In particular, this assumption holds if S is 2-simplicial and so $F(S) \geq \frac{5}{2}$ for strongly regular 2-simplicial 3-spheres and for strongly regular 2-simple 3-spheres.

Proof. If S is a 2-simplicial 3-sphere, then $f_{02} = 3f_2$ and by Theorem 1.1.14 (iv) we get that $f_{03} \leq \frac{2}{3}f_{02}$. Therefore, $f_{03} \leq 2f_2$.

Let us subdivide S to get a simplicial sphere, for which the above theorem gives a lower bound on the fatness. To do this, we triangulate every 2-face without introducing new vertices. This adds $f_{02} - 3f_2$ edges and substitutes the 2-faces by $f_{02} - 2f_2$ triangles. In a second step, we add a vertex inside every cell and cone to the boundary. This adds f_3 vertices, f_{03} edges and $f_{13} + f_{123} - 3f_{23} = 3f_{02} - 6f_2$ triangles and replaces the cells by $f_{023} - 2f_{23} = 2f_{02} - 4f_2$ tetrahedra.

Denote the new simplicial sphere by S'. It has the f-vector

$$\begin{aligned} f(S') &= (f_0(S'), f_1(S'), f_2(S'), f_3(S')) \\ &= (f_0 + f_3, f_1 + f_{02} - 3f_2 + f_{03}, 4f_{02} - 8f_2, 2f_{02} - 4f_2) \\ &= (f_0 + f_3, f_0 - 3f_3 + 2f_{03}, -8f_3 + 4f_{03}, -4f_3 + 2f_{03}). \end{aligned} \tag{1.7}$$

Therefore, the fatness of S' is

$$\frac{5}{2} \leq F(S') = \frac{f_0 - 11f_3 + 6f_{03} - 20}{f_0 - 3f_3 + 2f_{03} - 10}. \tag{1.8}$$

Since $f_{03} \leq 2f_2 = 2f_1 + 2f_3 - 2f_0$, we have

$$\begin{aligned} & 5(f_0 - 3f_3 + 2f_{03} - 10) \leq 2(f_0 - 11f_3 + 6f_{03} - 20) \\ \Leftrightarrow \quad & 3f_0 + 7f_3 - 2f_{03} - 10 \leq 0 && (1.9) \\ \Rightarrow \quad & -4f_0 + 4f_1 + 4f_3 \geq 2f_{03} \geq 3f_0 + 7f_3 - 10 \\ \Rightarrow \quad & 4f_1 \geq 7f_0 + 3f_3 - 10. && (1.10) \end{aligned}$$

Adding Euler's equation $-2f_1 + 2f_2 = -2f_0 + 2f_3$ we get

$$2f_1 + 2f_2 - 40 \geq 5f_0 + 5f_3 - 50. \tag{1.11}$$

Therefore,

$$F(S) = \frac{f_1 + f_2 - 20}{f_0 + f_3 - 10} \geq \frac{5}{2}. \tag{1.12}$$

□

However, this does not prove that a 2-simplicial, resp. 2-simple strongly regular 3-sphere S satisfies the same bounds on flag-vectors as 4-polytopes, since the complexity $C(S)$ could still be less than three, which would violate the g-Theorem. Indeed, there are 28 potential flag-vectors of 2-simplicial strongly regular 3-spheres with $f_0 = 9$ and $C < 3$. With $f_0 = 10$ there are 45 such vectors. The following lemma reduces the number of potential flag-vectors to 12 resp. 20. Table 1.1 lists all potential flag-vectors of 3-spheres with $C < 3$ but still satisfying the following lemma. The results of Chapter 2 give that there are no spheres with these flag-vectors.

Lemma 1.2.8. *Let S be a strongly regular 3-sphere with flag-vector $fl(S) = (f_0, f_1, f_3; f_{03})$.*

(i) *If $f_{03} \leq 4f_3 + 2$, then $C(S) \geq 3$.*

(ii) *Let $l \leq f_{02} - 3f_2 = f_0 - f_1 - 3f_3 + f_{03}$ denote the number of non-triangular 2-faces, then*

$$2f_0 + f_1 + 10f_3 - 3f_{03} \leq 3f_0 + 7f_3 - 2f_{03} - l \leq 10.$$

Proof. If $f_{03} = 4f_3$, then S is simplicial, for which the statement is already proven. So, let $f_{03} = 4f_3 + 1$. Thus, there is exactly one facet F which has five vertices whereas all other facets have four vertices. Therefore, all facets except F are tetrahedra and S is 2-simplicial. Since the only simplicial 3-polytope with five vertices is the bipyramid over the triangle, F has these combinatorics and we can triangulate it by introducing one 2-face, replacing F by two tetrahedra. The new sphere has complexity $C \geq 3$ and hence,

$$3(f_0 + f_3 + 1 - 10) \leq 4(f_3 + 1) - 20 \;\Rightarrow\; 3f_0 + 3f_3 - f_{03} \leq 10,$$

which is equivalent to $C(S) \geq 3$.

Next, let $f_{03} = 4f_3 + 2$. In this case, S has either one or two non-tetrahedral facets, which are then a simplicial 3-polytope with six vertices, two bipyramids over the triangle, or two pyramids over the square. In the first case S has a facet that is a 3-polytope with f-vector $(6, 12, 8)$. If we insert a vertex inside this facet and cone to the boundary, we get a simplicial 3-sphere S' with flag-vector $(f_0 + 1, f_1 + 6, f_3 + 7; f_{03} + 21)$. Hence, by $C(S') \geq 3$, we get $10 \geq 3(f_0 + 1) + 3(f_3 + 6) - (f_{03} + 21) = 3f_0 + 3f_3 - f_{03}$, so $C(S) \geq 3$.
In the second case, triangulating the two bipyramids via introducing one new triangle in each one will increase f_3 by two and f_{03} by six, giving a simplicial sphere for which $C \geq 3$ is known. So, $10 \geq 3f_0 + 3(f_3 + 2) - (f_{03} + 6) = 3f_0 + 3f_3 - f_{03}$.
In the third case, note that the two pyramids have the quadrilateral in common, so removing both pyramids from S will give a simplicial ball with $f_3 - 2$ tetrahedra, $n_b = 6$ boundary

$f_0 = 9$			
$(9, 19, 19, 9; 37)$	$(9, 20, 21, 10; 41)$	$(9, 21, 23, 11; 45)$	$(9, 22, 25, 12; 49)$
$(9, 19, 19, 9; 38)$	$(9, 20, 21, 10; 42)$	$(9, 21, 23, 11; 46)$	$(9, 23, 26, 12; 50)$
$(9, 20, 20, 9; 38)$	$(9, 21, 21, 9; 39)$	$(9, 22, 23, 10; 43)$	$(9, 23, 27, 13; 53)$
$(9, 20, 20, 9; 39)$	$(9, 21, 22, 10; 42)$	$(9, 22, 24, 11; 46)$	$(9, 24, 29, 14; 57)$
$f_0 = 10$			
$(10, 21, 21, 10; 41)$	$(10, 22, 23, 11; 47)$	$(10, 24, 24, 10; 44)$	$(10, 25, 27, 12; 51)$
$(10, 21, 21, 10; 42)$	$(10, 23, 23, 10; 43)$	$(10, 24, 25, 11; 47)$	$(10, 25, 28, 13; 54)$
$(10, 21, 21, 10; 43)$	$(10, 23, 23, 10; 44)$	$(10, 24, 26, 12; 50)$	$(10, 25, 29, 14; 57)$
$(10, 22, 22, 10; 42)$	$(10, 23, 24, 11; 46)$	$(10, 24, 26, 12; 51)$	$(10, 25, 29, 14; 58)$
$(10, 22, 22, 10; 43)$	$(10, 23, 24, 11; 47)$	$(10, 24, 27, 13; 53)$	$(10, 26, 29, 13; 55)$
$(10, 22, 23, 11; 45)$	$(10, 23, 25, 12; 49)$	$(10, 24, 27, 13; 54)$	$(10, 26, 30, 14; 58)$
$(10, 22, 23, 11; 46)$	$(10, 23, 25, 12; 50)$	$(10, 25, 26, 11; 48)$	$(10, 26, 31, 15; 61)$

Table 1.1: This is a complete list of potential flag-vectors $(f_0, f_1, f_2, f_3; f_{03})$ of 3-spheres with nine and ten vertices that violate Theorem 1.1.14 (iii), but satisfy Lemma 1.2.8. The results of Chapter 2 give that there are no spheres with these flag-vectors.

vertices and $n_i = f_0 - 6$ interior vertices. So, with Theorem 1.1.5 (the ball is not stacked) we have $f_3 - 2 > 6 + 3(f_0 - 6) - 3 = 3f_0 - 15$, so $3f_0 \leq f_3 + 12$. With $f_{03} = 4f_3 + 2$ it follows that

$$3f_0 + 3f_3 - f_{03} \leq 4f_3 + 12 - 4f_3 - 2 = 10,$$

which shows $C(S) \geq 3$.

For the general case, let $F_1, \ldots, F_k, T_{k+1}, \ldots, T_{f_3}$ be the facets of S, where the F_i's are not tetrahedra, but the T_j's are. Let us triangulate the F_i's by introducing a vertex inside every non-triangular 2-face and connecting it to all vertices of this 2-face to get a simplicial F_i' with $f_0(F_i) + l_i$ vertices and $2f_0(F_i) + 2l_i - 4$ 2-faces. Next, we add a vertex in the interior of each F_i and cone to the boundary. This adds $l + k$ vertices and replaces the k facets $F_1, \ldots, F_k$ by $2\sum_{i=1}^{k}(f_0(F_i) + l_i - 4)$ tetrahedra. Since $n = f_{03} - 4f_3$ is the number of vertex-facet-incidences that S has more than a simplicial sphere with the same number of facets, the sum of the vertices of the F_i's is $\sum_{i=1}^{k} f_0(F_i) = 4k + n$. Moreover, the sum of all non-triangular 2-faces of the F_i's is $\sum_{i=1}^{k} l_i = 2l$ by double-counting. Therefore, the triangulated sphere S' has $f_0(S') = f_0 + k + l$ vertices and $f_3(S') = f_3 + 3k + 4l + 2n$ facets. Again, with the gLBT for simplicial spheres, we get that

$$\begin{aligned} 10 &\geq 3f_0(S') + 3f_3(S') - f_{03}(S') \\ &= 3(f_0 + k + l) + 3(f_3 + 3k + 4l + 2n) - (4f_3 + 12k + 16l + 8n) \\ &= 3f_0 + 3f_3 - f_{03} - l - n. \end{aligned}$$

Finally, with $l \leq f_0 - f_1 - 3f_3 + f_{03}$ and $n = f_{03} - 4f_3$ we get $2f_0 + f_1 + 10f_3 - 3f_{03} \leq 3f_0 + 7f_3 - 2f_{03} - l$. □

Table 1.2 shows the fatness and complexity for (classes of) 2s2s 3-spheres that are described in the literature. The data from this table suggests the following conjecture:

Source, description	$(f_0, f_1; f_{03})$	F	C
simplex	$(5, 10; 20)$		
hypersimplex	$(10, 30; 50)$	4	3
glued hypersimplex	$(14, 48; 76)$	$4\frac{2}{9}$	$3\frac{1}{9}$
24-cell	$(24, 96; 144)$	$4\frac{10}{19}$	$3\frac{5}{19}$
[34] 720-cell	$(720, 3600; 5040)$	$4\frac{142}{143}$	$3\frac{53}{143}$
[30]	$(54n - 30, 252n - 156; 360n - 216)$	$4\frac{16}{17}$	$3\frac{1}{3}$
[56]	$(10 + 4n, 30 + 18n; 50 + 26n)$	$4\frac{1}{2}$	$3\frac{1}{4}$
[55] W_9	$(9, 26; 44)$	4	3
[55] W_{10}	$(10, 30; 50)$	4	3
[55] P_{11}	$(11, 34; 56)$	4	3
[55] $\mathcal{I}^2(\mathcal{I}^1(P_9; S)^n)^m$	$(9 + 4n + 5m, 26 + 16n + 20m;$ $44 + 24n + 30m)$	4	3
[55] $\mathcal{I}^2(\mathcal{I}^1(P_{10}; S)^n)^m$	$(10 + 4n + 5m, 30 + 16n + 20m;$ $50 + 24n + 30m)$	4	3
[55] $\mathcal{I}^2(\mathcal{I}^1(P_{11}; S)^n)^m$	$(11 + 4n + 5m, 34 + 16n + 20m;$ $56 + 24n + 30m)$	4	3
[72], Sec. 2.1; W_{12}^{39}	$(12, 39; 63)$	$4\frac{1}{7}$	$3\frac{1}{14}$
[72], Fig. 3.40; W_{12}^{40}	$(12, 40; 64)$	$4\frac{2}{7}$	$3\frac{1}{7}$

Table 1.2: This table shows the flag-vectors of some 2s2s 3-spheres and their fatness and complexity (for families of examples only the limits are shown).

Conjecture 1. *The fatness of 2s2s 3-spheres other than the boundary of the simplex is bounded from below by $F \geq 4$.*

If this conjecture holds, then $C \geq 3$ would hold for 2s2s 3-spheres as well. In the remainder of this Section we will prove a partial result.

Corollary 1.2.9. *A 2s2s 3-sphere S other than the simplex has fatness*

$$F(S) \geq 3.$$

Proof. The proof follows directly from Proposition 1.2.13 and Theorem 1.2.16 below. □

For the proof of this theorem, we will need the notion of pseudo-balls, since we will show it for these first, and then extend the result to 2s2s 3-spheres.

Definition 1.2.10. A *pseudo-ball* B is a 3-dimensional strongly regular cell complex, where no ridge is in three or more facets, with a specified vertex v_0, and a facet ordering $F_1, F_2, \ldots, F_k$ so that the intermediate complexes $B^j := \bigcup_{i=1}^{j} F_i$ for $1 \leq j \leq k$ satisfy:

(i) There is $r \geq 4$ such that B^r is homeomorphic to the 3-dimensional ball, v_0 is in the interior of B^r, and v_0 is the intersection of the facets $F_1, \ldots, F_r$;

(ii) The intersection $F_{j+1} \cap B^j$ is 2-dimensional and does not coincide with ∂F_{j+1} for $1 \leq j \leq k-1$.

Note that in this definition the last property of part (i) implies that v_0 is the only interior vertex of B^r, and that part (ii) implies that pseudo-balls are strongly connected.

Definition 1.2.11. A pseudo-ball B is called *2s2s* if:

(i) The facets $F_1, \ldots, F_k$ of B have the combinatorics of simplicial 3-polytopes;

(ii) Each edge e is in at most three facets and the facets containing an edge e intersect pairwise in distinct 2-dimensional faces.

Definition 1.2.12. The *extended flag-vector* of a 2s2s-pseudo-ball is

$$f = (f_0, f_1, f_2, f_3; f_{03}, f_{13}, f_{23}; f_0^r, f_1^{r1}, f_1^{r2}, f_2^r), \tag{1.13}$$

where f_0^r are the boundary vertices, f_1^{r1}, f_1^{r2} are the boundary edges in one, respectively two 3-cells, and f_2^r are the boundary triangles. Here, *boundary* refers to the subcomplex consisting of the triangles which are in exactly one 3-cell, and their faces. The faces not on the boundary are called *interior* faces.

Define the *fatness* of a 2s2s-pseudo-ball B other than $\partial\Delta \setminus F$ (the boundary of the simplex without one facet) as

$$F(B) := \frac{f_1(B) + f_2(B) - \frac{2}{3} f_1^{r1}(B) - 20}{f_0(B) + f_3(B) - 9}. \tag{1.14}$$

The following proposition shows the connection between pseudo-balls and 3-spheres, which gives the motivation to look at the fatness of pseudo-balls.

Proposition 1.2.13. *Let S be a strongly regular 3-sphere and $F \subset S$ a facet. Then $S \setminus F$ is a pseudo-ball. If S is 2s2s other than the boundary of the 4-simplex, then also $S \setminus F$ is 2s2s and has fatness $F(S \setminus F) = F(S)$.*

Proof. First, check the conditions of the pseudo-ball definition. Since S is a strongly regular 3-sphere, all ridges of S are in exactly two facets. To get the facet ordering, proceed in reverse order:

- If (i) of the definition is satisfied for $k = r$, one is done;
- Otherwise there is an interior vertex v_0 and a facet F_j not containing v_0 but with a 2-face on the boundary; remove F_j and iterate with $B' = B - F_j$.

The first condition guarantees that Definition 1.2.10 (ii) is satisfied for $1 \leq j \leq r$: Since B^r is strongly connected, it can be labelled appropriately by finding a spanning tree in its dual graph and deleting and labelling a leaf in any step from r to 1.

The fatness of $S \setminus F$ coincides with the fatness of S in the case that S is 2s2s other than $\partial\Delta$ as $f_1^{r1}(S \setminus F) = 0$ and $f_3(S \setminus F) = f_3(S) - 1$. □

Now, let us examine the structure of 2s2s-pseudo-balls a bit more in detail.

Lemma 1.2.14. *Let B be a 2s2s-pseudo-ball. If, additionally, B is simplicial (every facet is a simplex), then $B = \partial\Delta \setminus F$.*

Proof. Let $F_1, \ldots, F_k$ be the facet ordering of B, and let $r \geq 4$ be such that B^r is homeomorphic to the 3-ball with $\bigcap_{i=1}^{r} F_i = v_0$. Now, since all F_i's are tetrahedra, only three among $F_2, \ldots, F_r$ can intersect F_1 in a facet, call them $F_{i_1}, F_{i_2}, F_{i_3}$. On the other hand, since B is 2s2s, every edge is in at most three facets, so the F_{i_j} have to intersect pairwise in a facet, too. But then these four facets already form a 3-ball, which is combinatorically the boundary of the simplex without one facet. Therefore, $r = 4$ and all boundary edges of B^r are of type $r2$ (contained in two facets). Hence, B cannot have other facets than $F_1, \ldots, F_4$, so $B = B^4 = \partial\Delta \setminus F$. □

Lemma 1.2.15. *Let B be a 2s2s-pseudo-ball with facet ordering $F_1, \ldots, F_k$.*

(i) *The intersection $A^c := F_{j+1} \cap B^j$ has only pure 0- and 2- dimensional components for all $j = 1, \ldots, k-1$.*

(ii) *The edges in the boundary of the 2-dimensional components of A^c are of type $r1$ in B^j (i.e. contained in exactly one facet).*

(iii) *Denote by* $A := \overline{\partial F_{j+1} \setminus A^c}$ *the part of the boundary of* F_{j+1} *which is also part of the boundary of* B^{j+1}. *Then,*

$$f_1(\operatorname{int} A) = f_0(\operatorname{int} A) + f_2(\operatorname{int} A) - l,$$
$$f_2(\operatorname{int} A) = f_1(\partial A) - 2l + 2f_0(\operatorname{int} A),$$
$$f_1(\partial A) \geq 3l,$$

where l *is the number of components of* $\operatorname{int} A$.

Proof. Every edge of the boundary of B^j is either of type r1 or of type r2, since B is 2s2s. If an edge e of type r2 is in the intersection A^c, then F_{j+1} has to intersect both facets of B^j that contain e in a 2-face according to Definition 1.2.10 (ii). Therefore, e is in the interior of some 2-dimensional component of A^c. If, in turn, e is of the type r1, then, again by Definition 1.2.10 (ii), F_{j+1} has to intersect the facet of B^j which contains e in a 2-face. Hence, e is in the boundary of some 2-dimensional component of A^c, which proves part (i) of the statement.

The second part follows from the fact that the argument for edges of type r1 can be reversed in the sense that an edge in the boundary of some 2-dimensional component of A^c is only contained in one 2-face of A^c and so cannot be of type r2 in B^j.

For the third part assume that $\operatorname{int} A$ has only one component. Otherwise do the same argumentation for every component and sum up. Note that $A^c \neq \partial F_{j+1}$ and therefore $\dim(A) = 2$. Hence, $f_1(\partial A) \geq 3$. Moreover, since

$$f_0(\operatorname{int} A) = f_0(F_{j+1}) - \sum_{\substack{C \subset A^c \\ \text{2-dim. comp.}}} f_0(C) - \sharp\text{0-dimensional components}$$

and additional components of A^c only increase the number of egdes and 2-faces in the interior of A without increasing the number of vertices there, we may assume that the number of components of A^c is 1. Now, proceed by induction on $n = f_0(\operatorname{int} A)$, the number of interior vertices of A. If $n = 0$, then, since A is triangulated,

$$f_1(\operatorname{int} A) = 0 + f_2(\operatorname{int} A) - 1 = f_0(\operatorname{int} A) + f_2(\operatorname{int} A) - 1$$

and

$$f_2(\operatorname{int} A) = f_1(\partial A) - 2 = f_1(\partial A) - 2 + 2f_0(\operatorname{int} A).$$

So, assume that the statement is true for $n \leq k$ for some $k \in \mathbb{N}$ and let $f_0(\operatorname{int} A) = k+1$. Pick some interior vertex $v \in A$. Its link is a polygon whose vertices are exactly the neighbours of v, since A is triangulated. We can remove v from A and triangulate the polygon without new vertices which will reduce the number of vertices by one, the number of edges by three and the number of triangles by two. Moreover, since A was triangulated before, this is still regular. Therefore, the induction hypothesis applies to the new complex, and we get

$$f_2(\operatorname{int} A) = f_1(\partial A) - 2 + 2k + 2 = f_1(\partial A) - 2 + 2f_0(\operatorname{int} A),$$
$$f_1(\operatorname{int} A) = k + f_1(\partial A) - 2 + 2k - 1 + 3 = f_0(\operatorname{int} A) + f_2(\operatorname{int} A) - 1.$$

This completes the proof of the lemma. □

Theorem 1.2.16. *Let B be a 2s2s-pseudo-ball other than $\partial\Delta \setminus F$. Then*

$$F(B) \geq 3.$$

Proof. We will proceed by induction on the number k of facets of B, but we will start with $B^r = \bigcup_{i=1}^r F_i$, which contains exactly one interior vertex $v_0 = \bigcap_{i=1}^r F_i$.

Since B^r is a 2s2s-pseudo-ball, every F_i has the combinatorics of a simplicial 3-polytope, and thus $f(F_i) = (n_i, 3n_i - 6, 2n_i - 4)$. Denote by $f_1^{int}(B^r)$ the number of interior edges and by $f_2^{int}(B^r)$ the number of interior triangles of B^r.

The number $f_0(B^r)$ of vertices of B^r is the sum over all vertices of the cells $F_1, \ldots, F_r$, where we count the interior vertex r times and the other endpoints of the interior edges three times. Hence,

$$f_0(B^r) = \sum_{i=1}^{r} n_i - (r-1) - 2f_1^{int}(B^r). \tag{1.15}$$

The number $f_1(B^r)$ of edges of B^r is the sum over all edges of the cells $F_1, \ldots, F_r$, where we counted the interior edges three times and the boundary edges that are in two cells two times. Thus,

$$f_1(B^r) = 3\sum_{i=1}^{r} n_i - 6r - 2f_1^{int}(B^r) - f_1^{r2}(B^r). \tag{1.16}$$

The number $f_2(B^r)$ of 2-faces of B^r is the sum over all 2-faces of the cells $F_1, \ldots, F_r$, where we counted the interior triangles twice. Therefore,

$$f_2(B^r) = 2\sum_{i=1}^{r} n_i - 4r - f_2^{int}(B^r). \tag{1.17}$$

Furthermore, $f_1(B^r) = f_1^{int}(B^r) + f_1^{r1}(B^r) + f_1^{r2}(B^r)$ and, hence,

$$f_1^{r1}(B^r) = f_1(B^r) - f_1^{int}(B^r) - f_1^{r2}(B^r). \tag{1.18}$$

By construction of B^r every interior triangle has exactly one edge on the boundary and so we have that

$$f_1^{r2}(B^r) = f_2^{int}(B^r). \tag{1.19}$$

To calculate $f_1^{int}(B^r)$ and $f_2^{int}(B^r)$ let us intersect B^r with a small sphere around v_0. This results in a polytopal sphere with $v = f_1^{int}(B^r)$ vertices, $e = f_2^{int}(B^r)$ edges and $f = r$ 2-faces. Since all interior edges of B^r have degree 3, all vertices of the polytopal sphere have degree 3. Thus, $3v = 2e$. Moreover, from the Euler equation $v - e + f = 2$ we get

$$f_2^{int}(B^r) = e = 3r - 6; \quad f_1^{int}(B^r) = v = 2r - 4. \tag{1.20}$$

Therefore, with $N := \sum_{i=1}^r n_i$, we get that

$$\begin{aligned}
f_0(B^r) &\overset{(1.15)}{=} N - r + 1 - 2f_1^{int} &&\overset{(1.20)}{=} N - 5r + 9;\\
f_1(B^r) &\overset{(1.16)}{=} 3N - 6r - 2f_1^{int} - f_1^{r2} &&\overset{(1.19),(1.20)}{=} 3N - 13r + 14;\\
f_2(B^r) &\overset{(1.17)}{=} 2N - 4r - f_2^{int} &&\overset{(1.20)}{=} 2N - 7r + 6;\\
f_1^{r1}(B^r) &\overset{(1.18)}{=} f_1 - f_1^{int} - f_1^{r2} &&\overset{(1.19),(1.20),(1.21)}{=} 3N - 18r + 24;\\
f_3(B^r) &= &&\quad r.
\end{aligned} \tag{1.21}$$

Hence, the fatness of B^r is

$$F(B^r) = \frac{f_1(B^r) + f_2(B^r) - \frac{2}{3}f_1^{r1}(B^r) - 20}{f_0(B^r) + f_3(B^r) - 9} = \frac{3N - 8r - 16}{N - 4r}. \tag{1.22}$$

Since the F_i are simplicial 3-polytopes, they have $n_i \geq 4$ vertices. But if all F_i were tetrahedra, then B^r would be the simplex without one facet by Lemma 1.2.14. Thus, $N \geq 4r + 1$ and so the fatness in (1.22) is defined. Since $r \geq 4$, we get that

$$F(B^r) \overset{(1.22)}{=} \frac{3N - 8r - 16}{N - 4r} \geq \frac{3N - 12r}{N - 4r} \geq 3.$$

For the induction step, we assume that the theorem holds for all 2s2s-pseudo-balls with $k \geq r$ facets and at least one interior vertex. Let $B^{k+1} = \bigcup_{i=1}^{k+1} F_i$ be a 2s2s-pseudo-ball, such that $B^k = \bigcup_{i=1}^{k} F_i$ is also a 2s2s-pseudo-ball with interior vertex. Denote with $A := \partial B^{k+1} \cap F_{k+1} \subset \partial F_{k+1}$ the part of F_{k+1} which is on the boundary of B^{k+1}. Thus, the faces in the "interior" of A and the cell itself are the ones added. Moreover, the edges in ∂A are of type $r1$ in B^k and of type $r2$ in B^{k+1} by Lemma 1.2.15. Therefore,

$$\begin{aligned}
f_0(B^{k+1}) &= f_0(B^k) + f_0(\operatorname{int} A),\\
f_1(B^{k+1}) &= f_1(B^k) + f_1(\operatorname{int} A),\\
f_2(B^{k+1}) &= f_2(B^k) + f_2(\operatorname{int} A),\\
f_1^{r1}(B^{k+1}) &= f_1^{r1}(B^k) - f_1(\partial A) + f_1(\operatorname{int} A);\\
f_3(B^{k+1}) &= f_3(B^k) + 1.
\end{aligned}$$

Hence, the fatness of B^{k+1} is

$$F(B^{k+1}) = \frac{f_1(B^k) + f_2(B^k) - \frac{2}{3}f_1^{r1}(B^k) - 20 + \frac{1}{3}f_1(\operatorname{int} A) + f_2(\operatorname{int} A) + \frac{2}{3}f_1(\partial A)}{f_0(B^k) + f_3(B^k) - 9 + f_0(\operatorname{int} A) + 1}.$$

Since the fatness of B^k is bounded by $F(B^k) \geq 3$, it suffices to show

$$\frac{\frac{1}{3}f_1(\operatorname{int} A) + f_2(\operatorname{int} A) + \frac{2}{3}f_1(\partial A)}{f_0(\operatorname{int} A) + 1} \geq 3$$

in order to prove $F(B^{k+1}) \geq 3$. But with Lemma 1.2.15 (iii) this follows immediately. □

Chapter 2

Enumeration of manifolds

In the previous chapter we focused on the inequalities that hold for the sets of f-, resp. flag-vectors, in order to find differences in those sets for polytopes, spheres and Eulerian lattices. Another approach, which we will be following here to find differences between the sets $f(\mathcal{P}^4)$ and $f(\mathcal{S}^3)$, resp. $f\ell(\mathcal{P}^4)$ and $f\ell(\mathcal{S}^3)$, is to exhibit an f-, resp. flag-vector for which there are strongly regular 3-spheres, but no 4-polytopes. In order to do so, we need to enumerate all strongly regular 3-spheres for a given f-, resp. flag-vector. This has been done already extensively for simplicial 4-polytopes, 3-spheres, and 3-manifolds with up to 10 vertices (cf. [36], [10], [2], [3], [4], [45], [46]), for general 4-polytopes and 3-spheres with up to eight vertices (cf. [5], [6]), and for 2s2s 4-polytopes with up to 11 vertices [72]. In this chapter we will enumerate Eulerian 3-manifolds and strongly regular 3-spheres for certain f-vectors with up to 12 vertices.

As seen in Section 1.2, 2s2s 3-spheres (and 2s2s 3-manifolds) have a lot of combinatorial properties which make them easier to handle than general spheres. Therefore, in Section 2.1 we will describe an algorithm to enumerate 2s2s 3-manifolds with a given flag-vector. With this algorithm we will be able to show $f\ell(\mathcal{P}^4) \subsetneqq f\ell(\mathcal{S}^3)$ (Theorem 3.1). In order to extend this result to $f(\mathcal{P}^4) \subsetneqq f(\mathcal{S}^3)$ (Theorem 3.2), we introduce in Section 2.2 another algorithm that enumerates all Eulerian 3-manifolds with a given f-vector. Although the latter produces much stronger results and can also be used to reproduce the results of the former, both algorithms are presented here, since both have their particular strengths: The flag-vector algorithm is much faster than the f-vector algorithm and, therefore, one can obtain results for higher numbers of vertices f_0. The f-vector algorithm is stronger, since it enables results regarding the sets of f-vectors.

In this chapter we will only describe the enumeration algorithms and results of the enumeration, while in Chapter 3 we will give constructions and/or coordinates for polytopes with various f-vectors, as well as we will proof non-polytopality of all spheres with some special f-, resp. flag-vectors.

(0, 8, 4, 0)	(1, 6, 5, 0)	(2, 4, 6, 0)	(3, 2, 7, 0)	(4, 0, 8, 0)	(0, 9, 2, 1)
(1, 7, 3, 1)	(2, 5, 4, 1)	(3, 3, 5, 1)	(4, 1, 6, 1)	(0, 10, 0, 2)	(1, 8, 1, 2)
(2, 6, 2, 2)	(3, 4, 3, 2)	(4, 2, 4, 2)	(5, 0, 5, 2)	(2, 7, 0, 3)	(3, 5, 1, 3)
(4, 3, 2, 3)	(5, 1, 3, 3)	(4, 4, 0, 4)	(5, 2, 1, 4)	(6, 0, 2, 4)	(6, 1, 0, 5)

Table 2.1: These are the 24 p^3-vectors $(p_4^3, p_5^3, p_6^3, p_7^3)$ that are possible for the flag-vector $(12, 40, 40, 12; 120)$.

2.1 Enumeration of 2s2s 3-manifolds with given flag-vector

This section is based on the paper [25], which is joint work with Günter M. Ziegler.

Definition 2.1.1. Let M be a strongly regular 3-manifold. Then the *p^3-vector* of M is $p^3(M) = (p_4^3, p_5^3, \ldots)$, where p_i^3 is the number of facets of M with i vertices.

This is the analog to the p-vector for 3-polytopes as introduced by Grünbaum [35]. For any 2s2s 3-manifold with flag-vector $(f_0, f_1, f_2, f_3; f_{02}) = (n, m, m, n; 3m)$ we have $p_i^3 = 0$ for $2i - 4 \geq n$, since a facet with i vertices is a simplicial 3-polytope with $2i - 4$ faces and thus has $2i - 4$ neighboring facets. In particular, for $n = 12$ we have $p_i^3 = 0$ for $i > 7$. Moreover, we have $\sum_{i \geq 4} p_i^3 = n$, and $\sum_{i \geq 4} (2i - 4) p_i^3 = 2m$. This yields a finite list of possible p^3-vectors for any possible flag-vector. For example, for $f = (12, 40, 40, 12; 120)$ there are exactly 24 potential p^3-vectors that satisfy the three restrictions (see Table 2.1). To enumerate all 2s2s 3-manifolds with n vertices, note that

$$2n \leq m \leq \tfrac{1}{4} n(n + 3). \tag{2.1}$$

While the lower bound is trivial, the upper bound stems from Theorem 1.1.15 (iii).

The idea of the algorithm to enumerate all Eulerian 3-manifolds with a given flag-vector is to produce, for each p^3-vector, one symmetry representative of each set system (of vertex sets of facets) that has the given p^3-vector and is proper w.r.t. the given flag-vector. The resulting lists are then checked whether they correspond to Eulerian lattices of rank 5.

Definition 2.1.2. Let $f = (f_0, f_1, f_2, f_3; f_{02}) = (n, m, m, n; 3m)$ be a flag-vector. A set system F is *proper* w.r.t. f, if it consists of exactly f_3 sets F_i (facets) that are subsets of the vertex set $\{0, \ldots, f_0 - 1\}$, and if it satisfies the following conditions:

(I1) The intersection of two facets contains either 0, 1 or 3 vertices,

(I2) The intersection of three facets contains at most 2 vertices, and

(I3) The intersection of four facets contains at most 1 vertex.

This is where we crucially use the fact that we are looking for 2s2s 3-manifolds only: every edge is in preciseley three facets that intersect pairwise in triangles, whence the intersection of two facets cannot contain preciseley two vertices, and four facets cannot intersect in a

common egde; moreover, since all 2-faces are triangles, the intersection of two facets contains at most three vertices.

The idea for symmetry breaking in the enumeration, and thus to avoid producing re-labelled versions of the same facet lists too often, is to fix the labelling of the vertex set of a facet of maximal size i, and then to assign step by step vertex labels to a remaining facet of maximal size. It turns out that in some cases even more facets can be fixed, or at least up to re-labelling have only few distinct possibilities. In particular this is the case whenever $p_7^3 > 0$.

Algorithm 2.1.3. *find_facet_lists*(p^3)
INPUT: p^3*-vector* $(p_4^3, p_5^3, \ldots)$
OUTPUT: *the facet lists of all 2s2s rank* 5 *Eulerian lattices with this* p^3*-vector, up to combinatorial equivalence*

(1) $ind = \max\{i : p_i^3 > 0\}$

(2) $facet\_list = \{\{0, \ldots, \text{ind} - 1\}\}$

(3) $p_{ind}^3 = p_{ind}^3 - 1$

(4) $ind = \max\{i : p_i^3 > 0\}$

(5) $stc = \{\{i_0, \ldots, i_{ind}\} : \textit{intersection with facet\_list is proper}\}$

(6) *for* $F \in stc$*:*

(7) $\quad facet\_list = facet\_list \cup \{F\}$

(8) $\quad$ recursively add new facets to the list

(9) $\quad$ evaluate whenever there are enough $(= \sum p_i^3)$ facets in the list

(10) $\quad facet\_list = facet\_list \setminus \{F\}$

After roughly two weeks of computation on standard linux workstations with altogether 45 kernels, the algorithm had enumerated all connected 2s2s rank 5 Eulerian lattices with up to 12 vertices. This produced exactly the face lattices of the spheres listed in Theorem 2.1.4, and thus proves that theorem as well as the second part of Theorem 3.1.

Theorem 2.1.4. *The following is a complete list of combinatorial types of* 2*-simple* 2*-simplicial strongly connected Eulerian lattices of rank* 5 *with at most* 12 *vertices.*

f_0	*name*	*flag vector*	*reference*	*(realisation as) polytope*
5	Δ_5	$(5, 10, 10, 5; 30)$		simplex
9	W_9	$(9, 26, 26, 9; 78)$	[72]	[72, Thm. 4.2.2]
10	W_{10}	$(10, 30, 30, 10; 90)$	[55, Sect. 4.1]	[55, Sect. 4.1]
	$\Delta_4(2)$	$(10, 30, 30, 10; 90)$	[35, p. 65]	hypersimplex $\Delta_4(2)$
	$\Delta_4(2)^*$	$(10, 30, 30, 10; 90)$		dual of $\Delta_4(2)$
11	P_{11}	$(11, 34, 34, 11; 102)$	[55, Sect. 4.1]	[55, Sect. 4.1]
12	W_{12}^{39}	$(12, 39, 39, 12; 117)$	[72, Tbl. 7.1 right]	[51, Sect. 4.2]
	W_{12}^{40}	$(12, 40, 40, 12; 120)$	[72, Tbl. 7.1 left]	no: Theorem 3.2.9

All of these are 3-spheres, and, except for the hypersimplex and its dual, are self-dual.

We refer to the works by Paffenholz and Werner [54, 55, 72] for information and data on 2s2s 4-polytopes with more than 12 vertices.

2.2 Enumeration of 3-manifolds with given f-vector

This section is based on the paper [26], which is joint work with Günter M. Ziegler. For the enumeration algorithm presented here, we will introduce some more notation and strengthen some known inequalities for Eulerian 3-manifolds for special cases. However, this is not needed in order to understand and implement the algorithm; only to speed it up.

2.2.1 Bayer's inequality

In [11] Bayer proved some inequalities that hold for the set of flag-vectors of Eulerian 3-manifolds $f\ell(\mathcal{M}^3_e)$ (see Theorems 1.1.14, 1.1.15), among which is

$$f_{02} - 4f_2 + 3f_1 - 2f_0 \leq \binom{f_0}{2}. \tag{2.2}$$

With this we get for an Eulerian 3-manifold with symmetric f-vector (n, m, m, n):

$$3m \leq f_{02} \leq \frac{n^2 + 3n}{2} + m. \tag{2.3}$$

In order to understand Bayer's proof and to sharpen her result, we need some notation.

Definition 2.2.1. Let F be a 3-polytope. Then $m_b(F)$ is the number of pairs of vertices contained in some 2-face of F, but not forming an edge of F (boundary non-edges), and $m_i(F)$ is the number of pairs of vertices not contained in the same 2-face of F (interior non-edges). Similarly, if M is an Eulerian 3-manifold, then $m_i(M)$ is the number of pairs of vertices not forming an edge of M, but not lying in a common facet of M.

The proof of (2.2) relies on the following lemma:

Lemma 2.2.2 ([11, Lemma 3])**.** *If F is a 3-polytope, then*

$$\frac{1}{2}m_b(F) + m_i(F) \geq \frac{1}{2}(f_2(F) - 4) + \frac{1}{2}(f_{02}(F) - 3f_2(F)). \tag{2.4}$$

A look into the proof of this lemma reveals that the inequalities are not tight, so we can strengthen the result a bit.

Lemma 2.2.3. *In the same notation as before we have for a 3-polytope F with $f_0(F) \geq 7$ and for the simplex*

$$\frac{1}{2}(m_b(F) + m_i(F) - f_{02}(F) + 3f_2(F)) \geq \frac{1}{2}(f_{02}(F) - 2f_2(F) - 4).$$

Proof. First, note that the inequality holds with equality for the simplex, since both sides are 0. For $f_0(F) \geq 7$ we follow Bayer's proof of Lemma 3 in [11] to obtain

$$m_i(F^s) \geq f_{02}(F) - 2f_2(F) - 4. \tag{2.5}$$

Here, F^s is a simplicial polytope obtained from F by pulling vertices. Moving back to F, we see that some of the edges from $m_i(F^s)$ move to $m_b(F)$ and that the $f_{02}(F) - 3f_2(F)$ edges that appeared in F^s to triangulate the 2-faces of F now are in $m_b(F)$. Therefore, $m_i(F^s) = m_i(F) + m_b(F) - f_{02}(F) + 3f_2(F)$. The claim follows. □

Moreover, going through the list of the nine combinatorial types of 3-polytopes with five or six vertices [35] gives that inequality (2.4) from Lemma 2.2.2 is tight for those with five vertices, while the left hand side is larger by one than the right hand side in the case of six vertices, except for the pyramid over the pentagon, where it is larger by 0.5.

With this stronger lemma we can now also strengthen Bayer's inequality (2.2).

Proposition 2.2.4. *Let M be an Eulerian 3-manifold with flag vector $(f_0, f_1, f_2, f_3; f_{02})$, then*

$$\begin{aligned} f_{02} - 4f_2 + 3f_1 - 2f_0 \quad \leq \quad & \binom{f_0}{2} - m_i(M) - \frac{1}{2} \sum_{\substack{F \text{ facet} \\ f_0(F) \geq 7}} (m_i(F) + f_{02}(F) - 3f_2(F)) \\ & - \#\text{facets with 6 vertices} + \frac{1}{2}\#\text{pyramids over pentagon}. \end{aligned}$$

Proof. Bayer showed in the proof of Theorem 1.1.15 (iii) that for every Eulerian 3-manifold M (she actually showed it for 4-polytopes, but her proof is valid in this more general context, since it only uses the intersection property and the fact that the faces have the combinatorics of polytopes)

$$f_{02}(M) - 4f_2(M) + 3f_1(M) - 2f_0(M) = f_1(M) + \frac{1}{2} \sum_{\substack{F \subset M \\ facet}} (f_{02}(F) - 2f_2(F) - 4). \tag{2.6}$$

Applying the two lemmas above and the observation that $\frac{1}{2}\sum_{\substack{F \subset M \\ facet}} m_b(F) = \sum_{\substack{G \subset M \\ ridge}} m_i(G)$ (half the number of missing boundary edges of the facets is the number of missing interior edges of the ridges) yields

$$\begin{aligned} f_{02}(M) - 4f_2(M) + 3f_1(M) - 2f_0(M) \quad \leq \quad & f_1(M) + \sum_{\substack{F \subset M \\ facet}} m_i(F) + \sum_{\substack{G \subset M \\ ridge}} m_i(G) + m_i(M) \\ & - m_i(M) - \frac{1}{2} \sum_{\substack{F \text{ facet} \\ f_0(F) \geq 7}} (m_i(F) + f_{02}(F) - 3f_2(F)) \\ & - \#\text{facets with 6 vertices} \\ & + \frac{1}{2}\#\text{pyramids over pentagon}. \end{aligned} \tag{2.7}$$

Note that the first line of the right hand side of this inequality is the sum of the number of edges of M, the number of missing interior edges of M, the number of missing interior edges of the facets of M, and the number of missing interior edges of the ridges of M. Hence, it is $\binom{f_0}{2}$, the number of possible edges of M. □

Now, by inserting the f-vector (n, m, m, n) into the inequality from Proposition 2.2.4, we can strengthen inequality (2.3) to

$$\begin{aligned} 3m \leq \sum_{\substack{G \subset M \\ ridge}} f_0(G) = f_{02}(M) \quad \leq \quad & \frac{n^2+3n}{2} + m - \frac{1}{2} \sum_{\substack{F \, facet \\ f_0(F) \geq 7}} (m_i(F) + f_{02}(F) - 3f_2(F)) \\ & - m_i(M) - \#\text{facets with 6 vertices} \\ & + \frac{1}{2} \#\text{pyramids over pentagon.} \end{aligned} \tag{2.8}$$

2.2.2 Excluding polygons and 3-polytopes as faces

In order to make the enumeration of all Eulerian 3-manifolds with a given f-vector faster, we want to exclude as many lower dimensional polytopes as faces as possible. Since for smaller numbers of vertices and edges, the enumeration is fast anyway (cf. Table 2.3), we will focus on the higher numbers in this section.

Proposition 2.2.5. *An Eulerian 3-manifold M with f-vector $(10, m, m, 10)$, $m \neq 25$, cannot have ridges (2-faces) with 8 or more vertices, or facets with nine vertices.*

Proof. The only possibility to have a facet with 9 vertices is that M is the boundary of the pyramid over this facet. In this case the facet would also have 9 2-faces due to the symmetry of the f-vector. Hence, the facet has 16 edges, and M has 25 edges. Since an 8-gon can only occur in a facet with at least nine vertices, these cannot occur in M either. □

Proposition 2.2.6. *An Eulerian 3-manifold M with f-vector $(11, m, m, 11)$, $m \geq 29$, cannot have facets with 10 or more vertices, or ridges (2-faces) with 8 or more vertices.*

Proof. An Eulerian 3-manifold M with symmetric f-vector and $n = 11$ vertices can only have a facet with 10 vertices if M is the boundary of the pyramid over this facet and this facet has itself 10 2-faces. Therefore, the facet has 18 edges according to Theorem 1.1.1, and M has $m = 28$ edges.

Such a manifold also cannot have a ridge with 8 vertices: since there cannot be a facet with more than 9 vertices, the two facets containing the 8-gon would be pyramids. Since this is also true in the dual, the two apices that are in at least 9 facets anyway would be in at most 9 facets as well. Hence, both are in an edge that is contained in all neighbours of their respective pyramid. In the dual this edge corresponds to an 8-gon, of which there can only be one by $f_0(M^*) = 11$. Therefore, the two apices are joined by an edge. Thus, every neighbour of one of the two pyramids would contain the edge between the two apices, and would be neighbouring the other pyramid too. Hence, there would only be 10 facets in total. □

Proposition 2.2.7. *An Eulerian 3-manifold M with f-vector $(12, m, m, 12)$, $m \geq 40$, cannot have facets with 10 or more vertices, or ridges (2-faces) with 8 or more vertices.*

Proof. We proceed case by case.

(i) k-gon with $k \geq 11$ and 3-polytope F with $f_0(F) \geq 12$: since $f_0(S) = 12$.

(ii) k-gon with $k = 9, 10$: since $f_0(S) = 12$, there are $\binom{12}{2} = 66$ potential edges in M, but already a 9-gon has $\binom{9}{2} - 9 = 27$ missing edges. Hence, $f_1(S) \leq 39$. Therefore, there cannot be a 9- or 10-gon in M.

(iii) 3-polytope F with $f_0(F) = 11$: since $f_0(S) = 12$, F would be neighbouring all other facets. Hence, it would have f-vector $(11, 20, 11)$. But with the last vertex we can add at most 11 edges, which gives a total of 31 edges for M.

(iv) 3-polytope F with $f_0(F) = 10$: F would have at most 19 edges, but the remaining two vertices cannot both be connected to all other vertices. Moreover, there needs to be at least one 2-face of F of which the vertices are connected to only one of the two remaining vertices, since otherwise all facets of S that contain one of the two vertices would contain both. Therefore, there would be at most 39 edges in M.

(v) k-gon with $k = 8$: since there cannot be a facet with more than 9 vertices, the two facets containing the 8-gon would be pyramids. Since this is also true in the dual, the two apices that are in at least 9 facets anyway would be in at most 9 facets as well. Hence, both are in an edge that is contained in all neighbours of their respective pyramid. In the dual this edge corresponds to an 8-gon, of which there can only be one by $f_0(M^*) = 12$. Therefore, the two apices are joined by an edge. Thus, every neighbour of one of the two pyramids would contain the edge between the two apices, and would be neighbouring the other pyramid too. Hence, there would only be 10 facets in total. □

Now, to exclude more faces, such as 7-gons and facets with 9 vertices, we classify 3-polytopes according to their p-vector $(p_3, p_4, p_5, \ldots)$, where p_i counts the number of i-gonal faces of the polytope. With this we can calculate m_i, and $f_{02} - 3f_2$ in terms of the p-vector. So, let F be a 3-polytope with $f_0(F)$ vertices and $p_i(F) = 0$ for all $i \geq 8$. Then $m_i(F)$ is the number of possible edges between the vertices minus the number of edges of F and the numbers $m_i(G)$, where $G \subset F$ is a 2-face of F. Therefore,

$$m_i(F) = \binom{f_0(F)}{2} - f_1(F) - 14p_7 - 9p_6 - 5p_5 - 2p_4. \tag{2.9}$$

With Euler's formula $f_0(F) - f_1(F) + f_2(F) = 2$ and $f_2(F) = f_2(F^s) - 4p_7 - 3p_6 - 2p_5 - p_4$, we obtain

$$m_i(F) = \frac{1}{2}f_0(F)^2 - \frac{7}{2}f_0(F) + 6 - 10p_7 - 6p_6 - 3p_5 - p_4. \tag{2.10}$$

Here again F^s is the simplicial polytope obtained from F by pulling vertices, and the coefficients of the p_i are simply the numbers of new 2-faces that appear for any i-gon in that process. Therefore, we get

$$f_0(F) = 9: \quad m_i(F) = 15 - 10p_7 - 6p_6 - 3p_5 - p_4, \tag{2.11}$$
$$f_0(F) = 8: \quad m_i(F) = 10 - 10p_7 - 6p_6 - 3p_5 - p_4, \tag{2.12}$$
$$f_0(F) = 7: \quad m_i(F) = 6 - 6p_6 - 3p_5 - p_4. \tag{2.13}$$

For every 3-polytope F the term $f_{02} - 3f_2$ reads

$$f_{02}(F) - 3f_2(F) = \sum_{i\geq 3}(i-3)p_i, \tag{2.14}$$

so in our case we have $f_{02}(F) - 3f_2(F) = p_4 + 2p_5 + 3p_6 + 4p_7$.

Now, let us examine inequality (2.8). This gives

$$3m \leq \sum_{\substack{G\subset S\\ ridge}} f_0(G) \leq \frac{n^2+3n}{2} + m - \frac{1}{2}\sum_{\substack{F\ facet\\ f_0(F)\geq 7}} (m_i(F) + f_{02}(F) - 3f_2(F)) \tag{2.15}$$

and for a single facet $F \subset S$ with $f_0(F) \geq 7$ we get from (2.15)

$$p_4(F) + 2p_5(F) + 3p_6(F) + 4p_7(F) + \frac{1}{2}(m_i(F) + f_{02}(F) - 3f_2(F)) \leq \binom{n}{2} + 2n - 2m. \tag{2.16}$$

So, for the case $f_0(F) = 9$ we obtain the following system determining the allowed p-vectors:

$$10p_7 + 6p_6 + 3p_5 + p_4 \leq 15, \tag{2.17}$$
$$2p_7 + 3p_6 + 3p_5 + 2p_4 \leq n^2 + 3n - 4m - 15, \tag{2.18}$$
$$p_7 + p_6 + p_5 + p_4 + p_3 \geq 7, \tag{2.19}$$
$$p_7 + p_6 + p_5 + p_4 + p_3 \leq n - 1, \tag{2.20}$$
$$5p_7 + 4p_6 + 3p_5 + 2p_4 + p_3 = 14, \tag{2.21}$$
$$p_7 = 1 \Rightarrow p_5 = p_6 = 0. \tag{2.22}$$

Here, inequality (2.17) stems from $m_i(F) \geq 0$ and (2.11); inequality (2.18) is a combination of (2.11), (2.14), and (2.16); inequality (2.19) simply is the lower bound on the number of 2-faces of a 3-polytope with 9 vertices (see Theorem 1.1.1); inequality (2.20) reflects that we want the 3-manifold M to have $f_3(M) = n$, so no facet of M can have more than $n-1$ neighbours; equation (2.21) is a re-writing of $14 = f_2(F^s) = f_2(F) + 4p_7 + 3p_6 + 2p_5 + p_4$; the implication (2.22) comes from the fact that whenever a 3-polytope F with 9 vertices has a 7-gon as 2-face, then every potential pentagon would intersect this 7-gon in at least 3 vertices.

Similarly, for $f_0(F) = 8$ we obtain:

$$\begin{aligned}
10p_7 + 6p_6 + 3p_5 + p_4 &\leq 10, && (2.23)\\
2p_7 + 3p_6 + 3p_5 + 2p_4 &\leq n^2 + 3n - 4m - 10, && (2.24)\\
p_7 + p_6 + p_5 + p_4 + p_3 &\geq 6, && (2.25)\\
p_7 + p_6 + p_5 + p_4 + p_3 &\leq n - 1, && (2.26)\\
5p_7 + 4p_6 + 3p_5 + 2p_4 + p_3 &= 12, && (2.27)\\
p_7 = 1 &\Rightarrow p_4 = p_5 = p_6 = 0,\ p_3 = 7, && (2.28)\\
p_6 = 1 &\Rightarrow p_5 = 0,\ p_4 \leq 2. && (2.29)\\
p_5 &\leq 2 && (2.30)
\end{aligned}$$

Here, inequality (2.23) stems from $m_i(F) \geq 0$ and (2.12); inequality (2.24) is a combination of (2.12), (2.14), and (2.16); inequality (2.25) simply is the lower bound on the number of 2-faces of a 3-polytope with 8 vertices (see Theorem 1.1.1); inequality (2.26) reflects that we want the 3-manifold M to have $f_3(M) = n$, so no facet of S can have more than $n - 1$ neighbours; equation (2.27) is a re-writing of $14 = f_2(F^s) = f_2(F) + 4p_7 + 3p_6 + 2p_5 + p_4$; the implications (2.28) and (2.29) and inequality (2.30) come from the fact that $f_0(F) = 8$.

For $f_0(F) = 7$ we get:

$$\begin{aligned}
6p_6 + 3p_5 + p_4 &\leq 6, && (2.31)\\
3p_6 + 3p_5 + 2p_4 &\leq n^2 + 3n - 4m - 6, && (2.32)\\
p_6 + p_5 + p_4 + p_3 &\geq 6, && (2.33)\\
p_6 + p_5 + p_4 + p_3 &\leq 10, && (2.34)\\
4p_6 + 3p_5 + 2p_4 + p_3 &= 10, && (2.35)\\
p_6 = 1 &\Rightarrow p_4 = p_5 = 0,\ p_3 = 6, && (2.36)\\
p_5 &\leq 1, && (2.37)\\
p_5 = 1 &\Rightarrow p_4 \leq 2. && (2.38)
\end{aligned}$$

Here, inequality (2.31) stems from $m_i(F) \geq 0$ and (2.13); inequality (2.32) is a combination of (2.13), (2.14), and (2.16); inequality (2.33) resp. (2.34) simply is the lower resp. upper bound on the number of 2-faces of a 3-polytope with 7 vertices (see Theorem 1.1.1); equation (2.35) is a re-writing of $10 = f_2(F^s) = f_2(F) + 3p_6 + 2p_5 + p_4$; the implications (2.36) and (2.38) and inequality (2.37) come from the fact that $f_0(F) = 7$.

Finally, for $f_0(F) = 6$ the system reads:

$$\begin{aligned}
2p_5 + p_4 &\leq \frac{n^2 + 3n}{2} - 2m - \frac{1}{2}, && (2.39)\\
p_5 + p_4 + p_3 &\geq 5, && (2.40)\\
p_5 + p_4 + p_3 &\leq 8, && (2.41)\\
3p_5 + 2p_4 + p_3 &= 8, && (2.42)\\
p_5 &\leq 1, && (2.43)\\
p_5 = 1 &\Rightarrow p_4 = 0,\ p_3 = 5. && (2.44)
\end{aligned}$$

Here, inequality (2.39) is inequality (2.8) for a single facet with six vertices; the inequalities (2.40) and (2.41) are the lower and upper bound on the number of 2-faces of a 3-polytope with 6 vertices (see Theorem 1.1.1); equation (2.42) is a re-writing of $8 = f_2(F^s) = f_2(F)+2p_5+p_4$; inequality (2.43) and implication (2.44) come from the fact that $f_0(F) = 6$.

Table 2.2 contains all p-vectors $(p_i)_{i\geq 3}$ for 3-polytopes F with $4 \leq f_0(F) \leq 9$, $f_2 \leq 11$, $3 \leq i \leq 7$, satisfying inequality (2.16), and the p-vector satisfying the respective system of restrictions for at least one of the (n, m)-pairs with $n = 10$ and $m \geq 29$, or $n = 11$ and $m \geq 34$, or $n = 12$ and $m \geq 40$. Moreover, some values necessary for the inequalities above are provided.

Proposition 2.2.8. *An Eulerian 3-manifold M with f-vector $(10, m, m, 10)$, $m \geq 30$, or $(11, 36, 36, 11)$ cannot have a facet with 8 vertices.*

Proof. This follows from inequality (2.8) and the values of $\frac{1}{2}(m_i+f_{02}-3f_2)+4p_7+3p_6+2p_5+p_4$ for the facets with 8 vertices from Table 2.2. □

Proposition 2.2.9. *An Eulerian 3-manifold M with f-vector $(12, m, m, 12)$, $m \geq 40$, or $(11, m, m, 11)$, $m \geq 34$, or $(10, m, m, 10)$, $m \neq 25$, cannot have a facet $F \subset S$ with $f_0(F) = 9$, or a ridge $G \subset S$ with $f_0(G) = 7$.*

Proof. Facets with nine vertices can only occur for $n = 12$ and $m = 40$, resp. $n = 11$ and $m = 34$ according to Proposition 2.2.5, Table 2.2, and inequality (2.18). For this case, note that all possible facets of M with 9 vertices would reduce the gap between lower and upper bound on f_{02} from inequality (2.8) to at most 1.5, but will also require at least one other facet with at least 6 vertices. Comparison of the values from Table 2.2 yields that the only possibility for a facet with $f_0 = 9$ vertices exists for $n = 12$ and $m = 40$: combine a facet of type $F_{\{9,10,2\}}$ with one of type $F_{\{8,8,5\}}$. However, since they reduce the gap of inequality (2.8) to 0, all other facets can have at most 5 vertices. Hence, the total number of 2-faces of M would be at most $\frac{1}{2}(10 + 8 + 10 \cdot 6) = 39 < 40$ (these two facets together with 10 bipyramids over a triangle, type $F_{\{5,6,1\}}$). Therefore, this combination is not possible and we see that no facet with 9 vertices can occur.

Now, assume M would have a 7-gon G as a 2-face. Since all facets have at most 8 vertices, the two facets F_1, F_2 containing G have to be pyramids. The two apices of these pyramids, a_1, resp. a_2, will be in F_1, resp. F_2 and at least 7 other facets each (the neighbours of F_i at the triangles). However, all the restrictions to M hold also for the dual manifold, so no vertex of M can be in more than 8 facets. Hence, all facets that contain the apex a_1 of F_1 also have to contain some edge from this apex to some vertex not in F_1. Since these two edges are dual to a 7-gon of which there can only be one in the dual manifold, these edges are actually the same and a_1, a_2 are joined by an edge and all neighbours of F_1 are also neitghbours of F_2. Hence M has 9 facets: F_1, F_2 and the 7 tetrahedra containing an edge of G and both a_1 and a_2. □

f_0	f_2	$(p_3, p_4, p_5, p_6, p_7)$	$f_{02} - 3f_2 = 2f_0 - f_2 - 4$	m_i	$\frac{1}{2}(m_i + f_{02} - 3f_2) + 4p_7 + 3p_6 + 2p_5 + p_4$	label
4	4	$(4,0,0,0,0)$	0	0		$F_{\{4,4,1\}}$
5	5	$(4,1,0,0,0)$	1	0		$F_{\{5,5,1\}}$
	6	$(6,0,0,0,0)$	0	1		$F_{\{5,6,1\}}$
6	5	$(2,3,0,0,0)$	3	0		$F_{\{6,5,1\}}$
	6	$(4,2,0,0,0)$	2	1		$F_{\{6,6,1\}}$
		$(5,0,1,0,0)$	2	0		$F_{\{6,6,2\}}$
	7	$(6,1,0,0,0)$	1	2		$F_{\{6,7,1\}}$
	8	$(8,0,0,0,0)$	0	3		$F_{\{6,8,1\}}$
7	6	$(2,4,0,0,0)$	4	2	7	$F_{\{7,6,1\}}$
		$(3,2,1,0,0)$	4	1	6.5	$F_{\{7,6,2\}}$
	7	$(4,3,0,0,0)$	3	3	6	$F_{\{7,7,1\}}$
		$(5,1,1,0,0)$	3	2	5.5	$F_{\{7,7,2\}}$
		$(6,0,0,1,0)$	3	0	4.5	$F_{\{7,7,3\}}$
	8	$(6,2,0,0,0)$	2	4	5	$F_{\{7,8,1\}}$
		$(7,0,1,0,0)$	2	3	4.5	$F_{\{7,8,2\}}$
	9	$(8,1,0,0,0)$	1	5	4	$F_{\{7,9,1\}}$
	10	$(10,0,0,0,0)$	0	6	3	$F_{\{7,10,1\}}$
8	6	$(0,6,0,0,0)$	6	4	11	$F_{\{8,6,1\}}$
		$(1,4,1,0,0)$	6	3	10.5	$F_{\{8,6,2\}}$
		$(2,2,2,0,0)$	6	2	10	$F_{\{8,6,3\}}$
	7	$(2,5,0,0,0)$	5	5	10	$F_{\{8,7,1\}}$
		$(3,3,1,0,0)$	5	4	9.5	$F_{\{8,7,2\}}$
		$(4,1,2,0,0)$	5	3	9	$F_{\{8,7,3\}}$
		$(4,2,0,1,0)$	5	2	8.5	$F_{\{8,7,4\}}$
	8	$(4,4,0,0,0)$	4	6	9	$F_{\{8,8,1\}}$
		$(5,2,1,0,0)$	4	5	8.5	$F_{\{8,8,2\}}$
		$(6,0,2,0,0)$	4	4	8	$F_{\{8,8,3\}}$
		$(6,1,0,1,0)$	4	3	7.5	$F_{\{8,8,4\}}$
		$(7,0,0,0,1)$	4	0	6	$F_{\{8,8,5\}}$
	9	$(6,3,0,0,0)$	3	7	8	$F_{\{8,9,1\}}$
		$(7,1,1,0,0)$	3	6	7.5	$F_{\{8,9,2\}}$
		$(8,0,0,1,0)$	3	4	6.5	$F_{\{8,9,3\}}$
	10	$(8,2,0,0,0)$	2	8	7	$F_{\{8,10,1\}}$
		$(9,0,1,0,0)$	2	7	6.5	$F_{\{8,10,2\}}$
	11	$(10,1,0,0,0)$	1	9	6	$F_{\{8,11,1\}}$
9	9	$(7,1,0,0,1)$	5	4	9.5	$F_{\{9,9,1\}}$
	10	$(8,1,0,1,0)$	4	8	10	$F_{\{9,10,1\}}$
		$(9,0,0,0,1)$	4	5	8.5	$F_{\{9,10,2\}}$
	11	$(9,1,1,0,0)$	3	11	10	$F_{\{9,11,1\}}$
		$(10,0,0,1,0)$	3	9	9	$F_{\{9,11,2\}}$

Table 2.2: The table of p-vectors of 3-polytopes and some combinatorial values needed in the inequalities throughout this section. Column 6 shows for $f_0(F) \geq 7$ the left hand side of inequality (2.16). The last column gives a label for the respective facet type.

2.2.3 Facet-type-vectors

Lemma 2.2.10. *Let M be an Eulerian 3-manifold with f-vector (n, m, m, n). Then*

$$m_i(M) = \binom{n}{2} - m - \sum_{\substack{F \subset M \\ facet}} m_i(F) - \sum_{\substack{G \subset M \\ ridge}} m_i(G).$$

Proof. Since M has n vertices, there are $\binom{n}{2}$ potential edges in M. Since $f_1(M) = m$ and $m_i(M)$ is the number of pairs of vertices of M that do not form an edge, and do not lie in a common facet, we get

$$m_i(M) = \binom{n}{2} - m - \sum_{\substack{F \subset M \\ facet}} m_i(F) - \frac{1}{2} \sum_{\substack{F \subset M \\ facet}} m_b(F),$$

where $m_i(F)$ counts the pairs of vertices in F that do not form an edge of F and do not lie in a 2-face of F, and $m_b(F)$ is the number of pairs of vertices of F that lie in a common 2-face of F, but do not form an edge of F. Here, the $m_b(F)$ are counted with factor 0.5, since every 2-face is in two facets and so counted twice. For the same reason, half the sum over the $m_b(F)$ is the sum over the $m_i(G)$. □

Lemma 2.2.11. *Let M be an Eulerian 3-manifold with f-vector $(12, m, m, 12)$, $m \geq 40$, or $(11, m, m, 11)$, $m \geq 34$, or $(10, m, m, 10)$, $m \neq 25$. Then*

$$\begin{aligned} m - 2n \;=\; & \frac{1}{2} \sum_{\substack{F \text{ facet} \\ f_0(F) \geq 7}} (m_i(F) - f_{02}(F) + 3f_2(F)) + \sum_{\substack{F \text{ facet} \\ f_0(F) \leq 6}} m_i(F) \\ & + 6p_6(M) + 3p_5(M) + p_4(M) \\ & - \#\text{facets with 6 resp. 8 vertices} \\ & + \frac{1}{2} \#\text{pyramids over pentagon.} \end{aligned}$$

Proof. With Proposition 2.2.9 we know that M does not have facets with 9 or more vertices or ridges with 7 or more vertices. Moreover, with Table 2.2 we see that Lemma 2.2.2 holds with equality for all 3-polytopes with at most 5 vertices, the left hand side is by 0.5 larger than the right hand side in the case of the pyramid over the pentagon, and by 1 in all other cases with $f_0(F) = 6$. Similarly, we see that Lemma 2.2.3 is tight for $f_0(F) = 7$ and again the left hand side is larger by 1 than the right hand side for $f_0(F) = 8$. Taking this and Lemma 2.2.10 into account, the claim follows the same way we arrived at inequality (2.8). □

Definition 2.2.12. Let M be an Eulerian 3-manifold with f-vector (n, m, m, n). The *facet-type-vector* (ft-vector) of M is

$$ft(M) = (F_{\{i,j,k\}})_{i,j,k},$$

where by abuse of notation $F_{\{i,j,k\}}$ counts the number of facets of M with label $F_{\{i,j,k\}}$ (see Table 2.2). Note that $i = f_0(F)$ and $j = f_2(F)$ for any 3-polytope of type $F_{\{i,j,k\}}$.

The ft-vector of M satisfies the following system of linear equations and inequalities:

$$\sum_{i,j,k} F_{\{i,j,k\}} = n, \tag{2.45}$$

$$\sum_{i,j,k} jF_{\{i,j,k\}} = 2m, \tag{2.46}$$

$$\sum_{i,j,k} (i+j-2)F_{\{i,j,k\}} \geq 3m, \tag{2.47}$$

$$\sum_{i,j,k} (i+j-2)F_{\{i,j,k\}} \leq \frac{n^2+3n}{2} + m. \tag{2.48}$$

Here, equation (2.45) is the condition $f_3(M) = n$; equation (2.46) counts on the left hand side the 2-faces of the facets, which is $2f_2(M) = 2m$; the inequalities (2.47), and (2.48) have on their left hand side the sum over the numbers of edges of the facets, $f_{13}(M)$, which by the generalised Dehn–Sommerville relations (5) is the same as $f_{02}(M)$, which we bounded in (2.3).

With the ft-vectors we can now exclude even more possible faces for Eulerian 3-manifolds with certain f-vectors.

Proposition 2.2.13. *Let M be an Eulerian 3-manifold with f-vector $(10, 29, 29, 10)$. Then the only facet type with 8 vertices that can occur is $F_{\{8,9,3\}}$.*

Proof. Lemmas 2.2.10 and 2.2.11 together with the equalities/inequalities (2.8), (2.45)–(2.48) and the non-negativity and integrality of the occuring numbers (the p_i, $m_i(F)$, $m_i(M)$) give a system of inequalities in the entries of the ft-vector of M. Maximise the number of occurrences of a given facet type for every facet type with 8 vertices over this IP to get the result (checked with the sage MILP-solver). □

Proposition 2.2.14. *Let M be an Eulerian 3-manifold with f-vector $(10, 32, 32, 10)$. Then there is no feasible ft-vector.*

Proof. Construct the IP as in Proposition 2.2.13. According to the sage MILP-solver this system is infeasible. □

Proposition 2.2.15. *Let M be an Eulerian 3-manifold with f-vector $(11, 34, 34, 11)$. Then*

(i) $f_{02}(M) \leq 107$, $p_7(M), p_6(M) \leq 1$.

(ii) $p_5(M) \leq 2$, $p_4(M) \leq 4$.

(iii) *M has at most three facets with 7 vertices.*

(iv) *M has at most one facet with 8 vertices. In this case it is of one of the types $F_{\{8,7,3\}}$, $F_{\{8,8,1\}}$, $F_{\{8,8,2\}}$, $F_{\{8,8,3\}}$, $F_{\{8,9,1\}}$, $F_{\{8,9,2\}}$, $F_{\{8,9,3\}}$, $F_{\{8,10,1\}}$, or $F_{\{8,10,2\}}$.*

Proof. Construct the IP as in Proposition 2.2.13 and maximise $f_{02}(M)$, resp. the number of occurrences of a given facet type for every facet type with 7 or 8 vertices, or the numbers $p_4(M)$, $p_5(M)$ to get the result (checked with the sage MILP-solver). Note that the upper bound on $f_{02}(M)$ yields with $f_{02}(M) \geq 3f_2(M) = 102$ the restrictions on the $p_i(M)$, $i \geq 6$. □

Proposition 2.2.16. *Let M be an Eulerian 3-manifold with f-vector $(11, 35, 35, 11)$. Then*

(i) $f_{02}(M) \leq 108$, $p_7(M) = 0$, $p_6(M), p_5(M) \leq 1$.

(ii) $p_4(M) \leq 2$.

(iii) *M has at most two facets with 7 vertices. Only the types $F_{\{7,7,3\}}$, $F_{\{7,8,1\}}$, $F_{\{7,8,2\}}$, $F_{\{7,9,1\}}$, $F_{\{7,10,1\}}$ can occur.*

(iv) *M has at most one facet with 8 vertices. In this case it is of type $F_{\{8,10,1\}}$.*

Proof. Construct the IP as in Proposition 2.2.13 and maximise $f_{02}(M)$, resp. the number of occurrences of a given facet type for every facet type with 7 or 8 vertices, or the number $p_4(M)$ to get the result (checked with the sage MILP-solver). Note that the upper bound on $f_{02}(M)$ yields with $f_{02}(M) \geq 3f_2(M) = 105$ the restrictions on the $p_i(M)$, $i \geq 5$. □

Proposition 2.2.17. *Let M be an Eulerian 3-manifold with f-vector $(11, 36, 36, 11)$. Then*

(i) $f_{02}(M) \leq 109$, $p_7(M) = p_6(M) = p_5(M) = 0$, $p_4(M) \leq 1$.

(ii) *M has at most one facet with 7 vertices. In this case it is of type $F_{\{7,10,1\}}$.*

Proof. Construct the IP as in Proposition 2.2.13 and maximise $f_{02}(M)$, resp. the number of occurrences of a given facet type for every facet type with 7 vertices to get the result (checked with the sage MILP-solver). Note that the upper bound on $f_{02}(M)$ yields with $f_{02}(M) \geq 3f_2(M) = 108$ the restrictions on the $p_i(M)$. □

Proposition 2.2.18. *Let M be an Eulerian 3-manifold with f-vector $(12, 40, 40, 12)$. Then*

(i) $f_{02}(M) \leq 124$, $p_5(M) \leq 2$.

(ii) *M has at most one facet with 8 vertices. In that case, $f_{02}(M) \leq 122$. Moreover, only two types of facets with eight vertices can occur: $F_{\{8,10,2\}}$ and $F_{\{8,11,1\}}$.*

(iii) *M has no 2-face with 6 vertices, i.e. $p_6(M)$=0.*

(iv) $p_4(M) \leq 3$, $p_4(M) + 2p_5(M) \leq 4$.

Proof. Construct the IP as in Proposition 2.2.13. With suitable objective functions this can be viewed as an LP problem, of which the solution gives the claims (checked with the sage MILP-solver):

(i) Maximisation of $f_{02}(M)$ yields an optimum of 124. The bound on $p_5(M)$ directly follows.

(ii) Maximise the number of facets with 8 vertices to get the optimum 1. Fix this number and maximise $f_{02}(M)$ to get the second part. To see that only the given two facet types are valid, note that all except these two and $F_{\{8,10,1\}}$ are excluded by $f_{02}(S) \leq 122$. Now, maximise $p_4(M)$ with the additional constraint that there has to be a facet with eight vertices. The maximum is 1, but $F_{\{8,10,1\}}$ contains two squares, so this type is not valid.

(iii) From (i) we know $p_6(M) \leq 1$, and from (ii) we get that if $p_6(M) = 1$ neither M nor its dual have a facet with eight vertices, since then $123 \leq f_{02}(M) = f_{02}(M^*)$. Therefore, the hexagon will be contained in two pyramids F_1, F_2 (with 7 vertices each) and the two apices a_1, a_2 of these are only contained in the respective pyramid and its 6 neighbours. Hence, the edge adjacent to a_1 but not in F_1 is contained in 6 facets, so it is dual to a hexagon. This also holds for a_2 and since the dual M^* has at most one hexagon, it follows that a_1, a_2 are joined by an edge, which is inside every neighbour of F_1 and F_2. Thus, M would only have 8 facets.

(iv) Maximisation of $p_4(M)$ gives an optimum of 3, and maximisation of $p_4(M) + 2p_5(M)$ gives an optimum of 4. □

Proposition 2.2.19. *Let M be an Eulerian 3-manifold with f-vector $(12, 41, 41, 12)$. Then*

(i) *M has no 2-face with 6 vertices, i.e. $p_6(M)$=0, and no facet with 8 vertices.*

(ii) *$f_{02}(M) \leq 125$, $p_5(M) \leq 1$, and $p_4(M) \leq 1$.*

(iii) *M has at most two facets with 7 vertices.*

(iv) *M has at most eigth facets with 6 vertices.*

(v) *M has at most nine facets with 5 vertices.*

(vi) *M has at most three facets with 4 vertices.*

Proof. As in Proposition 2.2.13 we can construct a system of linear inequalities and equalities for the ft-vectors. All these bounds can be obtained from optimising suitable objective functions over this system. □

Proposition 2.2.20. *Let M be an Eulerian 3-manifold with f-vector $(12, m, m, 12)$. If $m = 42$, then M is 2s2s. For the case $m = 43$ there is no feasible ft-vector.*

Proof. As in Proposition 2.2.13 we can construct a system of linear inequalities and equalities for the ft-vectors. Mimimising f_{02} for the case $m = 42$ yields an objective value of $126 = 3m$. Therefore, any such manifold is 2s2s. For $m = 43$ this system is infeasible and so there is no ft-vector for this case. □

To the above restrictions on ft-vectors we can also add some restrictions that reflect the facts that $p_i(M) \geq \max(p_i(F), F \subset M)$ and that two facets cannot intersect in more than one ridge. These are

$$F_{\{7,7,1\}} = 1 \vee F_{\{6,5,1\}} = 1 \quad \Rightarrow \quad \begin{cases} p_4(S) \geq 3, & \text{if } n = 11, \\ p_4(S) = 3, F_{\{7,7,1\}} + F_{\{6,5,1\}} = 1, & \text{if } n = 12, \\ F_{\{7,8,1\}} = 0, F_{\{6,6,1\}} = 0, & \text{if } n = 12, \end{cases} \tag{2.49}$$

$$F_{\{7,6,2\}} = 1 \quad \Rightarrow \quad p_4(S) \geq 2, \tag{2.50}$$

$$F_{\{7,8,1\}} + F_{\{6,6,1\}} = 2 \quad \Rightarrow \quad p_4(S) \geq 3, \tag{2.51}$$

$$F_{\{7,8,1\}} + F_{\{6,6,1\}} = 1 \quad \Rightarrow \quad p_4(S) \geq 2. \tag{2.52}$$

For the case $(n, m) = (11, 34)$ these results give 527 possible ft-vectors, for $(n, m) = (11, 35)$ we get 82, for $(n, m) = (11, 36)$ we get 8, for $(n, m) = (12, 40)$ we get 201 and for $(n, m) = (12, 41)$ we get 21.

2.2.4 The algorithm

The algorithm presented here is the combination of our previous approach (Section 2.1) with an algorithm developed together with Katy Beeler, Hannah Schäfer Sjöberg, and Moritz Schmitt.

The rough idea of the algorithm is to construct the face lattices of the Eulerian 3-manifolds (strongly connected Eulerian lattices of rank 5) systematically starting from the graph of the manifold (vertices and edges), and then trying to find a family of facets that fits to this graph and all other constraints. The algorithm has the following outline:

Algorithm 2.2.21. *find_manifolds*(f)
INPUT: *f-vector* (f_0, f_1, f_2, f_3)
OUTPUT: *all Eulerian 3-manifolds with this f-vector*

(i) *enumerate all connected graphs on f_0 vertices and f_1 edges that are 4-connected;*

(ii) *for symmetric f-vectors: rule out all graphs of which the degree sequence does not fit to any possible ft-vector (optional, we did not do this in all cases);*

(iii) *for the remaining graphs find all planar induced non-separating subgraphs that are the graphs of 3-polytopes fitting to the possible facet types (optional, for those cases not treated above we used all 3-polytopes with less than f_0 vertices);*

(iv) *construct for every graph an integer program (IP) with binary variables corresponding to the possible facets and ridges (faces of the facets), and with constraints given by the f-vector, proper intersection, the Euler relation, and the graph;*

(v) *enumerate all feasible solutions of this IP;*

(vi) *check for every feasible solution whether it gives a manifold (resp. sphere, polytope) or not.*

Proposition 2.2.22. *Algorithm 2.2.21 enumerates all Eulerian 3-manifolds with given f-vector (f_0, f_1, f_2, f_3).*

Proof. Clearly, all graphs of Eulerian 3-manifolds satisfy (iii). The ft-vectors described in the previous sections determine the dual graphs of the Eulerian 3-manifolds with the given f-vectors. Since the f-vectors are symmetric, the dual of any Eulerian 3-manifolds with such an f-vector will have the same f-vector and its graph is the dual graph of the original manifold. Therefore, the ft-vectors also determine the graphs of the Eulerian 3-manifolds with the given f-vectors. Hence, (iv) will not exclude any graph of an Eulerian 3-manifold.

By Theorem 0.1 a simple planar graph is the graph of a 3-polytope if and only if it is 3-connected. Thus, with Step (v) we find all possible facets that a manifold with the given graph can have.

Given a graph G and a list $\mathcal{F}$ of potential facets, we can construct the list $\mathcal{R}$ of potential ridges simply from the faces of the facets. We now construct the IP such that feasible solutions will be Eulerian posets of rank 5 on this graph with f-vector (f_0, f_1, f_2, f_3), and such that all face lattices of Eulerian 3-manifolds with this graph and f-vector are feasible solutions. If the variables x_i represent the facets F_i, and the variables y_j the ridges R_j, then we get the constraints

$$\sum_i x_i = f_3 \tag{2.53}$$

$$\sum_j y_j = f_2 \tag{2.54}$$

$$2y_j - \sum_{F_i \supset R_j} x_i = 0 \tag{2.55}$$

$$x_i, y_j \in \{0, 1\}. \tag{2.56}$$

Equations (2.53) and (2.54) enforce that the total number of facets and ridges is f_3, resp. f_2. Equation (2.55) ensures that ridge R_j is in the poset if and only if precisely two facets containing it are also in the poset. Line (2.56) simply says that all variables are binary, which means that if a variable in the solution is 1 the corresponding face will be in the poset. Similarly to these constraints, we get constraints from the Euler relation for the intervals above the vertices and edges. Moreover, for every edge we get an inequality forcing the number of faces containing it to be larger than zero. Finally, we get inequalities $x_i + x_j \leq 1$ for pairs of facets F_i, F_j if their intersection is not *proper* (i.e. that not both can appear in a Eulerian 3-manifold simultaneuosly).

Since all strongly connected Eulerian lattices of rank 5 (Eulerian 3-manifolds) with the given f-vector satisfy the constraints of the IP for their graph, all of them will be in the set of feasible solutions to these IPs. Therefore, with the last steps we can complete the enumeration of all Eulerian 3-manifolds (strongly regular 3-spheres, 4-polytopes) with the given f-vector. □

We implemented this algorithm in sage [59], using the *geng*-function of nauty [47] (this is a built-in function of sage) to enumerate all graphs, and the MILP-library of sage to check the IPs for feasibility and to enumerate all their solutions. We enumerated all feasible solutions in a greedy way: given a feasible solution, store it and set the sum of the f_3 variables corresponding to the facets of this solution to be at most $f_3 - 1$. Thus, we excluded with an additional constraint preciseley the solution we just found and optimised again. By iterating this until no feasible solution exists, we could enumerate all feasible solutions of the original IP. All those solutions that turned out to be strongly connected Eulerian lattices of rank 5, and thus Eulerian 3-manifolds, we triangulated and calculated with sage the Betti numbers to filter out all homology spheres. Afterwards, with the help of BISTELLAR [44], we could find for each of these spheres a certificate that it is PL-homeomorphic to the boundary of the simplex. Finally, with the oriented matroid approach that will be explained in Chapter 3 we could get certificates of non-polytopality for some of the spheres.

The results of the enumerations are shown in Table 2.3.

Table 2.3

f-vector	# graphs	CPU time	# feas. IPs	# feas. sltns	$\#\mathcal{M}_e^3$	$\#\mathcal{S}^3$	#np	$\#\mathcal{P}^4$	
$(8,19,19,8)$	94	13 sec	12	15^*	13	13	0	13	[6]
$(8,20,20,8)$	90	13 sec	13	$14^\dagger$	12	12	0	12	[6]
$(8,21,21,8)$	66	9 sec	3	$2^\dagger$	2	2	0	2	[6]
$(8,19,20,9)$	94	12 sec	1	$1^\dagger$	1	1	0	1	[6]
$(8,20,21,9)$	90	18 sec	21	$31^\dagger$	31	31	0	31	[6]
$(8,22,23,9)$	41	11 sec	4	$7^\dagger$	7	7	0	7	[6]
$(8,20,22,10)$	90	12 sec	9	$10^\dagger$	7	7	0	7	[6]
$(8,21,23,10)$	66	42 sec	31	$71^\dagger$	71	71	0	71	[6]
$(8,22,24,10)$	41	1.5 min	20	$57^\dagger$	57	57	1	56	[6]
$(8,23,25,10)$	20	16 sec	2	$3^\dagger$	3	3	0	3	[6]
$(8,21,24,11)$	66	19 sec	17	30^*	26	26	0	26	[6]
$(8,23,26,11)$	20	6 min	14	$54^\dagger$	54	54	3	51	[6]
$(8,22,26,12)$	41	1.5 min	25	$75^\dagger$	75	75	0	75	[6]
$(8,23,27,12)$	20	6.5 min	15	$133^\dagger$	133	133	4	129	[6]
$(8,24,28,12)$	10	13h	9	$19^\dagger$	19	19	2	17	[6]
$(8,24,29,13)$	10	2.5h	9	$97^\dagger$	97	97	7	90	[6]
$(8,m,m+6,14)$	344	24 sec	0	0	0	0	0	0	$m \leq 21$
$(8,22,28,14)$	41	6 sec	4	4^*	3	3	0	3	[36]
$(8,23,29,14)$	20	23 sec	13	159^*	30	30	0	30	[6]
$(8,24,30,14)$	10	12 min	9	$1\,712^*$	105	105	2	103	[6]
$(8,25,31,14)$	5	10.5h	4	$1\,580^*$	35	35	5	30	[6]
$(8,26,32,14)$	2	2.5h	2	0^*	0	0	0	0	
$(8,m,m+6,14)$	2	2 sec	0	0	0	0	0	0	$m \geq 27$
$(9,m,m,9)$	15 470	4h	478	519					$18 \leq m \leq 36$
$(9,m,m,9)$	170				0	0	0	0	$m \leq 19$
$(9,20,20,9)$	713				1	1	0	1	Section 3.1
$(9,21,21,9)$	1 754				0	0	0	0	
$(9,22,22,9)$	2 770				129	129		≥ 42	Section 3.1
$(9,23,23,9)$	3 129				211	211	≥ 2	$\geq 113^*$	Figure 3.8
$(9,24,24,9)$	2 723				118	118	≥ 2	$\geq 81^*$	Figure 3.8

Table 2.3 – continued from previous page

f-vector	# graphs	CPU time	# feas. IPs	# feas. sltns	$\#\mathcal{M}_e^3$	$\#\mathcal{S}^3$	#np	$\#\mathcal{P}^4$	
$(9, 25, 25, 9)$	1 917				7	7	0	7^*	Figure 3.8
$(9, 26, 26, 9)$	1 154				1	1	0	1	W_9 [72, Thm. 4.2.2]
$(9, m, m, 9)$	1 132				0	0	0	0	$m \geq 27$
$(9, m, m+1, 10)$	2 673	9 min	0	0	0	0	0	0	$m \leq 21$
$(9, 22, 23, 10)$	2 770	16 min	15	24^*	12	12		$\geq 9^*$	Section 3.1
$(9, 23, 24, 10)$	3 129	20 min	267	463^*	398	398	≥ 1	$\geq 78^*$	Section 3.1
$(9, 24, 25, 10)$	2 723	20 min	470	$1\,125^*$	904	904	≥ 7	$\geq 27^*$	Figure 3.10
$(9, 25, 26, 10)$	1 917	15.5 min	286	762^*	524	524	≥ 15	$\geq 80^*$	Section 3.1
$(9, 26, 27, 10)$	1 154	9.5 min	83	140^*	67	67	≥ 2	$\geq 62^*$	Section 3.1
$(9, 27, 28, 10)$	610	5.5 min	15	0^*	0	0	0	0	
$(9, 28, 29, 10)$	294	2.5 min	4	0^*	0	0	0	0	
$(9, 29, 30, 10)$	133	1 min	1	0^*	0	0	0	0	
$(9, m, m+1, 10)$	95	51 sec	0	0	0	0	0	0	$m \geq 30$
$(9, m, m+2, 11)$	5 443	35 min	0	0	0	0	0	0	$m \leq 22$
$(9, 23, 25, 11)$	3 129	21.5 min	75	95^*	66	66		≥ 34	Section 3.1
$(9, 24, 26, 11)$	2 723	27 min	477	$1\,202^*$	1 188	1 188		≥ 105	Section 3.1
$(9, 25, 27, 11)$	1 917	45 min	624	$2\,650^\dagger$	2 650	2 650		≥ 52	Section 3.1
$(9, 26, 28, 11)$	1 154	45.5 min	348	$1\,344^\dagger$	1 344	1 344		≥ 1	Figure 3.14
$(9, 27, 29, 11)$	610	40 min	104	$125^\dagger$	125	125		≥ 60	Figure 3.15, Section 3.1
$(9, 28, 30, 11)$	294	45 min	20	$3^\dagger$	3	3	1	2	Figure 3.16
$(9, 29, 31, 11)$	133	35 min	3	$0^\dagger$	0	0	0	0	
$(9, m, m+2, 11)$	103	66 sec	0	0	0	0	0	0	$m \geq 30$
$(9, m, m+3, 12)$	5 443	33 min	0	0	0	0	0	0	$m \leq 22$
$(9, 23, 26, 12)$	3 129	19 min	3	$3^\dagger$	3	3	0	3	Section 3.1
$(9, 24, 27, 12)$	2 723	20 min	207	419^*	335	335		≥ 129	Section 3.1
$(9, 25, 28, 12)$	1 917	1h	669	$3\,296^*$	3 275	3 275		≥ 171	Section 3.1
$(9, 26, 29, 12)$	1 154	5h	560	$5\,929^*$	5 928	5 928		≥ 276	Section 3.1
$(9, 27, 30, 12)$	610	10.5h	305	$2\,171^\dagger$	2 171	2 171		≥ 516	Figure 3.18, Section 3.1
$(9, 28, 31, 12)$	294	4.5 days	110	$113^\dagger$	113	113		≥ 33	Figure 3.19, Section 3.1
$(9, 29, 32, 12)$	133	20.5 days	25	$0^\dagger$	0	0	0	0	

Table 2.3 – continued from previous page

f-vector	# graphs	CPU time	# feas. IPs	# feas. sltns	$\#\mathcal{M}_e^3$	$\#\mathcal{S}^3$	#np	$\#\mathcal{P}^4$	
$(9, 30, 33, 12)$	59	8 min	5	0^*	0	0	0	0	
$(9, m, m+3, 12)$	44	45 sec	0	0	0	0	0	0	$m \geq 31$
$(9, m, m+4, 13)$	8 536	53 min	0	0	0	0	0	0	$m \leq 23$
$(9, 24, 28, 13)$	2 723	21.5 min	52	160^*	33	33		$\geq 32^*$	Section 3.1
$(9, 25, 29, 13)$	1 917	21 min	373	$2\,486^*$	1 223	1 223	≥ 1	$\geq 387^*$	Section 3.1
$(9, 26, 30, 13)$	1 154	1h	597	$14\,683^*$	7 677	7 677	≥ 3	≥ 309	Section 3.1
$(9, 27, 31, 13)$	610	43 min	390	$24\,970^*$	9 773	9 773	≥ 32	≥ 13	Section 3.1
$(9, 28, 32, 13)$	294	16.5 days	201	$5\,399^\sharp$	2 136	2 136		≥ 439	Section 3.1
$(9, 29, 33, 13)$	133	1 month	68	$96^\sharp$	27	27	≥ 1	$\geq 9^*$	Figure 3.20
$(9, 30, 34, 13)$	59	16.5h	16	0^*	0	0	0	0	
$(9, m, m+4, 13)$	44	4 min	0	0	0	0	0	0	$m \geq 31$
$(9, 23, 28, 14)$	3 129	19 min	0	0	0	0	0	0	
$(9, 24, 29, 14)$	2 723	20 min	0	0	0	0	0	0	
$(10, m, m, 10)$	10 247	11h	0	0	0	0	0	0	$m \leq 22$
$(10, 23, 23, 10)$	35 219	1.5 days	5	$6^\dagger$	4	4	0	4	Figure 3.21
$(10, 24, 24, 10)$	87 014	4 days	12	$16^\dagger$	16	16		$\geq 2^*$	Section 3.1
$(10, 25, 25, 10)$	152 369							≥ 296	Section 3.1
$(10, 26, 26, 10)$	203 469	9.5 days	3 502	$5\,550^\dagger$	5 550	5 550	≥ 69	$\geq 2^*$	Figure 3.23
$(10, 27, 27, 10)$	217 596	10.5 days	3 463	$5\,561^\dagger$	5 561	5 561	≥ 204	$\geq 90^*$	Section 3.1
$(10, 28, 28, 10)$	192 964	9.5 days	1 175	$1\,662^\dagger$	1 662	1 662	≥ 143	$\geq 13^*$	
$(10, 29, 29, 10)$	145 773	7.5 days	114	$128^\dagger$	128	128	≥ 2	$\geq 21^*$	Section 3.1
$(10, 30, 30, 10)$	95 827	5.5 days	3	$3^\dagger$	3	3	0	3	$\Delta_4(2)$, its dual, and W_{10}
$(10, 31, 31, 10)$	55 762	3.5 days	0	0	0	0	0	0	
$(10, m, m, 10)$	53 718				0	0	0	0	$m \geq 32$
$(10, m, m+1, 11)$	45 469	42h	0	0	0	0	0	0	$m \leq 23$
$(10, 24, 25, 11)$	87 014	3.5 days	4	18^*	6	6		$\geq 2^*$	Section 3.1
$(10, 25, 26, 11)$	152 369	6.5 days	177	307^*	136	136		$\geq 10^*$	Figure 3.25
$(10, 26, 27, 11)$	203 469	8.5 days	4 476	$7\,351^*$	6 794	6 794	≥ 11	≥ 633	Section 3.1
$(10, 27, 28, 11)$	217 596	9.5 days	13 844	$26\,556^*$	24 915	24 915		≥ 22	Section 3.1
$(10, 28, 29, 11)$	192 964	9.5 days	16 749	$32\,797^*$	30 355	30 355	≥ 1	≥ 159	Section 3.1

Table 2.3 – continued from previous page

f-vector	# graphs	CPU time	# feas. IPs	# feas. sltns	$\#\mathcal{M}_e^3$	$\#\mathcal{S}^3$	#np	$\#\mathcal{P}^4$	
$(10, 29, 30, 11)$	145 773	7.5 days	9 737	13 617*	11 916	11 916		≥ 28	Section 3.1
$(10, 30, 31, 11)$	95 827	4.5 days	3 296	1 927*	1 441	1 441	≥ 61	≥ 1	Figure 3.27
$(10, 31, 32, 11)$	55 762	3 days	863	60*	35	35	≥ 9	≥ 20*	Section 3.1
$(10, 32, 33, 11)$	29 199	1.5 days	214	6*	2	**2**	**2**	**0**	
$(10, 33, 34, 11)$	13 981	19h	30	0*	0	0	0	0	
$(10, 34, 35, 11)$	6 202	7.5h	3	0*	0	0	0	0	
$(10, 35, 36, 11)$	2 600	3.5h	1	0*	0	0	0	0	
$(10, m, m+1, 11)$	1 736	2.5h	0	0	0	0	0	0	$m \geq 36$
$(10, m, m+2, 12)$	45 469	49h	0	0	0	0	0	0	$m \leq 23$
$(10, 24, 26, 12)$	87 014	4 days	2	2*	2	2		≥ 1	Section 3.1
$(10, 25, 27, 12)$	152 369	6.5 days	2	34*	2	2		≥ 1	Figure 3.28
$(10, 26, 28, 12)$	203 469	9 days	1 039	2 008*	1 051	1 051		≥ 178	Figure 3.29
$(10, 27, 29, 12)$	217 596	9.5 days	10 733	27 144*	23 884	23 884		≥ 768	Section 3.1
$(10, 28, 30, 12)$	192 964	10.5 days	26 240	101 157*	91 727	91 727		≥ 455	Section 3.1
$(10, 29, 31, 12)$	145 773	8.5 days	27 774	115 086*	112 266	112 266		≥ 256	Section 3.1
$(10, 30, 32, 12)$	95 827	6.5 days	17 682	59 311*	47 141	47 141	≥ 13	≥ 1	Figure 3.30
$(10, 31, 33, 12)$	55 762	6.5 days	7 191	8 991*	5 943	5 943	≥ 521	≥ 368	Section 3.1
$(10, 32, 34, 12)$	29 199	20 days		618♯	225	225		≥ 7	Section 3.1
$(10, 33, 35, 12)$	13 981	3.5 days	393	4*	1	**1**	**1**	**0**	
$(10, 34, 36, 12)$	6 202	2.5 days	45	0*	0	0	0	0	
$(10, 35, 37, 12)$	2 600	4.5h	3	0*	0	0	0	0	
$(10, m, m+2, 12)$	1 736	2.5h	0	0	0	0	0	0	$m \geq 36$
$(10, 24, 27, 13)$	87 014	4.5 days	0	0	0	0	0	0	
$(10, 25, 28, 13)$	152 369	7.5 days	1	1†	1	1	0	1	Section 3.1
$(10, 26, 29, 13)$	203 469	9.5 days	59	73*	43	43		≥ 29	Section 3.1
$(10, 25, 29, 14)$	152 369	7.2 days	0	0	0	0	0	0	
$(10, 26, 30, 14)$	203 469	6.5 days	0	0	0	0	0	0	
$(10, 26, 31, 15)$	203 469	9.5 days	0	0	0	0	0	0	
$(10, 27, 32, 15)$	217 596	10.5 days	12	12*	9	9	0	9	Section 3.1
$(10, 27, 33, 16)$	217 596	10.5 days	0	0	0	0	0	0	

Table 2.3 – continued from previous page

f-vector	# graphs	CPU time	# feas. IPs	# feas. sltns	$\#\mathcal{M}_e^3$	$\#\mathcal{S}^3$	#np	$\#\mathcal{P}^4$	
$(10, 28, 35, 17)$	192 964	9.5 days	0	0	0	0	0	0	
$(11, 22, 22, 11)$	265	6 min	0	0	0	0	0	0	
$(11, 23, 23, 11)$	10 391	4.5h	0	0	0	0	0	0	
$(11, 24, 24, 11)$	120 985	59h	0	0	0	0	0	0	
$(11, 25, 25, 11)$	696 184	14.5 days	0	0	0	0	0	0	
$(11, 26, 26, 11)$	2 504 998	53 days	28	56	21	21		≥ 1	Section 3.1
$(11, 27, 27, 11)$	6 383 318	138 days	257	730	322	322		≥ 1	Section 3.1
$(11, 28, 28, 11)$								≥ 2635	Section 3.1
$(11, 29, 29, 11)$								≥ 1	Figure 3.31
$(11, 30, 30, 11)$								≥ 1	Figure 3.32
$(11, 31, 31, 11)$								≥ 1	Figure 3.33
$(11, 32, 32, 11)$								≥ 104	Section 3.1
$(11, 33, 33, 11)$								≥ 1	Figure 3.34
$(11, 34, 34, 11)$	17 005 570	140 days*	19 784	39 193	100	100	≥ 15	≥ 1	P_{11}
$(11, 35, 35, 11)$	11 561 155	86 days*	1 979	3 750	2	**2**	**2**	**0**	
$(11, 36, 36, 11)$	7 134 337	7h*	18	33	0	0	0	0	
$(12, 39, 39, 12)$					≥ 1	≥ 1		≥ 1	W_{12}^{39}
$(12, 40, 40, 12)$	2 997 683 218	16 years*			4	**4**	**4**	**0**	
$(12, 41, 41, 12)$	2 037 876 411	160 days*	49	72	0	0	0	0	
$(12, m, m, 12)$					0	0	0	0	$m \geq 42$

Table 2.3: This table shows the results of the computation per f-vector: the numbers of graphs to check, CPU time needed for the enumeration (those marked with $*$ are the cases where the ft-sequences were used to reduce running time), on how many graphs there are feasible instances, how many solutions these have (those marked with $*$ are already reduced by the non-lattices, the ones marked with † are furthermore reduced by isomorphic copies; those marked with ♯ were not enumerated entirely, since some instances had too many feasible solutions), and the numbers of strongly regular 3-manifolds, strongly regular 3-spheres, non-polytopal spheres, and 4-polytopes (the last two either show an exact number, or lower bounds, since we did not realise all of which we do not have a certificate of non-polytopality; if it is a number with $*$, we have exact coordinates for at least one polytope and numerical coordinates for the others, a number marked with † indicates that we only have numerical coordinates). The CPU times are rounded. Blank spaces represent missing data (e.g. not enumerated or calculated).

Chapter 3

Special 4-Polytopes and 3-Spheres

In this chapter we will discuss some of the results of Chapter 2, i.e. for some of the f- and flag-vectors of which we have enumerated all Eulerian 3-manifolds (strongly regular 3-spheres) we will either give polytope coordinates (Section 3.1), or we will prove for all of them non-realisability as polytopes (Section 3.2). Hence, we will establish the following two results:

Theorem 3.1. *There is a unique strongly regular 3-sphere, but no convex 4-polytope, with flag-vector given by*

$$(f_0, f_1, f_2, f_3; f_{02}) = (12, 40, 40, 12; 120).$$

Thus, the set of flag-vectors of 4-polytopes is a proper subset of the set of flag-vectors of strongly regular 3-spheres:

$$f\ell(\mathcal{P}^4) \subsetneqq f\ell(\mathcal{S}^3).$$

Moreover, this is the smallest 2s2s flag-vector for which there is a 3-sphere but no 4-polytope.

Here *small* refers to the sum of vertices and facets, shifted by the value for the simplex: $\text{size}(f) = f_0 + f_3 - 10$.

Proof. Any strongly regular 3-sphere with the given flag-vector is 2-simple and 2-simplicial, since $f_{02} = 3f_2$ and $f_{13} = f_{02} = 3f_1$. An example for such a sphere is W_{12}^{40} (see Figure 3.40) found by Werner [72]. That this sphere is unique with the given flag-vector and that the flag-vector is the smallest for which there is a 3-sphere but no 4-polytope follows from Theorem 2.1.4. Therefore, all we need to show is non-polytopality. This we will do in two different ways: First, we show that it has no oriented matroid, and thus is not realisable (Theorem 3.2.9); this proof was found by computer, but can be verified by hand. The second proof is again a computer-based oriented matroid proof and shows that for exactly one of the facets this sphere does not even have a diagram based on this facet (Proposition 3.2.10). □

Theorem 3.2. *The set of f-vectors of 4-polytopes is a strict subset of that of f-vectors of strongly regular 3-spheres:*

$$f(\mathcal{P}^4) \subsetneqq f(\mathcal{S}^3).$$

In particular, there are strongly regular 3-spheres, but no 4-polytopes, with the f-vectors

$$\begin{aligned}
f_0, f_1, f_2, f_3) &= (10, 32, 33, 11),\\
(f_0, f_1, f_2, f_3) &= (11, 33, 32, 10),\\
(f_0, f_1, f_2, f_3) &= (10, 33, 35, 12),\\
(f_0, f_1, f_2, f_3) &= (12, 35, 33, 10),\\
(f_0, f_1, f_2, f_3) &= (11, 35, 35, 11),\\
(f_0, f_1, f_2, f_3) &= (12, 40, 40, 12).
\end{aligned}$$

Moreover, the f-vectors $(10, 32, 33, 11)$ and $(11, 33, 32, 10)$ are the smallest ones with that property and there are no other f-vectors of size $\operatorname{size}(f) \leq 12$ for which there are 3-spheres but no 4-polytopes other than the listed ones.

Proof. The enumeration results of Chapter 2 (Table 2.3) give that there are precisely

- two strongly regular 3-spheres with f-vector $(10, 32, 33, 11)$ (Figure 3.35),
- one strongly regular 3-sphere with f-vector $(10, 33, 35, 12)$ (Figure 3.37),
- two strongly regular 3-spheres with f-vector $(11, 35, 35, 11)$ (Figure 3.38),
- and four strongly regular 3-spheres with f-vector $(12, 40, 40, 12)$ (Figures 3.40, 3.41, 3.42, and 3.44).

We will prove non-polytopality of these spheres in the Theorems 3.2.1, 3.2.3, 3.2.5, 3.2.7, 3.2.9, 3.2.12, 3.2.14, and 3.2.16.

The results for the f-vectors $(11, 33, 32, 10)$ and $(12, 35, 33, 10)$ follow from dualising: they are both the opposite f-vector of one of the other four and so a complete enumeration of strongly regular 3-spheres (and even of the Eulerian lattices/3-manifolds) can be obtained by dualising all those spheres (lattices/manifolds) that were found for the opposite f-vector. The non-polytopality then follows from the fact that the dual of a polytope is a polytope again.

That these results are the smallest follows from Section 3.1: There we will see constructions, resp. give coordinates for polytopes for every f-vector f that has size $\operatorname{size}(f) \leq 12$ and at least nine vertices and satisfies $f_0 \leq f_3$. The polytopes and spheres with up to eight vertices have been enumerated completely by others (Altshuler & Steinberg [5, 6], Barnette [10], and Grünbaum & Sreedharan [36]) and do not yield an example of an f-vector that occurs for 3-spheres but not for 4-polytopes. The cases with $f_3 > f_0$ follow from duality. □

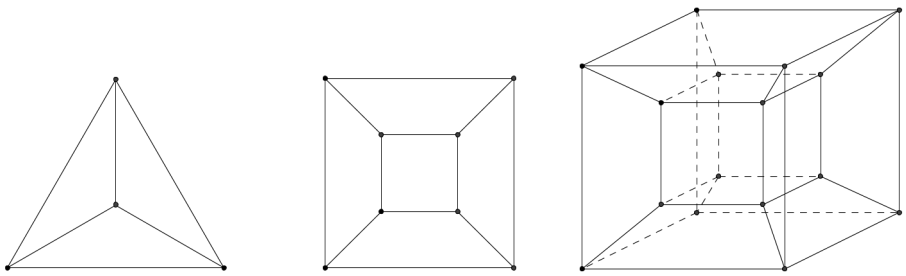

Figure 3.1: These are Schlegel diagrams of the tetrahedron, the 3-cube, and the 4-cube.

The first Theorem is from the paper [25], while the second is from [26]. Both papers are joint work with Günter M. Ziegler.

Apart from realising spheres as polytopes, one can ask whether a given sphere has some *diagram*, or is *embeddable* in some way. We will also study these properties and their relations (Section 3.3), as well as using their non-existence for non-polytopality proofs (Propositions 3.2.2, 3.2.4, 3.2.6, 3.2.10, 3.2.13, 3.2.15, 3.2.17). The description of these concepts is based on Ewald [31].

The motivation for studying diagrams is that they enable us to visualise an n-sphere in $\mathbb{R}^n$. In particular, a diagram of a strongly regular 3-sphere lives in $\mathbb{R}^3$ and, therefore, can be visualised. As often, this tool came up studying polytopes: imagine you have a 3-polytope and can look through the facets into its interior. If you put the polytope with one facet close enough in front of your eyes, you can see the rest of the polytope through (resp. *inside*) this facet. Hence, you've got a two dimensional projection from your polytope. This projection is called a *Schlegel diagram* (see Figure 3.1 for examples). In the following, we will define more general the notion of *diagrams* of a *polyhedral sphere* (i.e. every face is a polytope). Roughly speaking, a Schlegel diagram is a diagram of some polytope. A more precise definition can be found in [31, Sec. III.4].

Definition 3.3. *Let S be a polyhedral n-sphere, and $F \in S$ a facet of S. A* diagram *of S with* base *F is a polytopal complex C in $\mathbb{R}^n$ with*

(i) underlying space $|C| = F$ (where F is seen as a convex polytope),

(ii) every face $G \in S \setminus \{F\}$ is a face of C,

(iii) the boundary faces of C are precisely the faces of F.

*Sometimes the term n-*diagram *is used to clarify the dimension. One can also define a diagram independent from a sphere S as a cell complex with the above notations, but every n-diagram together with its base forms an n-sphere when viewed combinatorially.*

Since a polytope has a (Schlegel) diagram based on every facet, we can use the non-existence of some diagrams as a proof of non-polytopality for spheres. Another question is, whether a given sphere is *embeddable* (into $\mathbb{R}^{d+1}$). A *polyhedral embedding* of a sphere S is a continuous, injective map $\varphi : |S| \to \mathbb{R}^k$ for some k, such that φ has a continuous inverse on $\varphi(|S|)$ and every face $F \in S$ is mapped to a polytope in $\mathbb{R}^k$.

Clearly, every simplicial d-sphere (and more general every simplicial d-complex) is polyhedrally embeddable, since it can be realised as a subcomplex of a $(2d+2)$-dimensional cyclic polytope. However, for general spheres this is not true (see Proposition 3.3.3).

A stronger form of embeddability for spheres is the *star-shaped embedding*. A d-sphere S is *star-shaped* if it has a polyhedral embedding into $\mathbb{R}^{d+1}$ such that there is a point p that can *see* every point on S (i.e. that every ray from p through a point $q \in S$ hits S only in q). In other words, the fan consisting of the cones over the faces of S with apex p is a polyhedral fan.

A weaker form of a star-shaped embedding is the fan-like embedding. A d-sphere S is *fan-like*, if there exists a complete fan Σ together with an isomorphism that maps a face $F \in S$ to a cone $\operatorname{pos} F \in \Sigma$. In the simplicial case, both notions are equivalent, since given a fan-like embedding of a sphere S all choices of vertices as representatives of the 1-dimensional cones will give coplanar faces by the fact that all faces are simplices.

To show non-polytopality and non-existence of diagrams, fan-like embeddings, and star-shaped embeddings, we will use oriented matroid theory. The following description of this method is based on the paper [25], which is joint work with Günter M. Ziegler. The oriented matroid approach is a standard method for proving the non-realisability of polytopes as well as of polyhedral surfaces (see for example Bokowski & Sturmfels [23], Bokowski [20], Björner et al. [18, Chap. 8]), however, it seems that this has almost always been applied to simplicial polytopes or surfaces, and thus in a setting of uniform oriented matroids. An exception is Bremner's software package `mpc` [24], see Bokowski, Bremner & Gévay [21, Sect. 7].

The basic approach is as follows: Any set of points $v_0, \ldots, v_N \in \mathbb{R}^d$ leads to an orientation function $\chi : \{v_0, v_1, \ldots, v_N\}^{d+1} \to \{0, +1, -1\}$ by setting

$$\chi(v_{i_0}, v_{i_1}, \ldots, v_{i_d}) \;:=\; \operatorname{sign} \det \begin{pmatrix} v_{i_0} & v_{i_1} & \cdots & v_{i_d} \\ 1 & 1 & \cdots & 1 \end{pmatrix}.$$

This map is a *chirotope of rank* $d+1$. In addition to the condition that its support has to be a matroid (which we do not use; cf. [18, Thm. 3.6.2]), this means that

(C1) it is alternating, and

(C2) it satisfies the *three term Grassmann–Plücker relations*: For any $d-1$ points $\lambda = (v_{i_0}, \ldots, v_{i_{d-2}})$ and four points v_a, v_b, v_c, v_d the set

$$\{\, \chi(\lambda, v_a, v_b) \cdot \chi(\lambda, v_c, v_d), \quad -\chi(\lambda, v_a, v_c) \cdot \chi(\lambda, v_b, v_d), \quad \chi(\lambda, v_a, v_d) \cdot \chi(\lambda, v_b, v_c) \,\}$$

either equals $\{0\}$ or contains $\{-1, +1\}$.

If the points $v_0, \ldots, v_N$ are supposed to be the vertices of a d-dimensional polytope with a prescribed facet list $(F_0, \ldots, F_n)$, then the map must satisfy the following extra conditions:

(P1) If $v_{i_0}, \ldots, v_{i_d}$ are contained in a facet F_j, then $\chi(v_{i_0}, \ldots, v_{i_d}) = 0$.

(P2) If $v_{i_1}, \ldots, v_{i_d}$ are contained in a facet F_j which does not contain v_a or v_b, then

$$\chi(v_a, v_{i_1}, \ldots, v_{i_d}) = \chi(v_b, v_{i_1}, \ldots, v_{i_d}).$$

In the case of realisability of strongly regular 3-spheres as polytopes, we need to choose four vertices in a facet that will, in every (possible) realisation, form a tetrahedron and add a fifth point not on that facet to get five points of which the value of χ is non-zero. Fixing a sign for these five vertices, we can construct a partial chirotope. If we arrive at a contradiction, this will give a certificate of non-realisability. Similarly, we can use this method in the case of fan-like or star-shaped embeddings.

If we want to check existence of diagrams, then the realisation will be in $\mathbb{R}^3$ and we construct a partial chirotope as follows:

- Take three points in a ridge and some other point on a facet that contains this ridge, and choose a sign ($+1$ or -1) for the basis.
- Every ridge defines a plane that separates the two facets containing it. Therefore, the sign of the chirotope does not change when we exchange points on the same side, and flips otherwise. The only exception to this are the ridges on the boundary, which are the facets of the convex hull of the diagram.
- Use the Grassmann–Plücker relations to determine further entries of the partial chirotope.

However, the partial chirotope that we can construct with this method does not always directly give a certificate of non-realisability (i.e. a contradiction to (C2), or (P2)). In that case we can try to find a *biquadratic final polynomial* (bfp) (see [23, Ch. VII] for an introduction and [22] for the algorithm). To find these bfps we used an implementation of the algorithm by Moritz Firsching and Arnaul Padrol. If this still does not work, we can try to find a contradiction in filling the chirotope via backtracking.

Once we have found a partial chirotope, and no certificate of non-realisatility, we can follow an approach recently introduced by Firsching [32], and use SCIP [1] to find coordinates.

$(8^0_{22,24})$
$F_0 = \{v_0, v_2, v_4, v_6\}$
$F_1 = \{v_0, v_3, v_5, v_7\}$
$F_2 = \{v_1, v_3, v_5, v_7\}$
$F_3 = \{v_1, v_3, v_6, v_7\}$
$F_4 = \{v_1, v_4, v_5, v_7\}$
$F_5 = \{v_1, v_4, v_6, v_7\}$
$F_6 = \{v_0, v_2, v_4, v_5, v_7\}$
$F_7 = \{v_0, v_3, v_4, v_6, v_7\}$
$F_8 = \{v_1, v_2, v_4, v_5, v_6\}$
$F_9 = \{v_0, v_1, v_2, v_3, v_5, v_6\}$

Figure 3.2: This is the facet list of a 4-polytope with f-vector $(8, 22, 24, 10)$. This is one of the nine 4-polytopes of the class $15A^2$ in the classification in [6].

3.1 4-Polytopes

In this section we will prove the "smallest" part of Theorem 3.2. Namely, we will show constructions, resp. give coordinates for polytopes, if existent, for every f-vector f of size $\text{size}(f) \leq 12$ and with $f_0 \leq f_3$. These are the vectors of the form $(9, m, m, 9)$, $(9, m, m+1, 10)$, $(9, m, m+2, 11)$, $(9, m, m+3, 12)$, $(9, m, m+4, 13)$, $(10, m, m, 10)$, $(10, m, m+1, 11)$, $(10, m, m+2, 11)$, and $(11, m, m, 11)$, where $2f_0 \leq m \leq \binom{f_0}{2}$. The coordinates were mostly found via the oriented matroid approach explained above, or via a randomised search. The names of the polytopes are $(A^D_{B,C})$, where $A = f_0$ is the number of vertices, $B = f_1$ is the number of edges, $C = f_2$ is the number of ridges (omitted if it is the same as B), and D is the index of the polytope in the list of all spheres with this f-vector as it was given by our enumeration. This data is not part of the written thesis, but will be provided for download from a university server.

One non-standard construction of a polytope, which we will use, is the *beneath/beyond-method* (cf. Grünbaum [35]). Let P be a 4-polytope, let $F \subset P$ be a tetrahedron facet of P, and denote the vertices of F by $v_0, \ldots, v_3$. Let v_0 be non-simple, and assume furthermore that the three neighbours F_1, F_2, F_3 of F that meet F in the triangles $\{v_0, v_1, v_2\}$, $\{v_0, v_1, v_3\}$, resp. $\{v_0, v_2, v_3\}$ pairwise intersect only in the edges $\{v_0, v_1\}$, $\{v_0, v_2\}$, resp. $\{v_0, v_3\}$ (i.e. these edges are non-simple). Then the supporting hyperplanes of F_1, F_2, F_3 meet in a line L that meets P precisely in v_0, i.e. $P \cap L = \{v_0\}$. If we now place a point w onto L s.t. w is beyond the supporting hyperplane of F and beneath the supporting hyperplanes of all other facets of P except for F_1, F_2, F_3, then the convex hull of P and w will be a 4-polytope P' with one additional vertex w, four additional edges $\{w, v_i\}$, $i = 0, \ldots, 3$, three additional 2-faces (there are six new triangles of the form w plus edge of F, but since w is in the hyperplane supporting F_i, three previous triangles vanish), and without a new facet. Therefore, $f(P') = (f_0(P)+1, f_1(P)+4, f_2(P)+3, f_3(P))$. We will call this operation *beneath/beyond placing of* v_0 *on* F.

3.1.1 Polytopes with $f_0 \leq 8$

The polytopes with up to eight vertices have been classified long ago (Altshuler & Steinberg [5, 6], Barnette [10], and Grünbaum & Sreedharan [36]), so we refer to these for proofs of polytopality and further examples of polytopes with small vertex numbers. However, since we need some examples later on, they are shown here.

(i) $(8, 22, 24, 10)$: see Figure 3.2.

$(8^{1}_{21,24})$

$F_0 = \{v_0, v_2, v_4, v_6\}$
$F_1 = \{v_0, v_2, v_5, v_6\}$
$F_2 = \{v_0, v_3, v_5, v_7\}$
$F_3 = \{v_0, v_4, v_6, v_7\}$
$F_4 = \{v_0, v_5, v_6, v_7\}$
$F_5 = \{v_1, v_3, v_5, v_7\}$
$F_6 = \{v_1, v_4, v_6, v_7\}$
$F_7 = \{v_1, v_5, v_6, v_7\}$
$F_8 = \{v_0, v_1, v_3, v_4, v_7\}$
$F_9 = \{v_1, v_2, v_4, v_5, v_6\}$
$F_{10} = \{v_0, v_1, v_2, v_3, v_4, v_5\}$

Figure 3.3: This is the facet list of a 4-polytope with f-vector $(8, 21, 24, 11)$. This is one of the two 4-polytopes of the class 4 in the classification in [6].

$(8^{15}_{23,26})$

$F_0 = \{v_0, v_2, v_4, v_6\}$
$F_1 = \{v_0, v_3, v_4, v_6\}$
$F_2 = \{v_0, v_3, v_4, v_7\}$
$F_3 = \{v_0, v_3, v_5, v_7\}$
$F_4 = \{v_1, v_2, v_5, v_7\}$
$F_5 = \{v_1, v_3, v_4, v_6\}$
$F_6 = \{v_1, v_3, v_4, v_7\}$
$F_7 = \{v_1, v_3, v_5, v_7\}$
$F_8 = \{v_0, v_2, v_4, v_5, v_7\}$
$F_9 = \{v_1, v_2, v_4, v_6, v_7\}$
$F_{10} = \{v_0, v_1, v_2, v_3, v_5, v_6\}$

Figure 3.4: This is the facet list of a 4-polytope with f-vector $(8, 23, 26, 11)$. This is one of the four 4-polytopes of the class A^2C in the classification in [6].

$(8^{0}_{23,27})$

$F_0 = \{v_0, v_2, v_4, v_5\}$
$F_1 = \{v_0, v_2, v_4, v_6\}$
$F_2 = \{v_0, v_2, v_5, v_7\}$
$F_3 = \{v_0, v_2, v_6, v_7\}$
$F_4 = \{v_0, v_3, v_6, v_7\}$
$F_5 = \{v_1, v_3, v_6, v_7\}$
$F_6 = \{v_1, v_4, v_6, v_7\}$
$F_7 = \{v_2, v_4, v_6, v_7\}$
$F_8 = \{v_0, v_1, v_3, v_5, v_7\}$
$F_9 = \{v_1, v_2, v_4, v_5, v_7\}$
$F_{10} = \{v_0, v_3, v_4, v_5, v_6\}$
$F_{11} = \{v_1, v_3, v_4, v_5, v_6\}$

Figure 3.5: This is the facet list of a 4-polytope with f-vector $(8, 23, 27, 12)$. This is one of the 42 4-polytopes of the class $1A^2$ in the classification in [6].

$(8^{8}_{24,28})$

$F_0 = \{v_0, v_2, v_4, v_7\}$
$F_1 = \{v_0, v_3, v_4, v_6\}$
$F_2 = \{v_0, v_3, v_4, v_7\}$
$F_3 = \{v_1, v_3, v_4, v_6\}$
$F_4 = \{v_1, v_3, v_4, v_7\}$
$F_5 = \{v_1, v_3, v_5, v_7\}$
$F_6 = \{v_1, v_4, v_6, v_7\}$
$F_7 = \{v_2, v_4, v_6, v_7\}$
$F_8 = \{v_0, v_2, v_4, v_5, v_6\}$
$F_9 = \{v_0, v_2, v_3, v_5, v_7\}$
$F_{10} = \{v_0, v_1, v_3, v_5, v_6\}$
$F_{11} = \{v_1, v_2, v_5, v_6, v_7\}$

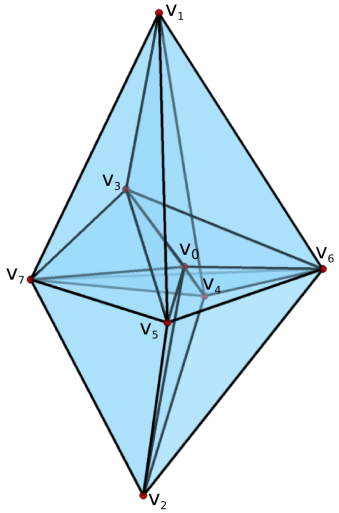

Figure 3.6: These are the facet list of a 4-polytope with f-vector $(8, 24, 28, 12)$, as well as a Schlegel diagram of it based on F_{11}. This is one of the 17 4-polytopes of the class A^4 in the classification in [6].

$(8^1_{24,29})$
$F_0 = \{v_0, v_3, v_4, v_6\}$
$F_1 = \{v_0, v_3, v_4, v_7\}$
$F_2 = \{v_0, v_3, v_5, v_7\}$
$F_3 = \{v_0, v_4, v_5, v_6\}$
$F_4 = \{v_1, v_3, v_4, v_6\}$
$F_5 = \{v_1, v_3, v_4, v_7\}$
$F_6 = \{v_1, v_3, v_5, v_7\}$
$F_7 = \{v_1, v_4, v_6, v_7\}$
$F_8 = \{v_2, v_4, v_5, v_6\}$
$F_9 = \{v_2, v_4, v_6, v_7\}$
$F_{10} = \{v_0, v_1, v_3, v_5, v_6\}$
$F_{11} = \{v_0, v_2, v_4, v_5, v_7\}$
$F_{12} = \{v_1, v_2, v_5, v_6, v_7\}$

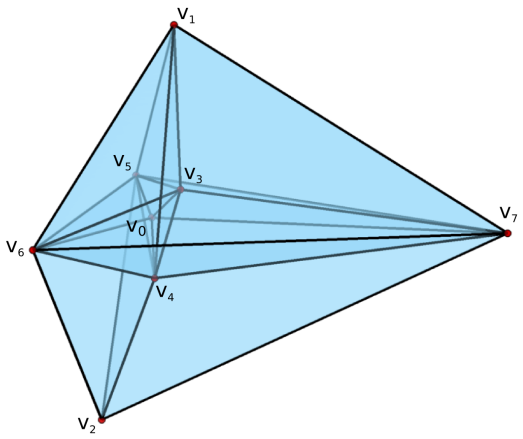

Figure 3.7: These are the facet list of a 4-polytope with f-vector $(8, 24, 29, 13)$, as well as a Schlegel diagram of it based on F_{12}. This is one of the 56 4-polytopes of the class A^3 in the classification in [6].

(ii) $(8, 21, 24, 11)$: see Figure 3.3.

(iii) $(8, 23, 26, 11)$: see Figure 3.4.

(iv) $(8, 23, 27, 12)$: see Figure 3.5.

(v) $(8, 24, 28, 12)$: see Figure 3.6.

(vi) $(8, 24, 29, 13)$: see Figure 3.7.

3.1.2 Polytopes with f-vector $(9, m, m, 9)$

As a result of the enumeration in Chapter 2, there are no strongly regular 3-spheres, and hence no 4-polytopes, with the f-vector $(9, m, m, 9)$ for $m \leq 19$, $m = 21$, and $m \geq 27$. The remaining cases are:

(i) $(9, 20, 20, 9)$: There is a unique strongly regular 3-sphere with this f-vector, which can be realised as a 4-polytope by taking the bipyramid over the tetrahedron (gives $f = (6, 14, 16, 8)$) and truncate a simple vertex (one of the two apices).

(ii) $(9, 22, 22, 9)$: Take any 3-polytope with f-vector $(8, 14, 8)$ and build a pyramid over it. This way we can construct 42 4-polytopes with f-vector $(9, 22, 22, 9)$.

(iii) $(9, 23, 23, 9)$: There are 211 strongly regular 3-spheres with this f-vector. A realisation of one of these as a 4-polytope is (9^2_{23}) in Figure 3.8.

(iv) $(9, 24, 24, 9)$: There are 118 strongly regular 3-spheres with this f-vector. A realisation of one of these as a 4-polytope is (9^0_{24}) in Figure 3.8.

Figure 3.8

$\underline{F_8}$

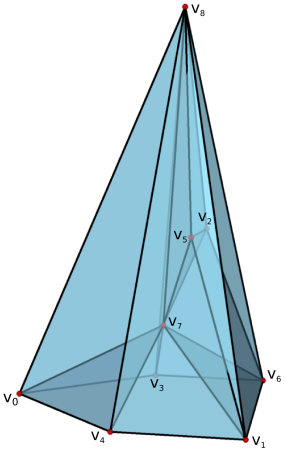

(9^2_{23})

$F_0 = \{v_0, v_3, v_7, v_8\}$
$F_1 = \{v_0, v_4, v_7, v_8\}$
$F_2 = \{v_2, v_5, v_7, v_8\}$
$F_3 = \{v_1, v_4, v_5, v_7, v_8\}$
$F_4 = \{v_2, v_3, v_6, v_7, v_8\}$
$F_5 = \{v_1, v_2, v_5, v_6, v_7\}$
$F_6 = \{v_1, v_2, v_5, v_6, v_8\}$
$F_7 = \{v_0, v_1, v_3, v_4, v_6, v_7\}$
$F_8 = \{v_0, v_1, v_3, v_4, v_6, v_8\}$

$v_0 = (0, 0, 0, 0)$
$v_1 = (7758/5, 7686/5, 7932/5, 7932/5)$
$v_2 = (1582, 1577, 1591, 1591)$
$v_3 = (261, 253, 246, 246)$
$v_4 = (258, 257, 269, 269)$
$v_5 = (39394/25, 15733/10, 15939/10, 15939/10)$
$v_6 = (1614, 7871/5, 7787/5, 7787/5)$
$v_7 = (1137271811/721818, 5684532109/3609090, 15881/10, 15881/10)$
$v_8 = (146, 146, 170, 170)$

(9^0_{24})

$F_0 = \{v_1, v_2, v_4, v_7, v_8\}$
$F_1 = \{v_1, v_3, v_5, v_7, v_8\}$
$F_2 = \{v_2, v_3, v_6, v_7, v_8\}$
$F_3 = \{v_0, v_1, v_4, v_5, v_7\}$
$F_4 = \{v_0, v_1, v_4, v_5, v_8\}$
$F_5 = \{v_0, v_2, v_4, v_6, v_7\}$
$F_6 = \{v_0, v_2, v_4, v_6, v_8\}$
$F_7 = \{v_0, v_3, v_5, v_6, v_7\}$
$F_8 = \{v_0, v_3, v_5, v_6, v_8\}$

$v_0 = (0, 0, 0, 0)$
$v_1 = (2888/15, 2842/15, 191, 191)$
$v_2 = (-20, -41/2, -18, -18)$
$v_3 = (88, 84, 175/2, 175/2)$
$v_4 = (76, 80, 78, 78)$
$v_5 = (152, 148, 150, 150)$
$v_6 = (-26, -27, -25, -25)$
$v_7 = 1/146460*(-941172, -2149963, -3092890, -3092890)$
$v_8 = (130, 128, 136, 136)$

$\underline{F_6}$

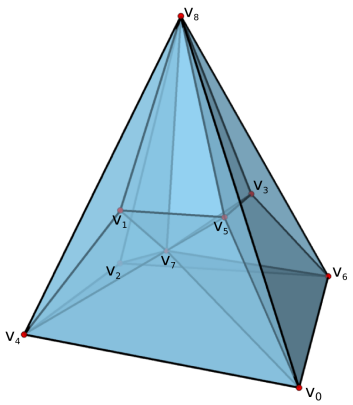

(9^0_{25})

$F_0 = \{v_2, v_4, v_6, v_7\}$
$F_1 = \{v_3, v_5, v_6, v_7\}$
$F_2 = \{v_0, v_2, v_4, v_6, v_8\}$
$F_3 = \{v_1, v_2, v_4, v_7, v_8\}$
$F_4 = \{v_0, v_3, v_5, v_6, v_8\}$
$F_5 = \{v_1, v_3, v_5, v_7, v_8\}$
$F_6 = \{v_2, v_3, v_6, v_7, v_8\}$
$F_7 = \{v_0, v_1, v_4, v_5, v_8\}$
$F_8 = \{v_0, v_1, v_4, v_5, v_6, v_7\}$

$v_0 = (76, 87, 77, 82)$
$v_1 = (82, 82, 82, 54)$
$v_2 = (47158/553, 44700/553, 43909/553, 81)$
$v_3 = (4582/57, 1465/19, 86, 81)$
$v_4 = (83, 85, 75, 68)$
$v_5 = (75, 84, 84, 68)$
$v_6 = (79, 78, 79, 87)$
$v_7 = (85, 73, 84, 59)$
$v_8 = (85, 87, 85, 99)$

$\underline{F_6}$

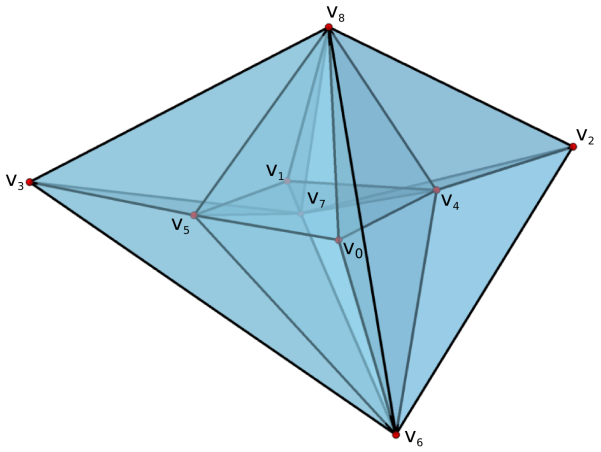

Figure 3.8: These are the facet list, coordinates, and a diagram for 4-polytopes with the f-vectors $(9, m, m, 9)$, $23 \leq m \leq 25$. The upper index is the index of the polytope in the list of all 3-spheres with that f-vector that were found by our enumeration.

$(9^{33}_{23,24})$
$F_0 = \{v_0, v_3, v_6, v_8\}$
$F_1 = \{v_0, v_5, v_6, v_8\}$
$F_2 = \{v_1, v_3, v_6, v_8\}$
$F_3 = \{v_1, v_3, v_7, v_8\}$
$F_4 = \{v_1, v_5, v_6, v_8\}$
$F_5 = \{v_2, v_4, v_7, v_8\}$
$F_6 = \{v_0, v_3, v_4, v_7, v_8\}$
$F_7 = \{v_0, v_2, v_4, v_5, v_8\}$
$F_8 = \{v_1, v_2, v_5, v_7, v_8\}$
$F_9 = \{v_0, v_1, v_2, v_3, v_4, v_5, v_6, v_7\}$

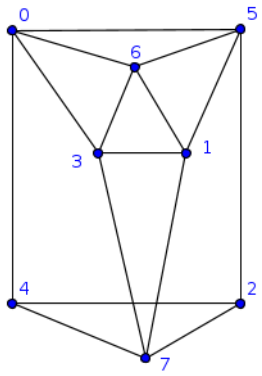

Figure 3.9: On the left hand side is the facet list of a 4-polytope with f-vector $(9, 23, 24, 10)$. It is the pyramid over the 3-polytope with f-vector $(8, 15, 9)$ shown on the right hand side.

$(9^{558}_{24,25})$
$F_0 = \{v_4, v_5, v_6, v_7\}$
$F_1 = \{v_2, v_4, v_5, v_7, v_8\}$
$F_2 = \{v_0, v_2, v_4, v_7\}$
$F_3 = \{v_0, v_3, v_4, v_6, v_7\}$
$F_4 = \{v_0, v_1, v_2, v_3, v_4, v_8\}$
$F_5 = \{v_0, v_1, v_2, v_3, v_6, v_7\}$
$F_6 = \{v_1, v_3, v_4, v_6\}$
$F_7 = \{v_1, v_4, v_5, v_6, v_8\}$
$F_8 = \{v_1, v_2, v_5, v_6, v_7\}$
$F_9 = \{v_1, v_2, v_5, v_8\}$

$v_0 = (0, 0, 0, 0)$
$v_1 = (2, 2, 1, 1)$
$v_2 = (0, 2, 0, 0)$
$v_3 = (0, 2, 0, 0)$
$v_4 = (0, 2, 2, 2)$
$v_5 = (1, 0, 2, 2)$
$v_6 = (2, 2, 0, 0)$
$v_7 = (1, 2, 0, 0)$
$v_8 = (2, 0, 2, 2)$

Figure 3.10: These are the facet list and coordinates of a 4-polytope with f-vector $(9, 24, 25, 10)$. This is polytope $p11_{166}$ in the list of polytopes provided by Höppner as data from her diploma thesis [38].

(v) $(9, 25, 25, 9)$: There are 7 strongly regular 3-spheres with this f-vector. For all of them we found numerical coordinates for a realisation as 4-polytope. One of these with exact values is (9^0_{25}) in Figure 3.8.

(vi) $(9, 26, 26, 9)$: There is a unique strongly regular 3-sphere W_9 with this f-vector, which was realised as 4-polytope in [72, Thm. 4.2.2].

3.1.3 Polytopes with f-vector $(9, m, m+1, 10)$

As a result of the enumeration in Chapter 2, there are no strongly regular 3-spheres, and hence no 4-polytopes, with the f-vector $(9, m, m+1, 10)$ for $m \leq 21$, and $m \geq 27$. The remaining cases are:

(i) $(9, 22, 23, 10)$: Again, take the bipyramid over the tetrahedron, but this time truncate one of the tetrahedra-vertices (they have valence 5). The new facet will be a bipyramid over the triangle, hence we get a 4-polytope with f-vector $(10, 23, 22, 9)$. If we dualise, we get a 4-polytope with f-vector $(9, 22, 23, 10)$. We obtain two more polytopes with this f-vector by taking the pyramid over one of the two 3-polytopes with f-vector $(7, 11, 6)$ and then stack one of the tetrahedra facets.

$(9^0_{23,25})$

$F_0 = \{v_1, v_3, v_5, v_7\}$
$F_1 = \{v_0, v_3, v_5, v_7\}$
$F_2 = \{v_0, v_5, v_7, v_8\}$
$F_3 = \{v_0, v_1, v_3, v_5, v_6\}$
$F_4 = \{v_1, v_3, v_4, v_6, v_7\}$
$F_5 = \{v_2, v_5, v_7, v_8\}$
$F_6 = \{v_1, v_2, v_4, v_5, v_7\}$
$F_7 = \{v_0, v_2, v_5, v_8\}$
$F_8 = \{v_0, v_1, v_2, v_4, v_5, v_6\}$
$F_9 = \{v_0, v_2, v_7, v_8\}$
$F_{10} = \{v_0, v_2, v_3, v_4, v_6, v_7\}$

Figure 3.11: This is the facet list of a 4-polytope with f-vector $(9, 23, 25, 11)$ that we obtained from stacking onto a 4-polytope with f-vector $(8, 19, 19, 8)$.

(ii) $(9, 23, 24, 10)$: Take any 3-polytope with f-vector $(8, 15, 9)$ and build a pyramid over it. In this way we can construct 74 4-polytopes with f-vector $(9, 23, 24, 10)$. One of these, $(9^{33}_{23,24})$, is shown in Figure 3.9.

(iii) $(9, 24, 25, 10)$: The facet list and vertex coordinates for one 4-polytope with this f-vector are in Figure 3.10.

(iv) $(9, 25, 26, 10)$: We want to perform the beneath/beyond operation explained at the beginning of this section. For this take for example the prism over the triangle, triangulate two of the quadrilateral faces, and stack onto one of the triangles. We can do this in a way that the resulting 3-polytope P has only two simple vertices v_1, v_2, and so that P has at least two triangles without a simple vertex. Moreover, $f(P) = (7, 14, 9)$, and $f(\text{pyr}(P)) = (8, 21, 23, 10)$. Denote the apex of $\text{pyr}(P)$ by w and the two tetrahedra above the triangles without a simple vertex with F_1, F_2. Then we can place w beneath/beyond on F_i for any $i \in \{1, 2\}$. The resulting 4-polytope has f-vector $(9, 25, 26, 10)$. Starting from different polytopes, we can construct 79 4-polytopes in this way.

(v) $(9, 26, 27, 10)$: We will perform a beneath/beyond operation with the polytope $(8^0_{22,24})$ from Figure 3.2. The facet $F_2 = \{v_1, v_3, v_5, v_7\}$ of this polytope is a tetrahedron, the vertex v_7 is non-simple, and the edges $\{v_1, v_7\}$, $\{v_3, v_7\}$, and $\{v_5, v_7\}$ are in four facets each. Therefore, we can place v_7 beneath/beyond on F_2 and obtain a 4-polytope with f-vector $(9, 26, 27, 10)$. Starting from different polytopes, we can construct 35 4-polytopes in this way.

3.1.4 Polytopes with f-vector $(9, m, m + 2, 11)$

As a result of the enumeration in Chapter 2, there are no strongly regular 3-spheres, and hence no 4-polytopes, with the f-vector $(9, m, m + 2, 11)$ for $m \leq 22$, and $m \geq 29$. The remaining cases are:

(i) $(9, 23, 25, 11)$: There are 13 4-polytopes with f-vector $(8, 19, 19, 8)$, eight of which are pyramids. All of these have at least one tetrahedron as a facet on which we can stack to get a 4-polytope with f-vector $(9, 23, 25, 11)$. In total, this construction yields 34 polytopes. The facet list of one of them is shown in Figure 3.11.

$(9^{11}_{24,26})$
$F_0 = \{v_0, v_2, v_4, v_8\}$
$F_1 = \{v_0, v_2, v_5, v_8\}$
$F_2 = \{v_0, v_4, v_6, v_8\}$
$F_3 = \{v_1, v_3, v_6, v_8\}$
$F_4 = \{v_1, v_3, v_7, v_8\}$
$F_5 = \{v_1, v_4, v_6, v_8\}$
$F_6 = \{v_2, v_5, v_7, v_8\}$
$F_7 = \{v_3, v_5, v_7, v_8\}$
$F_8 = \{v_0, v_3, v_5, v_6, v_8\}$
$F_9 = \{v_1, v_2, v_4, v_7, v_8\}$
$F_{10} = \{v_0, v_1, v_2, v_3, v_4, v_5, v_6, v_7\}$

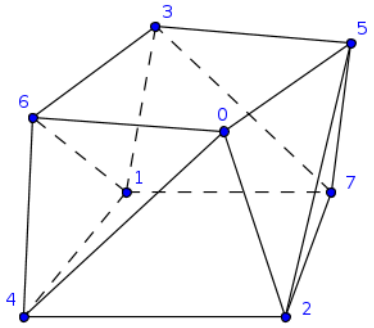

Figure 3.12: On the left hand side is the facet list of a 4-polytope with f-vector $(9, 24, 26, 11)$. It is the pyramid over the 3-polytope with f-vector $(8, 16, 10)$ shown on the right hand side.

$(9^{1900}_{25,27})$
$F_0 = \{v_0, v_2, v_4, v_6, v_8\}$
$F_1 = \{v_0, v_2, v_5, v_6\}$
$F_2 = \{v_0, v_3, v_5, v_7\}$
$F_3 = \{v_4, v_6, v_7, v_8\}$
$F_4 = \{v_0, v_5, v_6, v_7, v_8\}$
$F_5 = \{v_1, v_3, v_5, v_7\}$
$F_6 = \{v_1, v_4, v_6, v_7\}$
$F_7 = \{v_1, v_5, v_6, v_7\}$
$F_8 = \{v_0, v_1, v_3, v_4, v_7, v_8\}$
$F_9 = \{v_1, v_2, v_4, v_5, v_6\}$
$F_{10} = \{v_0, v_1, v_2, v_3, v_4, v_5\}$

Figure 3.13: This is the facet list of a 4-polytope with f-vector $(9, 25, 27, 11)$ that we obtained from stacking onto a 4-polytope with f-vector $(8, 23, 23, 8)$.

$(9^{500}_{26,28})$
$F_0 = \{v_0, v_2, v_7, v_8\}$
$F_1 = \{v_0, v_3, v_6, v_7, v_8\}$
$F_2 = \{v_2, v_3, v_5, v_6, v_7, v_8\}$
$F_3 = \{v_0, v_1, v_2, v_3, v_4, v_7\}$
$F_4 = \{v_0, v_1, v_2, v_8\}$
$F_5 = \{v_3, v_4, v_5, v_6\}$
$F_6 = \{v_0, v_1, v_4, v_5, v_6, v_8\}$
$F_7 = \{v_0, v_3, v_4, v_6\}$
$F_8 = \{v_1, v_2, v_4, v_5\}$
$F_9 = \{v_2, v_3, v_4, v_5\}$
$F_{10} = \{v_1, v_2, v_5, v_8\}$

$v_0 = (0, 0, 2, 2)$
$v_1 = (0, 2, 0, 0)$
$v_2 = (0, 2, 1, 1)$
$v_3 = (1, 0, 0, 0)$
$v_4 = (1, 0, 1, 1)$
$v_5 = (2, 2, 2, 2)$
$v_6 = (2, 0, 0, 0)$
$v_7 = (2, 0, 1, 1)$
$v_8 = (2, 0, 2, 2)$

Figure 3.14: These are the facet list and coordinates of a 4-polytope with f-vector $(9, 26, 28, 11)$. This is polytope $p12_{197}$ in the list of polytopes provided by Höppner as data from her diploma thesis [38].

$(9^{53}_{27,29})$
$F_0 = \{v_0, v_2, v_4, v_6, v_8\}$
$F_1 = \{v_0, v_3, v_6, v_8\}$
$F_2 = \{v_0, v_3, v_4, v_7, v_8\}$
$F_3 = \{v_0, v_3, v_5, v_7\}$
$F_4 = \{v_1, v_2, v_5, v_7\}$
$F_5 = \{v_1, v_3, v_4, v_6, v_8\}$
$F_6 = \{v_1, v_3, v_4, v_7\}$
$F_7 = \{v_1, v_3, v_5, v_7\}$
$F_8 = \{v_0, v_2, v_4, v_5, v_7\}$
$F_9 = \{v_1, v_2, v_4, v_6, v_7\}$
$F_{10} = \{v_0, v_1, v_2, v_3, v_5, v_6\}$

Figure 3.15: This is the facet list of a 4-polytope with f-vector $(9, 27, 29, 11)$ that we obtained via the beneath/beyond operation on the 4-polytope $(8^{15}_{23,26})$.

$(9^1_{28,30})$

$F_0 = \{v_0, v_4, v_5, v_7\}$
$F_1 = \{v_1, v_3, v_5, v_7\}$
$F_2 = \{v_1, v_3, v_6, v_8\}$
$F_3 = \{v_0, v_3, v_5, v_6, v_7\}$
$F_4 = \{v_0, v_2, v_4, v_6, v_7\}$
$F_5 = \{v_0, v_2, v_4, v_5, v_8\}$
$F_6 = \{v_0, v_2, v_3, v_6, v_8\}$
$F_7 = \{v_1, v_4, v_5, v_7, v_8\}$
$F_8 = \{v_1, v_3, v_4, v_6, v_7\}$
$F_9 = \{v_0, v_1, v_3, v_5, v_8\}$
$F_{10} = \{v_1, v_2, v_4, v_6, v_8\}$

$v_0 = (-922, -914, -907, -912)$
$v_1 = 1/63639437031882044478059 \cdot (4401456664486374673983666 8,$
$44487118764012306544495746,$
$41361085165253401203569137,$
$42754407461261313797050764)$
$v_2 = 1/31228482517380023801537 09 \cdot (-24808564715872743948585339 08,$
$-26212305955461143867388993 14,$
$-25789437883452262077245904 97,$
$-25131020518525483647614433 16)$
$v_3 = 1/25452430514683067 \cdot (21554745511127058338, 21236217599707481018,$
$21463612388041103607, 21741658090235972176)$
$v_4 = (-810, -826, -805, -826)$
$v_5 = (-755, -675, -687, -742)$
$v_6 = (196, 150, 204, 210)$
$v_7 = (215, 278, 347, 243)$
$v_8 = (122, 119, 58, 94)$

$(9^2_{28,30})$

$F_0 = \{v_0, v_2, v_4, v_7\}$
$F_1 = \{v_0, v_4, v_6, v_8\}$
$F_2 = \{v_1, v_3, v_7, v_8\}$
$F_3 = \{v_0, v_2, v_4, v_5, v_8\}$
$F_4 = \{v_0, v_2, v_5, v_6, v_7\}$
$F_5 = \{v_1, v_3, v_4, v_6, v_8\}$
$F_6 = \{v_1, v_3, v_5, v_6, v_7\}$
$F_7 = \{v_0, v_1, v_4, v_6, v_7\}$
$F_8 = \{v_1, v_2, v_4, v_7, v_8\}$
$F_9 = \{v_0, v_3, v_5, v_6, v_8\}$
$F_{10} = \{v_2, v_3, v_5, v_7, v_8\}$

$v_0 = (-1116085454470691691057583/1499741338601751219428,$
$-1205082269831604704216927/1499741338601751219428,$
$-2292003296124442906991331/2999482677203502438856,$
$-2376668700774594767633373/2999482677203502438856)$
$v_1 = 1/11993337569901975395257 \cdot (4344412408881811740455546,$
$48130762169231549030950 99,$
$47053029115779401533163 94,$
$45125067814054127380394 74)$
$v_2 = 1/373440771851165 \cdot (136044681970166693, 118413719696992144,$
$119898969135186327, 129453910329366809)$
$v_3 = (-393, -366, -370, -377)$
$v_4 = (-938, -953, -960, -972)$
$v_5 = (511, 452, 477, 503)$
$v_6 = (456, 439, 523, 452)$
$v_7 = (938, 922, 927, 937)$
$v_8 = (-953, -940, -960, -956)$

Figure 3.16: These are the facet lists and coordinates of the two 4-polytopes with f-vector $(9, 28, 30, 11)$. The sphere $(9^0_{28,30})$ with the same f-vector is non-polytopal.

$(9^{2147}_{26,29})$

$F_0 = \{v_0, v_3, v_5, v_7\}$
$F_1 = \{v_1, v_3, v_5, v_7\}$
$F_2 = \{v_0, v_2, v_6, v_8\}$
$F_3 = \{v_0, v_2, v_3, v_6, v_7\}$
$F_4 = \{v_1, v_3, v_6, v_7\}$
$F_5 = \{v_2, v_4, v_6, v_8\}$
$F_6 = \{v_0, v_4, v_6, v_8\}$
$F_7 = \{v_0, v_2, v_4, v_8\}$
$F_8 = \{v_0, v_2, v_4, v_5, v_7\}$
$F_9 = \{v_1, v_2, v_4, v_6, v_7\}$
$F_{10} = \{v_0, v_1, v_3, v_4, v_5, v_6\}$
$F_{11} = \{v_1, v_4, v_5, v_7\}$

Figure 3.17: This is the facet list of a 4-polytope with f-vector $(9, 26, 29, 12)$ that we obtained by stacking one 4-polytope with f-vector $(8, 22, 23, 9)$.

(ii) $(9, 24, 26, 11)$: Take any of the 76 3-polytopes with f-vector $(8, 16, 10)$ and build a pyramid over it. In this way we can construct 76 4-polytopes with f-vector $(9, 24, 26, 11)$. One of these is shown in Figure 3.12. Additionally we could stack one of the 12 4-polytopes with f-vector $(8, 20, 20, 8)$, which yields 29 different 4-polytopes with f-vector $(9, 24, 26, 11)$.

(iii) $(9, 25, 27, 11)$: There are two 4-polytopes with f-vector $(8, 21, 21, 8)$. Both have a tetrahedron as facet on which we can stack to get a 4-polytope with f-vector $(9, 25, 27, 11)$. In total, we can construct four different polytopes in this way.
We also can perform a beneath/beyond operation with the polytope $(8^1_{21,24})$ from Figure 3.3. The facet $F_3 = \{v_0, v_4, v_6, v_7\}$ of this polytope is a tetrahedron, the vertex v_0 is non-simple, and the edges $\{v_0, v_4\}$, $\{v_0, v_6\}$, and $\{v_0, v_7\}$ are in four facets each. Therefore, we can place v_0 beneath/beyond on F_3 and obtain a 4-polytope $(9^{1900}_{25,27})$ with f-vector $(9, 25, 27, 11)$. The facet list of $(9^{1900}_{25,27})$ is shown in Figure 3.13. Starting from different polytopes, we can construct 48 different 4-polytopes in this way.

(iv) $(9, 26, 28, 11)$: The facet list and vertex coordinates for one 4-polytope with this f-vector are in Figure 3.14.

(v) $(9, 27, 29, 11)$: We will perform a beneath/beyond operation with the polytope $(8^{15}_{23,26})$ from Figure 3.4. The facet $F_1 = \{v_0, v_3, v_4, v_6\}$ of this polytope is a tetrahedron, the vertex v_4 is non-simple, and the edges $\{v_0, v_4\}$, $\{v_3, v_4\}$, and $\{v_4, v_6\}$ are in four facets each. Therefore, we can place v_4 beneath/beyond on F_1 and obtain a 4-polytope $(9^{53}_{27,29})$ with f-vector $(9, 27, 29, 11)$. The facet list of $(9^{53}_{27,29})$ is shown in Figure 3.15. Starting from different polytopes, we can construct 60 different 4-polytopes in this way.

(vi) $(9, 28, 30, 11)$: There are precisely three strongly regular 3-spheres with this f-vector, two of which are polytopes (see Figure 3.16), and one is non-polytopal.

3.1.5 Polytopes with f-vector $(9, m, m + 3, 12)$

As a result of the enumeration in Chapter 2, there are no strongly regular 3-spheres, and hence no 4-polytopes, with the f-vector $(9, m, m + 3, 12)$ for $m \leq 22$, and $m \geq 29$. The remaining cases are:

(i) $(9, 23, 26, 12)$: There is one 4-polytope with f-vector $(8, 19, 20, 9)$. Since it has a tetrahedral facet, we can stack on it to obtain a 4-polytope with f-vector $(9, 23, 26, 12)$. In total, we get three different 4-polytopes in this way.

$(9^{1363}_{27,30})$

$F_0 = \{v_0, v_2, v_4, v_5, v_8\}$	$F_4 = \{v_0, v_3, v_6, v_7\}$	$F_8 = \{v_0, v_1, v_3, v_5, v_7, v_8\}$
$F_1 = \{v_0, v_2, v_4, v_6\}$	$F_5 = \{v_1, v_3, v_6, v_7\}$	$F_9 = \{v_1, v_2, v_4, v_5, v_7\}$
$F_2 = \{v_2, v_5, v_7, v_8\}$	$F_6 = \{v_1, v_4, v_6, v_7\}$	$F_{10} = \{v_0, v_3, v_4, v_5, v_6\}$
$F_3 = \{v_0, v_2, v_6, v_7, v_8\}$	$F_7 = \{v_2, v_4, v_6, v_7\}$	$F_{11} = \{v_1, v_3, v_4, v_5, v_6\}$

Figure 3.18: This is the facet list of a 4-polytope with f-vector $(9, 27, 30, 12)$ that we obtained via the beneath/beyond operation on the polytope $(8^0_{23,27})$.

$(9^{100}_{28,31})$

$F_0 = \{v_0, v_2, v_4, v_7\}$	$F_4 = \{v_1, v_3, v_4, v_7\}$	$F_8 = \{v_0, v_2, v_4, v_5, v_6, v_8\}$
$F_1 = \{v_0, v_3, v_6, v_8\}$	$F_5 = \{v_1, v_3, v_5, v_7\}$	$F_9 = \{v_0, v_2, v_3, v_5, v_7\}$
$F_2 = \{v_0, v_3, v_4, v_7, v_8\}$	$F_6 = \{v_1, v_4, v_6, v_7\}$	$F_{10} = \{v_0, v_1, v_3, v_5, v_6\}$
$F_3 = \{v_1, v_3, v_4, v_6, v_8\}$	$F_7 = \{v_2, v_4, v_6, v_7\}$	$F_{11} = \{v_1, v_2, v_5, v_6, v_7\}$

Figure 3.19: This is the facet list of a 4-polytope with f-vector $(9, 28, 31, 12)$ that we obtained via the beneath/beyond operation on the polytope $(8^8_{24,28})$.

(ii) $(9, 24, 27, 12)$: There are 31 4-polytopes with f-vector $(8, 20, 21, 9)$, 11 of which are pyramids. All of these have a tetrahedron as facet on which we can stack to get in total 129 4-polytopes with f-vector $(9, 24, 27, 12)$.

(iii) $(9, 25, 28, 12)$: Take any 3-polytope with f-vector $(8, 17, 11)$ and build a pyramid over it. In this way we can construct 38 4-polytopes with f-vector $(9, 25, 28, 12)$. Additionally, we can stack one of the 37 4-polytopes with f-vector $(8, 21, 22, 9)$ to get in total 133 more 4-polytopes with f-vector $(9, 25, 28, 12)$.

(iv) $(9, 26, 29, 12)$: There are 7 4-polytopes with f-vector $(8, 22, 23, 9)$. All of these have a tetrahedron as a facet on which we can stack to get a 4-polytopes with f-vector $(9, 26, 29, 12)$. In total, we can construct 19 different 4-polytopes in this way. One of these is $(9^{2147}_{26,29})$ from Figure 3.17. We can construct 257 more 4-polytopes with this f-vector using the beneath/beyond operation.

(v) $(9, 27, 30, 12)$: We will perform a beneath/beyond operation with the polytope $(8^0_{23,27})$ from Figure 3.5. The facet $F_2 = \{v_0, v_2, v_5, v_7\}$ of this polytope is a tetrahedron, the vertex v_0 is non-simple, and the edges $\{v_0, v_2\}$, $\{v_0, v_5\}$, and $\{v_0, v_7\}$ are in four facets each. Therefore, we can place v_0 beneath/beyond on F_2 and obtain a 4-polytope $(9^{1363}_{27,30})$ with f-vector $(9, 27, 30, 12)$. The facet list of $(9^{1363}_{27,30})$ is shown in Figure 3.18. Starting from different polytopes, we can construct 516 different 4-polytopes in this way.

(vi) $(9, 28, 31, 12)$: We will perform a beneath/beyond operation with the polytope $(8^8_{24,28})$ from Figure 3.6. The facet $F_1 = \{v_0, v_3, v_4, v_6\}$ of this polytope is a tetrahedron, the vertex v_4 is non-simple, and the edges $\{v_0, v_4\}$, $\{v_3, v_4\}$, and $\{v_4, v_6\}$ are in four, resp. five facets each. Therefore, we can place v_4 beneath/beyond on F_1 and obtain a 4-polytope $(9^{100}_{28,31})$ with f-vector $(9, 28, 31, 12)$. The facet list of $(9^{100}_{28,31})$ is shown in Figure 3.19. Starting from different polytopes, we can construct 33 different 4-polytopes in this way.

$(9^{12}_{29,33})$

$F_0 = \{v_0, v_2, v_5, v_7\}$
$F_1 = \{v_0, v_2, v_5, v_8\}$
$F_2 = \{v_1, v_3, v_5, v_7\}$
$F_3 = \{v_1, v_3, v_6, v_8\}$
$F_4 = \{v_1, v_4, v_5, v_7\}$
$F_5 = \{v_1, v_4, v_5, v_8\}$
$F_6 = \{v_0, v_3, v_5, v_6, v_7\}$
$F_7 = \{v_0, v_2, v_3, v_6, v_8\}$
$F_8 = \{v_1, v_3, v_4, v_6, v_7\}$
$F_9 = \{v_2, v_4, v_5, v_7, v_8\}$
$F_{10} = \{v_0, v_2, v_4, v_6, v_7\}$
$F_{11} = \{v_0, v_1, v_3, v_5, v_8\}$
$F_{12} = \{v_1, v_2, v_4, v_6, v_8\}$

$v_0 = (28574669507189857/142389477734700, 1,$
$70362818914253729/427168433204100, -1/15)$
$v_1 = 1/(290617454696910775122700570849389469576955168584561766112728 1\ldots$
$\ldots 790244165525922825332611280995560639505296730980814117005128005 66)$
$(320851580877762580580458886201502332545703790652103187580859011527663 78\ldots$
$\ldots 155965642698411644353451327176291343723087863527361193281 35,$
$290617454696910775122700570849389469576955168584561766112728179024 4\ldots$
$\ldots 165525922825332611280995560639505296730980814117005128005660,$
$-417272899338216949986458526045253495207966159341763383283871132910\ldots$
$\ldots 511909534503287071497319314242430053875436989382812178802167015,$
$136467747643726275112950854318717320467947934353074278262617302582\ldots$
$\ldots 027792141663832830138193306411683834653926236507295871167420)$
$v_2 = (0, 10000, 0, 0)$
$v_3 = (0, 0, 10000, 0)$
$v_4 = (63930, 63883, 97033, 1023)$
$v_5 = (60080, 6003, -73830, 202)$
$v_6 = (14913, 26356, 60991, 404)$
$v_7 = 1/39539836381066428781413441628579768230205206040 8$
$(272017618176617330245752276273551477502835152506346 75,$
$232197689147812603018850435963834688931880072474598 00,$
$294105845656621494348086952786691153896447729097297 75,$
$383421658626273968987848530747849554217744421927200)$
$v_8 = 1/10397330064439359167693859514512013200094$
$(-113469957294796154054280100230844295901007599,$
$-907582941324911661747996997021753632236205 26,$
$-354323856463965163406904105220181439476568375,$
$-305398402579230010125582670761997028283750 0)$

Figure 3.20: These are the facet list and coordinates of a 4-polytope with f-vector $(9, 29, 33, 13)$.

3.1.6 Polytopes with f-vector $(9, m, m+4, 13)$

As a result of the enumeration in Chapter 2, there are no strongly regular 3-spheres, and hence no 4-polytopes, with the f-vector $(9, m, m+4, 13)$ for $m \leq 23$, and $m \geq 30$. The remaining cases are:

(i) $(9, 24, 28, 13)$: There are seven 4-polytopes with f-vector $(8, 20, 22, 10)$. All of these have a tetrahedron as a facet on which we can stack to get in total ten 4-polytopes with f-vector $(9, 24, 28, 13)$.

(ii) $(9, 25, 29, 13)$: There are 71 4-polytopes with f-vector $(8, 21, 23, 10)$, eight of which are pyramids. All of these have a tetrahedron as facet on which we can stack to get in total 354 4-polytopes with f-vector $(9, 25, 29, 13)$.

(iii) $(9, 26, 30, 13)$: Take any 3-polytope with f-vector $(8, 18, 12)$ and build a pyramid over it. In this way we can construct 14 4-polytopes with f-vector $(9, 26, 30, 13)$. Additionally, we can stack one of the 56 4-polytopes with f-vector $(8, 22, 24, 10)$ to get in total 295 more 4-polytopes with f-vector $(9, 26, 30, 13)$.

(iv) $(9, 27, 31, 13)$: There are three 4-polytopes with f-vector $(8, 23, 25, 10)$. All of these have a tetrahedron as facet on which we can stack to get in total 13 4-polytopes with f-vector $(9, 27, 31, 13)$.

(v) $(9, 28, 32, 13)$: We will perform a beneath/beyond operation with the polytope $(8^0_{24,29})$ from Figure 3.7. The facet $F_0 = \{v_0, v_3, v_4, v_6\}$ of this polytope is a tetrahedron, the vertex v_4 is non-simple, and the edges $\{v_0, v_4\}$, $\{v_3, v_4\}$, and $\{v_4, v_6\}$ are in four, resp. five facets each. Therefore, we can place v_4 beneath/beyond on F_0 and obtain a 4-polytope with f-vector $(9, 28, 32, 13)$. Starting from different polytopes, we can construct 470 different 4-polytopes in this way.

(vi) $(9, 29, 33, 13)$: One polytope with this f-vector can be found in Figure 3.20.

3.1.7 Polytopes with f-vector $(10, m, m, 10)$

As a result of the enumeration in Chapter 2, there are no strongly regular 3-spheres, and hence no 4-polytopes, with the f-vector $(10, m, m, 10)$ for $m \leq 22$ and $m \geq 31$. The remaining cases are:

(i) $(10, 23, 23, 10)$: There are precisely four strongly regular 3-spheres with this f-vector, all of which are polytopes. The facet lists and coordinates are in Figure 3.21.

(ii) $(10, 24, 24, 10)$: Take a prism over the triangle and triangulate such that a vertex remains simple (there is one combinatorial type of this; it has two simple vertices that cannot be distinguished: see Figure 3.22). This 3-polytope P has f-vector $(6, 12, 8)$. Now, take the pyramid over P, the two simple vertices remain simple (now in the 4-polytope $\mathrm{pyr}(P)$); the pyramid has f-vector $(7, 18, 20, 9)$, and we can truncate one of the simple vertices to get a 4-polytope with f-vector $(10, 24, 24, 10)$.

Figure 3.21

(10^0_{23})

$F_0 = \{v_0, v_3, v_5, v_7\}$
$F_1 = \{v_1, v_4, v_6, v_8\}$
$F_2 = \{v_1, v_4, v_6, v_9\}$
$F_3 = \{v_1, v_4, v_8, v_9\}$
$F_4 = \{v_2, v_6, v_8, v_9\}$
$F_5 = \{v_4, v_6, v_8, v_9\}$
$F_6 = \{v_0, v_2, v_3, v_5, v_8, v_9\}$
$F_7 = \{v_0, v_1, v_3, v_7, v_8, v_9\}$
$F_8 = \{v_0, v_1, v_2, v_5, v_6, v_7, v_8\}$
$F_9 = \{v_1, v_2, v_3, v_5, v_6, v_7, v_9\}$

$v_0 = (1000, 1000, 1000, 0)$
$v_1 = (0, 1000, 0, 0)$
$v_2 = (1000, 0, 0, 0)$
$v_3 = (1000, 1000, 1000, 1000)$
$v_4 = (-960, 10, 19, 9)$
$v_5 = (2000, 1000, 0, 0)$
$v_6 = (0, 0, 0, 0)$
$v_7 = (1000, 2000, 0, 0)$
$v_8 = (0, 0, 1000, 0)$
$v_9 = (0, 0, 1000, 1000)$

F_8

$v_0 = (1500, 1500, 1000)$
$v_1 = (0, 1000, 0)$
$v_2 = (1000, 0, 0)$
$v_3 = (1000, 1000, 500)$
$v_4 = (250, 500, 375)$
$v_5 = (2000, 1000, 0)$
$v_6 = (0, 0, 0)$
$v_7 = (1000, 2000, 0)$
$v_8 = (500, 500, 1000)$
$v_9 = (500, 500, 500)$

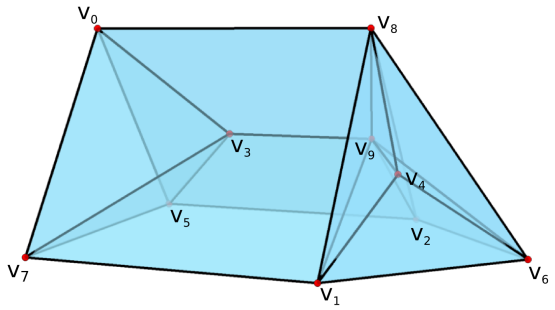

(10^1_{23})

$F_0 = \{v_0, v_3, v_5, v_8\}$
$F_1 = \{v_0, v_3, v_6, v_8\}$
$F_2 = \{v_1, v_4, v_7, v_9\}$
$F_3 = \{v_2, v_4, v_7, v_9\}$
$F_4 = \{v_0, v_1, v_3, v_5, v_7, v_9\}$
$F_5 = \{v_0, v_2, v_3, v_6, v_7, v_9\}$
$F_6 = \{v_0, v_1, v_4, v_5, v_7, v_8\}$
$F_7 = \{v_0, v_2, v_4, v_6, v_7, v_8\}$
$F_8 = \{v_1, v_3, v_4, v_5, v_8, v_9\}$
$F_9 = \{v_2, v_3, v_4, v_6, v_8, v_9\}$

$v_0 = (0, 0, 10, 0)$
$v_1 = (10, 10, 10, 90)$
$v_2 = (0, 0, 0, 100)$
$v_3 = (0, 10, 0, 0)$
$v_4 = (10, 0, 0, 100)$
$v_5 = (10, 10, 10, 10)$
$v_6 = (0, 0, 0, 0)$
$v_7 = (0, 0, 10, 100)$
$v_8 = (10, 0, 0, 0)$
$v_9 = (0, 10, 0, 100)$

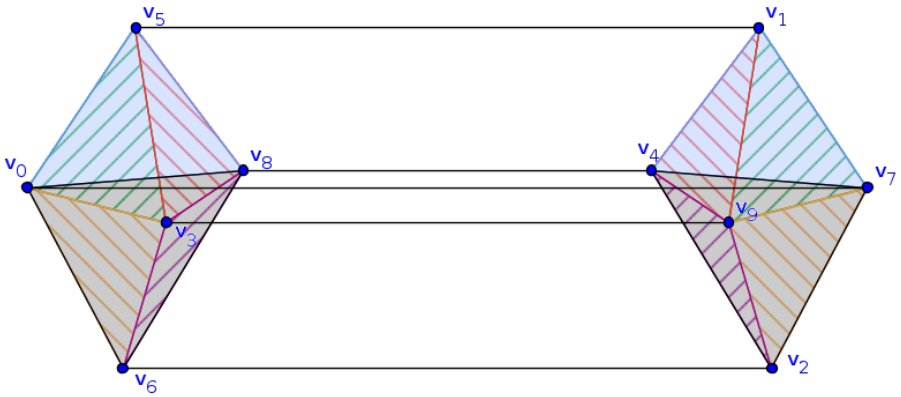

(10^2_{23})
$F_0 = \{v_6, v_7, v_8, v_9\}$
$F_1 = \{v_0, v_3, v_4, v_5\}$
$F_2 = \{v_1, v_2, v_4, v_5\}$
$F_3 = \{v_2, v_3, v_4, v_5\}$
$F_4 = \{v_0, v_1, v_2, v_3, v_4\}$
$F_5 = \{v_0, v_1, v_2, v_3, v_5\}$
$F_6 = \{v_0, v_4, v_5, v_6, v_8, v_9\}$
$F_7 = \{v_1, v_4, v_5, v_7, v_8, v_9\}$
$F_8 = \{v_0, v_1, v_4, v_6, v_7, v_8\}$
$F_9 = \{v_0, v_1, v_5, v_6, v_7, v_9\}$

$v_0 = (0, 0, 0, 0)$
$v_1 = (100, 0, 0, 0)$
$v_2 = (100, 100, 0, 0)$
$v_3 = (0, 100, 0, 0)$
$v_4 = (50, 50, 40, 0)$
$v_5 = (50, 50, 40, -100)$
$v_6 = (40, 12, 26, -20)$
$v_7 = (60, 12, 26, -20)$
$v_8 = (50, 22, 34, -20)$
$v_9 = (50, 22, 34, -40)$

$\underline{F_4}$
$v_0 = (0, 0, 0)$
$v_1 = (100, 0, 0)$
$v_2 = (100, 100, 0)$
$v_3 = (0, 100, 0)$
$v_4 = (50, 50, 40)$
$v_5 = (50, 50, 100)$
$v_6 = (40, 20, 25)$
$v_7 = (60, 20, 25)$
$v_8 = (30, 50, 33)$
$v_9 = (30, 50, 45)$

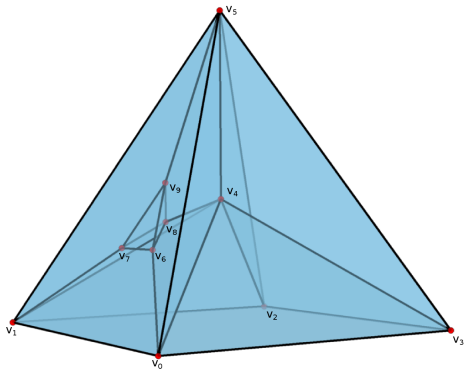

(10^3_{23})
$F_0 = \{v_0, v_6, v_7, v_8\}$
$F_1 = \{v_1, v_4, v_5, v_6, v_8, v_9\}$
$F_2 = \{v_2, v_3, v_4, v_5\}$
$F_3 = \{v_0, v_6, v_7, v_9\}$
$F_4 = \{v_2, v_4, v_5, v_7, v_8, v_9\}$
$F_5 = \{v_1, v_3, v_4, v_5\}$
$F_6 = \{v_0, v_6, v_8, v_9\}$
$F_7 = \{v_0, v_7, v_8, v_9\}$
$F_8 = \{v_1, v_2, v_3, v_4, v_6, v_7, v_8\}$
$F_9 = \{v_1, v_2, v_3, v_5, v_6, v_7, v_9\}$

Figure 3.21: These are the 4-polytopes with f-vector $(10, 23, 23, 10)$ found by our enumeration. (10^2_{23}) and (10^3_{23}) are dual to each other, the other two are self-dual. We show here the facet lists and coordinates for a realisation as convex polytope. Additionally there are a diagram each of (10^0_{23}) and (10^3_{23}) with coordinates given and a drawing of (10^2_{23}). This is basically the prism over the bipyramid over the triangle, but with the apices wiggled, so four tetrahedra appear. The triangles with the same colouring and style are matched by a prism over a triangle.

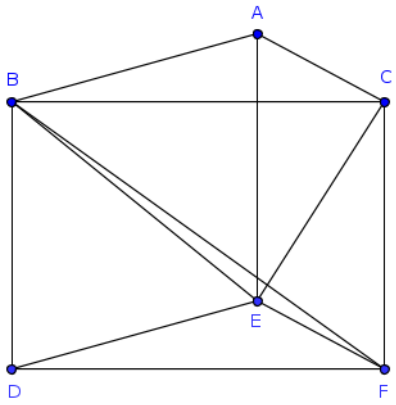

Figure 3.22: This figure shows a triangulation of the prism over the triangle with simple vertices (A, D).

(10^{1}_{26})
$F_0 = \{v_0, v_4, v_8, v_9\}$
$F_1 = \{v_1, v_6, v_7, v_9\}$
$F_2 = \{v_0, v_2, v_6, v_8, v_9\}$
$F_3 = \{v_3, v_4, v_7, v_8, v_9\}$
$F_4 = \{v_0, v_4, v_6, v_7, v_8\}$
$F_5 = \{v_0, v_4, v_6, v_7, v_9\}$
$F_6 = \{v_1, v_2, v_5, v_6, v_9\}$
$F_7 = \{v_1, v_3, v_5, v_7, v_9\}$
$F_8 = \{v_2, v_3, v_5, v_8, v_9\}$
$F_9 = \{v_1, v_2, v_3, v_5, v_6, v_7, v_8\}$

$v_0 = (787, 3170, 30, 30)$
$v_1 = (1000, 0, 1000, 1000)$
$v_2 = (0, 0, 0, 0)$
$v_3 = (0, 1000, 1000, 1000)$
$v_4 = (787, 3250, 110, 110)$
$v_5 = (0, 0, 1000, 1000)$
$v_6 = (1000, 0, 0, 0)$
$v_7 = (1000, 1000, 1000, 1000)$
$v_8 = (0, 1000, 0, 0)$
$v_9 = (1400, 8500, 100, 100)$

Figure 3.23: These are the facet list and coordinates for one of the 4-polytopes with f-vector $(10, 26, 26, 10)$ found by our enumeration. The coordinates were found with the oriented matroid approach (SCIP gave numerical coordinates, the exact ones had to be obtained by hand from these).

(10^{913}_{28})
$F_0 = \{v_0, v_1, v_2, v_3, v_4, v_5\}$
$F_1 = \{v_0, v_3, v_5, v_7\}$
$F_2 = \{v_0, v_1, v_2, v_6, v_8\}$
$F_3 = \{v_0, v_1, v_3, v_4, v_6, v_7, v_8\}$
$F_4 = \{v_2, v_6, v_8, v_9\}$
$F_5 = \{v_4, v_6, v_8, v_9\}$
$F_6 = \{v_1, v_2, v_4, v_5, v_6, v_9\}$
$F_7 = \{v_4, v_7, v_8, v_9\}$
$F_8 = \{v_0, v_2, v_5, v_7, v_8, v_9\}$
$F_9 = \{v_3, v_4, v_5, v_7, v_9\}$

$v_0 = (0, 0, 1, 2)$
$v_1 = (0, 1, 2, 1)$
$v_2 = (0, 1, 2, 2)$
$v_3 = (1, 0, 1, 1)$
$v_4 = (1, 1, 2, 0)$
$v_5 = (2, 2, 2, 1)$
$v_6 = (1, 1, 2, 2)$
$v_7 = (1, 2, 2, 0)$
$v_8 = (2, 0, 0, 1)$
$v_9 = (2, 2, 1, 0)$

Figure 3.24: These are the facet list and coordinates of a 4-polytopes with f-vector $(10, 28, 28, 10)$. The coordinates were found by a randomised approach that has also been used in [38].

$(10^{70}_{25,26})$

$F_0 = \{v_0, v_1, v_2, v_3\}$
$F_1 = \{v_0, v_2, v_3, v_4, v_5, v_6, v_7\}$
$F_2 = \{v_0, v_1, v_2, v_8\}$
$F_3 = \{v_0, v_2, v_4, v_6, v_8\}$
$F_4 = \{v_0, v_1, v_8, v_9\}$
$F_5 = \{v_0, v_1, v_3, v_9\}$
$F_6 = \{v_1, v_2, v_3, v_8, v_9\}$
$F_7 = \{v_0, v_4, v_5, v_8, v_9\}$
$F_8 = \{v_2, v_3, v_6, v_7, v_8, v_9\}$
$F_9 = \{v_4, v_5, v_6, v_7, v_8, v_9\}$
$F_{10} = \{v_0, v_3, v_5, v_7, v_9\}$

$v_0 = (0, 0, 2, 1)$
$v_1 = (0, 1, 1, 2)$
$v_2 = (0, 2, 0, 1)$
$v_3 = (0, 2, 2, 1)$
$v_4 = (1, 1, 1, 0)$
$v_5 = (1, 1, 2, 0)$
$v_6 = (1, 2, 0, 0)$
$v_7 = (1, 2, 2, 0)$
$v_8 = (2, 0, 1, 2)$
$v_9 = (2, 0, 2, 2)$

Figure 3.25: These are the facet list and coordinates of a 4-polytopes with f-vector $(10, 25, 26, 11)$. The coordinates were found by a randomised approach that has also been used in [38].

$(10^{9078}_{28,29})$

$F_0 = \{v_0, v_2, v_4, v_9\}$
$F_1 = \{v_0, v_2, v_5, v_8, v_9\}$
$F_2 = \{v_0, v_4, v_6, v_8, v_9\}$
$F_3 = \{v_1, v_3, v_6, v_8\}$
$F_4 = \{v_1, v_3, v_7, v_8\}$
$F_5 = \{v_1, v_4, v_6, v_8\}$
$F_6 = \{v_2, v_5, v_7, v_8\}$
$F_7 = \{v_3, v_5, v_7, v_8\}$
$F_8 = \{v_0, v_3, v_5, v_6, v_8\}$
$F_9 = \{v_1, v_2, v_4, v_7, v_8, v_9\}$
$F_{10} = \{v_0, v_1, v_2, v_3, v_4, v_5, v_6, v_7\}$

Figure 3.26: This is the facet list of the 4-polytopes with f-vector $(10, 28, 29, 11)$ that we obtained via the beneath/beyond operation on the polytope $(9^{11}_{24,26})$.

(iii) $(10, 25, 25, 10)$: Take any 3-polytope with f-vector $(9, 16, 9)$ and build a pyramid over it. This way we can construct 296 4-polytopes with f-vector $(10, 25, 25, 10)$.

(iv) $(10, 26, 26, 10)$: One example of a 4-polytope with this f-vector is shown in Figure 3.23.

(v) $(10, 27, 27, 10)$: We will perform a beneath/beyond operation with the polytope $(9^{33}_{23,24})$ from Figure 3.7. The facet $F_0 = \{v_0, v_3, v_6, v_8\}$ of this polytope is a tetrahedron, the vertex v_8 is non-simple, and the edges $\{v_0, v_8\}$, $\{v_3, v_8\}$, and $\{v_6, v_8\}$ are in four, resp. five facets each. Therefore, we can place v_8 beneath/beyond on F_0 and obtain a 4-polytope with f-vector $(10, 27, 27, 10)$. Starting from different polytopes, we can construct 82 different 4-polytopes in this way.

(vi) $(10, 28, 28, 10)$: One example of a 4-polytope with this f-vector is shown in Figure 3.24. With the beneath/beyond operation we can construct six other 4-polytopes with this f-vector.

(vii) $(10, 29, 29, 10)$: We can do a second beneath/beyond operation as described at the beginning of this section to the 4-polytope we have constructed with f-vector $(9, 25, 26, 10)$, since we had two independent choices of tetrahedra for the first beneath/beyond operation. Therefore, we get a 4-polytope with f-vector $(10, 29, 29, 10)$. Starting from different polytopes, we can construct 7 different 4-polytopes in this way.

(viii) $(10, 30, 30, 10)$: There are three 3-spheres with this f-vector, all of which are polytopes: the hypersimplex $\Delta_4(2)$ (see [35, p. 65]), its dual, and W_{10} (see [55, Sect. 4.1]).

$(10^1_{30,31})$

$F_0 = \{v_0, v_2, v_5, v_9\}$
$F_1 = \{v_0, v_4, v_6, v_8\}$
$F_2 = \{v_1, v_4, v_6, v_9\}$
$F_3 = \{v_0, v_2, v_4, v_6, v_9\}$
$F_4 = \{v_1, v_3, v_6, v_7, v_9\}$
$F_5 = \{v_1, v_3, v_4, v_6, v_8\}$
$F_6 = \{v_2, v_3, v_5, v_7, v_9\}$
$F_7 = \{v_1, v_2, v_4, v_7, v_9\}$
$F_8 = \{v_1, v_3, v_5, v_7, v_8\}$
$F_9 = \{v_0, v_3, v_5, v_6, v_8, v_9\}$
$F_{10} = \{v_0, v_1, v_2, v_4, v_5, v_7, v_8\}$

$v_0 = (20521463681081/3252460630, 6601, 6132, 6523)$
$v_1 = (-2307, -2668, -1675, -2181)$
$v_2 = (4509622001/568217, 4519939375/568217, 8278, 8206)$
$v_3 = (\frac{-25985124705405339698607404154044818563734760975365399977935389700058672756339419680240887662}{766595796705833631267546913272954229505659623865449444893172924362880641928656581418 5751}$,
$\frac{-76417836445276352492618413986580094568747996547330322448796134579361017742165212434281373534}{22997873901175008938026407398188626885169788715963483346795187730886419257859697442557253}$,
$\frac{-25930717387931103036322580668138542421907225376988584086395659750605758514936833539976222227}{766595796705833631267546913272954229505659623865449444893172924362880641928656581418 5751}$,
$\frac{-74612002567221463603584858340733930142608203423739211535177957825233625971274084834331283598}{22997873901175008938026407398188626885169788715963483346795187730886419257859697442557253})$
$v_4 = (4668, 4294, 4532, 3902)$
$v_5 = (9475961739/2601286, 5018450138/1300643, 3779, 4090)$
$v_6 = (\frac{260359927539115367267943447878919284 1633}{753974750091009917782027510496625 7880}, 189, -250,$
$-1402120313474421031643372033021/231816718436653272504647507 6)$
$v_7 = (-43, -293, 582, 214)$
$v_8 = (-26, 404, -539, 177)$
$v_9 = (5120, 5058, 5187, 4970)$

Figure 3.27: These are the facet list and coordinates of one of the 4-polytopes with f-vector $(10, 30, 31, 11)$ that was found by our enumeration.

3.1.8 Polytopes with f-vector $(10, m, m+1, 11)$

As a result of the enumeration in Chapter 2, there are no strongly regular 3-spheres, and hence no 4-polytopes, with the f-vector $(10, m, m+1, 11)$ for $m \leq 23$ and $m \geq 33$. The remaining cases are:

(i) $(10, 24, 25, 11)$: Take the pyramid over the bipyramid over the triangle. This 4-polytope P has simple vertices (the apices of the bipyramid) as well as tetrahedral facets (the pyramids over the triangular faces of the bipyramid). If we perform one truncation and one stacking operation on P, then we get a 4-polytope P' with f-vector $(10, 24, 25, 11)$. Since there are two simple vertices and six tetrahedral facets, we have several options to perform these operations.

(ii) $(10, 25, 26, 11)$: One example of a 4-polytope with this f-vector is shown in Figure 3.25.

(iii) $(10, 26, 27, 11)$: Take any 3-polytope with f-vector $(9, 17, 10)$ and build a pyramid over it. In this way we can construct 633 4-polytopes with f-vector $(10, 26, 27, 11)$.

(iv) $(10, 27, 28, 11)$: We will perform a beneath/beyond operation with the polytope $(9^0_{23,25})$ from Figure 3.11. The facet $F_1 = \{v_0, v_3, v_5, v_7\}$ of this polytope is a tetrahedron, the vertex v_7 is non-simple, and the edges $\{v_0, v_7\}$, $\{v_3, v_7\}$, and $\{v_5, v_7\}$ are in at least four facets each. Therefore, we can place v_7 beneath/beyond on F_1 and obtain a 4-polytope with f-vector $(10, 27, 28, 11)$. Starting from different polytopes, we can construct 22 different 4-polytopes in this way.

$(10^{0}_{25,27})$

$F_0 = \{v_0, v_2, v_4, v_6\}$
$F_1 = \{v_1, v_3, v_5, v_7\}$
$F_2 = \{v_0, v_2, v_4, v_8\}$
$F_3 = \{v_0, v_2, v_6, v_8\}$
$F_4 = \{v_0, v_1, v_3, v_6, v_7, v_8\}$
$F_5 = \{v_2, v_4, v_8, v_9\}$
$F_6 = \{v_0, v_3, v_4, v_5, v_7, v_8, v_9\}$
$F_7 = \{v_2, v_6, v_8, v_9\}$
$F_8 = \{v_2, v_4, v_6, v_9\}$
$F_9 = \{v_0, v_4, v_6, v_9\}$
$F_{10} = \{v_0, v_1, v_5, v_6, v_7, v_9\}$
$F_{11} = \{v_1, v_3, v_5, v_6, v_8, v_9\}$

$v_0 = (0, 0, 0, 1)$
$v_1 = (0, 0, 1, 0)$
$v_2 = (0.2, 0.1, 0.5, 1.3)$
$v_3 = (1, 0, 0, 0)$
$v_4 = (0.25, 0.25, 0, 1.5)$
$v_5 = (0, 1, 0, 0)$
$v_6 = (0, 0, 1, 1)$
$v_7 = (0, 0, 0, 0)$
$v_8 = (1, 0, 0, 1)$
$v_9 = (0, 1, 0, 1)$

Figure 3.28: These are the facet list and coordinates of a 4-polytopes with f-vector $(10, 25, 27, 12)$. The coordinates were found by a randomised approach that has also been used in [38].

(v) $(10, 28, 29, 11)$: We will perform a beneath/beyond operation with the polytope $(9^{11}_{24,26})$ from Figure 3.12. The facet $F_0 = \{v_0, v_2, v_4, v_8\}$ of this polytope is a tetrahedron, the vertex v_8 is non-simple, and the edges $\{v_0, v_8\}$, $\{v_2, v_8\}$, and $\{v_4, v_8\}$ are in at least four facets each. Therefore, we can place v_8 beneath/beyond on F_0 and obtain a 4-polytope with f-vector $(10, 28, 29, 11)$. Starting from different polytopes, we can construct 159 different 4-polytopes in this way.

(vi) $(10, 29, 30, 11)$: We will perform a beneath/beyond operation with the polytope $(9^{1900}_{25,27})$ from Figure 3.13. The facet $F_7 = \{v_1, v_5, v_6, v_7\}$ of this polytope is a tetrahedron, the vertex v_5 is non-simple, and the edges $\{v_1, v_5\}$, $\{v_5, v_6\}$, and $\{v_5, v_7\}$ are in four facets each. Therefore, we can place v_5 beneath/beyond on F_7 and obtain a 4-polytope with f-vector $(10, 29, 30, 11)$. Starting from different polytopes, we can construct 28 different 4-polytopes in this way.

(vii) $(10, 30, 31, 11)$: The facet list and coordinates for one 4-polytope with this f-vector are in Figure 3.27.

(viii) $(10, 31, 32, 11)$: We will perform a beneath/beyond operation with the polytope $(9^{53}_{27,29})$ from Figure 3.15. The facet $F_6 = \{v_1, v_3, v_4, v_7\}$ of this polytope is a tetrahedron, the vertex v_7 is non-simple, and the edges $\{v_1, v_7\}$, $\{v_3, v_7\}$, and $\{v_4, v_7\}$ are in four facets each. Therefore, we can place v_7 beneath/beyond on F_6 and obtain a 4-polytope with f-vector $(10, 31, 32, 11)$. Starting from different polytopes, we can construct 7 different 4-polytopes in this way.

(ix) $(10, 32, 33, 11)$: The two strongly regular 3-spheres with this f-vector are non-polytopal (Theorems 3.2.1 and 3.2.3).

3.1.9 Polytopes with f-vector $(10, m, m + 2, 12)$

As a result of the enumeration in Chapter 2, there are no strongly regular 3-spheres, and hence no 4-polytopes, with the f-vector $(10, m, m + 2, 12)$ for $m \leq 23$ and $m \geq 34$. The remaining cases are:

$(10^{240}_{26,28})$

$F_0 = \{v_0, v_1, v_2, v_3, v_4, v_5\}$
$F_1 = \{v_0, v_1, v_2, v_7\}$
$F_2 = \{v_1, v_2, v_5, v_7\}$
$F_3 = \{v_0, v_1, v_6, v_7\}$
$F_4 = \{v_1, v_5, v_6, v_7\}$
$F_5 = \{v_0, v_1, v_4, v_5, v_6, v_8\}$
$F_6 = \{v_5, v_6, v_7, v_8, v_9\}$
$F_7 = \{v_2, v_3, v_5, v_7, v_9\}$
$F_8 = \{v_0, v_4, v_6, v_7, v_8, v_9\}$
$F_9 = \{v_4, v_5, v_8, v_9\}$
$F_{10} = \{v_3, v_4, v_5, v_9\}$
$F_{11} = \{v_0, v_2, v_3, v_4, v_7, v_9\}$

$v_0 = (1, 0, 2, 0)$
$v_1 = (1, 0, 2, 1)$
$v_2 = (1, 1, 1, 0)$
$v_3 = (1, 2, 1, 0)$
$v_4 = (1, 2, 2, 0)$
$v_5 = (1, 2, 2, 2)$
$v_6 = (2, 0, 2, 1)$
$v_7 = (2, 1, 0, 0)$
$v_8 = (2, 1, 2, 1)$
$v_9 = (2, 2, 0, 0)$

Figure 3.29: These are the facet list and coordinates of a 4-polytopes with f-vector $(10, 26, 28, 12)$. The coordinates were found by a randomised approach that has also been used in [38].

$(10^{7373}_{30,32})$

$F_0 = \{v_0, v_1, v_2, v_3, v_4, v_5\}$
$F_1 = \{v_1, v_2, v_3, v_5, v_7\}$
$F_2 = \{v_1, v_3, v_6, v_7\}$
$F_3 = \{v_0, v_2, v_4, v_8\}$
$F_4 = \{v_1, v_6, v_7, v_8\}$
$F_5 = \{v_0, v_1, v_2, v_7, v_8\}$
$F_6 = \{v_6, v_7, v_8, v_9\}$
$F_7 = \{v_0, v_1, v_3, v_6, v_8, v_9\}$
$F_8 = \{v_0, v_3, v_4, v_9\}$
$F_9 = \{v_3, v_4, v_5, v_6, v_7, v_9\}$
$F_{10} = \{v_2, v_4, v_5, v_7, v_8, v_9\}$
$F_{11} = \{v_0, v_4, v_8, v_9\}$

$v_0 = (1, 1, 1, 3)$
$v_1 = (1, 2, 0, 3)$
$v_2 = (1, 2, 3, 3)$
$v_3 = (1, 3, 0, 2)$
$v_4 = (1, 3, 3, 1)$
$v_5 = (1, 3, 3, 2)$
$v_6 = (2, 3, 1, 2)$
$v_7 = (2, 3, 3, 3)$
$v_8 = (3, 1, 3, 3)$
$v_9 = (3, 3, 3, 1)$

Figure 3.30: These are the facet list and coordinates of a 4-polytopes with f-vector $(10, 30, 32, 12)$. The coordinates were found by a randomised approach that has also been used in [38].

(i) $(10, 24, 26, 12)$: The 4-polytope with f-vector $(9, 20, 20, 9)$ described above has a simplex facet. Stack on it to obtain a 4-polytope with f-vector $(10, 24, 26, 12)$.

(ii) $(10, 25, 27, 12)$: Take the 4-polytope with f-vector $(9, 20, 20, 9)$ (the stacked prism over the tetrahedron). Let us now place a new vertex beyond one of the tetrahedron facets, onto one of the hyperplanes defined by the facets that are triangular prisms, and beneath all other facet defining hyperplanes. The new polytope has an additional vertex, four additional edges, and replaces the tetrahedron by three new tetrahedra, while enlarging one of the triangular prisms. Therefore, the new polytope has f-vector $(9, 20, 19, 8)$. If we now place a tenth vertex beyond of two of the new tetrahedra, but beneath all other facets, we get a polytope P with an additional vertex, five additional edges, and we replace the two tetrahedra by six new tetrahedra. Hence, we obtain a polytope P' with f-vector $(10, 25, 27, 12)$.
The facet list and coordinates of this polytope, obtained by our construction, can be found in Figure 3.28.

(iii) $(10, 26, 28, 12)$: One example of a 4-polytope with this f-vector is shown in Figure 3.29. By stacking onto 4- olytopes with f-vector $(9, 22, 22, 9)$ we can construct in total 177 additional 4-polytopes with f-vector $(10, 26, 28, 12)$.

(iv) $(10, 27, 29, 12)$: Take any 3-polytope with f-vector $(9, 18, 11)$ and build a pyramid over it. In this way we can construct 768 4-polytopes with f-vector $(10, 27, 29, 12)$.

(v) $(10, 28, 30, 12)$: Take the bipyramid over the cube as one example. By stacking operations we can construct 204 more 4-polytopes with this f-vector, and with the beneath/beyond operation we get another 250 polytopes.

(vi) $(10, 29, 31, 12)$: The 4-polytope W_9 has a simplex facet. If we stack on that, we obtain a 4-polytope with f-vector $(10, 29, 31, 12)$. In total we can construct 17 4-polytopes with f-vector $(10, 29, 31, 12)$ in this way. Another 239 we get out of the beneath/beyond operation.

(vii) $(10, 30, 32, 12)$: One example of a 4-polytope with this f-vector is shown in Figure 3.30.

(viii) $(10, 31, 33, 12)$: We will perform a beneath/beyond operation with the polytope $(9^{1363}_{27,30})$ from Figure 3.18. The facet $F_4 = \{v_0, v_3, v_6, v_7\}$ of this polytope is a tetrahedron, the vertex v_6 is non-simple, and the edges $\{v_0, v_6\}$, $\{v_3, v_6\}$, and $\{v_6, v_7\}$ are in four, resp. five facets each. Therefore, we can place v_6 beneath/beyond on F_4 and obtain a 4-polytope with f-vector $(10, 31, 33, 12)$. Starting from different polytopes, we can construct 368 different 4-polytopes in this way.

(ix) $(10, 32, 34, 12)$: We will perform a beneath/beyond operation with the polytope $(9^{100}_{28,31})$ from Figure 3.19. The facet $F_4 = \{v_1, v_3, v_4, v_7\}$ of this polytope is a tetrahedron, the vertex v_7 is non-simple, and the edges $\{v_1, v_7\}$, $\{v_3, v_7\}$, and $\{v_4, v_7\}$ are in four facets each. Therefore, we can place v_7 beneath/beyond on F_4 and obtain a 4-polytope with f-vector $(10, 32, 34, 12)$. Starting from different polytopes, we can construct 7 4-polytopes in this way.

(x) $(10, 33, 35, 12)$: The unique strongly regular 3-sphere with this f-vector is non-polytopal (Theorem 3.2.5).

$$
\begin{array}{ll}
F_0 = \{v_0, v_2, v_4, v_5, v_6, v_7\} & v_0 = (0,0,1,0) \\
F_1 = \{v_0, v_1, v_2, v_3, v_5, v_7\} & v_1 = (0,0,2,1) \\
F_2 = \{v_0, v_1, v_4, v_5, v_8\} & v_2 = (0,2,1,0) \\
F_3 = \{v_4, v_5, v_6, v_7, v_9\} & v_3 = (0,2,2,1) \\
F_4 = \{v_4, v_5, v_8, v_9\} & v_4 = (1,0,1,0) \\
F_5 = \{v_0, v_1, v_2, v_3, v_8, v_{10}\} & v_5 = (1,0,2,0) \\
F_6 = \{v_2, v_3, v_7, v_{10}\} & v_6 = (1,1,1,0) \\
F_7 = \{v_1, v_3, v_5, v_7, v_8, v_9, v_{10}\} & v_7 = (1,1,2,0) \\
F_8 = \{v_4, v_6, v_8, v_9, v_{10}\} & v_8 = (2,0,2,2) \\
F_9 = \{v_0, v_2, v_4, v_6, v_8, v_{10}\} & v_9 = (2,1,2,1) \\
F_{10} = \{v_2, v_6, v_7, v_9, v_{10}\} & v_{10} = (2,2,2,2)
\end{array}
$$

Figure 3.31: These are the facet list and coordinates of a 4-polytopes with f-vector $(11, 29, 29, 11)$. The coordinates were found by a randomised approach that has also been used in [38].

3.1.10 Polytopes with other f-vectors and $f_0 = 10$

(i) $(10, 25, 28, 13)$: We will start with the prism over the tetrahedron, which has f-vector $(8, 16, 14, 6)$. Now, we stack one of the two tetrahedra, to get a 4-polytope P with f-vector $(9, 20, 20, 9)$. Finally, we can place a vertex v beyond two of the new facets of P and beneath all others. This adds another five edges, and substitutes the two tetrahedra beyond whom we placed v by six new tetrahedra. In total, we get a 4-polytope P' with f-vector $(10, 25, 28, 13)$.

(ii) $(10, 26, 29, 13)$: Take for example one of the 4-polytopes with f-vector $(9, 22, 23, 10)$ we constructed earlier. At least one of them has a tetrahedron as facet. Stack on this to obtain a 4-polytope with f-vector $(10, 26, 29, 13)$. In total we get 29 4-polytopes in this way.

(iii) $(10, 27, 32, 15)$: Take the 4-polytope with f-vector $(9, 23, 26, 12)$ we constructed earlier. This has a tetrahedron as facet on which we can stack to obtain a 4-polytope with f-vector $(10, 27, 32, 15)$. With this method we can construct nine 4-polytopes with this f-vector.

3.1.11 Polytopes with f-vector $(11, m, m, 11)$

As a result of the enumeration in Chapter 2, there are no strongly regular 3-spheres, and hence no 4-polytopes, with the f-vector $(11, m, m, 11)$ for $m \leq 25$ and $m \geq 36$. The remaining cases are:

(i) $(11, 26, 26, 11)$: Take the prism over the pyramid over the square, which has f-vector $(10, 21, 18, 7)$, and stack inside one of the pyr($square$)-facets. The resulting 4-polytope has f-vector $(11, 26, 26, 11)$.

$$
\begin{array}{ll}
F_0 = \{v_0, v_1, v_2, v_3, v_4, v_5, v_6, v_7\} & v_0 = (0,0,0,2) \\
F_1 = \{v_0, v_1, v_2, v_3, v_8\} & v_1 = (0,0,1,0) \\
F_2 = \{v_0, v_1, v_6, v_8, v_9\} & v_2 = (0,0,1,2) \\
F_3 = \{v_0, v_6, v_7, v_9\} & v_3 = (0,0,2,1) \\
F_4 = \{v_0, v_2, v_5, v_7, v_8, v_9, v_{10}\} & v_4 = (0,1,2,0) \\
F_5 = \{v_6, v_7, v_9, v_{10}\} & v_5 = (0,1,2,2) \\
F_6 = \{v_2, v_3, v_5, v_8, v_{10}\} & v_6 = (0,2,1,0) \\
F_7 = \{v_1, v_4, v_6, v_8, v_9, v_{10}\} & v_7 = (0,2,2,2) \\
F_8 = \{v_1, v_3, v_4, v_8, v_{10}\} & v_8 = (2,0,1,0) \\
F_9 = \{v_3, v_4, v_5, v_7, v_{10}\} & v_9 = (2,1,1,0) \\
F_{10} = \{v_4, v_6, v_7, v_{10}\} & v_{10} = (2,1,2,0)
\end{array}
$$

Figure 3.32: These are the facet list and coordinates of a 4-polytopes with f-vector $(11, 30, 30, 11)$. The coordinates were found by a randomised approach that has also been used in [38].

$$
\begin{array}{ll}
F_0 = \{v_0, v_1, v_2, v_5\} & v_0 = (0,2,0,0) \\
F_1 = \{v_0, v_1, v_3, v_6\} & v_1 = (0,2,2,2) \\
F_2 = \{v_0, v_1, v_4, v_5, v_6, v_7\} & v_2 = (1,2,0,2) \\
F_3 = \{v_1, v_2, v_5, v_8\} & v_3 = (1,2,2,0) \\
F_4 = \{v_0, v_2, v_4, v_5, v_8\} & v_4 = (2,0,0,0) \\
F_5 = \{v_0, v_3, v_4, v_6, v_9\} & v_5 = (2,0,0,2) \\
F_6 = \{v_0, v_4, v_8, v_9\} & v_6 = (2,0,2,0) \\
F_7 = \{v_0, v_1, v_2, v_3, v_8, v_9, v_{10}\} & v_7 = (2,0,2,1) \\
F_8 = \{v_1, v_3, v_6, v_7, v_9, v_{10}\} & v_8 = (2,2,2,1) \\
F_9 = \{v_4, v_5, v_6, v_7, v_8, v_9, v_{10}\} & v_9 = (2,2,0,2) \\
F_{10} = \{v_1, v_5, v_7, v_8, v_{10}\} & v_{10} = (2,2,2,0)
\end{array}
$$

Figure 3.33: These are the facet list and coordinates of a 4-polytopes with f-vector $(11, 31, 31, 11)$. The coordinates were found by a randomised approach that has also been used in [38].

$$
\begin{array}{ll}
F_0 = \{v_0, v_1, v_2, v_3, v_4, v_5\} & v_0 = (0,0,1,2) \\
F_1 = \{v_0, v_1, v_3, v_6\} & v_1 = (0,0,2,0) \\
F_2 = \{v_0, v_1, v_2, v_6, v_7, v_8\} & v_2 = (0,0,2,1) \\
F_3 = \{v_0, v_2, v_4, v_8\} & v_3 = (0,1,0,2) \\
F_4 = \{v_1, v_2, v_5, v_9\} & v_4 = (0,1,1,2) \\
F_5 = \{v_1, v_2, v_7, v_8, v_9\} & v_5 = (0,2,1,1) \\
F_6 = \{v_3, v_4, v_5, v_{10}\} & v_6 = (2,0,0,1) \\
F_7 = \{v_1, v_3, v_5, v_6, v_7, v_9, v_{10}\} & v_7 = (2,0,1,0) \\
F_8 = \{v_6, v_7, v_8, v_9, v_{10}\} & v_8 = (2,0,1,1) \\
F_9 = \{v_0, v_3, v_4, v_6, v_8, v_{10}\} & v_9 = (2,1,1,0) \\
F_{10} = \{v_2, v_4, v_5, v_8, v_9, v_{10}\} & v_{10} = (2,2,0,1)
\end{array}
$$

Figure 3.34: These are the facet list and coordinates of a 4-polytopes with f-vector $(11, 33, 33, 11)$. The coordinates were found by a randomised approach that has also been used in [38].

(ii) $(11, 27, 27, 11)$: Take the pyramid over the square and stack on a triangle to get a 3-polytope P with f-vector $(7, 14, 9)$ and a simple vertex (the new vertex). The pyramid $\mathrm{pyr}(P)$ has f-vector $(8, 21, 23, 10)$ and contains a simple vertex. Truncate this vertex to get a 4-polytope with f-vector $(11, 27, 27, 11)$.

(iii) $(11, 28, 28, 11)$: Take any 3-polytope with f-vector $(10, 18, 10)$ and build a pyramid over it. This way we can construct 2635 4-polytopes with f-vector $(11, 28, 28, 11)$.

(iv) $(11, 29, 29, 11)$: One example of a 4-polytope with this f-vector is shown in Figure 3.31.

(v) $(11, 30, 30, 11)$: One example of a 4-polytope with this f-vector is shown in Figure 3.32.

(vi) $(11, 31, 31, 11)$: One example of a 4-polytope with this f-vector is shown in Figure 3.33.

(vii) $(11, 32, 32, 11)$: We will perform a beneath/beyond operation with the polytope $(10^{9078}_{28,29})$ from Figure 3.26. The facet $F_3 = \{v_1, v_3, v_6, v_8\}$ of this polytope is a tetrahedron, the vertex v_8 is non-simple, and the edges $\{v_1, v_8\}$, $\{v_3, v_8\}$, and $\{v_6, v_8\}$ are in four facets each. Therefore, we can place v_8 beneath/beyond on F_3 and obtain a 4-polytope with f-vector $(11, 32, 32, 11)$. Starting from different polytopes, we can construct 104 4-polytopes in this way.

(viii) $(11, 33, 33, 11)$: One example of a 4-polytope with this f-vector is shown in Figure 3.34.

(ix) $(11, 34, 34, 11)$: The polytope P_{11} from [55, Sect. 4.1] has this f-vector.

(x) $(11, 35, 35, 11)$: The two strongly regular 3-spheres with this f-vector are non-polytopal (Theorem 3.2.7).

3.2 3-Spheres

In this section we will show non-polytopality of some of the strongly regular 3-spheres that were found in the enumeration of Chapter 2. We will do this via the oriented matroid approach explained at the beginning of this chapter.

3.2.1 The spheres with f-vector $(10, 32, 33, 11)$

The enumeration from Chapter 2 gives that there are preciseley two strongly regular 3-spheres with this f-vector. Since the f-vector is non-symmetric, they cannot be duals. Therefore, we have to check non-polytopality of both.

Theorem 3.2.1. *The sphere* $(10^{0}_{32,33})$ *is non-polytopal.*

Figure 3.35

$(10^0_{32,33})$

$F_0 = \{v_0, v_2, v_4, v_5, v_9\}$
$F_1 = \{v_0, v_2, v_4, v_6, v_8\}$
$F_2 = \{v_1, v_3, v_6, v_7, v_9\}$
$F_3 = \{v_1, v_3, v_4, v_6, v_8\}$
$F_4 = \{v_0, v_2, v_5, v_7, v_8\}$
$F_5 = \{v_1, v_3, v_5, v_7, v_8\}$
$F_6 = \{v_0, v_1, v_4, v_6, v_9\}$
$F_7 = \{v_2, v_3, v_5, v_7, v_9\}$
$F_8 = \{v_1, v_2, v_4, v_7, v_8\}$
$F_9 = \{v_1, v_2, v_4, v_7, v_9\}$
$F_{10} = \{v_0, v_3, v_5, v_6, v_8, v_9\}$

$\underline{F_0}$
$v_0 = (1000, 0, 0)$
$v_1 = (2392813869/13207550, 381, 276)$
$v_2 = (2090, 170, 9922)$
$v_3 = (6424, 8503, 7556)$
$v_4 = (0, 0, 0)$
$v_5 = (8777, 9816, 9824)$
$v_6 = (824, 986, 741)$
$v_7 = (2853, 5415, 5279)$
$v_8 = (1626, 1854, 1794)$
$v_9 = (2475, 9921, 173)$

$\underline{F_1}$
$v_0 = (7981, 7859, 3376)$
$v_1 = (5371881977/730222, 7122, 7709)$
$v_2 = (0, 0, 0)$
$v_3 = (7754, 7611, 7158)$
$v_4 = (7844, 7087, 8215)$
$v_5 = (5684, 5640, 4911)$
$v_6 = (7847, 7653, 7106)$
$v_7 = (1930, 1923, 2023)$
$v_8 = (7640, 8545, 8112)$
$v_9 = (7318, 7134, 6591)$

$\underline{F_2}$
$v_0 = (906, 197, 915)$
$v_1 = (228623/5810, 18, 986)$
$v_2 = (90, 942, 119)$
$v_3 = (983, 18, 10)$
$v_4 = (485, 502, 941)$
$v_5 = (448, 647, 296)$
$v_6 = (974, 18, 908)$
$v_7 = (18, 977, 14)$
$v_8 = (665, 333, 592)$
$v_9 = (983, 990, 985)$

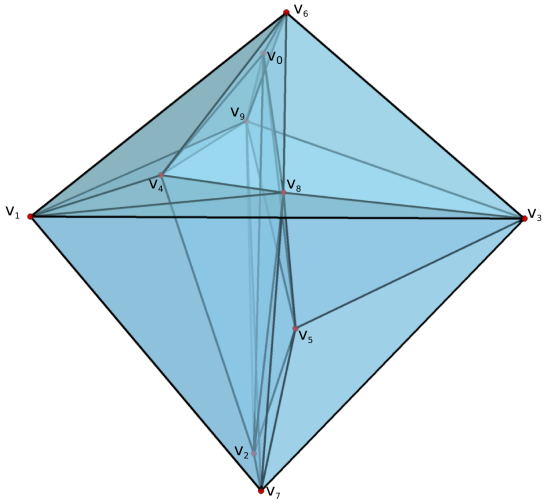

$\underline{F_3}$
$v_0 = (703, 448, 352)$
$v_1 = (708266/17855, 10, 983)$
$v_2 = (880, 90, 57)$
$v_3 = (91, 974, 981)$
$v_4 = (985, 18, 22)$
$v_5 = (84, 906, 802)$
$v_6 = (989, 983, 981)$
$v_7 = (58, 485, 497)$
$v_8 = (14, 983, 9)$
$v_9 = (407, 665, 666)$

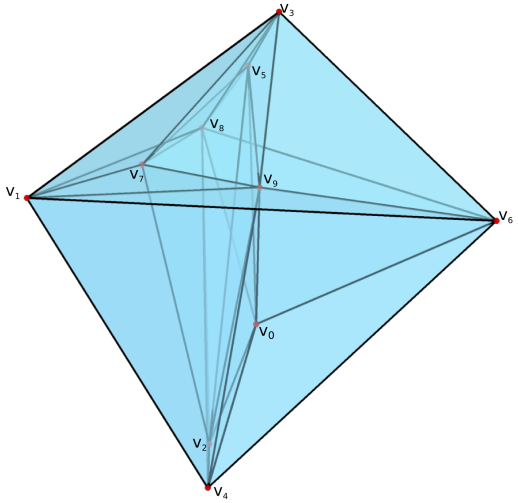

Figure 3.35

$\underline{F_4}$
$v_0 = (1246, 1435, 392)$
$v_1 = (247090199/211895, 1147, 2340)$
$v_2 = (0, 0, 0)$
$v_3 = (1364, 1586, 1319)$
$v_4 = (974, 390, 500)$
$v_5 = (1671, 3216, 1296)$
$v_6 = (1291, 1293, 446)$
$v_7 = (1139, 1306, 2761)$
$v_8 = (3126, 1046, 1277)$
$v_9 = (1242, 1444, 807)$

$\underline{F_5}$
$v_0 = (4899, 4062, 4834)$
$v_1 = (6032911744/1202089, 7287, 2570)$
$v_2 = (4891, 4775, 5244)$
$v_3 = (4267, 2905, 3485)$
$v_4 = (5164, 6695, 3058)$
$v_5 = (4691, 3910, 4916)$
$v_6 = (5052, 5091, 3653)$
$v_7 = (3331, 4668, 6618)$
$v_8 = (6697, 4400, 4280)$
$v_9 = (4711, 4234, 4649)$

$\underline{F_6}$
$v_0 = (15912, 7963, 10803)$
$v_1 = (6927, 23734, 19696)$
$v_2 = (7858, 8406, 1158)$
$v_3 = (14951, 14410, 15415)$
$v_4 = (1, 7, 222)$
$v_5 = (15331, 8769, 9222)$
$v_6 = (24766, 13072, 28804)$
$v_7 = (82639117319/10873358, 21326, 16203)$
$v_8 = (14794, 10433, 12426)$
$v_9 = (23451, 23521, 2)$

$\underline{F_7}$
$v_0 = (56526, 53907, 72852)$
$v_1 = (60147, 64874, 50685)$
$v_2 = (63121, 32157, 95245)$
$v_3 = (56822, 74239, 49380)$
$v_4 = (61846, 35512, 90754)$
$v_5 = (55365, 67804, 73783)$
$v_6 = (54606, 72640, 49095)$
$v_7 = (3321754766/35161, 58527, 56600)$
$v_8 = (58315, 65444, 59285)$
$v_9 = (30376, 70655, 44286)$

$(10^1_{32,33})$
$F_0 = \{v_0, v_3, v_5, v_6, v_8\}$
$F_1 = \{v_0, v_4, v_5, v_7, v_8\}$
$F_2 = \{v_0, v_3, v_4, v_6, v_7\}$
$F_3 = \{v_0, v_1, v_3, v_5, v_7\}$
$F_4 = \{v_1, v_3, v_5, v_8, v_9\}$
$F_5 = \{v_1, v_3, v_6, v_7, v_9\}$
$F_6 = \{v_0, v_2, v_4, v_6, v_8\}$
$F_7 = \{v_2, v_4, v_6, v_7, v_9\}$
$F_8 = \{v_2, v_4, v_5, v_8, v_9\}$
$F_9 = \{v_1, v_4, v_5, v_7, v_9\}$
$F_{10} = \{v_2, v_3, v_6, v_8, v_9\}$

$\underline{F_0}$
$v_0 = (11, 10, 26)$
$v_1 = (13, 16, 10)$
$v_2 = (9, 10, 11)$
$v_3 = (16, 8, 10)$
$v_4 = (9, 11, 14)$
$v_5 = (12, 24, 9)$
$v_6 = (11, 9, 11)$
$v_7 = (11, 14, 16)$
$v_8 = (5, 10, 8)$
$v_9 = (11, 13, 10)$

$\underline{fan}$
$v_0 = (100, 0, 0, 0)$
$v_1 = (0, 100, 0, 0)$
$v_2 = (0, 0, 100, 100)$
$v_3 = (0, 0, 0, 0)$
$v_4 = (108, 45, 64, 64)$
$v_5 = (-53, -54, -130, -130)$
$v_6 = (103, 2, 125, 125)$
$v_7 = (141, 135, 20, 20)$
$v_8 = (-83, -159, -23, -23)$
$v_9 = (-74, 98, 114, 114)$
$o = (-2, 8, 24, 24)$

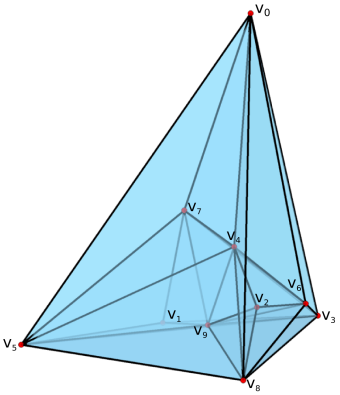

Figure 3.35

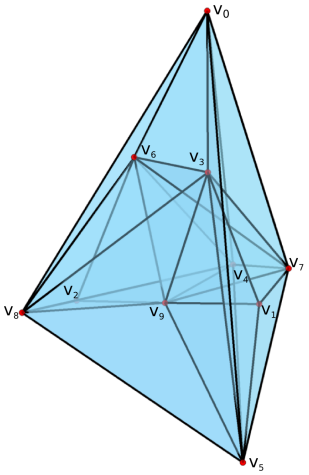

$\underline{F_1}$
$v_0 = (196, 203, 529)$
$v_1 = (232, 378, 286)$
$v_2 = (417, 212, 239)$
$v_3 = (243, 295, 401)$
$v_4 = (234, 235, 241)$
$v_5 = (296, 510, 214)$
$v_6 = (308, 214, 398)$
$v_7 = (191, 348, 296)$
$v_8 = (484, 190, 230)$
$v_9 = (321, 296, 261)$

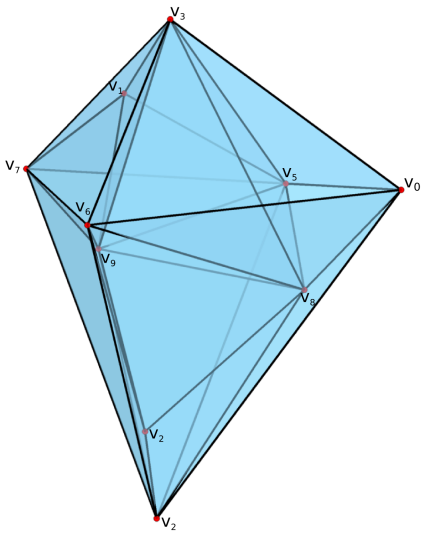

$\underline{F_2}$
$v_0 = (98, 98, 97)$
$v_1 = (7, 90, 64)$
$v_2 = (68, 7, 30)$
$v_3 = (1, 91, 97)$
$v_4 = (96, 1, 1)$
$v_5 = (68, 92, 74)$
$v_6 = (3, 1, 97)$
$v_7 = (3, 98, 1)$
$v_8 = (90, 64, 66)$
$v_9 = (26, 46, 44)$

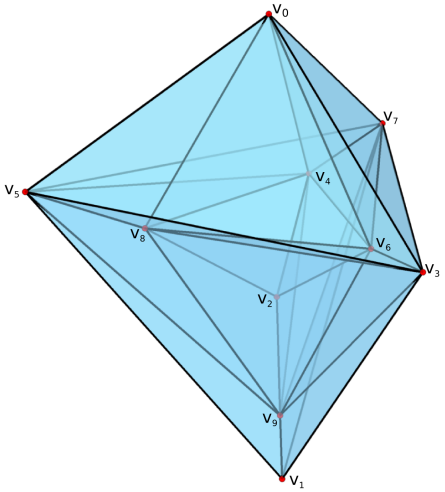

$\underline{F_3}$
$v_0 = (3, 96, 96)$
$v_1 = (97, 2, 2)$
$v_2 = (56, 43, 43)$
$v_3 = (2, 1, 97)$
$v_4 = (72, 83, 69)$
$v_5 = (2, 97, 1)$
$v_6 = (30, 27, 83)$
$v_7 = (98, 97, 97)$
$v_8 = (16, 69, 27)$
$v_9 = (82, 17, 17)$

$\underline{F_4}$
$v_0 = (234, 309, 255)$
$v_1 = (541, 194, 423)$
$v_2 = (213, 249, 239)$
$v_3 = (157, 115, 352)$
$v_4 = (324, 265, 291)$
$v_5 = (195, 548, 120)$
$v_6 = (212, 175, 317)$
$v_7 = (434, 215, 371)$
$v_8 = (91, 447, 113)$
$v_9 = (228, 193, 246)$

$\underline{F_5}$
$v_0 = (110, 191, 118)$
$v_1 = (27, 0, 354)$
$v_2 = (206, 76, 71)$
$v_3 = (50, 459, 69)$
$v_4 = (151, 85, 116)$
$v_5 = (69, 52, 265)$
$v_6 = (147, 278, 35)$
$v_7 = (141, 78, 109)$
$v_8 = (116, 134, 160)$
$v_9 = (280, 15, 17)$

$\underline{F_6}$
$v_0 = (19, 15, 37)$
$v_1 = (14, 15, 16)$
$v_2 = (17, 11, 15)$
$v_3 = (21, 12, 36)$
$v_4 = (2, 14, 0)$
$v_5 = (10, 25, 7)$
$v_6 = (28, 6, 55)$
$v_7 = (9, 13, 11)$
$v_8 = (9, 32, 4)$
$v_9 = (15, 13, 15)$

$\underline{F_7}$
$v_0 = (28, 38, 41)$
$v_1 = (52, 53, 30)$
$v_2 = (43, 32, 56)$
$v_3 = (41, 62, 41)$
$v_4 = (3, 0, 37)$
$v_5 = (41, 37, 39)$
$v_6 = (36, 70, 46)$
$v_7 = (22, 33, 25)$
$v_8 = (40, 35, 50)$
$v_9 = (72, 63, 27)$

$\underline{F_8}$
$v_0 = (33, 40, 33)$
$v_1 = (19, 20, 23)$
$v_2 = (50, 18, 24)$
$v_3 = (32, 28, 23)$
$v_4 = (27, 30, 53)$
$v_5 = (21, 58, 30)$
$v_6 = (43, 22, 26)$
$v_7 = (25, 25, 40)$
$v_8 = (36, 71, 26)$
$v_9 = (13, 2, 14)$

$\underline{F_9}$
$v_0 = (256, 233, 270)$
$v_1 = (185, 146, 345)$
$v_2 = (253, 225, 183)$
$v_3 = (197, 183, 307)$
$v_4 = (301, 248, 153)$
$v_5 = (127, 400, 160)$
$v_6 = (232, 206, 245)$
$v_7 = (317, 205, 293)$
$v_8 = (207, 278, 184)$
$v_9 = (255, 202, 182)$

$\underline{F_{10}}$
$v_0 = (105, 191, 219)$
$v_1 = (337, 127, 99)$
$v_2 = (113, 188, 180)$
$v_3 = (123, 107, 316)$
$v_4 = (134, 186, 179)$
$v_5 = (139, 285, 94)$
$v_6 = (40, 61, 417)$
$v_7 = (216, 125, 190)$
$v_8 = (36, 425, 35)$
$v_9 = (502, 44, 49)$

Figure 3.35: These are the two 3-spheres with f-vector $(10, 32, 33, 11)$. Both spheres are non-polytopal. The first does not have a diagram based on one of the facets F_8, F_9, or F_{10}, and has no fan-like embedding. The second sphere has all diagrams, is fan-like, but we couldn't decide the existence of a star-shaped embedding.

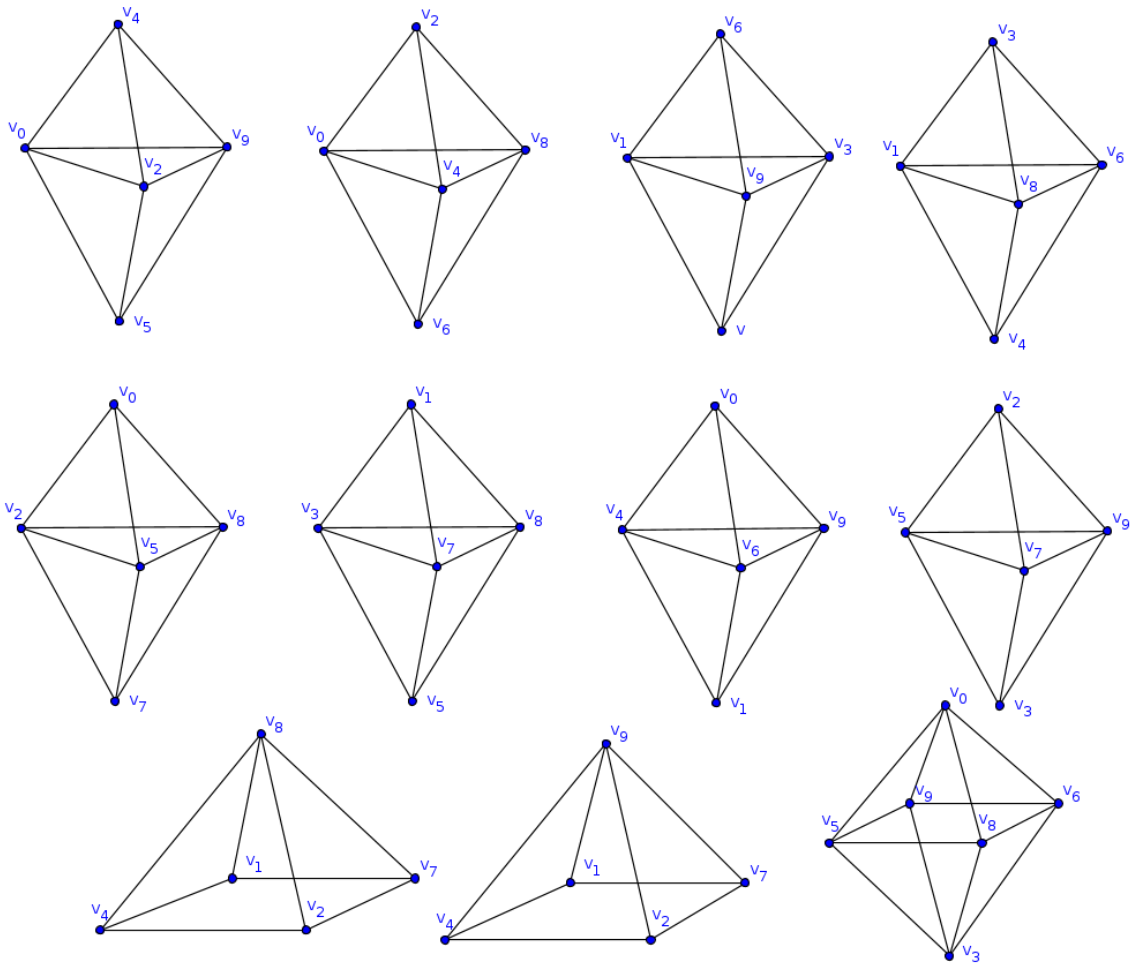

Figure 3.36: These are the facets of the sphere $(10^0_{32,33})$ from F_0 (top left) to F_{10} (bottom right).

Proof. Since five points in a common facet are colinear, we get:

$$\chi(v_3, v_5, v_6, v_8, v_9) \overset{F_{10}}{=} 0. \tag{3.1}$$

From facet F_0 we may choose $\chi(v_0\ , v_2\ , v_4\ , v_9\ , v_i\ ) = \ \ 1$ (see Figure 3.36 for an image of F_0), where $v_i \notin F_0$. With this we can derive:

$$\chi(v_0, v_1, v_2, v_4, v_9) = -1 \overset{F_9}{\Rightarrow} \chi(v_1, v_2, v_4, v_5, v_9) = \ \ 1 \overset{F_0}{\Rightarrow} \chi(v_2, v_4, v_5, v_8, v_9) = -1, \tag{3.2}$$

$$\begin{aligned}\chi(v_0, v_2, v_4, v_8, v_9) = -1 &\overset{F_1}{\Rightarrow} \chi(v_0, v_1, v_2, v_4, v_8) = \ \ 1 \overset{F_8}{\Rightarrow} \chi(v_1, v_2, v_4, v_6, v_8) = -1\\ &\overset{F_1}{\Rightarrow} \chi(v_2, v_4, v_6, v_8, v_9) = -1,\end{aligned} \tag{3.3}$$

$$\chi(v_0, v_2, v_4, v_8, v_9) = -1 \overset{F_1}{\Rightarrow} \chi(v_0, v_2, v_4, v_7, v_8) = \ \ 1 \overset{F_8}{\Rightarrow} \chi(v_2, v_4, v_7, v_8, v_9) = \ \ 1, \tag{3.4}$$

$$\begin{aligned}\chi(v_0, v_2, v_4, v_8, v_9) = -1 &\overset{F_1}{\Rightarrow} \chi(v_0, v_2, v_4, v_5, v_8) = \ \ 1 \overset{F_4}{\Rightarrow} \chi(v_0, v_2, v_5, v_6, v_8) = -1\\ &\overset{F_1}{\Rightarrow} \chi(v_0, v_2, v_3, v_6, v_8) = -1 \overset{F_{10}}{\Rightarrow} \chi(v_0, v_1, v_3, v_6, v_8) = -1\\ &\overset{F_3}{\Rightarrow} \chi(v_1, v_3, v_6, v_8, v_9) = -1 \overset{F_{10}}{\Rightarrow} \chi(v_2, v_3, v_6, v_8, v_9) = -1,\end{aligned} \tag{3.5}$$

$$\begin{aligned}\chi(v_0, v_2, v_4, v_6, v_9) = -1 &\overset{F_1}{\Rightarrow} \chi(v_0, v_1, v_2, v_4, v_6) = \ \ 1 \overset{F_6}{\Rightarrow} \chi(v_0, v_1, v_4, v_6, v_8) = \ \ 1\\ &\overset{F_3}{\Rightarrow} \chi(v_1, v_4, v_6, v_8, v_9) = \ \ 1,\end{aligned} \tag{3.6}$$

$$\begin{aligned}\chi(v_0, v_2, v_4, v_5, v_8) = \ \ 1 &\overset{F_4}{\Rightarrow} \chi(v_0, v_2, v_3, v_5, v_8) = \ \ 1 \overset{F_{10}}{\Rightarrow} \chi(v_0, v_3, v_5, v_7, v_8) = \ \ 1\\ &\overset{F_4}{\Rightarrow} \chi(v_0, v_1, v_5, v_7, v_8) = \ \ 1 \overset{F_5}{\Rightarrow} \chi(v_1, v_5, v_7, v_8, v_9) = \ \ 1,\end{aligned} \tag{3.7}$$

$$\begin{aligned}\chi(v_0, v_1, v_2, v_4, v_6) \overset{(3.6)}{=} \ \ 1 &\overset{F_6}{\Rightarrow} \chi(v_0, v_1, v_3, v_4, v_6) = \ \ 1 \overset{F_3}{\Rightarrow} \chi(v_1, v_3, v_4, v_6, v_9) = \ \ 1\\ &\overset{F_2}{\Rightarrow} \chi(v_0, v_1, v_3, v_6, v_9) = \ \ 1 \overset{F_{10}}{\Rightarrow} \chi(v_0, v_3, v_6, v_7, v_9) = \ \ 1\\ &\overset{F_2}{\Rightarrow} \chi(v_3, v_6, v_7, v_8, v_9) = -1,\end{aligned} \tag{3.8}$$

$$\chi(v_0, v_1, v_3, v_6, v_9) \overset{(3.8)}{=} \ \ 1 \overset{F_6}{\Rightarrow} \chi(v_0, v_1, v_6, v_7, v_9) = -1 \overset{F_2}{\Rightarrow} \chi(v_1, v_6, v_7, v_8, v_9) = \ \ 1, \tag{3.9}$$

$$\chi(v_0, v_2, v_3, v_6, v_8) \overset{(3.5)}{=} -1 \overset{F_{10}}{\Rightarrow} \chi(v_0, v_3, v_4, v_6, v_8) = \ \ 1 \overset{F_3}{\Rightarrow} \chi(v_3, v_4, v_6, v_8, v_9) = \ \ 1, \tag{3.10}$$

$$\begin{aligned}\chi(v_0, v_2, v_4, v_7, v_8) \overset{(3.4)}{=} \ \ 1 &\overset{F_4}{\Rightarrow} \chi(v_0, v_1, v_2, v_7, v_8) = -1 \overset{F_8}{\Rightarrow} \chi(v_1, v_2, v_5, v_7, v_8) = -1\\ &\overset{F_4}{\Rightarrow} \chi(v_2, v_5, v_7, v_8, v_9) = -1,\end{aligned} \tag{3.11}$$

$$\chi(v_0, v_1, v_2, v_7, v_8) \overset{(3.11)}{=} -1 \overset{F_8}{\Rightarrow} \chi(v_1, v_2, v_3, v_7, v_8) = -1 \overset{F_5}{\Rightarrow} \chi(v_1, v_3, v_7, v_8, v_9) = \ \ 1, \tag{3.12}$$

$$\chi(v_0, v_3, v_5, v_7, v_8) \overset{(3.7)}{=} \ \ 1 \overset{F_5}{\Rightarrow} \chi(v_3, v_5, v_7, v_8, v_9) = \ \ 1, \tag{3.13}$$

With these values for the partial chirotope, we can find some new values of χ using the Grassmann-Plücker-relations:

$$\begin{aligned}\{\chi(v_7,v_8,v_9,v_1,v_3)\chi(v_7,v_8,v_9,v_5,v_6), &\quad \chi(v_7,v_8,v_9,v_1,v_5)\chi(v_7,v_8,v_9,v_3,v_6),\\ &\quad \chi(v_7,v_8,v_9,v_1,v_6)\chi(v_7,v_8,v_9,v_3,v_5)\}\\ \overset{(3.12),(3.7),(3.8),(3.9),(3.13)}{=} \{1\cdot\chi(v_7,v_8,v_9,v_5,v_6), &\quad -1\cdot(-1),\\ &\quad 1\cdot 1\},\\ &\quad \Rightarrow \chi(v_7,v_8,v_9,v_5,v_6)=-1, \end{aligned} \tag{3.14}$$

$$\begin{aligned}\{\chi(v_6,v_8,v_9,v_2,v_3)\chi(v_6,v_8,v_9,v_5,v_7), &\quad \chi(v_6,v_8,v_9,v_2,v_5)\chi(v_6,v_8,v_9,v_3,v_7),\\ &\quad \chi(v_6,v_8,v_9,v_2,v_7)\chi(v_6,v_8,v_9,v_3,v_5)\}\\ \overset{(3.5),(3.14),(3.8),(3.1)}{=} \{(-1)\cdot 1, &\quad -\chi(v_6,v_8,v_9,v_2,v_5)\cdot 1,\\ &\quad 0\},\\ &\quad \Rightarrow \chi(v_6,v_8,v_9,v_2,v_5)=-1, \end{aligned} \tag{3.15}$$

$$\begin{aligned}\{\chi(v_6,v_8,v_9,v_1,v_3)\chi(v_6,v_8,v_9,v_4,v_7), &\quad \chi(v_6,v_8,v_9,v_1,v_4)\chi(v_6,v_8,v_9,v_3,v_7),\\ &\quad \chi(v_6,v_8,v_9,v_1,v_7)\chi(v_6,v_8,v_9,v_3,v_4)\}\\ \overset{(3.5),(3.6),(3.8),(3.9),(3.10)}{=} \{(-1)\cdot\chi(v_6,v_8,v_9,v_4,v_7), &\quad -1\cdot(-1),\\ &\quad (-1)\cdot 1\},\\ &\quad \Rightarrow \chi(v_6,v_8,v_9,v_4,v_7)=-1, \end{aligned} \tag{3.16}$$

$$\begin{aligned}\{\chi(v_6,v_8,v_9,v_3,v_4)\chi(v_6v_8,v_9,v_5,v_7), &\quad \chi(v_6,v_8,v_9,v_3,v_5)\chi(v_6,v_8,v_9,v_4,v_7),\\ &\quad \chi(v_6,v_8,v_9,v_3,v_7)\chi(v_6,v_8,v_9,v_4,v_5)\}\\ \overset{(3.10),(3.14),(3.1),(3.8)}{=} \{1\cdot 1, &\quad 0,\\ &\quad 1\cdot\chi(v_6,v_8,v_9,v_4,v_5)\},\\ &\quad \Rightarrow \chi(v_6,v_8,v_9,v_4,v_5)=-1, \end{aligned} \tag{3.17}$$

$$\begin{aligned}\{\chi(v_5,v_8,v_9,v_2,v_4)\chi(v_5,v_8,v_9,v_6,v_7), &\quad \chi(v_5,v_8,v_9,v_2,v_6)\chi(v_5,v_8,v_9,v_4,v_7),\\ &\quad \chi(v_5,v_8,v_9,v_2,v_7)\chi(v_5,v_8,v_9,v_4,v_6)\}\\ \overset{(3.2),(3.14),(3.15),(3.11),(3.17)}{=} \{(-1)\cdot(-1), &\quad -1\cdot\chi(v_5,v_8,v_9,v_4,v_7),\\ &\quad (-1)\cdot(-1)\},\\ &\quad \Rightarrow \chi(v_5,v_8,v_9,v_4,v_7)= \quad 1, \end{aligned} \tag{3.18}$$

Finally, we get the Grassmann-Plücker-relation

$$\begin{aligned}\{\chi(v_4,v_8,v_9,v_2,v_5)\chi(v_4,v_8,v_9,v_6,v_7), &\quad \chi(v_4,v_8,v_9,v_2,v_6)\chi(v_4,v_8,v_9,v_5,v_7),\\ &\quad \chi(v_4,v_8,v_9,v_2,v_7)\chi(v_4,v_8,v_9,v_5,v_6)\}\\ \overset{(3.2),(3.16),(3.3),(3.18),(3.4),(3.17)}{=} \{1\cdot 1, &\quad -1\cdot(-1),\\ &\quad (-1)\cdot(-1)\}, \end{aligned} \tag{3.19}$$

which is neither $\{0\}$, nor contains $\{-1, 1\}$. Therefore, the Grassmann-Plücker-relations cannot be satisfied, whence the sphere $(10^0_{32,33})$ does not support an oriented matroid. Hence, it is non-polytopal. □

Proposition 3.2.2. *The sphere $(10^0_{32,33})$ has a diagram based on each of the facets F_0, F_1, F_2, F_3, F_4, F_5, F_6, and F_7, but not based on one of F_8, F_9, or F_{10}. Moreover, it is not fan-like.*

Proof. We construct partial chirotopes as explained at the beginning of the chapter for each of the cases and solve with SCIP. The coordinates of diagrams based on each of the facets F_0, F_1, F_2, F_3, F_4, F_5, F_6, and F_7 can be found in Figure 3.35.

In the other cases we get certificates of non-realisability:

- F_8 and F_9: the partial chirotope obtained from orienting and the Grassmann–Plücker relations has a bfp;
- F_{10}: backtracking reveals that every partial chirotope, and hence every oriented matroid, fails the Grassmann–Plücker relations.

For the case of the fan-like embedding, we constructed a partial chirotope and tested via backtracking all partial chirotopes with a size of at least 15% of the size of an oriented matroid for this case ($\binom{11}{5} = 462$) for the existence of a bfp and all of them turned out to have one. Therefore, there is no oriented matroid for this case and $(10^0_{32,33})$ has no fan-like embedding. □

Theorem 3.2.3. *The sphere $(10^1_{32,33})$ is non-polytopal.*

Proof. From facet F_0 we may choose $\chi(v_0\ , v_3\ , v_5\ , v_6\ , v_i\ ) = \ \ 1$, where $v_i \notin F_0$ (see Figure 3.35 for a picture of F_0). Furthermore, we can get the signs

$$\chi(v_0, v_5, v_6, v_7, v_8) \ = \ \ 1, \tag{3.20}$$
$$\chi(v_3, v_5, v_6, v_7, v_8) \ = \ -1, \tag{3.21}$$

by extending the orientation inside F_0. With this we can derive:

$$\chi(v_0, v_3, v_5, v_6, v_7) = \ \ 1 \overset{F_2}{\Rightarrow} \chi(v_0, v_3, v_6, v_7, v_8) = \ \ 1, \tag{3.22}$$
$$\chi(v_0, v_3, v_5, v_6, v_7) = \ \ 1 \overset{F_2}{\Rightarrow} \chi(v_0, v_3, v_6, v_7, v_9) = \ \ 1 \overset{F_5}{\Rightarrow} \chi(v_3, v_6, v_7, v_8, v_9) = -1, \tag{3.23}$$
$$\chi(v_0, v_3, v_5, v_6, v_7) = \ \ 1 \overset{F_2}{\Rightarrow} \chi(v_0, v_1, v_3, v_6, v_7) = -1 \overset{F_5}{\Rightarrow} \chi(v_1, v_3, v_4, v_6, v_7) = -1$$
$$\overset{F_2}{\Rightarrow} \chi(v_3, v_4, v_6, v_7, v_8) = -1, \tag{3.24}$$
$$\chi(v_0, v_3, v_5, v_6, v_7) = \ \ 1 \overset{F_3}{\Rightarrow} \chi(v_0, v_3, v_4, v_5, v_7) = -1 \overset{F_1}{\Rightarrow} \chi(v_0, v_4, v_5, v_6, v_7) = -1$$
$$\overset{F_2}{\Rightarrow} \chi(v_0, v_4, v_6, v_7, v_9) = -1 \overset{F_7}{\Rightarrow} \chi(v_4, v_6, v_7, v_8, v_9) = \ \ 1, \tag{3.25}$$
$$\chi(v_0, v_3, v_4, v_5, v_7) \overset{(3.25)}{=} -1 \overset{F_1}{\Rightarrow} \chi(v_0, v_1, v_4, v_5, v_7) = -1 \overset{F_9}{\Rightarrow} \chi(v_1, v_4, v_5, v_7, v_8) = -1$$
$$\overset{F_1}{\Rightarrow} \chi(v_4, v_5, v_6, v_7, v_8) = -1, \tag{3.26}$$
$$\chi(v_0, v_4, v_5, v_6, v_7) \overset{(3.25)}{=} -1 \overset{F_2}{\Rightarrow} \chi(v_0, v_4, v_6, v_7, v_8) = -1, \tag{3.27}$$

With these values for the partial chirotope, we can find some new values of χ using the Grassmann-Plücker-relations:

$$\begin{aligned} &\{\chi(v_6,v_7,v_8,v_3,v_4)\chi(v_6,v_7,v_8,v_5,v_9), && \chi(v_6,v_7,v_8,v_3,v_5)\chi(v_6,v_7,v_8,v_4,v_9),\\ &&& \chi(v_6,v_7,v_8,v_3,v_9)\chi(v_6,v_7,v_8,v_4,v_5)\}\\ &\overset{(3.24),(3.21),(3.25),(3.23),(3.26)}{=} \{(-1)\cdot\chi(v_6,v_7,v_8,v_5,v_9), && -(-1)\cdot(-1),\\ &&& 1\cdot(-1)\},\\ &&& \Rightarrow \chi(v_6,v_7,v_8,v_5,v_9) = -1, \end{aligned} \tag{3.28}$$

$$\begin{aligned} &\{\chi(v_6,v_7,v_8,v_0,v_4)\chi(v_6,v_7,v_8,v_5,v_9), && \chi(v_6,v_7,v_8,v_0,v_5)\chi(v_6,v_7,v_8,v_4,v_9),\\ &&& \chi(v_6,v_7,v_8,v_0,v_9)\chi(v_6,v_7,v_8,v_4,v_5)\}\\ &\overset{(3.27),(3.28),(3.20),(3.25),(3.26)}{=} \{(-1)\cdot(-1), && -1\cdot(-1),\\ &&& \chi(v_6,v_7,v_8,v_0,v_9)\cdot(-1)\},\\ &&& \Rightarrow \chi(v_6,v_7,v_8,v_0,v_9) = \quad 1, \end{aligned} \tag{3.29}$$

Finally, we get the Grassmann-Plücker-relation

$$\begin{aligned} &\{\chi(v_6,v_7,v_8,v_0,v_3)\chi(v_6,v_7,v_8,v_5,v_9), && \chi(v_6,v_7,v_8,v_0,v_5)\chi(v_6,v_7,v_8,v_3,v_9),\\ &&& \chi(v_6,v_7,v_8,v_0,v_9)\chi(v_6,v_7,v_8,v_3,v_5)\}\\ &\overset{(3.22),(3.28),(3.20),(3.23),(3.29),(3.21)}{=} \{1\cdot(-1), && -1\cdot 1,\\ &&& 1\cdot(-1)\}, \end{aligned} \tag{3.30}$$

which is neither $\{0\}$, nor contains $\{-1,1\}$. Therefore, the Grassmann-Plücker-relations cannot be satisfied, whence the sphere $(10^1_{32,33})$ does not support an oriented matroid. Hence, it is non-polytopal. □

Proposition 3.2.4. *The sphere* $(10^1_{32,33})$ *has a diagram based on every facet and has a fan-like embedding.*

Proof. We construct partial chirotopes as explained at the beginning of the chapter for each of the cases and solve with SCIP. The coordinates can be found in Figure 3.35. □

Remark. The sphere $(10^1_{32,33})$ has an oriented matroid for the star-shaped embedding, but we couldn't find coordinates, so this case remains open.

3.2.2 The spheres with f-vector $(10, 33, 35, 12)$

The enumeration from Chapter 2 gives that there is a unique strongly regular 3-spheres with this f-vector.

Theorem 3.2.5. *The sphere* $(10_{33,35})$ *is non-polytopal.*

Figure 3.37

$(10_{33,35})$

$F_0 = \{v_1, v_4, v_7, v_9\}$
$F_1 = \{v_2, v_4, v_7, v_9\}$
$F_2 = \{v_0, v_2, v_4, v_5, v_8\}$
$F_3 = \{v_0, v_2, v_4, v_6, v_9\}$
$F_4 = \{v_1, v_3, v_6, v_7, v_8\}$
$F_5 = \{v_1, v_3, v_4, v_6, v_9\}$
$F_6 = \{v_0, v_2, v_5, v_7, v_9\}$
$F_7 = \{v_1, v_3, v_5, v_7, v_9\}$
$F_8 = \{v_0, v_1, v_4, v_6, v_8\}$
$F_9 = \{v_1, v_2, v_4, v_7, v_8\}$
$F_{10} = \{v_2, v_3, v_5, v_7, v_8\}$
$F_{11} = \{v_0, v_3, v_5, v_6, v_8, v_9\}$

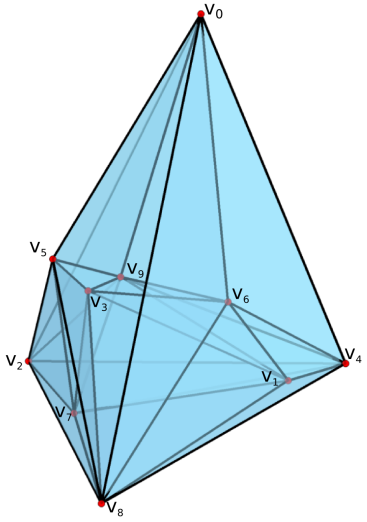

$\underline{F_2}$
$v_0 = (1306, 2451, 4264)$
$v_1 = (2471, 990, 1976)$
$v_2 = (2881, 3713, 856)$
$v_3 = (1412, 2367, 1947)$
$v_4 = (2812, 766, 2282)$
$v_5 = (1451, 2517, 2110)$
$v_6 = (1965, 1505, 2347)$
$v_7 = (1772, 2235, 976)$
$v_8 = (636, 941, 864)$
$v_9 = (1612, 2283, 2145)$

$\underline{F_3}$
$v_0 = (251, 200, 593)$
$v_1 = (210, 223, 145)$
$v_2 = (234, 510, 186)$
$v_3 = (230, 181, 246)$
$v_4 = (70, 171, 153)$
$v_5 = (246, 270, 275)$
$v_6 = (219, 163, 280)$
$v_7 = (237, 447, 175)$
$v_8 = (223, 218, 271)$
$v_9 = (370, 114, 99)$

$\underline{F_4}$
$v_0 = (4180, 8229, 2205)$
$v_1 = (0, 0, 0)$
$v_2 = (4423, 900, 9533)$
$v_3 = (1000, 0, 0)$
$v_4 = (4832, 6300, 6118)$
$v_5 = (4154, 2628, 7085)$
$v_6 = (3419, 8273, 82)$
$v_7 = (4255, 63, 9818)$
$v_8 = (7681, 9940, 9900)$
$v_9 = (3678, 4352, 4308)$

$\underline{F_5}$
$v_0 = (7102, 4363, 5262)$
$v_1 = (0, 0, 0)$
$v_2 = (8692, 5055, 6983)$
$v_3 = (0, 1000, 0)$
$v_4 = (9482, 5345, 7160)$
$v_5 = (478, 1478, 1687)$
$v_6 = (9623, 4905, 884)$
$v_7 = (1239, 1816, 4019)$
$v_8 = (4195, 2920, 3030)$
$v_9 = (727, 3700, 9685)$

$\underline{F_6}$
$v_0 = (3006, 2643, 6791)$
$v_1 = (4181, 5347, 1887)$
$v_2 = (3239, 8185, 3576)$
$v_3 = (3911, 3982, 3610)$
$v_4 = (2712, 5287, 4419)$
$v_5 = (4947, 1181, 5132)$
$v_6 = (2846, 3348, 5999)$
$v_7 = (4627, 5556, 1115)$
$v_8 = (3526, 3796, 4671)$
$v_9 = (1888, 2188, 5759)$

Figure 3.37

$\underline{F_7}$
$v_0 = (5600, 5977, 5306)$
$v_1 = (0, 0, 0)$
$v_2 = (5161, 6365, 4872)$
$v_3 = (1000, 0, 0)$
$v_4 = (593, 563, 703)$
$v_5 = (5754, 6479, 4967)$
$v_6 = (1776, 1482, 1811)$
$v_7 = (5339, 9907, 2380)$
$v_8 = (3707, 4125, 3207)$
$v_9 = (5187, 391, 9908)$

$\underline{F_8}$
$v_0 = (9829, 8194, 9859)$
$v_1 = (0, 0, 0)$
$v_2 = (3949, 2515, 1177)$
$v_3 = (1145, 1213, 1810)$
$v_4 = (9915, 3519, 146)$
$v_5 = (7639, 6463, 7415)$
$v_6 = (167, 2805, 9905)$
$v_7 = (336, 252, 144)$
$v_8 = (0, 1000, 0)$
$v_9 = (2914, 2566, 3439)$

$\underline{F_{10}}$
$v_0 = (2231, 1723, 1538)$
$v_1 = (4624, 3492, 5230)$
$v_2 = (0, 0, 0)$
$v_3 = (3382, 2901, 3791)$
$v_4 = (1599, 1014, 1096)$
$v_5 = (0, 1000, 0)$
$v_6 = (3809, 3016, 3718)$
$v_7 = (2541, 3327, 7926)$
$v_8 = (8340, 4590, 3386)$
$v_9 = (3015, 2607, 3363)$

Figure 3.37: This is the 3-sphere with f-vector $(10, 33, 35, 12)$. This sphere is non-polytopal, has no diagram based on one of the facets F_0, F_1, F_9, or F_{11}, and it has no fan-like embedding.

Proof. Since five points in a common facet are colinear, we get:

$$\chi(v_3, v_5, v_6, v_8, v_9) = \quad 0. \tag{3.31}$$

From the tetrahedron facet F_0 we may choose $\chi(v_1\ , v_4\ , v_7\ , v_9\ , v_i\ ) = \quad 1$, where $v_i \notin F_0$. With this we can derive:

$$\chi(v_1, v_4, v_5, v_7, v_9) = \quad 1 \overset{F_7}{\Rightarrow} \chi(v_1, v_5, v_7, v_8, v_9) = \quad 1, \tag{3.32}$$

$$\begin{aligned}\chi(v_1, v_4, v_7, v_8, v_9) = -1 &\overset{F_9}{\Rightarrow} \chi(v_0, v_1, v_4, v_7, v_8) = -1 \overset{F_8}{\Rightarrow} \chi(v_0, v_1, v_2, v_4, v_8) = \quad 1\\ &\overset{F_9}{\Rightarrow} \chi(v_1, v_2, v_4, v_5, v_8) = -1 \overset{F_2}{\Rightarrow} \chi(v_2, v_4, v_5, v_8, v_9) = -1,\end{aligned} \tag{3.33}$$

$$\chi(v_1, v_4, v_6, v_7, v_9) = \quad 1 \overset{F_5}{\Rightarrow} \chi(v_1, v_2, v_4, v_6, v_9) = \quad 1 \overset{F_3}{\Rightarrow} \chi(v_2, v_4, v_6, v_8, v_9) = -1, \tag{3.34}$$

$$\chi(v_0, v_1, v_2, v_4, v_8) \overset{(3.33)}{=} \quad 1 \overset{F_2}{\Rightarrow} \chi(v_0, v_2, v_4, v_7, v_8) = \quad 1 \overset{F_9}{\Rightarrow} \chi(v_2, v_4, v_7, v_8, v_9) = \quad 1, \tag{3.35}$$

$$\begin{aligned}\chi(v_1, v_3, v_4, v_7, v_9) = -1 &\overset{F_5}{\Rightarrow} \chi(v_1, v_3, v_4, v_5, v_9) = -1 \overset{F_7}{\Rightarrow} \chi(v_1, v_3, v_5, v_6, v_9) = \quad 1\\ &\overset{F_5}{\Rightarrow} \chi(v_1, v_3, v_6, v_8, v_9) = -1,\end{aligned} \tag{3.36}$$

$$\chi(v_1, v_4, v_6, v_7, v_9) \overset{(3.34)}{=} \quad 1 \overset{F_5}{\Rightarrow} \chi(v_1, v_4, v_6, v_8, v_9) = \quad 1, \tag{3.37}$$

$$\begin{aligned}\chi(v_1, v_4, v_7, v_8, v_9) \overset{(3.33)}{=} -1 &\overset{F_9}{\Rightarrow} \chi(v_1, v_4, v_6, v_7, v_8) = -1 \overset{F_4}{\Rightarrow} \chi(v_0, v_1, v_6, v_7, v_8) = \quad 1\\ &\overset{F_8}{\Rightarrow} \chi(v_0, v_1, v_3, v_6, v_8) = -1 \overset{F_{11}}{\Rightarrow} \chi(v_0, v_3, v_6, v_7, v_8) = -1\\ &\overset{F_4}{\Rightarrow} \chi(v_3, v_6, v_7, v_8, v_9) = -1,\end{aligned} \tag{3.38}$$

$$\chi(v_1,v_4,v_6,v_7,v_8) \overset{(3.38)}{=} -1 \overset{F_4}{\Rightarrow} \chi(v_1,v_6,v_7,v_8,v_9) = 1, \tag{3.39}$$

$$\begin{aligned}\chi(v_1,v_3,v_5,v_6,v_9) &\overset{(3.36)}{=} 1 \overset{F_5}{\Rightarrow} \chi(v_0,v_1,v_3,v_6,v_9) = 1 \overset{F_{11}}{\Rightarrow} \chi(v_0,v_3,v_4,v_6,v_9) = -1\\ &\overset{F_5}{\Rightarrow} \chi(v_3,v_4,v_6,v_8,v_9) = 1,\end{aligned} \tag{3.40}$$

$$\chi(v_1,v_3,v_4,v_7,v_9) \overset{(3.36)}{=} -1 \overset{F_7}{\Rightarrow} \chi(v_1,v_3,v_7,v_8,v_9) = 1, \tag{3.41}$$

$$\begin{aligned}\chi(v_0,v_1,v_2,v_4,v_8) &\overset{(3.33)}{=} 1 \overset{F_2}{\Rightarrow} \chi(v_0,v_2,v_4,v_8,v_9) = -1 \overset{F_3}{\Rightarrow} \chi(v_0,v_2,v_4,v_5,v_9) = -1\\ &\overset{F_2}{\Rightarrow} \chi(v_0,v_2,v_4,v_5,v_7) = -1 \overset{F_6}{\Rightarrow} \chi(v_0,v_2,v_5,v_7,v_8) = -1\\ &\overset{F_{10}}{\Rightarrow} \chi(v_2,v_5,v_7,v_8,v_9) = -1,\end{aligned} \tag{3.42}$$

$$\begin{aligned}\chi(v_0,v_2,v_5,v_7,v_8) &\overset{(3.42)}{=} -1 \overset{F_2}{\Rightarrow} \chi(v_0,v_2,v_3,v_5,v_8) = 1 \overset{F_{11}}{\Rightarrow} \chi(v_0,v_3,v_5,v_7,v_8) = 1\\ &\overset{F_{10}}{\Rightarrow} \chi(v_3,v_5,v_7,v_8,v_9) = 1,\end{aligned} \tag{3.43}$$

$$\chi(v_1,v_3,v_6,v_8,v_9) \overset{(3.36)}{=} -1 \overset{F_{11}}{\Rightarrow} \chi(v_2,v_3,v_6,v_8,v_9) = -1, \tag{3.44}$$

With these values for the partial chirotope, we can find some new values of χ using the Grassmann-Plücker-relations:

$$\begin{aligned}&\{\chi(v_1,v_3,v_7,v_8,v_9)\chi(v_5,v_6,v_7,v_8,v_9), \quad \chi(v_1,v_5,v_7,v_8,v_9)\chi(v_3,v_6,v_7,v_8,v_9),\\ &\qquad\qquad \chi(v_1,v_6,v_7,v_8,v_9)\chi(v_3,v_5,v_7,v_8,v_9)\}\\ &\overset{(3.41),(3.32),(3.38),(3.39),(3.43)}{=} \{1\cdot\chi(v_5,v_6,v_7,v_8,v_9), \quad -1\cdot(-1),\\ &\qquad\qquad 1\cdot 1\},\\ &\qquad\qquad \Rightarrow \chi(v_5,v_6,v_7,v_8,v_9) = -1,\end{aligned} \tag{3.45}$$

$$\begin{aligned}&\{\chi(v_2,v_3,v_6,v_8,v_9)\chi(v_5,v_6,v_7,v_8,v_9), \quad \chi(v_2,v_5,v_6,v_8,v_9)\chi(v_3,v_6,v_7,v_8,v_9),\\ &\qquad\qquad \chi(v_2,v_6,v_7,v_8,v_9)\chi(v_3,v_5,v_6,v_8,v_9)\}\\ &\overset{(3.44),(3.45),(3.38),(3.31)}{=} \{(-1)\cdot(-1), \quad -\chi(v_2,v_5,v_6,v_8,v_9)\cdot(-1),\\ &\qquad\qquad 1\cdot 0\},\\ &\qquad\qquad \Rightarrow \chi(v_2,v_5,v_6,v_8,v_9) = -1,\end{aligned} \tag{3.46}$$

$$\begin{aligned}&\{\chi(v_1,v_3,v_6,v_8,v_9)\chi(v_4,v_6,v_7,v_8,v_9), \quad \chi(v_1,v_4,v_6,v_8,v_9)\chi(v_3,v_6,v_7,v_8,v_9),\\ &\qquad\qquad \chi(v_1,v_6,v_7,v_8,v_9)\chi(v_3,v_4,v_6,v_8,v_9)\}\\ &\overset{(3.36),(3.37),(3.38),(3.39),(3.40)}{=} \{(-1)\cdot\chi(v_4,v_6,v_7,v_8,v_9), \quad -1\cdot(-1),\\ &\qquad\qquad 1\cdot 1\},\\ &\qquad\qquad \Rightarrow \chi(v_4,v_6,v_7,v_8,v_9) = 1,\end{aligned} \tag{3.47}$$

$$\begin{aligned}&\{\chi(v_3,v_4,v_6,v_8,v_9)\chi(v_5,v_6,v_7,v_8,v_9), \quad \chi(v_3,v_5,v_6,v_8,v_9)\chi(v_4,v_6,v_7,v_8,v_9),\\ &\qquad\qquad \chi(v_3,v_6,v_7,v_8,v_9)\chi(v_4,v_5,v_6,v_8,v_9)\}\\ &\overset{(3.40),(3.45),(3.31),(3.47),(3.38)}{=} \{1\cdot(-1), \quad -0\cdot 1,\\ &\qquad\qquad (-1)\cdot\chi(v_4,v_5,v_6,v_8,v_9)\},\\ &\qquad\qquad \Rightarrow \chi(v_4,v_5,v_6,v_8,v_9) = -1,\end{aligned} \tag{3.48}$$

$$\begin{aligned}
&\{\chi(v_2,v_4,v_5,v_8,v_9)\chi(v_5,v_6,v_7,v_8,v_9), && \chi(v_2,v_5,v_6,v_8,v_9)\chi(v_4,v_5,v_7,v_8,v_9),\\
&&& \chi(v_2,v_5,v_7,v_8,v_9)\chi(v_4,v_5,v_6,v_8,v_9)\}\\
&\overset{(3.33),(3.45),(3.46),(3.42),(3.48)}{=} \{(-1)\cdot(-1), && -(-1)\cdot\chi(v_4,v_5,v_7,v_8,v_9),\\
&&& (-1)\cdot(-1)\},\\
&&& \Rightarrow \chi(v_4,v_5,v_7,v_8,v_9) = -1, \qquad (3.49)
\end{aligned}$$

Finally, we get the Grassmann-Plücker-relation

$$\begin{aligned}
&\{\chi(v_2,v_4,v_5,v_8,v_9)\chi(v_4,v_6,v_7,v_8,v_9), && \chi(v_2,v_4,v_6,v_8,v_9)\chi(v_4,v_5,v_7,v_8,v_9),\\
&&& \chi(v_2,v_4,v_7,v_8,v_9)\chi(v_4,v_5,v_6,v_8,v_9)\}\\
&\overset{(3.33),(3.47),(3.34),(3.49),(3.35),(3.48)}{=} \{(-1)\cdot 1, && -(-1)\cdot(-1),\\
&&& 1\cdot(-1)\}, \qquad (3.50)
\end{aligned}$$

which is neither $\{0\}$, nor contains $\{-1,1\}$. Therefore, the Grassmann-Plücker-relations cannot be satisfied, whence the sphere $(10_{33,35})$ does not support an oriented matroid. Hence, it is non-polytopal. □

Proposition 3.2.6. *The sphere $(10_{33,35})$ has a diagram based on each of the facets F_2, F_3, F_4, F_5, F_6, F_7, F_8, and F_{10}, but not based on one of F_0, F_1, F_9, or F_{11}. Moreover, it is not fan-like.*

Proof. We construct partial chirotopes as explained at the beginning of the chapter for each of the cases and solve with SCIP. The coordinates can be found in Figure 3.37.

In the other cases we get certificates of non-realisability:

- F_0 and F_1: the partial chirotope obtained from orienting and the Grassmann–Plücker relations has a bfp;
- F_9 and F_{11}: backtracking reveals that every partial chirotope, and hence every oriented matroid, either has a bfp, or fails the Grassmann–Plücker relations.

For the case of the fan-like embedding, we constructed a partial chirotope and tested via backtracking all partial chirotopes with a size of at least 15% of the size of an oriented matroid for this case ($\binom{11}{5} = 462$) for the existence of a bfp and all of them turned out to have one. Therefore, there is no oriented matroid for this case and $(10_{33,35})$ has no fan-like embedding. □

(11^0_{35})

$F_0 = \{v_1, v_2, v_4, v_6, v_9\}$
$F_1 = \{v_3, v_5, v_7, v_8, v_9\}$
$F_2 = \{v_0, v_6, v_7, v_8, v_{10}\}$
$F_3 = \{v_2, v_3, v_4, v_8, v_9\}$
$F_4 = \{v_0, v_1, v_2, v_5, v_6, v_{10}\}$
$F_5 = \{v_3, v_4, v_7, v_8, v_{10}\}$
$F_6 = \{v_1, v_5, v_6, v_7, v_9\}$
$F_7 = \{v_0, v_1, v_2, v_4, v_8, v_{10}\}$
$F_8 = \{v_3, v_5, v_6, v_7, v_{10}\}$
$F_9 = \{v_0, v_2, v_6, v_7, v_8, v_9\}$
$F_{10} = \{v_1, v_3, v_4, v_5, v_9, v_{10}\}$

$\underline{F_4}$

$v_0 = (0, 0, 0)$
$v_1 = (6260, 6277, 6133)$
$v_2 = (9696, 9708, 9758)$
$v_3 = (1000, 0, 0)$
$v_4 = (4738, 5466, 5515)$

$\underline{F_6}$

$v_0 = (0, 0, 0)$
$v_1 = (1797, 1585, 512)$
$v_2 = (2009, 2395, 1622)$
$v_3 = (460, 1113, 648)$
$v_4 = (0, 0, 1000)$
$v_5 = (8565805/4137, 2055, 1316)$
$v_6 = (2850, 426, 139)$
$v_7 = (521, 1238, 853)$
$v_8 = (2946124555/1064794, 1020, 770)$
$v_9 = (423, 2580, 139)$
$v_{10} = (1161, 1055, 677)$

(11^1_{35})

$F_0 = \{v_2, v_4, v_7, v_9\}$
$F_1 = \{v_0, v_4, v_6, v_7, v_{10}\}$
$F_2 = \{v_0, v_3, v_4, v_7, v_9\}$
$F_3 = \{v_1, v_3, v_5, v_8, v_{10}\}$
$F_4 = \{v_0, v_3, v_5, v_7, v_{10}\}$
$F_5 = \{v_1, v_4, v_6, v_8, v_{10}\}$
$F_6 = \{v_0, v_2, v_4, v_6, v_8, v_9\}$
$F_7 = \{v_1, v_2, v_5, v_6, v_8, v_9\}$
$F_8 = \{v_1, v_2, v_3, v_5, v_7, v_9\}$
$F_9 = \{v_0, v_1, v_3, v_6, v_9, v_{10}\}$
$F_{10} = \{v_2, v_4, v_5, v_7, v_8, v_{10}\}$

$v_5 = (908013392/92217, 9868, 9870)$
$v_6 = (384, 508, 355)$
$v_7 = (6167, 5314, 9780)$
$v_8 = (9952112546/1102971, 9174, 9091)$
$v_9 = (3089, 3051, 3074)$
$v_{10} = (6651, 9788, 4876)$

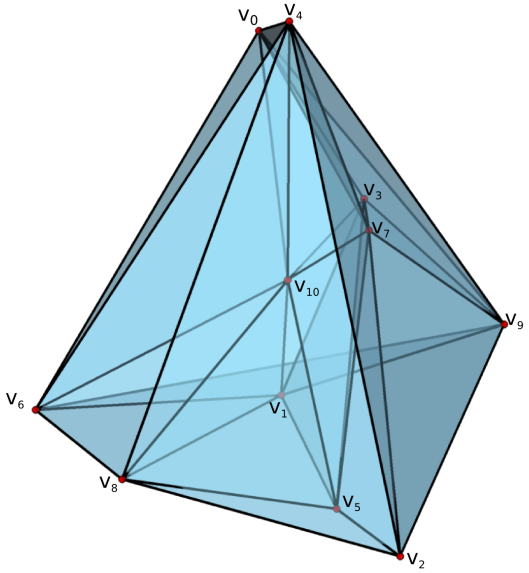

Figure 3.38: These are the facet lists of the two 3-spheres with f-vector $(11, 35, 35, 11)$. The two spheres are dual to each other. Furthermore, this figure shows diagrams of (11^1_{35}) based on F_4 and F_6.

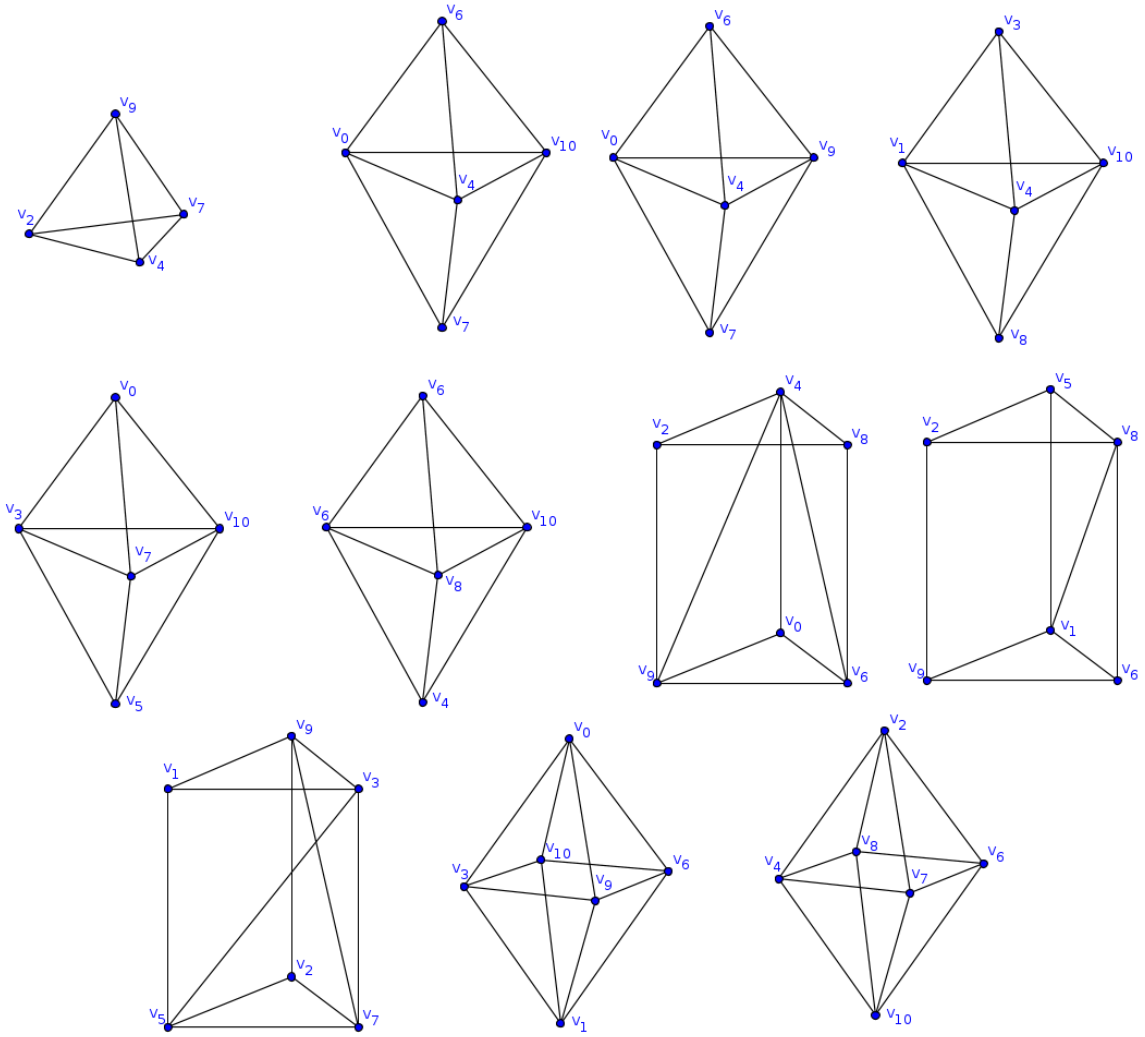

Figure 3.39: These are the facets of the sphere (11^1_{35}) from F_0 (top left) to F_{10} (bottom right).

3.2.3 The spheres with f-vector $(11, 35, 35, 11)$

The enumeration from Chapter 2 gives that there are preciseley two strongly regular 3-spheres with this f-vector. Since they are dual to each other, we only need to show non-polytopality of one of them.

Theorem 3.2.7. *The two spheres from Figure 3.38 are non-polytopal. In particular, they do not have an oriented matroid.*

Proof. To prove that neither sphere has an oriented matroid, we construct a partial chirotope and derive a contradiction in the Grassmann–Plücker relations. Since the two spheres are dual to each other, one non-polytopality proof suffices to show non-polytopality for both spheres. Here, we will present a proof for the sphere (11^1_{35}) not having an oriented matroid.

For an orientation of the vertices of the sphere (11^1_{35}) we may choose one sign that is non-zero arbitrarily. Since facet F_9 is an octahedron with opposite pairs v_0/v_1, v_3/v_6, and v_9/v_{10} (Figure 3.39), the vertices v_1, v_6, v_9, v_{10} form a tetrahedron, so we can set

$$\chi(v_1, v_6, v_7, v_9, v_{10}) := 1. \tag{3.51}$$

From this we can find orientations for the other tetrahedra in F_9 and we get

$$\begin{aligned}
\chi(v_1, v_6, v_8, v_9, v_{10}) &= 1, && (3.52)\\
\chi(v_1, v_3, v_8, v_9, v_{10}) &= -1, && (3.53)\\
\chi(v_0, v_3, v_7, v_9, v_{10}) &= 1, && (3.54)\\
\chi(v_0, v_6, v_7, v_9, v_{10}) &= -1, && (3.55)\\
\chi(v_0, v_3, v_6, v_8, v_9\ ) &= 1, && (3.56)\\
\chi(v_0, v_3, v_6, v_7, v_{10}) &= -1, && (3.57)\\
\chi(v_0, v_1, v_4, v_6, v_{10}) &= 1. && (3.58)
\end{aligned}$$

Since five points in a facet lie on a hyperplane, we have from F_9

$$\chi(v_1, v_3, v_6, v_9, v_{10}) = 0. \tag{3.59}$$

Now, every time we have four vertices on a facet F_i while the fifth is not on that facet, we can exchange that vertex with any other vertex not in F_i without changing the sign of the determinant. Note that a permutation of the vertices (columns) changes the sign. Therefore, we get (the "F_i" above the arrow indicates which facet is used)

$$\begin{aligned}
\chi(v_0, v_3, v_6, v_8, v_9\ ) = 1 &\overset{F_6}{\Rightarrow} \chi(v_0, v_5, v_6, v_8, v_9\ ) = 1 \overset{F_7}{\Rightarrow} \chi(v_5, v_6, v_8, v_9, v_{10}) = 1, && (3.60)\\
\chi(v_0, v_3, v_6, v_7, v_{10}) = -1 &\overset{F_4}{\Rightarrow} \chi(v_0, v_3, v_4, v_7, v_{10}) = -1 \overset{F_1}{\Rightarrow} \chi(v_0, v_4, v_5, v_7, v_{10}) = 1\\
&\overset{F_4}{\Rightarrow} \chi(v_0, v_2, v_5, v_7, v_{10}) = 1 \overset{F_{10}}{\Rightarrow} \chi(v_1, v_2, v_5, v_7, v_{10}) = 1 && (3.61)\\
&\overset{F_8}{\Rightarrow} \chi(v_1, v_2, v_5, v_7, v_8\ ) = 1 \overset{F_7}{\Rightarrow} \chi(v_1, v_2, v_3, v_5, v_8\ ) = -1\\
&\overset{F_3}{\Rightarrow} \chi(v_1, v_3, v_5, v_8, v_9\ ) = 1 \overset{F_7}{\Rightarrow} \chi(v_1, v_5, v_8, v_9, v_{10}) = -1,\\
\chi(v_0, v_3, v_5, v_6, v_{10}) = 1 &\overset{F_4}{\Rightarrow} \chi(v_0, v_3, v_5, v_8, v_{10}) = 1 \overset{F_3}{\Rightarrow} \chi(v_3, v_5, v_8, v_9, v_{10}) = -1, && (3.62)\\
\chi(v_0, v_1, v_4, v_6, v_{10}) = 1 &\overset{F_5}{\Rightarrow} \chi(v_1, v_4, v_6, v_7, v_{10}) = -1 \overset{F_1}{\Rightarrow} \chi(v_4, v_6, v_7, v_9, v_{10}) = 1, && (3.63)\\
\chi(v_0, v_1, v_4, v_6, v_{10}) = 1 &\overset{F_1}{\Rightarrow} \chi(v_0, v_2, v_4, v_6, v_{10}) = 1 \overset{F_6}{\Rightarrow} \chi(v_0, v_2, v_4, v_6, v_7\ ) = 1\\
&\overset{F_1}{\Rightarrow} \chi(v_0, v_4, v_6, v_7, v_9\ ) = -1 \overset{F_7}{\Rightarrow} \chi(v_0, v_4, v_7, v_9, v_{10}) = -1, && (3.64)\\
\chi(v_0, v_3, v_6, v_7, v_9\ ) = 1 &\overset{F_2}{\Rightarrow} \chi(v_0, v_2, v_3, v_7, v_9\ ) = -1 \overset{F_8}{\Rightarrow} \chi(v_2, v_3, v_4, v_7, v_9\ ) = -1\\
&\overset{F_2}{\Rightarrow} \chi(v_3, v_4, v_7, v_9, v_{10}) = -1. && (3.65)
\end{aligned}$$

Note that we use all vertices and all facets except the facet F_0 for this proof.

Now, consider the following Grassmann–Plücker relations:

$$\begin{aligned}&\{\chi(v_8,v_9,v_{10},v_1,v_3)\chi(v_8,v_9,v_{10},v_5,v_6), && -\chi(v_8,v_9,v_{10},v_1,v_5)\chi(v_8,v_9,v_{10},v_3,v_6),\\ &&& \chi(v_8,v_9,v_{10},v_1,v_6)\chi(v_8,v_9,v_{10},v_3,v_5)\}\\ &\overset{(3.53),(3.60),(3.61),(3.52),(3.62)}{=} \{(-1)\cdot 1, && -(-1)\cdot\chi(v_8,v_9,v_{10},v_3,v_6),\\ &&& 1\cdot(-1)\},\end{aligned} \tag{3.66}$$

$$\begin{aligned}&\{\chi(v_7,v_9,v_{10},v_0,v_3)\chi(v_7,v_9,v_{10},v_4,v_6), && -\chi(v_7,v_9,v_{10},v_0,v_4)\chi(v_7,v_9,v_{10},v_3,v_6),\\ &&& \chi(v_7,v_9,v_{10},v_0,v_6)\chi(v_7,v_9,v_{10},v_3,v_4)\}\\ &\overset{(3.54),(3.63),(3.64),(3.55),(3.65)}{=} \{1\cdot 1, && -(-1)\cdot\chi(v_7,v_9,v_{10},v_3,v_6),\\ &&& (-1)\cdot(-1)\}.\end{aligned} \tag{3.67}$$

Since these sets either have to contain $\{-1,1\}$ or to be $\{0\}$, we can conclude

$$\chi(v_8,v_9,v_{10},v_3,v_6) = 1, \tag{3.68}$$

$$\chi(v_7,v_9,v_{10},v_3,v_6) = -1. \tag{3.69}$$

Therefore, we have the Grassmann–Plücker relation

$$\begin{aligned}&\{\chi(v_6,v_9,v_{10},v_1,v_3)\chi(v_6,v_9,v_{10},v_7,v_8), && -\chi(v_6,v_9,v_{10},v_1,v_7)\chi(v_6,v_9,v_{10},v_3,v_8),\\ &&& \chi(v_6,v_9,v_{10},v_1,v_8)\chi(v_6,v_9,v_{10},v_3,v_7)\}\\ &\overset{(3.59),(3.51),(3.68),(3.52),(3.69)}{=} \{0, && -(-1)\cdot(-1),\\ &&& (-1)\cdot 1\},\end{aligned} \tag{3.70}$$

which is neither $\{0\}$ nor contains $\{-1,1\}$. Hence, the sphere (11^1_{35}) does not have an oriented matroid and thus is non-polytopal. □

Proposition 3.2.8. *The spheres (11^0_{35}) and (11^1_{35}) are not fan-like, hence have no star-shaped embedding. Moreover, (11^0_{35}) does not have a diagram with base F_6, F_9, or F_{10}, and sphere (11^1_{35}) has a diagram based on each F_4 and F_6, but does not have a diagram with base F_0, F_1, F_3, F_5, F_9, or F_{10}.*

Proof. We construct partial chirotopes as explained at the beginning of the chapter.

The resulting partial chirotopes for the different facets as bases of a diagram give already the signs of 131 to 276 elements out of $\binom{11}{4} = 330$, which is the size of an oriented matroid for a diagram of (11^0_{35}), resp. (11^1_{35}). With SCIP we can find coordinates for diagrams of (11^1_{35}) with bases F_4 and F_6 (see Figure 3.38), while in the other cases we get certificates of non-realisability:
(11^0_{35})

- F_6 and F_9: the partial chirotope obtained from orienting and the Grassmann–Plücker relations has a bfp;
- F_{10}: backtracking reveals that every partial chirotope, and hence every oriented matroid, either has a bfp, or fails the Grassmann–Plücker relations.

(11^1_{35})

- F_1 and F_3: the Grassmann–Plücker relations fail;
- F_0: the partial chirotope obtained from orienting and the Grassmann–Plücker relations has a bfp;
- F_5, F_9 and F_{10}: backtracking reveals that every partial chirotope, and hence every oriented matroid, either has a bfp, or fails the Grassmann–Plücker relations.

For the case of the fan-like embedding, we constructed (for each sphere) a partial chirotope and tested via backtracking all partial chirotopes with a size of at least 15% of the size of an oriented matroid for this case ($\binom{12}{5} = 792$) for the existence of a bfp and all of them turned out to have one. Therefore, there is no oriented matroid for this case and both spheres have no fan-like embedding. □

Remark. We could not decide the cases of diagrams for (11^0_{35}) with basis F_0, F_1, F_2, F_3, F_4, F_5, F_7, or F_8, and the cases of diagrams for (11^1_{35}) with basis F_2, F_7, or F_8, since there are oriented matroids whithout bfps, but we could not find coordinates.

3.2.4 The spheres with f-vector $(12, 40, 40, 12)$

The work on the sphere W^{40}_{12} is based on the paper [25], which is joint work with Günter M. Ziegler.

According to Table 2.3 there are preciseley four strongly regular 3-spheres with f-vector $(12, 40, 40, 12)$, one of them (W^{40}_{12}) is even 2s2s and we showed in Theorem 2.1.4 that it is the only sphere with flag-vector $(12, 40, 40, 12; 120)$. The facet lists of these spheres can be found in Figures 3.40, 3.41, 3.42, and 3.44.

Theorem 3.2.9. *The sphere W^{40}_{12} is non-polytopal.*

Proof. The sphere W^{40}_{12} is given as a list of facets in Figure 3.40. In order to prove non-polytopality of this sphere, we will show that there is no chirotope compatible with its facet list.

In the sphere, $\{v_8, v_9, v_{10}\} = F_6 \cap F_9$ is the vertex set of a triangle 2-face, so the vertices $\{v_7, v_8, v_9, v_{10}\} \subset F_6$ span a tetrahedron, while $v_2 \notin F_6$. Thus, in any realisation, we have

Figure 3.40

W_{12}^{40}

$F_0 = \{v_0, v_1, v_2, v_3\}$
$F_1 = \{v_0, v_2, v_3, v_4, v_5, v_6, v_7\}$
$F_2 = \{v_0, v_1, v_3, v_4, v_8, v_9\}$
$F_3 = \{v_0, v_1, v_2, v_6, v_9, v_{10}\}$
$F_4 = \{v_0, v_4, v_7, v_8\}$
$F_5 = \{v_0, v_5, v_6, v_{10}\}$
$F_6 = \{v_0, v_5, v_7, v_8, v_9, v_{10}\}$
$F_7 = \{v_1, v_2, v_3, v_4, v_{10}, v_{11}\}$
$F_8 = \{v_2, v_5, v_6, v_8, v_{10}, v_{11}\}$
$F_9 = \{v_1, v_8, v_9, v_{10}, v_{11}\}$
$F_{10} = \{v_1, v_4, v_5, v_7, v_8, v_{11}\}$
$F_{11} = \{v_2, v_4, v_5, v_{11}\}$

$\underline{F_0}$

$v_0 = (77, 80, 42)$
$v_1 = (71, 94, 91)$
$v_2 = (92, 64, 81)$
$v_3 = (57, 58, 76)$
$v_4 = (62, 63, 73)$
$v_5 = (74, 70, 67)$
$v_6 = (88, 67, 74)$
$v_7 = (70, 70, 64)$
$v_8 = (70, 78, 71)$
$v_9 = (74, 86, 67)$
$v_{10} = (79, 79, 77)$
$v_{11} = (74, 77, 75)$

$\underline{F_1}$

$v_0 = (74, 20, 23)$
$v_1 = (44, 70, 47)$
$v_2 = (30, 60, 110)$
$v_3 = (28, 100, 39)$
$v_4 = (44, 120, 50)$
$v_5 = (91, 88, 102)$
$v_6 = (44, 40, 117)$
$v_7 = (104, 97, 77)$
$v_8 = (83, 76, 58)$
$v_9 = (67, 45, 46)$
$v_{10} = (61, 44, 83)$
$v_{11} = (60, 71, 71)$

$\underline{fan}$

$v_0 = (9, 2, 4, -1)$
$v_1 = (-3, 14, -16, 6)$
$v_2 = (-8, -2, -4, -16)$
$v_3 = (1, 23, -1, -9)$
$v_4 = (-1, 12, 4, -1)$
$v_5 = (-14, -11, 27, -11)$
$v_6 = (-5, -9, 2, -16)$
$v_7 = (-1, 2, 14, -1)$
$v_8 = (-1, 2, 4, 9)$
$v_9 = (9, -7, -12, 21)$
$v_{10} = (-6, -13, -5, -1)$
$v_{11} = (-14, 4, 1, -3)$

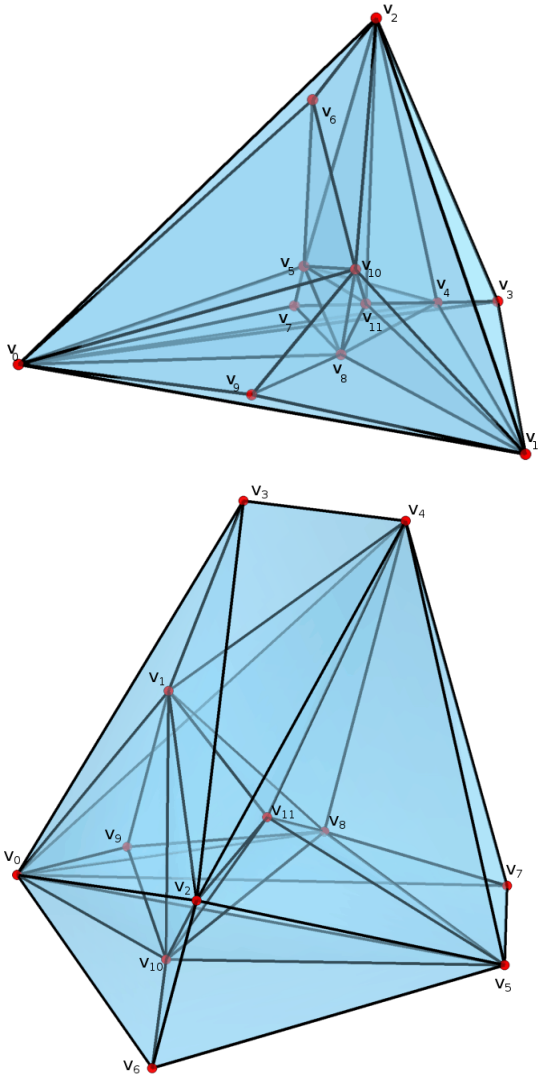

Figure 3.40

$\underline{F_2}$

$v_0 = (62, 66, 44)$
$v_1 = (68, 95, 94)$
$v_2 = (66, 79, 73)$
$v_3 = (73, 90, 68)$
$v_4 = (84, 86, 71)$
$v_5 = (75, 68, 74)$
$v_6 = (64, 73, 70)$
$v_7 = (77, 67, 73)$
$v_8 = (84, 63, 84)$
$v_9 = (57, 65, 90)$
$v_{10} = (61, 69, 86)$
$v_{11} = (72, 76, 80)$

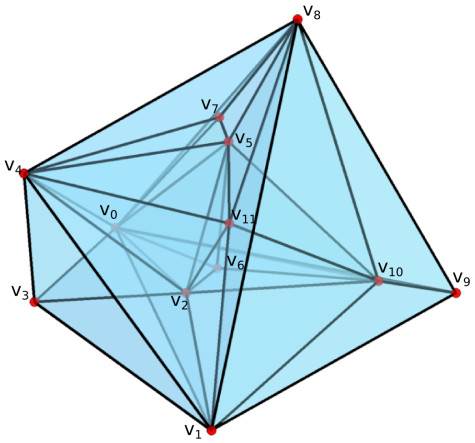

$\underline{F_3}$

$v_0 = (76, 57, 100)$
$v_1 = (65, 98, 80)$
$v_2 = (87, 85, 72)$
$v_3 = (72, 83, 85)$
$v_4 = (71, 81, 82)$
$v_5 = (74, 67, 73)$
$v_6 = (86, 71, 70)$
$v_7 = (71, 66, 78)$
$v_8 = (61, 70, 71)$
$v_9 = (53, 67, 70)$
$v_{10} = (72, 73, 48)$
$v_{11} = (71, 78, 72)$

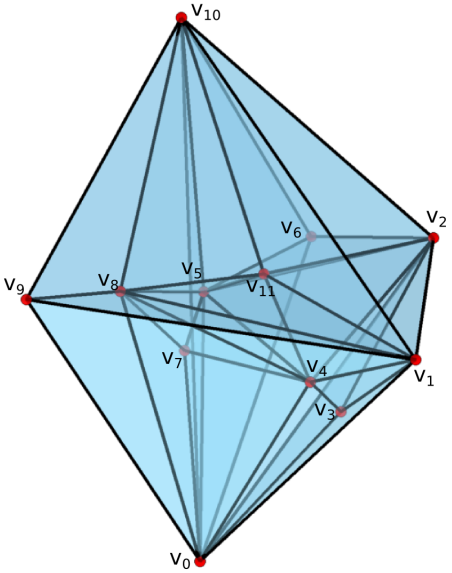

$\underline{F_4}$

$v_0 = (74, 90, 45)$
$v_1 = (71, 81, 76)$
$v_2 = (77, 75, 69)$
$v_3 = (84, 86, 80)$
$v_4 = (87, 86, 88)$
$v_5 = (77, 60, 71)$
$v_6 = (76, 72, 64)$
$v_7 = (79, 54, 72)$
$v_8 = (54, 73, 80)$
$v_9 = (62, 79, 68)$
$v_{10} = (67, 74, 69)$
$v_{11} = (72, 75, 74)$

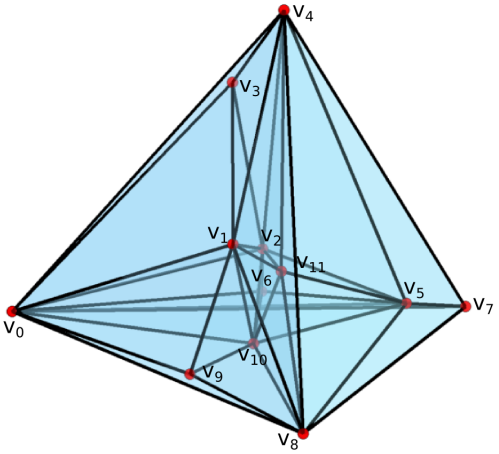

Figure 3.40

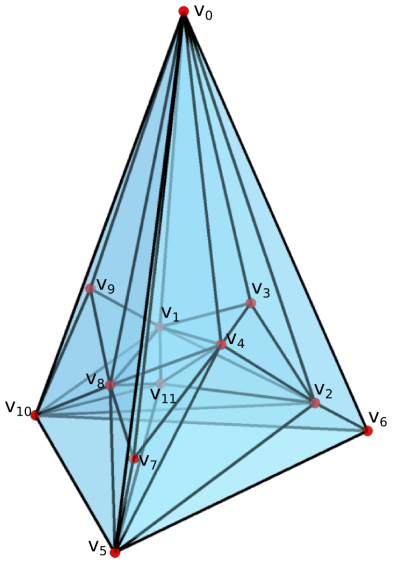

$\underline{F_5}$

$v_0 = (74, 95, 100)$
$v_1 = (79, 81, 69)$
$v_2 = (89, 66, 71)$
$v_3 = (81, 75, 79)$
$v_4 = (77, 73, 76)$
$v_5 = (58, 60, 67)$
$v_6 = (93, 61, 71)$
$v_7 = (62, 66, 72)$
$v_8 = (70, 77, 67)$
$v_9 = (76, 89, 67)$
$v_{10} = (77, 87, 47)$
$v_{11} = (75, 75, 68)$

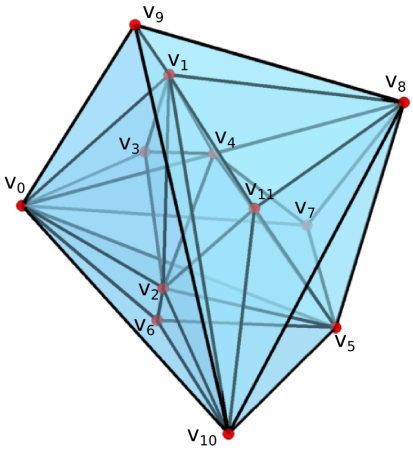

$\underline{F_6}$

$v_0 = (62, 64, 47)$
$v_1 = (65, 86, 78)$
$v_2 = (68, 67, 78)$
$v_3 = (68, 76, 66)$
$v_4 = (74, 77, 68)$
$v_5 = (87, 63, 74)$
$v_6 = (68, 64, 78)$
$v_7 = (86, 70, 65)$
$v_8 = (87, 86, 78)$
$v_9 = (61, 90, 79)$
$v_{10} = (68, 63, 99)$
$v_{11} = (75, 75, 78)$

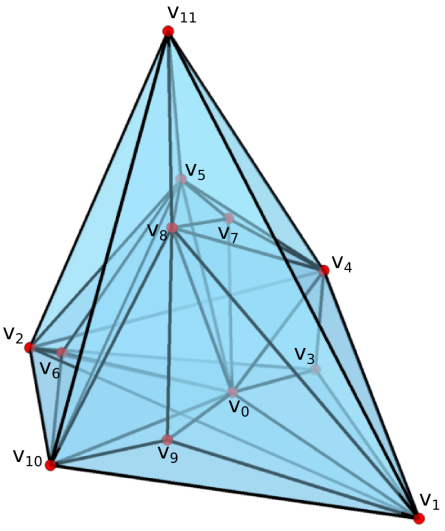

$\underline{F_7}$

$v_0 = (77, 79, 78)$
$v_1 = (72, 97, 89)$
$v_2 = (87, 59, 72)$
$v_3 = (81, 86, 69)$
$v_4 = (76, 84, 61)$
$v_5 = (65, 69, 66)$
$v_6 = (80, 63, 77)$
$v_7 = (68, 74, 66)$
$v_8 = (62, 70, 75)$
$v_9 = (72, 75, 89)$
$v_{10} = (69, 67, 97)$
$v_{11} = (50, 65, 65)$

$\underline{F_8}$
$v_0 = (73, 68, 80)$
$v_1 = (74, 87, 70)$
$v_2 = (90, 65, 81)$
$v_3 = (83, 76, 71)$
$v_4 = (83, 79, 66)$
$v_5 = (64, 57, 62)$
$v_6 = (79, 63, 84)$
$v_7 = (66, 65, 66)$
$v_8 = (61, 78, 71)$
$v_9 = (64, 80, 78)$
$v_{10} = (69, 87, 99)$
$v_{11} = (82, 95, 55)$

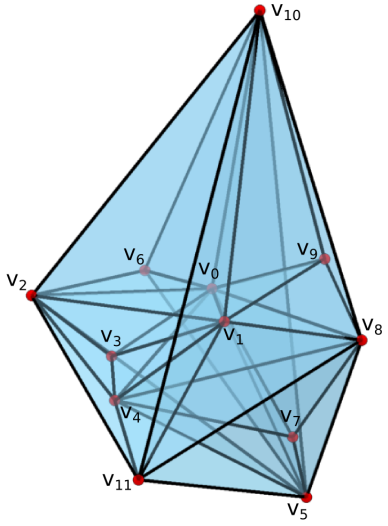

$\underline{F_9}$
$v_0 = (78, 80, 62)$
$v_1 = (90, 54, 75)$
$v_2 = (79, 77, 80)$
$v_3 = (82, 66, 70)$
$v_4 = (79, 65, 71)$
$v_5 = (68, 74, 70)$
$v_6 = (78, 80, 78)$
$v_7 = (67, 73, 68)$
$v_8 = (54, 66, 67)$
$v_9 = (81, 83, 55)$
$v_{10} = (77, 90, 98)$
$v_{11} = (71, 63, 88)$

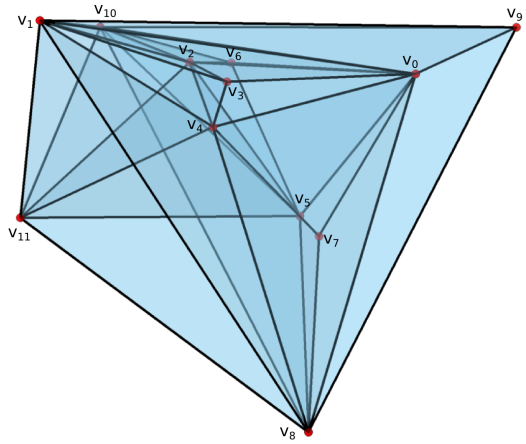

$\underline{F_{10}}$
$v_0 = (72, 69, 70)$
$v_1 = (61, 64, 87)$
$v_2 = (77, 86, 82)$
$v_3 = (60, 77, 71)$
$v_4 = (54, 81, 65)$
$v_5 = (83, 80, 64)$
$v_6 = (78, 82, 77)$
$v_7 = (77, 72, 61)$
$v_8 = (80, 57, 72)$
$v_9 = (67, 63, 82)$
$v_{10} = (73, 76, 90)$
$v_{11} = (83, 92, 99)$

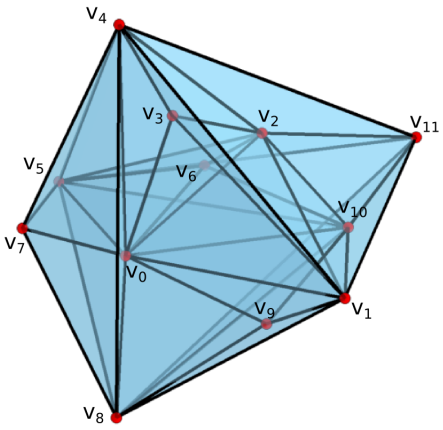

Figure 3.40: These are the facet list of the 3-sphere W_{12}^{40}, which was found by Werner and described in [72, Table 7.1, left], together with the coordinates of a fan-like embedding and diagrams based on the facets F_0, F_1, F_2, F_3, F_4, F_5, F_6, F_7, F_8, F_9, and F_{10}.

$\chi(v_7, v_8, v_{10}, v_2, v_9) \neq 0$. Therefore, we may fix an orientation of the realisation by setting $\chi(v_7, v_8, v_{10}, v_2, v_9) := +1$. Starting with this, we obtain the following implications:

$$\begin{aligned}
\chi(v_7\ , v_8\ , v_{10}, v_2\ , v_9\ ) = \ \ 1 \quad &\overset{F_6}{\Rightarrow} \chi(v_7\ , v_8\ , v_{10}, v_{11}, v_9\ ) = \ \ 1 \\
&\overset{F_9}{\Rightarrow} \chi(v_8\ , v_{10}, v_{11}, v_2\ , v_9\ ) = -1 && (3.71)\\
&\overset{F_8}{\Rightarrow} \chi(v_7\ , v_8\ , v_{10}, v_{11}, v_2\ ) = -1, && (3.72)\\
\chi(v_8\ , v_{10}, v_{11}, v_2\ , v_9\ ) \overset{(3.71)}{=} -1 \quad &\overset{F_8}{\Rightarrow} \chi(v_4\ , v_8\ , v_{10}, v_{11}, v_2\ ) = -1, && (3.73)\\
\chi(v_7\ , v_8\ , v_{10}, v_2\ , v_9\ ) = \ \ 1 \quad &\overset{F_6}{\Rightarrow} \chi(v_7\ , v_8\ , v_{10}, v_4\ , v_9\ ) = \ \ 1, && (3.74)\\
\chi(v_7\ , v_8\ , v_{10}, v_2\ , v_9\ ) = \ \ 1 \quad &\overset{F_6}{\Rightarrow} \chi(v_7\ , v_8\ , v_{10}, v_1\ , v_9\ ) = \ \ 1 && (3.75)\\
&\overset{F_9}{\Rightarrow} \chi(v_8\ , v_{10}, v_2\ , v_1\ , v_9\ ) = \ \ 1\\
&\overset{F_3}{\Rightarrow} \chi(v_4\ , v_{10}, v_2\ , v_1\ , v_9\ ) = \ \ 1\\
&\overset{F_7}{\Rightarrow} \chi(v_4\ , v_8\ , v_{10}, v_2\ , v_1\ ) = -1, && (3.76)\\
\chi(v_7\ , v_8\ , v_{10}, v_1\ , v_9\ ) \overset{(3.75)}{=} \ \ 1 \quad &\overset{F_9}{\Rightarrow} \chi(v_8\ , v_{10}, v_0\ , v_1\ , v_9\ ) = \ \ 1\\
&\overset{F_2}{\Rightarrow} \chi(v_8\ , v_7\ , v_0\ , v_1\ , v_9\ ) = \ \ 1\\
&\overset{F_6}{\Rightarrow} \chi(v_8\ , v_7\ , v_0\ , v_4\ , v_9\ ) = \ \ 1 && (3.77)\\
&\overset{F_4}{\Rightarrow} \chi(v_8\ , v_7\ , v_0\ , v_4\ , v_5\ ) = \ \ 1\\
&\overset{F_1}{\Rightarrow} \chi(v_{11}, v_7\ , v_0\ , v_4\ , v_5\ ) = \ \ 1\\
&\overset{F_{10}}{\Rightarrow} \chi(v_{11}, v_7\ , v_2\ , v_4\ , v_5\ ) = \ \ 1\\
&\overset{F_{11}}{\Rightarrow} \chi(v_{11}, v_1\ , v_2\ , v_4\ , v_5\ ) = \ \ 1\\
&\overset{F_7}{\Rightarrow} \chi(v_{11}, v_1\ , v_2\ , v_4\ , v_8\ ) = \ \ 1\\
&\overset{F_{11}}{\Rightarrow} \chi(v_4\ , v_8\ , v_{10}, v_{11}, v_1\ ) = \ \ 1, && (3.78)
\end{aligned}$$

$$\begin{aligned}
\chi(v_8\ , v_7\ , v_0\ , v_4\ , v_9\ ) \overset{(3.77)}{=} \ \ 1 \quad &\overset{F_4}{\Rightarrow} \chi(v_8\ , v_7\ , v_0\ , v_4\ , v_{11}) = \ \ 1\\
&\overset{F_{10}}{\Rightarrow} \chi(v_4\ , v_8\ , v_{10}, v_7\ , v_{11}) = \ \ 1, && (3.79)\\
\chi(v_8\ , v_7\ , v_0\ , v_4\ , v_9\ ) \overset{(3.77)}{=} \ \ 1 \quad &\overset{F_4}{\Rightarrow} \chi(v_8\ , v_7\ , v_0\ , v_4\ , v_1\ ) = \ \ 1\\
&\overset{F_{10}}{\Rightarrow} \chi(v_4\ , v_8\ , v_{10}, v_7\ , v_1\ ) = \ \ 1, && (3.80)
\end{aligned}$$

Note that this chain of arguments uses all facets except for F_0 and F_5; all vertices occur except for v_3 and v_6.

Given the values of χ that we have obtained, the contradiction appears in the three term Grassmann–Plücker relations:
Let $\lambda_1 = (v_7, v_8, v_{10})$, $a_1 = v_4$, $b_1 = v_{11}$, $c_1 = v_2$, $d_1 = v_9$,
and $\lambda_2 = (v_4, v_8, v_{10})$, $a_2 = v_7$, $b_2 = v_{11}$, $c_2 = v_2$, $d_2 = v_1$.

Then using the values of χ from above we get

$$\begin{aligned}
&\{\,\chi(\lambda_1,a_1,b_1)\cdot\chi(\lambda_1,c_1,d_1), && -\chi(\lambda_1,a_1,c_1)\cdot\chi(\lambda_1,b_1,d_1),\\
&&& \chi(\lambda_1,a_1,d_1)\cdot\chi(\lambda_1,b_1,c_1)\,\}\\
&\overset{(3.79),(3.72),(3.74),(3.72)}{=} \{(-1)\cdot(+1), && -\chi(v_7,v_8,v_{10},v_4,v_2)\cdot(+1), \quad (+1)\cdot(-1)\};\\
&\{\,\chi(\lambda_2,a_2,b_2)\cdot\chi(\lambda_2,c_2,d_2), && -\chi(\lambda_2,a_2,c_2)\cdot\chi(\lambda_2,b_2,d_2),\\
&&& \chi(\lambda_2,a_2,d_2)\cdot\chi(\lambda_2,b_2,c_2)\,\}\\
&\overset{(3.73),(3.76),(3.78),(3.80),(3.73)}{=} \{(+1)\cdot(-1), && -\chi(v_4,v_8,v_{10},v_7,v_2)\cdot(+1), \quad (+1)\cdot(-1)\}.
\end{aligned}$$

Thus, both sets contain -1, while by the alternating property of χ not both of them can contain $+1$. Therefore, there is no chirotope, and hence no oriented matroid for the sphere W_{12}^{40}. This shows that it is non-polytopal. □

Proposition 3.2.10. *The sphere W_{12}^{40} has a diagram based on each of the facets F_0, F_1, F_2, F_3, F_4, F_5, F_6, F_7, F_8, F_9, and F_{10}, but not based on F_{11}.*

Proof. We construct partial chirotopes as explained at the beginning of the chapter.

The resulting partial chirotopes for the different facets as bases give already the signs of 199 to 328 elements out of $\binom{12}{4} = 495$, which is the size of an oriented matroid for a diagram of W_{12}^{40}. With SCIP we can find coordinates for the diagrams with bases $F_0,\dots,F_{10}$ (see Figure 3.40), while in the case of the diagram with base F_{11} we used backtracking to find a partial chirotope of size at least 435 (i.e. of roughly 87.5%) for every oriented matroid. For all of these partial chirotopes we checked the existence of a bfp. The bfps for the partial chirotopes will also be bfps for all oriented matroids that would complete this partial chirotope, so in finding bfps at this stage we could decrease the size of the search tree by a factor of 2^{60}. There were 6098 such partial chirotopes. To prove existence of the bfps for all these partial chirotopes, we needed roughly one week of computing time on a usual Linux workstation. □

Proposition 3.2.11. *The sphere W_{12}^{40} is fan-like, but not polyhedrally embeddable, and hence it is not star-shaped.*

Proof. The coordinates of a fan-like embedding of W_{12}^{40} are in Figure 3.40 and were found as described above.

The rest of the proof heavily depends on the structure of W_{12}^{40}, and establishes the following:

(i) If W_{12}^{40} is polyhedrally embeddable into some $\mathbb{R}^k$, $k \geq 4$, then it is also polyhedrally embeddable into $\mathbb{R}^4$.

(ii) If W_{12}^{40} is polyhedrally embedded into $\mathbb{R}^4$, then this is a polyhedral embedding as convex polytope.

Let us assume that W_{12}^{40} is polyhedrally embedded in some $\mathbb{R}^k$, that is, it is realised by a polytopal complex Γ (where each of the facets is realised as a convex 3-polytope).

For (i) we note that v_3 is a simple vertex, that is, a vertex that is contained in only 4 facets, or equivalently, in only 4 edges. The 4 facets are each contained in the affine span of 3 of these edges, so all 4 facets are contained in the affine span of the 4 edges. Moreover, each of the 12 vertices of the sphere is contained in at least one of the 4 facets, which are F_0, F_1, F_2 and F_7. So the complete embedded sphere is contained in this affine 4-dimensional subspace of $\mathbb{R}^k$.

For (ii) note that the argument for (i) implies that in addition each of the facets F_0, F_1, F_2 and F_7 is also a facet of the convex hull of Γ, that is, all of Γ is contained in a closed halfspace of the hyperplane spanned by the facet, while only the vertices of the facet lie on the boundary hyperplane. Exactly the same arguments are valid for the other three simple vertices of W_{12}^{40} and the facets they are contained in: the vertex v_6 and the facets F_1, F_3, F_5 and F_8, the vertex v_7 and the facets F_1, F_4, F_6 and F_{10}, as well as the vertex v_9 and the facets F_2, F_3, F_6 and F_9. Thus, we have established for all facets F_i of Γ, except for the tetrahedron F_{11}, that it is also a facet of the convex hull of Γ. As mentioned above, F_{11} is special in the way that it is the only facet that does not contain a simple vertex.

To see that also F_{11} is a facet of the convex hull of Γ, consider its neighbours F_1, F_7, F_8, and F_{10}. Since these are all facets of the convex hull of Γ, they cannot lie in the same hyperplane as F_{11}. The facet F_1 gives that the vertices v_0, v_3, v_6, and v_7 lie on the same side of the hyperplane H_{11} spanned by F_{11}. Now, the facet F_7 contains v_3, the facet F_8 contains v_6, and the facet F_{10} contains v_7, whence the points from these facets not in F_{11} are also all on the same side of H_{11}. Therefore, we have that all points, except possibly v_9, lie in, say, H_{11}^+. Since F_9 is a bipyramid over the triangle v_1, v_8, v_{10} with apices v_9 and v_{11}, and since v_{11} is in F_{11}, it follows $v_9 \in H_{11}^+$. This completes the proof of (ii). □

Theorem 3.2.12. *The sphere* (12_{40}^0) *is non-polytopal.*

Proof. The proof of this theorem works the same way as described above: we construct a partial chirotope for the oriented matroid of the respective sphere starting out with one sign we may choose, and derive a contradiction from that.

Since five points in a common facet are colinear, we get:

$$\chi(v_2\ , v_3\ , v_9\ , v_{10}, v_{11}) \overset{F_{11}}{=} \quad 0. \tag{3.81}$$

(3.82)

Figure 3.41

(12^{0}_{40})

$F_0 = \{v_0, v_3, v_5, v_6, v_9\}$
$F_1 = \{v_0, v_3, v_6, v_8, v_{10}\}$
$F_2 = \{v_1, v_4, v_5, v_7, v_{11}\}$
$F_3 = \{v_2, v_4, v_6, v_8, v_{10}\}$
$F_4 = \{v_2, v_4, v_7, v_{10}, v_{11}\}$
$F_5 = \{v_1, v_3, v_5, v_9, v_{11}\}$
$F_6 = \{v_0, v_2, v_6, v_8, v_9\}$
$F_7 = \{v_0, v_1, v_5, v_7, v_8, v_9\}$
$F_8 = \{v_0, v_1, v_4, v_7, v_8, v_{10}\}$
$F_9 = \{v_0, v_3, v_5, v_7, v_{10}, v_{11}\}$
$F_{10} = \{v_1, v_2, v_4, v_8, v_9, v_{11}\}$
$F_{11} = \{v_2, v_3, v_6, v_9, v_{10}, v_{11}\}$

fan

$v_0 = (6112414565/6116143, 1, 1, 1)$
$v_1 = (0, 1000, 0, 0)$
$v_2 = (0, 0, 1000, 1000)$
$v_3 = (-7039, -8138, -7583, -7583)$
$v_4 = (-5446, -5189, -4988, -4988)$
$v_5 = (-7835, -7713, -8073, -8073)$
$v_6 = (-4748, -5199, -4854, -4854)$
$v_7 = (-9340, -9008, -9408, -9408)$
$v_8 = (-5113, -5255, -5021, -5021)$
$v_9 = (-5653, -5930, -5776, -5776)$
$v_{10} = (-9145, -9575, -8834, -8834)$
$v_{11} = (-9736, -9931, -9836, -9836)$
$o = (-8540, -8572, -8407, -8407)$

F_0

$v_0 = (0, 0, 0)$
$v_1 = (3663675077/823706, 4709, 7994)$
$v_2 = (3398, 2004, 3990)$
$v_3 = (0, 1000, 0)$
$v_4 = (3024, 2760, 4663)$
$v_5 = (79, 8760, 9935)$
$v_6 = (1000, 0, 0)$
$v_7 = (511, 7372, 8602)$
$v_8 = (3488, 2474, 4898)$
$v_9 = (9942, 1968, 8296)$
$v_{10} = (2301, 1993, 3245)$
$v_{11} = (2839, 2787, 4369)$

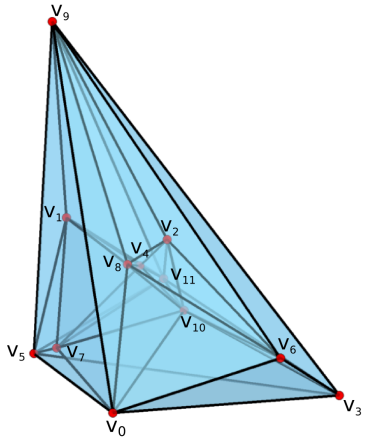

F_1

$v_0 = (0, 0, 0)$
$v_1 = (23101429342/2712507, 8906, 8868)$
$v_2 = (8521, 8542, 8393)$
$v_3 = (5000, 0, 0)$
$v_4 = (8996, 8976, 9106)$
$v_5 = (8221, 8083, 8077)$
$v_6 = (0, 5000, 0)$
$v_7 = (8449, 8031, 8271)$
$v_8 = (8016, 9420, 9026)$
$v_9 = (8021, 8039, 7900)$
$v_{10} = (9866, 8741, 9326)$
$v_{11} = (8386, 8229, 8232)$

F_2

$v_0 = (6232, 8707, 42764)$
$v_1 = (0, 0, 0)$
$v_2 = (32864, 8157, 9543)$
$v_3 = (59562, 11577, 7683)$
$v_4 = (82130, 12399, 24586)$
$v_5 = (0, 10000, 0)$
$v_6 = (18874, 8520, 27912)$
$v_7 = (81446107666/7665509, 13064, 99514)$
$v_8 = (5354, 7569, 35414)$
$v_9 = (1821, 5524, 1369)$
$v_{10} = (25201, 9550, 36358)$
$v_{11} = (98778, 12894, 11865)$

F_3

$v_0 = (7283, 6303, 7216)$
$v_1 = (1637096393/1051950, 714, 750)$
$v_2 = (0, 0, 0)$
$v_3 = (5577, 4509, 5351)$
$v_4 = (1000, 0, 0)$
$v_5 = (4261, 3248, 3823)$
$v_6 = (5084, 4532, 5178)$
$v_7 = (3895, 2472, 3028)$
$v_8 = (6909, 8614, 8644)$
$v_9 = (4591, 3942, 4526)$
$v_{10} = (8672, 3555, 5902)$
$v_{11} = (3100, 2041, 2495)$

Figure 3.41

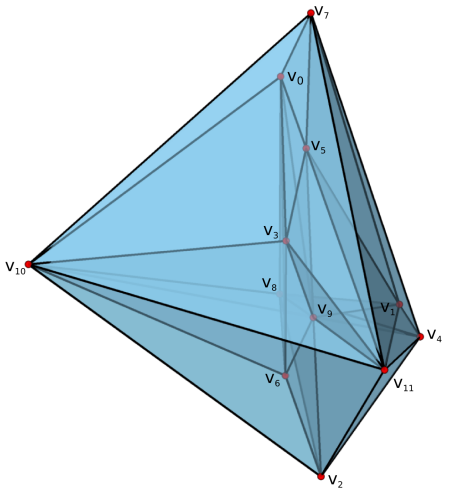

$\underline{F_4}$

$v_0 = (991, 1187, 1244)$
$v_1 = (14125049/14795, 179, 227)$
$v_2 = (0, 0, 0)$
$v_3 = (397, 703, 1025)$
$v_4 = (1000, 0, 0)$
$v_5 = (739, 868, 1228)$
$v_6 = (299, 442, 84)$
$v_7 = (1155, 1192, 1542)$
$v_8 = (631, 722, 161)$
$v_9 = (377, 444, 622)$
$v_{10} = (0, 1891, 0)$
$v_{11} = (0, 0, 1286)$

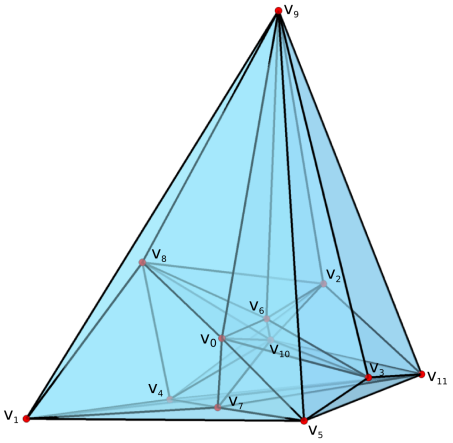

$\underline{F_5}$

$v_0 = (384, 345, 53)$
$v_1 = (1410, 0, 1)$
$v_2 = (230, 567, 862)$
$v_3 = (0, 90, 486)$
$v_4 = (947, 9, 543)$
$v_5 = (0, 0, 0)$
$v_6 = (320, 406, 385)$
$v_7 = (9491655/22373, 15, 46)$
$v_8 = (789, 689, 40)$
$v_9 = (1, 1705, 1)$
$v_{10} = (329, 304, 436)$
$v_{11} = (18, 1, 1733)$

$\underline{F_8}$

$v_0 = (0, 0, 0)$
$v_1 = (34, 0, 30)$
$v_2 = (55, 372, 2045/108)$
$v_3 = (15, 373, 1)$
$v_4 = (68, 338, 21)$
$v_5 = (7, 67, 28)$
$v_6 = (38, 299, 1)$
$v_7 = (0, 0, 33)$
$v_8 = (100, 0, 0)$
$v_9 = (30, 216, 11)$
$v_{10} = (0, 848, 0)$
$v_{11} = (11, 186, 24)$

$\underline{F_9}$

$v_0 = (0, 0, 0)$
$v_1 = (401115135/174449, 1485, 1005)$
$v_2 = (2781, 1654, 1816)$
$v_3 = (1000, 0, 9332)$
$v_4 = (2674, 1594, 1320)$
$v_5 = (0, 1000, 0)$
$v_6 = (1276, 737, 987)$
$v_7 = (2732, 1924, 868)$
$v_8 = (1287, 761, 706)$
$v_9 = (1293, 801, 991)$
$v_{10} = (3454, 1458, 2371)$
$v_{11} = (2842, 1765, 2239)$

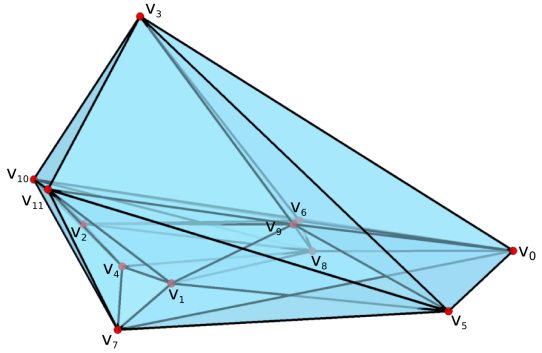

$\underline{F_{10}}$
$v_0 = (61588, 30185, 7355)$
$v_1 = (1, 1, -1898048173/1624776653)$
$v_2 = (71539, 37218, 136996)$
$v_3 = (4893, 70116, 50009)$
$v_4 = (6321, 100, 62535)$
$v_5 = (8829, 69736, 7535)$
$v_6 = (64999, 29956, 46275)$
$v_7 = (14943, 24541, 5979)$
$v_8 = (100000, 0, 0)$
$v_9 = (4670, 151643, 137)$
$v_{10} = (41589, 30763, 58881)$
$v_{11} = (387, 38247, 87801)$

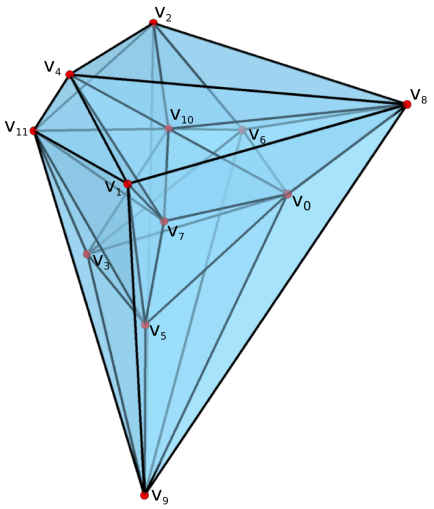

Figure 3.41: These are the facet list, coordinates for a fan-like embedding, and the diagrams (resp. coordinates for these) with bases F_0, F_1, F_2, F_3, F_4, F_5, F_8, F_9, and F_{10} of the first of the three 3-spheres with f-vector $(12, 40, 40, 12)$ that were found by our enumeration and not described before. This sphere is self-dual and non-polytopal.

From facet F_0 (see Figure 3.41 for a drawing) we may choose $\chi(v_0\ , v_3\ , v_6\ , v_9\ , v_i\ ) = \ \ 1$, where $v_i \notin F_0$. With this we can derive:

$$
\begin{aligned}
\chi(v_0\ , v_3\ , v_6\ , v_9\ , v_{10}) = \ \ 1 \quad &\overset{F_1}{\Rightarrow} \chi(v_0\ , v_3\ , v_6\ , v_7\ , v_{10}) = \ \ 1 \\
&\overset{F_9}{\Rightarrow} \chi(v_0\ , v_3\ , v_7\ , v_8\ , v_{10}) = -1 \\
&\overset{F_1}{\Rightarrow} \chi(v_0\ , v_1\ , v_3\ , v_8\ , v_{10}) = \ \ 1 \\
&\overset{F_8}{\Rightarrow} \chi(v_0\ , v_1\ , v_8\ , v_9\ , v_{10}) = -1 \\
&\overset{F_7}{\Rightarrow} \chi(v_0\ , v_1\ , v_2\ , v_8\ , v_9\ ) = -1 \\
&\overset{F_{10}}{\Rightarrow} \chi(v_1\ , v_2\ , v_7\ , v_8\ , v_9\ ) = -1 \\
&\overset{F_7}{\Rightarrow} \chi(v_1\ , v_3\ , v_7\ , v_8\ , v_9\ ) = -1, \qquad (3.83) \\
\chi(v_0\ , v_2\ , v_3\ , v_6\ , v_9\ ) = -1 \quad &\overset{F_6}{\Rightarrow} \chi(v_0\ , v_2\ , v_5\ , v_6\ , v_9\ ) = -1 \\
&\overset{F_0}{\Rightarrow} \chi(v_0\ , v_1\ , v_5\ , v_6\ , v_9\ ) = -1 \\
&\overset{F_7}{\Rightarrow} \chi(v_0\ , v_1\ , v_5\ , v_9\ , v_{11}) = \ \ 1 \\
&\overset{F_5}{\Rightarrow} \chi(v_1\ , v_2\ , v_5\ , v_9\ , v_{11}) = -1 \\
&\overset{F_{10}}{\Rightarrow} \chi(v_1\ , v_2\ , v_3\ , v_9\ , v_{11}) = -1 \\
&\overset{F_5}{\Rightarrow} \chi(v_1\ , v_3\ , v_7\ , v_9\ , v_{11}) = \ \ 1, \qquad (3.84)
\end{aligned}
$$

$$\begin{aligned}
\chi(v_0,v_3,v_6,v_9,v_{10}) = 1 &\overset{F_1}{\Rightarrow} \chi(v_0,v_3,v_6,v_{10},v_{11}) = -1\\
&\overset{F_9}{\Rightarrow} \chi(v_0,v_2,v_3,v_{10},v_{11}) = 1\\
&\overset{F_{11}}{\Rightarrow} \chi(v_2,v_3,v_7,v_{10},v_{11}) = 1\\
&\overset{F_9}{\Rightarrow} \chi(v_3,v_7,v_9,v_{10},v_{11}) = 1, \qquad (3.85)\\
\chi(v_0,v_3,v_6,v_7,v_{10}) \overset{(3.83)}{=} 1 &\overset{F_9}{\Rightarrow} \chi(v_0,v_3,v_4,v_7,v_{10}) = 1\\
&\overset{F_8}{\Rightarrow} \chi(v_0,v_2,v_4,v_7,v_{10}) = 1\\
&\overset{F_4}{\Rightarrow} \chi(v_1,v_2,v_4,v_7,v_{10}) = 1\\
&\overset{F_8}{\Rightarrow} \chi(v_1,v_3,v_4,v_7,v_{10}) = 1, \qquad (3.86)\\
\chi(v_2,v_3,v_7,v_{10},v_{11}) \overset{(3.85)}{=} 1 &\overset{F_9}{\Rightarrow} \chi(v_3,v_4,v_7,v_{10},v_{11}) = -1, \qquad (3.87)\\
\chi(v_2,v_3,v_7,v_{10},v_{11}) \overset{(3.85)}{=} 1 &\overset{F_9}{\Rightarrow} \chi(v_1,v_3,v_7,v_{10},v_{11}) = 1, \qquad (3.88)\\
\chi(v_0,v_1,v_8,v_9,v_{10}) \overset{(3.83)}{=} -1 &\overset{F_7}{\Rightarrow} \chi(v_0,v_1,v_8,v_9,v_{11}) = -1\\
&\overset{F_{10}}{\Rightarrow} \chi(v_1,v_7,v_8,v_9,v_{11}) = 1, \qquad (3.89)\\
\chi(v_0,v_3,v_7,v_8,v_{10}) \overset{(3.83)}{=} -1 &\overset{F_1}{\Rightarrow} \chi(v_0,v_3,v_8,v_9,v_{10}) = 1, \qquad (3.90)\\
\chi(v_1,v_2,v_7,v_8,v_9) \overset{(3.83)}{=} -1 &\overset{F_7}{\Rightarrow} \chi(v_1,v_7,v_8,v_9,v_{10}) = 1, \qquad (3.91)\\
\chi(v_0,v_1,v_8,v_9,v_{10}) \overset{(3.83)}{=} -1 &\overset{F_7}{\Rightarrow} \chi(v_0,v_1,v_6,v_8,v_9) = -1\\
&\overset{F_6}{\Rightarrow} \chi(v_0,v_6,v_7,v_8,v_9) = 1\\
&\overset{F_7}{\Rightarrow} \chi(v_0,v_7,v_8,v_9,v_{10}) = -1, \qquad (3.92)\\
\chi(v_0,v_3,v_6,v_{10},v_{11}) \overset{(3.85)}{=} -1 &\overset{F_9}{\Rightarrow} \chi(v_0,v_3,v_9,v_{10},v_{11}) = -1\\
&\overset{F_{11}}{\Rightarrow} \chi(v_3,v_8,v_9,v_{10},v_{11}) = 1, \qquad (3.93)\\
\chi(v_0,v_2,v_4,v_7,v_{10}) \overset{(3.86)}{=} 1 &\overset{F_4}{\Rightarrow} \chi(v_2,v_3,v_4,v_7,v_{10}) = -1, \qquad (3.94)\\
\chi(v_0,v_1,v_2,v_8,v_9) \overset{(3.83)}{=} -1 &\overset{F_6}{\Rightarrow} \chi(v_0,v_2,v_8,v_9,v_{11}) = 1\\
&\overset{F_{10}}{\Rightarrow} \chi(v_2,v_8,v_9,v_{10},v_{11}) = -1, \qquad (3.95)\\
\chi(v_0,v_6,v_7,v_8,v_9) \overset{(3.92)}{=} 1 &\overset{F_7}{\Rightarrow} \chi(v_0,v_7,v_8,v_9,v_{11}) = -1, \qquad (3.96)\\
\chi(v_0,v_2,v_8,v_9,v_{11}) \overset{(3.95)}{=} 1 &\overset{F_{10}}{\Rightarrow} \chi(v_2,v_7,v_8,v_9,v_{11}) = -1, \qquad (3.97)\\
\chi(v_0,v_1,v_3,v_8,v_{10}) \overset{(3.83)}{=} 1 &\overset{F_8}{\Rightarrow} \chi(v_0,v_1,v_8,v_{10},v_{11}) = 1, \qquad (3.98)\\
\chi(v_0,v_3,v_7,v_8,v_{10}) \overset{(3.83)}{=} -1 &\overset{F_1}{\Rightarrow} \chi(v_0,v_3,v_8,v_{10},v_{11}) = -1, \qquad (3.99)\\
\chi(v_0,v_1,v_8,v_9,v_{11}) \overset{(3.89)}{=} -1 &\overset{F_{10}}{\Rightarrow} \chi(v_1,v_8,v_9,v_{10},v_{11}) = 1, \qquad (3.100)\\
\chi(v_0,v_2,v_3,v_{10},v_{11}) \overset{(3.85)}{=} 1 &\overset{F_{11}}{\Rightarrow} \chi(v_2,v_3,v_8,v_{10},v_{11}) = 1, \qquad (3.101)\\
\chi(v_0,v_1,v_2,v_8,v_9) \overset{(3.83)}{=} -1 &\overset{F_6}{\Rightarrow} \chi(v_0,v_2,v_8,v_9,v_{10}) = 1, \qquad (3.102)
\end{aligned}$$

$$\chi(v_0\ ,v_3\ ,v_7\ ,v_8\ ,v_{10}) \overset{(3.83)}{=} -1 \quad \overset{F_1}{\Rightarrow} \chi(v_0\ ,v_3\ ,v_4\ ,v_8\ ,v_{10}) = -1$$
$$\overset{F_8}{\Rightarrow} \chi(v_0\ ,v_2\ ,v_4\ ,v_8\ ,v_{10}) = -1$$
$$\overset{F_3}{\Rightarrow} \chi(v_1\ ,v_2\ ,v_4\ ,v_8\ ,v_{10}) = -1$$
$$\overset{F_8}{\Rightarrow} \chi(v_1\ ,v_4\ ,v_8\ ,v_{10},v_{11}) = \ \ 1, \tag{3.103}$$
$$\chi(v_0\ ,v_2\ ,v_4\ ,v_8\ ,v_{10}) \overset{(3.103)}{=} -1 \quad \overset{F_3}{\Rightarrow} \chi(v_2\ ,v_4\ ,v_8\ ,v_{10},v_{11}) = -1. \tag{3.104}$$
$$\chi(v_0\ ,v_3\ ,v_6\ ,v_7\ ,v_{10}) \overset{(3.83)}{=} \ \ 1 \quad \overset{F_9}{\Rightarrow} \chi(v_0\ ,v_1\ ,v_3\ ,v_7\ ,v_{10}) = -1$$
$$\overset{F_8}{\Rightarrow} \chi(v_0\ ,v_1\ ,v_7\ ,v_{10},v_{11}) = -1$$
$$\overset{F_9}{\Rightarrow} \chi(v_0\ ,v_2\ ,v_7\ ,v_{10},v_{11}) = -1$$
$$\overset{F_4}{\Rightarrow} \chi(v_2\ ,v_7\ ,v_8\ ,v_{10},v_{11}) = -1, \tag{3.105}$$
$$\chi(v_0\ ,v_1\ ,v_3\ ,v_7\ ,v_{10}) \overset{(3.105)}{=} -1 \quad \overset{F_8}{\Rightarrow} \chi(v_0\ ,v_1\ ,v_5\ ,v_7\ ,v_{10}) = -1$$
$$\overset{F_7}{\Rightarrow} \chi(v_0\ ,v_1\ ,v_4\ ,v_5\ ,v_7\ ) = -1$$
$$\overset{F_2}{\Rightarrow} \chi(v_1\ ,v_4\ ,v_5\ ,v_7\ ,v_8\ ) = -1$$
$$\overset{F_7}{\Rightarrow} \chi(v_1\ ,v_5\ ,v_7\ ,v_8\ ,v_{10}) = \ \ 1$$
$$\overset{F_8}{\Rightarrow} \chi(v_1\ ,v_7\ ,v_8\ ,v_{10},v_{11}) = -1, \tag{3.106}$$
$$\chi(v_0\ ,v_2\ ,v_4\ ,v_7\ ,v_{10}) \overset{(3.86)}{=} \ \ 1 \quad \overset{F_4}{\Rightarrow} \chi(v_2\ ,v_4\ ,v_7\ ,v_8\ ,v_{10}) = -1$$
$$\overset{F_8}{\Rightarrow} \chi(v_4\ ,v_7\ ,v_8\ ,v_{10},v_{11}) = -1, \tag{3.107}$$

With these values for the partial chirotope, we can find some new values of χ using the Grassmann-Plücker-relations:

$$\{\chi(v_8,v_{10},v_{11},v_1,v_2)\chi(v_8,v_{10},v_{11},v_4,v_7),\quad \chi(v_8,v_{10},v_{11},v_1,v_4)\chi(v_8,v_{10},v_{11},v_2,v_7),$$
$$\chi(v_8,v_{10},v_{11},v_1,v_7)\chi(v_8,v_{10},v_{11},v_2,v_4)\}$$
$$\overset{(3.107),(3.103),(3.105),(3.106),(3.104)}{=} \{\chi(v_1,v_2,v_8,v_{10},v_{11})\cdot(-1), -1\cdot(-1),$$
$$(-1)\cdot(-1)\},$$
$$\Rightarrow \chi(v_8,v_{10},v_{11},v_1,v_2) = \ \ 1 \tag{3.108}$$
$$\{\chi(v_8,v_{10},v_{11},v_1,v_2)\chi(v_8,v_{10},v_{11},v_3,v_9),\quad \chi(v_8,v_{10},v_{11},v_1,v_3)\chi(v_8,v_{10},v_{11},v_2,v_9),$$
$$\chi(v_8,v_{10},v_{11},v_1,v_9)\chi(v_8,v_{10},v_{11},v_2,v_3)\}$$
$$\overset{(3.108),(3.93),(3.95),(3.100),(3.101)}{=} \{1\cdot(-1), -\chi(v_8,v_{10},v_{11},v_1,v_3)\cdot 1,$$
$$(-1)\cdot 1\},$$
$$\Rightarrow \chi(v_1,v_3,v_8,v_{10},v_{11}) = -1 \tag{3.109}$$
$$\{\chi(v_8,v_{10},v_{11},v_0,v_1)\chi(v_8,v_{10},v_{11},v_3,v_9),\quad \chi(v_8,v_{10},v_{11},v_0,v_3)\chi(v_8,v_{10},v_{11},v_1,v_9),$$
$$\chi(v_8,v_{10},v_{11},v_0,v_9)\chi(v_8,v_{10},v_{11},v_1,v_3)\}$$
$$\overset{(3.98),(3.93),(3.99),(3.100),(3.109)}{=} \{1\cdot(-1), -(-1)\cdot(-1),$$
$$\chi(v_8,v_{10},v_{11},v_0,v_9)\cdot(-1)\},$$
$$\Rightarrow \chi(v_8,v_{10},v_{11},v_0,v_9) = -1 \tag{3.110}$$

$$\{\chi(v_8,v_9,v_{10},v_0,v_2)\chi(v_8,v_9,v_{10},v_3,v_{11}),\quad \chi(v_8,v_9,v_{10},v_0,v_3)\chi(v_8,v_9,v_{10},v_2,v_{11}),$$
$$\chi(v_8,v_9,v_{10},v_0,v_{11})\chi(v_8,v_9,v_{10},v_2,v_3)\}$$
$$\overset{(3.102),(3.93),(3.90),(3.95),(3.110)}{=} \{1\cdot(-1),-1\cdot 1,$$
$$(-1)\cdot\chi(v_8,v_9,v_{10},v_2,v_3)\},$$
$$\Rightarrow \chi(v_8,v_9,v_{10},v_2,v_3)=-1 \tag{3.111}$$

$$\{\chi(v_3,v_9,v_{10},v_2,v_7)\chi(v_3,v_9,v_{10},v_8,v_{11}),\quad \chi(v_3,v_9,v_{10},v_2,v_8)\chi(v_3,v_9,v_{10},v_7,v_{11}),$$
$$\chi(v_3,v_9,v_{10},v_2,v_{11})\chi(v_3,v_9,v_{10},v_7,v_8)\}$$
$$\overset{(3.93),(3.111),(3.85),(3.81)}{=} \{\chi(v_3,v_9,v_{10},v_2,v_7)\cdot 1,-1\cdot 1,$$
$$0\},$$
$$\Rightarrow \chi(v_3,v_9,v_{10},v_2,v_7)=\quad 1 \tag{3.112}$$

$$\{\chi(v_8,v_9,v_{11},v_0,v_2)\chi(v_8,v_9,v_{11},v_7,v_{10}),\quad \chi(v_8,v_9,v_{11},v_0,v_7)\chi(v_8,v_9,v_{11},v_2,v_{10}),$$
$$\chi(v_8,v_9,v_{11},v_0,v_{10})\chi(v_8,v_9,v_{11},v_2,v_7)\}$$
$$\overset{(3.95),(3.96),(3.95),(3.110),(3.97)}{=} \{1\cdot\chi(v_8,v_9,v_{11},v_7,v_{10}),-(-1)\cdot(-1),$$
$$1\cdot(-1)\},$$
$$\Rightarrow \chi(v_8,v_9,v_{11},v_7,v_{10})=\quad 1 \tag{3.113}$$

$$\{\chi(v_3,v_7,v_{10},v_2,v_4)\chi(v_3,v_7,v_{10},v_9,v_{11}),\quad \chi(v_3,v_7,v_{10},v_2,v_9)\chi(v_3,v_7,v_{10},v_4,v_{11}),$$
$$\chi(v_3,v_7,v_{10},v_2,v_{11})\chi(v_3,v_7,v_{10},v_4,v_9)\}$$
$$\overset{(3.94),(3.85),(3.112),(3.87),(3.85)}{=} \{1\cdot(-1),-1\cdot 1,$$
$$(-1)\cdot\chi(v_3,v_7,v_{10},v_4,v_9)\},$$
$$\Rightarrow \chi(v_3,v_7,v_{10},v_4,v_9)=-1 \tag{3.114}$$

$$\{\chi(v_3,v_7,v_{10},v_1,v_4)\chi(v_3,v_7,v_{10},v_9,v_{11}),\quad \chi(v_3,v_7,v_{10},v_1,v_9)\chi(v_3,v_7,v_{10},v_4,v_{11}),$$
$$\chi(v_3,v_7,v_{10},v_1,v_{11})\chi(v_3,v_7,v_{10},v_4,v_9)\}$$
$$\overset{(3.86),(3.85),(3.87),(3.88),(3.114)}{=} \{(-1)\cdot(-1),-\chi(v_3,v_7,v_{10},v_1,v_9)\cdot(-1),$$
$$(-1)\cdot(-1)\},$$
$$\Rightarrow \chi(v_3,v_7,v_{10},v_1,v_9)=-1 \tag{3.115}$$

$$\{\chi(v_8,v_9,v_{10},v_0,v_3)\chi(v_8,v_9,v_{10},v_7,v_{11}),\quad \chi(v_8,v_9,v_{10},v_0,v_7)\chi(v_8,v_9,v_{10},v_3,v_{11}),$$
$$\chi(v_8,v_9,v_{10},v_0,v_{11})\chi(v_8,v_9,v_{10},v_3,v_7)\}$$
$$\overset{(3.90),(3.113),(3.92),(3.93),(3.110)}{=} \{1\cdot(-1),-(-1)\cdot(-1),$$
$$(-1)\cdot\chi(v_8,v_9,v_{10},v_3,v_7)\},$$
$$\Rightarrow \chi(v_8,v_9,v_{10},v_3,v_7)=-1 \tag{3.116}$$

$$\begin{aligned}\{\chi(v_7,v_8,v_9,v_1,v_3)\chi(v_7,v_8,v_9,v_{10},v_{11}), \quad & \chi(v_7,v_8,v_9,v_1,v_{10})\chi(v_7,v_8,v_9,v_3,v_{11}),\\ & \chi(v_7,v_8,v_9,v_1,v_{11})\chi(v_7,v_8,v_9,v_3,v_{10})\}\\ \overset{(3.83),(3.113),(3.91),(3.89),(3.116)}{=} \quad & \{(-1)\cdot 1, -(-1)\cdot\chi(v_7,v_8,v_9,v_3,v_{11}),\\ & \qquad (-1)\cdot 1\},\\ & \Rightarrow \chi(v_7,v_8,v_9,v_3,v_{11}) = \quad 1 \end{aligned} \tag{3.117}$$

Finally, we get the Grassmann-Plücker-relation

$$\begin{aligned}\{\chi(v_3,v_7,v_9,v_1,v_8)\chi(v_3,v_7,v_9,v_{10},v_{11}), \quad & \chi(v_3,v_7,v_9,v_1,v_{10})\chi(v_3,v_7,v_9,v_8,v_{11}),\\ & \chi(v_3,v_7,v_9,v_1,v_{11})\chi(v_3,v_7,v_9,v_8,v_{10})\}\\ \overset{(3.83),(3.85),(3.115),(3.117),(3.84),(3.116)}{=} \quad & \{(-1)\cdot 1, -1\cdot 1, (-1)\cdot 1\}, \end{aligned} \tag{3.118}$$

which is neither $\{0\}$, nor contains $\{-1,1\}$. Therefore, the Grassmann-Plücker-relations cannot be satisfied, whence the sphere (12^0_{40}) does not support an oriented matroid. Hence, it is non-polytopal. □

Proposition 3.2.13. *The sphere (12^0_{40}) is fan-like and has a diagram based on each of the facets F_0, F_1, F_2, F_3, F_4, F_5, F_8, F_9, and F_{10}, but does not have a diagram based on F_{11}.*

Proof. We construct partial chirotopes as explained at the beginning of the chapter.

The resulting partial chirotopes for the different facets as bases of a diagram give already the signs of 177 to 386 elements out of $\binom{12}{4} = 495$, which is the size of an oriented matroid for a diagram of (12^0_{40}). With SCIP we can find coordinates for the diagrams with bases F_0, F_1, F_2, F_3, F_4, F_5, F_8, F_9, and F_{10}, as well as for the fan-like embedding (see Figure 3.42), while in the case F_{11} backtracking revealed that all chirotopes violate the Grassmann–Plücker relations. □

Remark. We could not decide the case of a star-shaped embedding, nor that of a diagram based on F_6, or F_7, since in these cases oriented matroids exist, but we could not find coordinates.

Theorem 3.2.14. *The sphere (12^1_{40}) is non-polytopal.*

Proof. The proof of this theorem works the same way as described above: we construct a partial chirotope for the oriented matroid of the respective sphere starting out with one sign we may choose, and derive a contradiction from that.

From five points in a facet we get:

$$\chi(v_2\ ,v_4\ ,v_6\ ,v_9\ ,v_{10}) \overset{F_{10}}{=} \quad 0. \tag{3.119}$$

(12^1_{40})

$F_0 = \{v_0, v_5, v_7, v_{10}, v_{11}\}$
$F_1 = \{v_1, v_4, v_5, v_9, v_{11}\}$
$F_2 = \{v_1, v_5, v_6, v_{10}, v_{11}\}$
$F_3 = \{v_0, v_3, v_6, v_7, v_{11}\}$
$F_4 = \{v_2, v_4, v_5, v_8, v_9\}$
$F_5 = \{v_2, v_6, v_7, v_{10}, v_{11}\}$
$F_6 = \{v_1, v_3, v_6, v_9, v_{11}\}$
$F_7 = \{v_0, v_1, v_4, v_5, v_8, v_{10}\}$
$F_8 = \{v_2, v_3, v_6, v_7, v_8, v_9\}$
$F_9 = \{v_0, v_3, v_5, v_8, v_9, v_{11}\}$
$F_{10} = \{v_1, v_2, v_4, v_6, v_9, v_{10}\}$
$F_{11} = \{v_0, v_2, v_3, v_4, v_7, v_8, v_{10}\}$

$\underline{F_5}$

$v_0 = (521, 4578, 4178)$
$v_1 = (672, 1830, 3000)$
$v_2 = (0, 0, 0)$
$v_3 = (401, 6045, 1566)$
$v_4 = (86, 380, 985)$
$v_5 = (665, 2997, 3461)$
$v_6 = (1000, 0, 0)$
$v_7 = (489, 9490, 566)$
$v_8 = (583973976764177/2663388909400,$
$3674158187655449/2130711127520, 1859)$
$v_9 = (416, 1241, 1414)$
$v_{10} = (458, 561, 9801)$
$v_{11} = (689, 2862, 3212)$

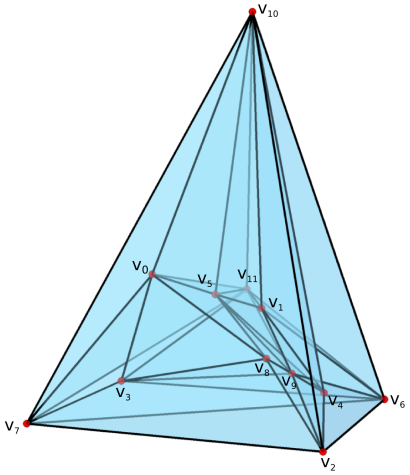

$\underline{F_6}$

$v_0 = (5836, 459, 9688)$
$v_1 = (3027, 3506, 2175)$
$v_2 = (1926, 1192, 1673)$
$v_3 = (5839, 58, 9971)$
$v_4 = (2793, 3230, 2045)$
$v_5 = (4325, 5528, 3616)$
$v_6 = (1000, 0, 0)$
$v_7 = (3878, 136, 5878)$
$v_8 = (4923105551293448/1175442365237,$
$1329420300780956/1175442365237, 6391)$
$v_9 = (0, 0, 0)$
$v_{10} = (3047, 3422, 2253)$
$v_{11} = (7588, 9974, 6203)$

$\underline{F_7}$

$v_0 = (0, 0, 0)$
$v_1 = (4047, 2473, 5124)$
$v_2 = (5674, 4092, 7945)$
$v_3 = (1248, 1140, 1564)$
$v_4 = (7991, 9933, 9605)$
$v_5 = (1000, 0, 0)$
$v_6 = (3748, 1615, 5027)$
$v_7 = (2001, 176, 3252)$
$v_8 = (221733789996629/79162757410,$
$418107710362426/39581378705, 357)$
$v_9 = (3845, 2457, 4849)$
$v_{10} = (5770, 91, 9945)$
$v_{11} = (2604, 236, 3411)$

Figure 3.42: These are the facet list and the diagrams (resp. coordinates for these) with bases F_5, F_6, and F_7 of the second of the three 3-spheres with f-vector $(12, 40, 40, 12)$ that were found by our enumeration and not described before. This sphere is self-dual and non-polytopal.

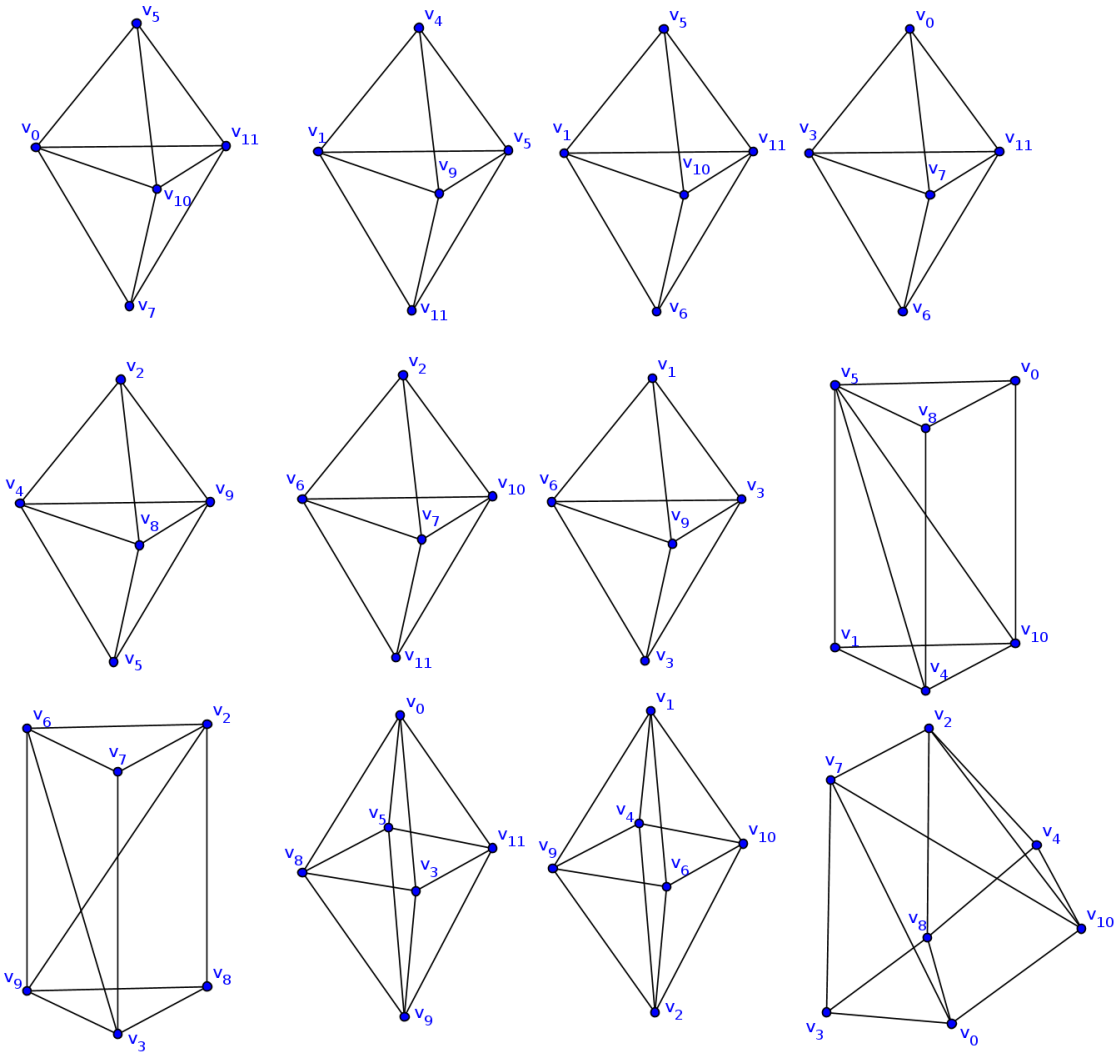

Figure 3.43: These are the facets of the sphere (12^1_{40}) from F_0 (top left) to F_{11} (bottom right).

From facet F_0 (see Figure 3.43) we may choose $\chi(v_0\ , v_5\ , v_{10}, v_{11}, v_i\ ) = \ \ 1$, where $v_i \notin F_0$. With this we can derive:

$$\begin{aligned}
\chi(v_0\ , v_3\ , v_5\ , v_{10}, v_{11}) = -1 \quad &\overset{F_9}{\Rightarrow} \chi(v_0\ , v_3\ , v_5\ , v_6\ , v_{11}) = -1 \\
&\overset{F_3}{\Rightarrow} \chi(v_0\ , v_3\ , v_6\ , v_8\ , v_{11}) = \ \ 1 \\
&\overset{F_9}{\Rightarrow} \chi(v_0\ , v_3\ , v_4\ , v_8\ , v_{11}) = \ \ 1 \\
&\overset{F_{11}}{\Rightarrow} \chi(v_0\ , v_3\ , v_4\ , v_5\ , v_8\ ) = -1 \\
&\overset{F_7}{\Rightarrow} \chi(v_0\ , v_2\ , v_4\ , v_5\ , v_8\ ) = -1 \\
&\overset{F_{11}}{\Rightarrow} \chi(v_0\ , v_2\ , v_4\ , v_8\ , v_9\ ) = \ \ 1 \\
&\overset{F_4}{\Rightarrow} \chi(v_2\ , v_4\ , v_6\ , v_8\ , v_9\ ) = \ \ 1 \\
&\overset{F_8}{\Rightarrow} \chi(v_2\ , v_6\ , v_8\ , v_9\ , v_{10}) = -1, \qquad (3.120) \\
\chi(v_0\ , v_1\ , v_5\ , v_{10}, v_{11}) = -1 \quad &\overset{F_7}{\Rightarrow} \chi(v_0\ , v_1\ , v_5\ , v_7\ , v_{10}) = \ \ 1 \\
&\overset{F_0}{\Rightarrow} \chi(v_0\ , v_2\ , v_5\ , v_7\ , v_{10}) = \ \ 1 \\
&\overset{F_{11}}{\Rightarrow} \chi(v_0\ , v_2\ , v_6\ , v_7\ , v_{10}) = \ \ 1 \\
&\overset{F_5}{\Rightarrow} \chi(v_2\ , v_6\ , v_7\ , v_9\ , v_{10}) = -1 \\
&\overset{F_{10}}{\Rightarrow} \chi(v_2\ , v_6\ , v_9\ , v_{10}, v_{11}) = -1, \qquad (3.121) \\
\chi(v_0\ , v_4\ , v_5\ , v_{10}, v_{11}) = -1 \quad &\overset{F_7}{\Rightarrow} \chi(v_0\ , v_4\ , v_5\ , v_7\ , v_{10}) = \ \ 1 \\
&\overset{F_{11}}{\Rightarrow} \chi(v_0\ , v_1\ , v_4\ , v_7\ , v_{10}) = -1 \\
&\overset{F_7}{\Rightarrow} \chi(v_0\ , v_1\ , v_4\ , v_9\ , v_{10}) = -1 \\
&\overset{F_{10}}{\Rightarrow} \chi(v_1\ , v_4\ , v_9\ , v_{10}, v_{11}) = -1, \qquad (3.122) \\
\chi(v_0\ , v_5\ , v_6\ , v_{10}, v_{11}) = \ \ 1 \quad &\overset{F_2}{\Rightarrow} \chi(v_5\ , v_6\ , v_9\ , v_{10}, v_{11}) = \ \ 1, \qquad (3.123) \\
\chi(v_0\ , v_3\ , v_5\ , v_{10}, v_{11}) = -1 \quad &\overset{F_9}{\Rightarrow} \chi(v_0\ , v_3\ , v_5\ , v_7\ , v_{11}) = -1 \\
&\overset{F_0}{\Rightarrow} \chi(v_0\ , v_5\ , v_7\ , v_9\ , v_{11}) = -1 \\
&\overset{F_9}{\Rightarrow} \chi(v_0\ , v_1\ , v_5\ , v_9\ , v_{11}) = \ \ 1 \\
&\overset{F_1}{\Rightarrow} \chi(v_1\ , v_5\ , v_9\ , v_{10}, v_{11}) = -1, \qquad (3.124) \\
\chi(v_0\ , v_1\ , v_5\ , v_{10}, v_{11}) = -1 \quad &\overset{F_7}{\Rightarrow} \chi(v_0\ , v_1\ , v_5\ , v_6\ , v_{10}) = \ \ 1 \\
&\overset{F_2}{\Rightarrow} \chi(v_1\ , v_5\ , v_6\ , v_9\ , v_{10}) = -1 \\
&\overset{F_{10}}{\Rightarrow} \chi(v_1\ , v_6\ , v_9\ , v_{10}, v_{11}) = \ \ 1, \qquad (3.125) \\
\chi(v_0\ , v_5\ , v_7\ , v_9\ , v_{11}) \overset{(3.124)}{=} -1 \quad &\overset{F_9}{\Rightarrow} \chi(v_0\ , v_4\ , v_5\ , v_9\ , v_{11}) = \ \ 1 \\
&\overset{F_1}{\Rightarrow} \chi(v_4\ , v_5\ , v_9\ , v_{10}, v_{11}) = -1, \qquad (3.126) \\
\chi(v_0\ , v_3\ , v_6\ , v_8\ , v_{11}) \overset{(3.120)}{=} \ \ 1 \quad &\overset{F_9}{\Rightarrow} \chi(v_0\ , v_2\ , v_3\ , v_8\ , v_{11}) = -1 \\
&\overset{F_{11}}{\Rightarrow} \chi(v_0\ , v_2\ , v_3\ , v_8\ , v_9\ ) = -1 \\
&\overset{F_8}{\Rightarrow} \chi(v_2\ , v_3\ , v_8\ , v_9\ , v_{10}) = -1, \qquad (3.127)
\end{aligned}$$

$$\chi(v_0\ ,v_2\ ,v_4\ ,v_8\ ,v_9\ ) \overset{(3.120)}{=} 1 \quad \overset{F_4}{\Rightarrow} \chi(v_2\ ,v_4\ ,v_8\ ,v_9\ ,v_{10}) = 1, \tag{3.128}$$

$$\chi(v_0\ ,v_2\ ,v_3\ ,v_8\ ,v_9\ ) \overset{(3.127)}{=} -1 \quad \overset{F_9}{\Rightarrow} \chi(v_0\ ,v_3\ ,v_6\ ,v_8\ ,v_9\ ) = 1$$

$$\overset{F_8}{\Rightarrow} \chi(v_3\ ,v_6\ ,v_8\ ,v_9\ ,v_{10}) = 1, \tag{3.129}$$

$$\chi(v_0\ ,v_2\ ,v_4\ ,v_5\ ,v_8\ ) \overset{(3.120)}{=} -1 \quad \overset{F_4}{\Rightarrow} \chi(v_2\ ,v_4\ ,v_5\ ,v_8\ ,v_{10}) = -1$$

$$\overset{F_{11}}{\Rightarrow} \chi(v_1\ ,v_2\ ,v_4\ ,v_8\ ,v_{10}) = -1$$

$$\overset{F_7}{\Rightarrow} \chi(v_1\ ,v_3\ ,v_4\ ,v_8\ ,v_{10}) = -1$$

$$\overset{F_{11}}{\Rightarrow} \chi(v_3\ ,v_4\ ,v_8\ ,v_9\ ,v_{10}) = 1, \tag{3.130}$$

With these values for the partial chirotope, we can find some new values of χ using the Grassmann-Plücker-relations:

$$\begin{aligned}\{\chi(v_8,v_9,v_{10},v_2,v_3)\chi(v_8,v_9,v_{10},v_4,v_6), &\quad \chi(v_8,v_9,v_{10},v_2,v_4)\chi(v_8,v_9,v_{10},v_3,v_6),\\ &\quad \chi(v_8,v_9,v_{10},v_2,v_6)\chi(v_8,v_9,v_{10},v_3,v_4)\}\\ \overset{(3.127),(3.128),(3.129),(3.120),(3.130)}{=} &\quad \{(-1)\cdot\chi(v_8,v_9,v_{10},v_4,v_6), -1\cdot 1,\\ &\qquad (-1)\cdot 1\},\\ &\quad \Rightarrow \chi(v_8,v_9,v_{10},v_4,v_6) = -1,\end{aligned} \tag{3.131}$$

$$\begin{aligned}\{\chi(v_9,v_{10},v_{11},v_1,v_4)\chi(v_9,v_{10},v_{11},v_5,v_6), &\quad \chi(v_9,v_{10},v_{11},v_1,v_5)\chi(v_9,v_{10},v_{11},v_4,v_6),\\ &\quad \chi(v_9,v_{10},v_{11},v_1,v_6)\chi(v_9,v_{10},v_{11},v_4,v_5)\}\\ \overset{(3.122),(3.123),(3.124),(3.125),(3.126)}{=} &\quad \{(-1)\cdot 1, -(-1)\cdot\chi(v_9,v_{10},v_{11},v_4,v_6),\\ &\qquad 1\cdot(-1)\},\\ &\quad \Rightarrow \chi(v_9,v_{10},v_{11},v_4,v_6) = 1,\end{aligned} \tag{3.132}$$

Finally, we get the Grassmann-Plücker-relation

$$\begin{aligned}\{\chi(v_6,v_9,v_{10},v_2,v_4)\chi(v_6,v_9,v_{10},v_8,v_{11}), &\quad \chi(v_6,v_9,v_{10},v_2,v_8)\chi(v_6,v_9,v_{10},v_4,v_{11}),\\ &\quad \chi(v_6,v_9,v_{10},v_2,v_{11})\chi(v_6,v_9,v_{10},v_4,v_8)\}\\ \overset{(3.119),(3.120),(3.132),(3.121),(3.131)}{=} &\quad \{0, -1\cdot(-1),\\ &\qquad 1\cdot 1\},\end{aligned} \tag{3.133}$$

which is neither $\{0\}$, nor contains $\{-1,1\}$. Therefore, the Grassmann-Plücker-relations cannot be satisfied, whence the sphere (12^1_{40}) does not support an oriented matroid. Hence, it is non-polytopal. □

Proposition 3.2.15. *The sphere (12^1_{40}) has a diagram based on F_5, F_6, and F_7, but does not have a diagram based on one of the facets F_0, F_1, F_3, F_4, F_8, F_9, F_{10}, and F_{11}. Furthermore, it is not fan-like.*

Proof. We construct partial chirotopes as explained at the beginning of the chapter.

The resulting partial chirotopes for the different facets as bases of a diagram give already the signs of 177 to 386 elements out of $\binom{12}{4} = 495$, which is the size of an oriented matroid for a diagram of (12^1_{40}). With SCIP we can find coordinates for the diagrams with bases F_5, F_6, and F_7 (see Figure 3.42), while in the other cases we get certificates of non-realisability:

- F_3 and F_{11}: the Grassmann–Plücker relations fail;
- F_0, F_1, F_8, and F_9: the partial chirotope obtained from orienting and the Grassmann–Plücker relations has a bfp;
- F_4 and F_{10}: backtracking reveals that every partial chirotope, and hence every oriented matroid, either has a bfp, or fails the Grassmann–Plücker relations.

For the case of the fan-like embedding, we constructed a partial chirotope and tested via backtracking all partial chirotopes with a size of at least 15% of the size of an oriented matroid for this case ($\binom{13}{5} = 1287$) for the existence of a bfp and all of them turned out to have one. Therefore, there is no oriented matroid for this case and (12^1_{40}) has no fan-like embedding. □

Remark. We could not decide, whether the sphere (12^1_{40}) has a diagram based on F_2, since in that case oriented matroids without a bfp exist, but we coul not find coordinates.

Theorem 3.2.16. *The sphere* (12^2_{40}) *is non-polytopal.*

Proof. The proof of this theorem works the same way as described above: we construct a partial chirotope for the oriented matroid of the respective sphere starting out with one sign we may choose, and derive a contradiction from that.

From the tetrahedron facet F_0 we may choose $\chi(v_2\ , v_5\ , v_9\ , v_{11}, v_i\ ) = -1$, where $v_i \notin F_0$. With this we can derive:

$$\chi(v_2\ , v_3\ , v_5\ , v_9\ , v_{11}) = \quad 1 \quad \overset{F_{11}}{\Rightarrow} \chi(v_3\ , v_5\ , v_9\ , v_{10}, v_{11}) = -1, \tag{3.134}$$

$$\begin{aligned} \chi(v_1\ , v_2\ , v_5\ , v_9\ , v_{11}) = -1 \quad &\overset{F_{10}}{\Rightarrow} \chi(v_0\ , v_1\ , v_2\ , v_5\ , v_{11}) = \quad 1 \\ &\overset{F_{11}}{\Rightarrow} \chi(v_0\ , v_1\ , v_5\ , v_6\ , v_{11}) = -1 \\ &\overset{F_{10}}{\Rightarrow} \chi(v_1\ , v_5\ , v_6\ , v_8\ , v_{11}) = \quad 1 \\ &\overset{F_4}{\Rightarrow} \chi(v_1\ , v_6\ , v_8\ , v_9\ , v_{11}) = \quad 1 \\ &\overset{F_6}{\Rightarrow} \chi(v_6\ , v_8\ , v_9\ , v_{10}, v_{11}) = -1, \end{aligned} \tag{3.135}$$

$$\begin{aligned} \chi(v_0\ , v_1\ , v_2\ , v_5\ , v_{11}) \overset{(3.135)}{=} \quad 1 \quad &\overset{F_{11}}{\Rightarrow} \chi(v_0\ , v_1\ , v_4\ , v_5\ , v_{11}) = \quad 1 \\ &\overset{F_5}{\Rightarrow} \chi(v_0\ , v_1\ , v_3\ , v_4\ , v_{11}) = -1 \\ &\overset{F_3}{\Rightarrow} \chi(v_0\ , v_3\ , v_4\ , v_9\ , v_{11}) = -1 \\ &\overset{F_{11}}{\Rightarrow} \chi(v_0\ , v_3\ , v_6\ , v_9\ , v_{11}) = -1 \\ &\overset{F_6}{\Rightarrow} \chi(v_3\ , v_6\ , v_9\ , v_{10}, v_{11}) = \quad 1, \end{aligned} \tag{3.136}$$

Figure 3.44

(12^2_{40})

$F_0 = \{v_2, v_5, v_9, v_{11}\}$
$F_1 = \{v_0, v_4, v_7, v_9, v_{10}\}$
$F_2 = \{v_0, v_3, v_8, v_9, v_{10}\}$
$F_3 = \{v_0, v_3, v_4, v_8, v_{11}\}$
$F_4 = \{v_1, v_4, v_6, v_8, v_{11}\}$
$F_5 = \{v_0, v_1, v_4, v_7, v_{11}\}$
$F_6 = \{v_2, v_3, v_6, v_8, v_9, v_{11}\}$
$F_7 = \{v_0, v_2, v_4, v_6, v_8, v_{10}\}$
$F_8 = \{v_2, v_5, v_7, v_8, v_9, v_{10}\}$
$F_9 = \{v_1, v_4, v_5, v_6, v_7, v_{10}\}$
$F_{10} = \{v_1, v_2, v_5, v_6, v_{10}, v_{11}\}$
$F_{11} = \{v_0, v_1, v_3, v_5, v_7, v_9, v_{11}\}$

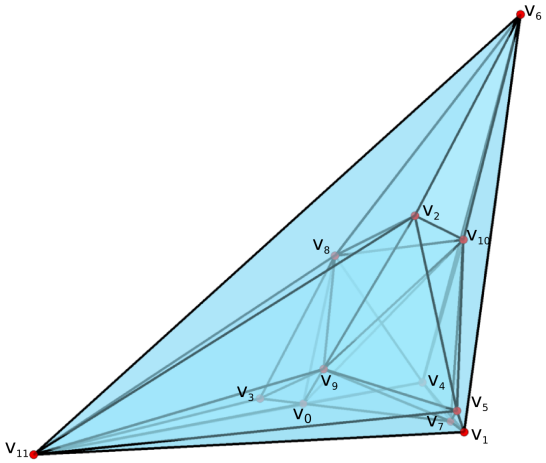

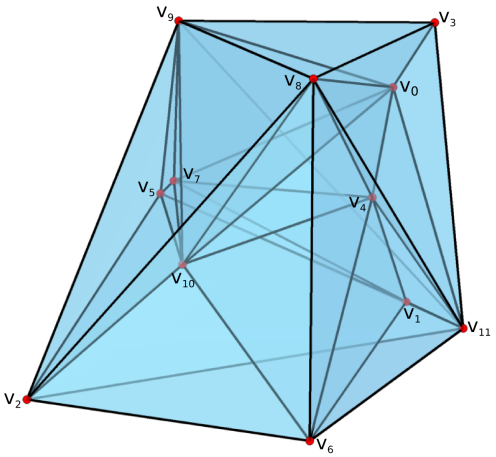

$\underline{F_4}$
$v_0 = (60, 109, 3)$
$v_1 = (31291466/6900155,$
$24661781/6900155, 1/10)$
$v_2 = (20, 52, 156)$
$v_3 = (44, 146, 15)$
$v_4 = (100, 0, 0)$
$v_5 = (11, 8, 14)$
$v_6 = (0, 0, 298)$
$v_7 = (22, 7, 1)$
$v_8 = (32, 89, 116)$
$v_9 = (36, 103, 39)$
$v_{10} = (20, 14, 139)$
$v_{11} = (0, 305, 0)$

$\underline{F_6}$
$v_0 = (1736, 8768, 2375)$
$v_1 = (8998, 8341, 821)$
$v_2 = (9878, 55, 9929)$
$v_3 = (47, 9536, 872)$
$v_4 = (4435, 9019, 4749)$
$v_5 = (40929711125/8014191, 1294, 3878)$
$v_6 = (9572, 9287, 9878)$
$v_7 = (12907764250/2811809, 1959, 4041)$
$v_8 = (114, 9938, 9934)$
$v_9 = (130, 53, 69)$
$v_{10} = (6414, 3625, 6500)$
$v_{11} = (9961, 9938, 48)$

$\underline{F_7}$
$v_0 = (0, 0, 0)$
$v_1 = (156, 229, 296)$
$v_2 = (107, 299, 262)$
$v_3 = (5, 8, 18)$
$v_4 = (100, 0, 0)$
$v_5 = (3084285/37657, 274, 125)$
$v_6 = (183, 311, 397)$
$v_7 = (87781/1491, 235, 41)$
$v_8 = (29, 28, 314)$
$v_9 = (11, 89, 14)$
$v_{10} = (30, 394, 40)$
$v_{11} = (139, 193, 269)$

$\underline{F_8}$
$v_0 = (-900, -360, 390)$
$v_2 = (-657, 1663, 59)$
$v_4 = (-648, -392, 490)$
$v_6 = (-650, 500, 250)$
$v_8 = (-868, 262, 202)$
$v_{10} = (-600, -410, 2000)$
$v_1 = (-29280086/12100455,$
$64710914/4033485, 1)$
$v_3 = (-937, 30, -28)$
$v_5 = (530, -470, -25)$
$v_7 = (-300, -480, 360)$
$v_9 = (-1194, -509, -769)$
$v_{11} = (-70, 190, -95)$

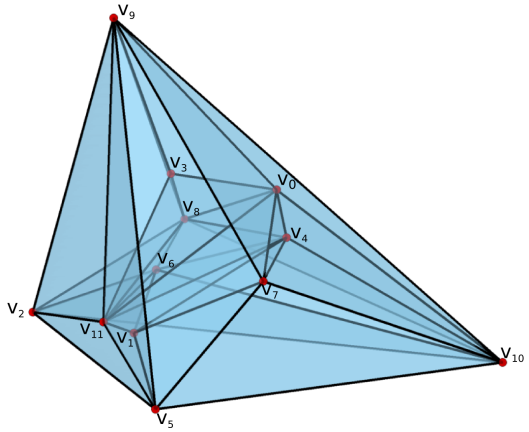

Figure 3.44: These are the facet list and the diagrams (resp. coordinates for these) with bases F_4, F_6, F_7, and F_8 of the third of the 3-spheres with f-vector $(12, 40, 40, 12)$ that were found by our enumeration and not described before. This sphere is self-dual and non-polytopal.

$$\begin{aligned}
\chi(v_0, v_1, v_4, v_5, v_{11}) \overset{(3.136)}{=} 1 \quad &\overset{F_5}{\Rightarrow} \chi(v_0, v_1, v_4, v_8, v_{11}) = 1 \\
&\overset{F_3}{\Rightarrow} \chi(v_0, v_2, v_4, v_8, v_{11}) = 1 \\
&\overset{F_7}{\Rightarrow} \chi(v_0, v_2, v_3, v_4, v_8) = 1 \\
&\overset{F_3}{\Rightarrow} \chi(v_0, v_3, v_4, v_8, v_{10}) = -1 \\
&\overset{F_2}{\Rightarrow} \chi(v_0, v_2, v_3, v_8, v_{10}) = 1 \\
&\overset{F_7}{\Rightarrow} \chi(v_0, v_2, v_8, v_9, v_{10}) = -1 \\
&\overset{F_2}{\Rightarrow} \chi(v_0, v_5, v_8, v_9, v_{10}) = -1 \\
&\overset{F_8}{\Rightarrow} \chi(v_5, v_8, v_9, v_{10}, v_{11}) = -1, \qquad (3.137)
\end{aligned}$$

$$\begin{aligned}
\chi(v_0, v_2, v_3, v_4, v_8) \overset{(3.137)}{=} 1 \quad &\overset{F_3}{\Rightarrow} \chi(v_0, v_3, v_4, v_8, v_9) = -1 \\
&\overset{F_2}{\Rightarrow} \chi(v_0, v_2, v_3, v_8, v_9) = 1 \\
&\overset{F_6}{\Rightarrow} \chi(v_2, v_3, v_8, v_9, v_{10}) = 1 \\
&\overset{F_2}{\Rightarrow} \chi(v_3, v_8, v_9, v_{10}, v_{11}) = 1, \qquad (3.138)
\end{aligned}$$

$$\begin{aligned}
\chi(v_0, v_3, v_4, v_8, v_{10}) \overset{(3.137)}{=} -1 \quad &\overset{F_7}{\Rightarrow} \chi(v_0, v_4, v_8, v_9, v_{10}) = -1 \\
&\overset{F_1}{\Rightarrow} \chi(v_0, v_4, v_6, v_9, v_{10}) = -1 \\
&\overset{F_7}{\Rightarrow} \chi(v_0, v_4, v_5, v_6, v_{10}) = 1 \\
&\overset{F_9}{\Rightarrow} \chi(v_4, v_5, v_6, v_{10}, v_{11}) = 1 \\
&\overset{F_{10}}{\Rightarrow} \chi(v_5, v_6, v_9, v_{10}, v_{11}) = 1. \qquad (3.139)
\end{aligned}$$

With these values for the partial chirotope, we get the Grassmann-Plücker-relation

$$\{\chi(v_9,v_{10},v_{11},v_3,v_5)\chi(v_9,v_{10},v_{11},v_6,v_8),\quad \chi(v_9,v_{10},v_{11},v_3,v_6)\chi(v_9,v_{10},v_{11},v_5,v_8),$$
$$\chi(v_9,v_{10},v_{11},v_3,v_8)\chi(v_9,v_{10},v_{11},v_5,v_6)\}$$
$$\overset{(3.134),(3.135),(3.136),(3.137),(3.138),(3.139)}{=} \{(-1)\cdot(-1), -1\cdot(-1), 1\cdot 1\}, \tag{3.140}$$

which is neither $\{0\}$, nor contains $\{-1,1\}$. Therefore, the Grassmann-Plücker-relations cannot be satisfied, whence the sphere (12^2_{40}) does not support an oriented matroid. Hence, it is non-polytopal. □

Proposition 3.2.17. *The sphere (12^2_{40}) has a diagram based on F_4, F_6, F_7, and F_8, but does not have a diagram based on one of the facets F_0, F_1, F_2, F_{10}, and F_{11}.*

Proof. We construct partial chirotopes as explained at the beginning of the chapter.

The resulting partial chirotopes for the different facets as bases of a diagram give already the signs of 348 to 402 elements out of $\binom{12}{4} = 495$, which is the size of an oriented matroid for a diagram of (12^2_{40}). With SCIP we can find coordinates for the diagrams with bases F_4, F_6, F_7, and F_8 (see Figure 3.44), while in the cases F_0, F_1, F_2, F_{10}, and F_{11} the Grassmann–Plücker relations fail. □

Remark. We could not decide, whether the sphere (12^2_{40}) has a diagram based on F_3, F_5, or F_9, since in these cases oriented matroids without a bfp exist, but we could not find coordinates. For the fan-like embedding, we checked via backtracking some of the partial chirotopes, they all have a bfp. However, we could only check a tiny fraction of the entire search tree. Since we could not find coordinates either, this case remains open.

3.3 Diagrams and Embeddability

Polytopes have a lot of structure and come together with several properties, for example they are shellable, have a Schlegel diagram, and are star-shaped (see e.g. [35] or [76]). Trivially, all polytopal spheres have these properties as well, but also non-polytopal spheres can have some of these. In this section we will prove relations between these properties and give examples for the failure of other properties. For a better visualisation, we will draw a chart that depicts all implications from polytopes on the one side to spheres on the other side (see Figure 3.46).

A classical example of a non-polytopal sphere is the *Barnette sphere*. This sphere is also a first example of a sphere that has some diagram, but not with every facet as base (see [31, Sec. III.4] for the proof and Figure 3.45 for the facet list and a diagram).

At the beginning of this chapter we have seen that for simplicial spheres the notions of star-shaped embedding and fan-like embedding are equivalent, but we have seen in Section 3.2 that this does not hold in general (Proposition 3.2.11). Another connection between the properties of Figure 3.46 that does not hold in general, but for simplicial spheres, is that the existence of a diagram implies the existence of a star-shaped embedding.

$\{1,3,5,7\},\{1,2,3,4\},\{3,4,5,6\},$
$\{1,2,5,6\},\{1,2,4,7\},\{1,3,4,7\},$
$\{3,4,6,7\},\{3,5,6,7\},\{1,2,5,7\},$
$\{2,5,6,7\},\{2,4,6,7\},\{1,2,3,8\},$
$\{2,3,4,8\},\{3,4,5,8\},\{4,5,6,8\},$
$\{1,2,6,8\},\{1,5,6,8\},\{1,3,5,8\},$
$\{2,4,6,8\}$

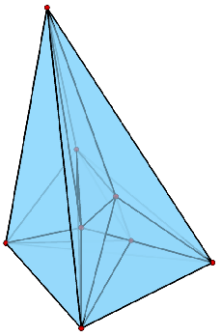

Figure 3.45: The Barnette Sphere: on the left is a list with the facets, and on the right a diagram is shown.

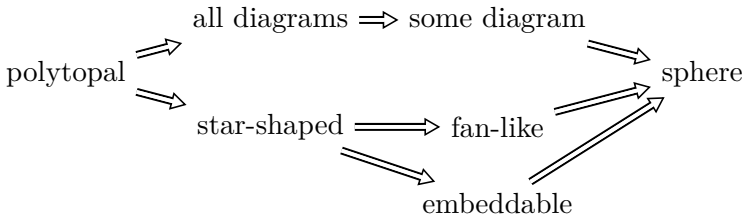

Figure 3.46: This diagram shows the implications that hold between polytopes, diagrams, embeddability and spheres.

Proposition 3.3.1. *Let S be a d-sphere with a diagram based on the facet $F \in S$ and with a vertex $v \in F$, such that every facet $F' \in S$ that contains v is a pyramid with apex v. Then S is also star-shaped. This holds in particular for simplicial spheres.*

Proof. The proof is essentially the same as the one in [31, Sec. III.5] for the fact that the Barnette sphere is star-shaped. The diagram with base F gives a polyhedral embedding of $S \setminus F$ into $\mathbb{R}^d$. If we now lift this onto a hyperplane in $\mathbb{R}^{d+1}$ and move v out of this hyperplane, then the facets containing v remain convex polytopes and do not change combinatorics, since they are pyramids with apex v. In total, we obtain a pyramid with apex v and base $S \setminus v$, which is star-shaped. □

The known connections between all the properties introduced in this section are depicted in Figure 3.46. For many of the "missing" implications of that chart there are counterexamples, but not for all of them.

Conjecture 2. *Figure 3.46 is complete in the sense that missing implications do not hold in general.*

Theorem 3.3.2 (Ewald [31, Thm. 5.7])**.** *The Ewald sphere from Figure 3.47 is fan-like, but not polyhedrally embeddable into any $\mathbb{R}^k$.*

Proposition 3.3.3. *None of the implications of Figure 3.46 holds in the other direction as well. Furthermore, we have:*

$$\begin{aligned}
\text{polyhedrally embeddable} &\not\Rightarrow \text{fan-like},\\
\text{polyhedrally embeddable} &\not\Rightarrow \text{some diagram},\\
\text{fan-like} &\not\Rightarrow \text{polyhedrally embeddable},\\
\text{some diagram} &\not\Rightarrow \text{polyhedrally embeddable},\\
\text{some diagram} &\not\Rightarrow \text{fan-like},\\
\text{fan-like} &\not\Rightarrow \text{all diagrams},\\
\text{star-shaped} &\not\Rightarrow \text{all diagrams}.
\end{aligned}$$

Proof. For this proof we use four examples: the Barnette Sphere (Figure 3.45), the Ewald Sphere (Figure 3.47), the sphere obtained from gluing two copies of the Barnette Sphere along a facet that does not serve as a base of a diagram (this construction is from [31, Thm. 5.5]), and the sphere $(10^0_{32,33})$ from Figure 3.35.

The Barnette Sphere has some diagram, but not all, it is star-shaped, but not polytopal (Proposition 3.3.1, see also [31, Sec. III.5]). Therefore, it shows:

$$\begin{aligned}
\text{star-shaped} &\not\Rightarrow \text{all diagrams},\\
\text{star-shaped} &\not\Rightarrow \text{polytopal},\\
\text{fan-like} &\not\Rightarrow \text{all diagrams},\\
\text{some diagram} &\not\Rightarrow \text{all diagrams}.
\end{aligned}$$

The Ewald Sphere has a diagram based on every facet (see Figure 3.47), it is fan-like, but not polyhedrally embeddable, hence not star-shaped (Theorem 3.3.2). Therefore, it shows:

$$\begin{aligned}
\text{all diagrams} &\not\Rightarrow \text{polytopal},\\
\text{all/some diagram(s)} &\not\Rightarrow \text{star-shaped},\\
\text{all/some diagram(s)} &\not\Rightarrow \text{polyhedrally embeddable},\\
\text{fan-like} &\not\Rightarrow \text{polyhedrally embeddable},\\
\text{fan-like} &\not\Rightarrow \text{star-shaped},\\
\text{sphere} &\not\Rightarrow \text{polyhedrally embeddable}.
\end{aligned}$$

The gluing of the two copies of the Barnette Sphere is polyhedrally embeddable, but not fan-like [31, Thm. 5.7]. Furthermore, it does not have any diagram, since every diagram would include a diagram of one of the copies of the Barnette Sphere based on the facet along it was glued to the other sphere, which does not exist by construction. Therefore, it shows:

$$\begin{aligned}
\text{polyhedrally embeddable} &\not\Rightarrow \text{fan-like},\\
\text{polyhedrally embeddable} &\not\Rightarrow \text{star-shaped},\\
\text{polyhedrally embeddable} &\not\Rightarrow \text{all/some diagram(s)},\\
\text{sphere} &\not\Rightarrow \text{fan-like},\\
\text{sphere} &\not\Rightarrow \text{some diagram}.
\end{aligned}$$

The sphere $(10^0_{32,33})$ has some diagrams, but is not fan-like (Proposition 3.2.2). Therefore, it shows:

$$\text{some diagram} \quad \not\Rightarrow \quad \text{fan-like}.$$

□

Remark. To finish the proof of Conjecture 2 we would need to show the following:

$$\begin{aligned} \text{all diagrams} &\quad \not\Rightarrow \quad \text{fan-like}, \\ \text{fan-like} &\quad \not\Rightarrow \quad \text{some diagram}, \\ \text{star-shaped} &\quad \not\Rightarrow \quad \text{some diagram}. \end{aligned}$$

However, at the moment we do not have any example or at least a candidate at hand that would show one of these.

Figure 3.47

Ewald Sphere

F_0: $\{v_1, v_2, v_3, v_4\}$
F_1: $\{v_1, v_2, v_3, v_8\}$
F_2: $\{v_1, v_2, v_4, v_5, v_6\}$
F_3: $\{v_1, v_3, v_4, v_5, v_7\}$
F_4: $\{v_2, v_3, v_4, v_7\}$
F_5: $\{v_2, v_4, v_6, v_7\}$
F_6: $\{v_1, v_2, v_5, v_6, v_8\}$
F_7: $\{v_1, v_3, v_5, v_7, v_8\}$
F_8: $\{v_2, v_3, v_6, v_7, v_8\}$
F_9: $\{v_4, v_5, v_6, v_7, v_8\}$

$\underline{F_0}$
$v_0 = (-160, 190, 70)$
$v_1 = (-138, 1020, -120)$
$v_2 = (-143011/595, -79, 401)$
$v_3 = (240, -40, -50)$
$v_4 = (-280, -2, 18)$
$v_5 = (-220, 210, 20)$
$v_6 = (-230, 80, 160)$
$v_7 = (-22258/4585, 1, 1)$

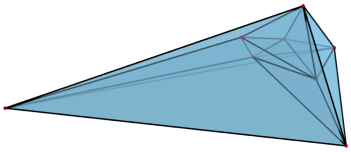

$\underline{F_1}$
$v_0 = (-13, 13, -3)$
$v_1 = (-8, -12, -24)$
$v_2 = (-20.6046511627907, -18, 0)$
$v_3 = (334/21, -4, 7)$
$v_4 = (-7, -11, -6)$
$v_5 = (-10, -2, -11)$
$v_6 = (-15, -5, -2)$
$v_7 = (0, 0, 0)$

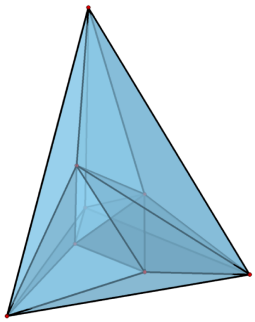

$\underline{F_2}$
$v_0 = (-13, -1, -8)$
$v_1 = (-18, -16, -10)$
$v_2 = (-7, -12, -21)$
$v_3 = (-93/13, -8.5, -5.5)$
$v_4 = (8, 1, 7)$
$v_5 = (-22, -1, 1)$
$v_6 = (-2095/209, 8, -9)$
$v_7 = (0, 0, 0)$

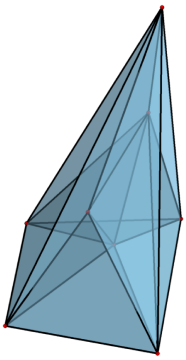

$\underline{F_3}$
$v_0 = (11, 2, 12)$
$v_1 = (13, 16, 36)$
$v_2 = (15, 18, 15)$
$v_3 = (-2, 19, 16)$
$v_4 = (28, 20, 3)$
$v_5 = (17, -8, 18)$
$v_6 = (2177/135, 10, 11)$
$v_7 = (2/89, 1, 1)$

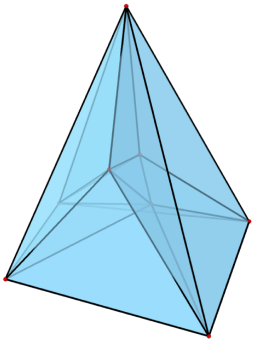

$\underline{F_4}$
$v_0 = (20, 25, 20)$
$v_1 = (5, 50, 38)$
$v_2 = (98, -2, -1)$
$v_3 = (-135/52, 99, 0)$
$v_4 = (-2, -2, 99)$
$v_5 = (5, 31, 35)$
$v_6 = (11639/195, 0, 12)$
$v_7 = (0, 0, 0)$

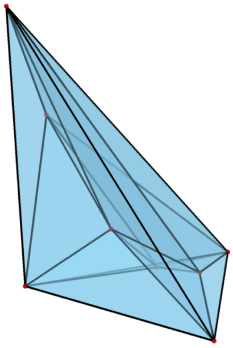

$\underline{F_5}$
$v_0 = (-1, 4, 42)$
$v_1 = (24, 25, 6)$
$v_2 = (44988/547, -11, -12)$
$v_3 = (12800/557, 14, -4)$
$v_4 = (-14, 88, -13)$
$v_5 = (-2, 28, 29)$
$v_6 = (-14, -12, 87)$
$v_7 = (0, 0, 0)$

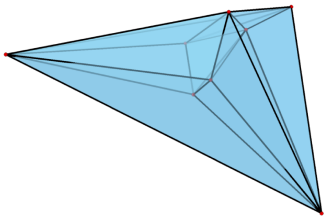

$\underline{F_6}$
$v_0 = (-11, -41, 103)$
$v_1 = (-47, 60, -67)$
$v_2 = (69, 17, -50)$
$v_3 = (-7629/1946, 15, -9)$
$v_4 = (16, -3, -27)$
$v_5 = (-53, -16, -47)$
$v_6 = (4093/36, -5, -42)$
$v_7 = (0, 0, 0)$

$\underline{F_7}$
$v_0 = (1, 14, 40)$
$v_1 = (12, -21, 26)$
$v_2 = (11, -4, 25)$
$v_3 = (3722/169, -2, 11)$
$v_4 = (0, -6, 11)$
$v_5 = (-10, -17, 13)$
$v_6 = (934/217, -1, 21)$
$v_7 = (0, 0, 0)$

$\underline{F_8}$
$v_0 = (11, -1, 90)$
$v_1 = (6, 19, 6)$
$v_2 = (7, 23, -1)$
$v_3 = (21/59, 16, 3)$
$v_4 = (20, 12, 6)$
$v_5 = (18, 12, 10)$
$v_6 = (22, 13, 6)$
$v_7 = (0, 0, 0)$

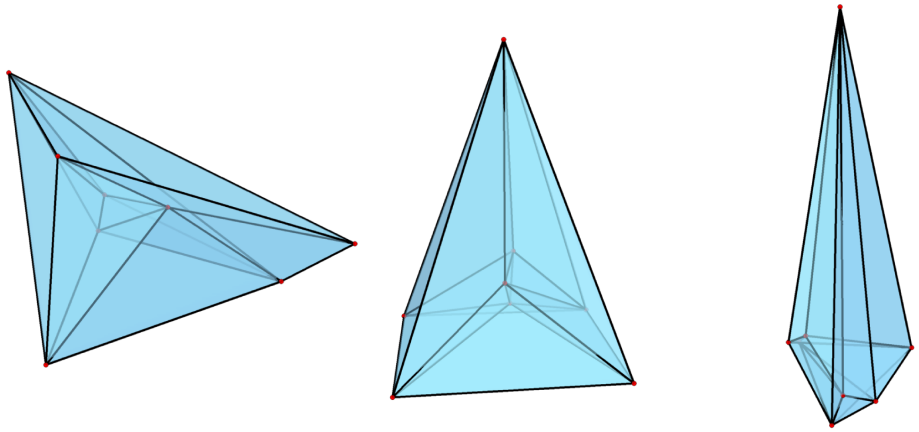

$\underline{F_9}$
$v_0 = (-3, 12, 31)$
$v_1 = (-8, 19, 9)$
$v_2 = (5, 22, 12)$
$v_3 = (5/7, 11, 9)$
$v_4 = (3, 24, -8)$
$v_5 = (-18, 23, 5)$
$v_6 = (37/3, 30, 12)$
$v_7 = (0, 0, 0)$

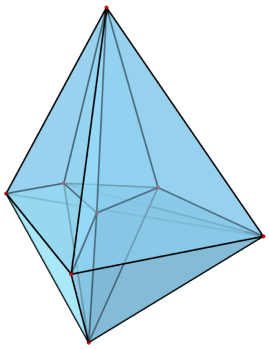

Figure 3.47: These are the facet list and diagrams based on every facet of the Ewald Sphere. See also [31, Thm. 5.3].

List of Figures

...“and what is the use of a book”,
thought Alice, “without pictures or conversation?”
(Lewis Carrol, Alice’s Adventures in Wonderland, 1865)

To create the pictures in some of the figures, I used external software. These were Geogebra [37] (Figures 3.1, 3.12, 3.21, 3.22, 3.36, 3.39, 3.43), JavaView [58] (Figures 3.6, 3.7, 3.8, 3.16, 3.21, 3.27, 3.35, 3.37, 3.38, 3.40, 3.41, 3.42, 3.44, 3.45, 3.47,), and sage [59] (Figure 1).

List of Tables

Index

Bibliography

[1] Tobias Achterberg. SCIP: solving constraint integer programs. *Math. Prog. Comp.*, 1(1):1–41, 2009.

[2] Amos Altshuler. Combinatorial 3-manifolds with few vertices. *Journal of Combinatorial Theory, Series A*, 16:165–173, 1974.

[3] Amos Altshuler. Neighborly 4-polytopes and neighborly combinatorial 3-manifolds with ten vertices. *Canadian Journal of Mathematics*, 29:400–420, 1977.

[4] Amos Altshuler, Jürgen Bokowski, and Leon Steinberg. The classification of simplicial 3-spheres with nine vertices into polytopes and nonpolytopes. *Discrete Mathematics*, 31:115–124, 1980.

[5] Amos Altshuler and Leon Steinberg. Enumeration of the quasisimplicial 3-spheres and 4-polytopes with eight vertices. *Pacific Journal of Mathematics*, 113:269–288, 1984.

[6] Amos Altshuler and Leon Steinberg. The complete enumeration of the 4-polytopes and 3-spheres with eight vertices. *Pacific Journal of Mathematics*, 117:1–16, 1985.

[7] David W. Barnette. The minimum number of vertices of a simple polytope. *Israel Journal of Mathematics*, 10:121–125, 1971.

[8] David W. Barnette. Inequalities for f-vectors of 4-polytopes. *Israel Journal of Mathematics*, 11:284–291, 1972.

[9] David W. Barnette. A proof of the lower bound conjecture for convex polytopes. *Pacific Journal of Mathematics*, 46(2):349–354, 1973.

[10] David W. Barnette. The triangulations of the 3-sphere with up to 8 vertices. *Journal of Combinatorial Theory, Series A*, 14:37–53, 1973.

[11] Margaret M. Bayer. The extended f-vectors of 4-polytopes. *Journal of Combinatorial Theory, Series A*, 44:141–151, 1987.

[12] Margaret M. Bayer. Face numbers and subdivisions of convex polytopes. In T. Bisztriczky, P. McMullen, R. Schneider, and A. Ivić Weiss, editors, *POLYTOPES: Abstract, Convex and Computational*, volume 440 of *NATO ASI Series C: Mathematical and Physical Sciences*, pages 155–171. Kluwer Academic Publishers, 1994.

[13] Margaret M. Bayer and Louis J. Billera. Generalized Dehn–Sommerville relations for polytopes, spheres and Eulerian partially ordered sets. *Inventiones Mathematicae*, 79:143–157, 1985.

[14] Louis J. Billera and Anders Björner. Face numbers of polytopes and complexes. In J. E. Goodman and J. O'Rourke, editors, *Handbook of Discrete and Computational Geometry*, chapter 15, pages 291–310. CRC Press, Boca Raton, FL, 1997.

[15] Louis J. Billera and Carl W. Lee. Sufficieny of McMullen's conditions for f-vectors of simplicial polytopes. *Bulletin of the American Mathematical Society*, 2:181–185, 1980.

[16] Louis J. Billera and Carl W. Lee. A proof of the sufficiency of McMullen's conditions for f-vectors of simplicial polytopes. *Journal of Combinatorial Theory, Series A*, 31:237–255, 1981.

[17] Anders Björner. The minimum number of faces of a simple polyhedron. *European Journal of Combinatorics*, 1:27–31, 1980.

[18] Anders Björner, Michel Las Vergnas, Bernd Sturmfels, Neil White, and Günter M. Ziegler. *Oriented Matroids*, volume 46 of *Encyclopedia of Mathematics*. Cambridge University Press, Cambridge, second edition, 1998.

[19] Gerd Blind and Roswitha Blind. Shellings and the lower bound theorem. *Discrete & Computational Geometry*, 21:519–526, 1999.

[20] Jürgen Bokowski. Oriented matroids. In P. Gruber and J. Wills, editors, *Handbook of Convex Geometry*, pages 555–602. North-Holland, Amsterdam, 1993.

[21] Jürgen Bokowski, David Bremner, and G. Gévay. Symmetric matroid polytopes and their generation. *European Journal of Combinatorics*, 30:1758–1777, 2009.

[22] Jürgen Bokowski and Jürgen Richter. On the finding of final polynomials. *European Journal of Combinatorics*, 11:21–34, 1990.

[23] Jürgen Bokowski and Bernd Sturmfels. *Computational Synthetic Geometry*. Number 1355 in Lecture Notes in Mathematics. Springer, Berlin Heidelberg, 1989.

[24] David Bremner. `mpc`, Software package for matroid polytopes. `http://www.cs.unb.ca/profs/bremner/software/mpc/`, 2012. Software.

[25] Philip Brinkmann and Günter M. Ziegler. A flag vector of a 3-sphere that is not the flag vector of a 4-polytope. *Mathematika*. to appear.

[26] Philip Brinkmann and Günter M. Ziegler. Small f-vectors of 3-spheres and of 4-polytopes. Preprint, October 2016, 19 pages, arXiv:1610.01028.

[27] Arne Brøndsted. *An Introduction to Convex Polytopes*, volume 90 of *Graduate Texts in Mathematics*. Springer, New York, 1983.

[28] George E. Cooke and Ross L. Finney. *Homology of Cell Complexes*. Princeton University Press, Princeton, 1967.

[29] Max Dehn. Die Eulersche Polyederformel im Zusammenhange mit dem Inhalt in der Nicht-Euklidischen Geometrie. *Mathematische Annalen*, 61:561–586, 1905.

[30] David Eppstein, Greg Kuperberg, and Günter M. Ziegler. Fat 4-polytopes and fatter 3-spheres. In A. Bezdek, editor, *Discrete Geometry: In honor of W. Kuperberg's 60th birthday*, volume 253 of *Pure and Applied Mathematics*, pages 239–265. Marcel Dekker Inc., New York, 2003.

[31] Günter Ewald. *Combinatorial Convexity and Algebraic Geometry*, volume 168 of *Graduate Texts in Mathematics*. Springer, New York, 1996.

[32] Moritz Firsching. Realizability and inscribability for simplicial polytopes via nonlinear optimization. http://arxiv.org/abs/1508.02531, 2015.

[33] Jacob E. Goodman and Richard Pollack. Upper bounds for configurations and polytopes in $\mathbb{R}^d$. *Discrete & Computational Geometry*, 1:219–227, 1986.

[34] Thorold Gosset. On the regular and semi-regular figures in space of n dimensions. *Messenger of mathematics*, 29:43–48, 1900.

[35] Branko Grünbaum. *Convex Polytopes*, volume 221 of *Graduate Texts in Math.* Springer, New York, 2003. Second edition prepared by V. Kaibel, V. Klee and G. M. Ziegler (original edition: Interscience, London 1967).

[36] Branko Grünbaum and Vadakekkara P. Sreedharan. An enumeration of simplicial 4-polytopes with 8 vertices. *Journal of Combinatorial Theory*, 2:437–467, 1967.

[37] Markus Hohenwarter, Michael Borcherds, Zsolt Lavicza, Stephen Jull, et al. GeoGebra 4.2. http://www.geogebra.org/, 2013. Software.

[38] Andrea Höppner. F-Vektoren und Fahnenvektoren von 4-dimensionalen Polytopen, 1998. Diplomarbeit, Technische Universität Berlin, Germany.

[39] Andrea Höppner and Günter M. Ziegler. A census of flag-vectors of 4-polytopes. In G. Kalai and G. M. Ziegler, editors, *Polytopes — Combinatorics and Computation*, volume 29 of *DMV Seminars*, pages 105–110. Birkhäuser-Verlag, Basel, 2000.

[40] Gil Kalai. Rigidity and the lower bound theorem i. *Inventiones Mathematicea*, 88:125–151, 1987.

[41] Gil Kalai. Many triangulated spheres. *Discrete & Computational Geometry*, 3:1–14, 1988.

[42] Kalle Karu. Hard Lefschetz theorem for nonrational polytopes. *Inventiones Mathematicae*, 157:419–447, 2004.

[43] Joseph M. Ling. New non-linear inequalities for flag-vectors of 4-polytopes. *Discrete & Computational Geometry*, 37:455–469, 2007.

[44] Frank H. Lutz. GAP-program BISTELLAR. Second version (first version 1997 with A. Björner). page.math.tu-berlin.de/~lutz/, 1999. Software.

[45] Frank H. Lutz. *Triangulated Manifolds with Few Vertices and Vertex-Transitive Group Actions*. PhD thesis, Technische Universität Berlin, Germany, 1999.

[46] Frank H. Lutz. Combinatorial 3-manifolds with 10 vertices. *Beiträge zur Algebra und Geometrie*, 49:97–106, 2008.

[47] Brendan T. McKay and Adolfo Piperno. Practical graph isomorphism, II. *Journal of Symbolic Computation*, 60:94–112, 2014.

[48] Peter McMullen. The maximum numbers of faces of a convex polytope. *Mathematika*, 17:179–184, 1970.

[49] Peter McMullen. The numbers of faces of simplicial polytopes. *Israel Journal of Mathematics*, 9:559–570, 1971.

[50] Peter McMullen and David W. Walkup. A generalized lower-bound conjecture for simplicial polytopes. *Mathematika*, 18:264–273, 1971.

[51] Hiroyuki Miyata. *Studies on Classifications and Constructions od combinatorial Structures related to Oriented Matroids*. PhD thesis, University of Tokio, Japan, 2011.

[52] Eran Nevo, Francisco Santos, and Stedman Wilson. Many triangulated odd-dimensional spheres. *Mathematische Annalen*, 364:737–762, 2016.

[53] Isabella Novik. Upper bound theorems for homology manifolds. *Israel Journal of Mathematics*, 108:45–82, 1998.

[54] Andreas Paffenholz. The 2s2s Pages. web page with data, 2005–2011, http://polymake.org/polytopes/paffenholz/www/2s2s.html.

[55] Andreas Paffenholz and Axel Werner. Constructions for 4-polytopes and the cone of flag vectors. In *Algebraic and Geometric Combinatorics*, pages 283–303. American Mathematical Society (AMS), Providence, RI, 2006.

[56] Andreas Paffenholz and Günter M. Ziegler. The e_t-construction for lattices, spheres and polytopes. *Discrete & Computational Geometry*, 32(4):601–621, 2004.

[57] Julian Pfeifle and Günter M. Ziegler. Many triangulated 3-spheres. *Mathematische Annalen*, 330:829–837, 2004.

[58] Konrad Polthier, Klaus Hildebrandt, Ulrich Preuß, Ulrich Reitebuch, et al. JavaView 4.0. http://www.javaview.de, 1999-2013. Software.

[59] Sage community. Sage 6.2, Sage Mathematical Software System. http://www.sagemath.org/. Software.

[60] Duncan M. Y. Sommerville. The relations connecting the angle-sums and volume of a polytope in space of n dimensions. *Proceedings of the Royal Society London, Series A*, 115:103–119, 1927.

[61] Richard P. Stanley. The upper bound conjecture and Cohen-Macaulay rings. *Studies in Applied Mathematics*, 54:135–142, 1975.

[62] Richard P. Stanley. The number of faces of simplicial convex polytopes. *Advances in Mathematics*, 35:236–238, 1980.

[63] Richard P. Stanley. The number of faces of simplicial polytopes and spheres. *Annals of the New York Acadamy of Sciences*, 440:212–223, 1985.

[64] Richard P. Stanley. *Enumerative Combinatorics*, volume 1. Wadsworth & Brooks/Cole, Bekmont, California, 1986. Second edition, Cambridge U.P., 1997.

[65] Richard P. Stanley. Generalized H-vectors, intersection cohomology of toric varieties, and related results. In M. Nagata and H. Matsumura, editor, *Commutative Algebra and Combinatorics*, volume 11 of *Advanced Studies in Pure Mathematics*, pages 187–213. Kinokuniya, Tokyo, and North-Holland, Amsterdam/New York, 1987.

[66] Ernst Steinitz. Über die Eulersche Polyederrelation. *Archiv der Mathematik und Physik, Series 3*, 11:86–88, 1906.

[67] Ernst Steinitz. Polyeder und Raumeinteilungen. In W. Fr. Meyer and H. Mohrmann, editors, *Encyklopädie der mathematischen Wissenschaften mit Einschluss ihrer Anwendungen, Band III.1.2*, volume 9, chapter AB12, pages 1–139. Teubner, Leipzig, 1922.

[68] Ernst Steinitz and Hans Rademacher. *Vorlesungen über die Theorie der Polyeder*. Springer-Verlag, Berlin, 1934. Reprint, Springer-Verlag 1976.

[69] Edward Swartz. Thirty-five years and counting. Preprint, arXiv:1411.0987, 2014.

[70] Tiong-Seng Tay. Lower-bound theorems for pseudomanifolds. *Discrete & Computational Geometry*, 13:203–216, 1995.

[71] David W. Walkup. The lower bound conjecture for 3- and 4-manifolds. *Acta Mathematica*, 125:75–107, 1970.

[72] Axel Werner. *Linear constraints on Face numbers of Polytopes*. PhD thesis, Technische Universität Berlin, Germany, 2009. Published at https://opus4.kobv.de/.

[73] Walter Whiteley. Infinitesimally rigid polyhedra. I. Statics of frameworks. *Transactions of the American Mathematical Society*, 285:431–465, 1984.

[74] Günter M. Ziegler. Face numbers of 4-polytopes and 3-spheres. In Daqian Li, editor, *Proceedings of the International Congress of Mathematicians: Beijing 2002, August 20 - 28. 3. Invited lectures*, volume III, pages 625–636. Beijing: Higher Education Press, 2002.

[75] Günter M. Ziegler. Convex polytopes: Extremal constructions and f-vector shapes. In E. Miller and V. Reiner and B. Sturmfels, editor, *"Geometric Combinatorics", Proc. Park City Mathematical Institute (PCMI) 2004*, pages 617–691. American Mathematical Society, Providence, RI, 2007. With an appendix by Th. Schröder and N. Witte.

[76] Günter M. Ziegler. *Lectures on Polytopes*, volume 152 of *Graduate Texts in Mathematics*. Springer, New York, updated seventh printing of the first edition, 2007.

Zusammenfassung

Die vorliegende Arbeit beschäftigt sich mit den f-Vektoren von 4-dimensionalen Polytopen und deren Verallgemeinerungen (3-Sphären/3-Mannigfaltigkeiten und Eulersche Verbände von Rang 5). Die Beschreibung der Menge aller f-Vektoren von d-Polytopen, $d \geq 4$ (der Fall $d = 3$ wurde 1906 von Ernst Steinitz gelöst) ist eines der großen offenen Probleme der Diskreten Geometrie. Damit eng verbunden ist die Frage, ob 4-Polytope und 3-Sphären die gleichen Mengen von f-Vektoren haben, oder wo Unterschiede bestehen. Dies ist insbesondere deshalb spannend, da zwar schon lange bekannt ist, dass die Menge der kombinatorischen Typen von 3-Sphären echt größer ist als die Menge von kombinatorischen Typen von 4-Polytopen (vgl. Introduction S. 5), und es auch einfach zu zeigen ist, dass in höheren Dimensionen Mannigfaltigkeiten f-Vektoren haben können, die nicht bei Polytopen auftauchen (Theorem 1.1.11), es aber bisher noch kein Beispiel eines f-Vektors, der f-Vektor einer 3-Sphäre aber nicht eines 4-Polytops ist, gibt.

Kapitel 1 beschäftigt sich mit Ungleichungen, die für die Menge der f-Vektoren (oder etwas spezieller der Menge der Fahnenvektoren) von Polytopen, Sphären und Mannigfaltigkeiten gelten. Dabei zeige ich, dass Mannigfaltigkeiten f-Vektoren haben können, die bei Polytopen nicht auftauchen (Theorem 1.1.11), sowie einige neue Ungleichungen für die Mengen der f-Vektoren, bzw. Fahnenvektoren, von speziellen Klassen von 3-Sphären (Propositions 1.2.3 und 1.2.7, Lemma 1.2.8, und Corollary 1.2.9).

Kapitel 2 und 3 verfolgen eine andere Strategie, um Unterschiede in den Mengen der f-Vektoren von 4-Polytopen und 3-Sphären zu zeigen: ich stelle einen Algorithmus vor, mit dem alle 3-Mannigfaltigkeiten mit gegebenem f-Vektor enumeriert werden können, und bei einigen von ihnen zeige ich, dass alle Sphären mit diesem f-Vektor nichtpolytopal sind. Das heißt, ich beweise, dass die Menge der f-Vektoren von 4-Polytopen eine echte Teilmenge derjenigen von f-Vektoren von 3-Sphären ist (Theorem 3.2).

Erklärung

Gemäß §7 (4), der Promotionsordnung des Fachbereichs Mathematik und Informatik der Freien Universität Berlin vom 8. Januar 2007 versichere ich hiermit, dass ich alle Hilfsmittel und Hilfen angegeben und auf dieser Grundlage die vorliegende Arbeit selbständig verfasst habe. Des Weiteren versichere ich, dass ich diese Arbeit nicht bereits zu einem früheren Promotionsverfahren eingereicht habe.

Berlin, den

Philip Brinkmann